

Engineering Mechanics Division
IIT Research Institute
10 West 35th Street
Chicago, Illinois 60616

PB80-191794



Final Report
IITRI Project J6309
Contract HSM 95-73-27
September 1975

MOLTEN ALUMINUM-WATER EXPLOSION
INITIATION MECHANISM STUDY

Prepared by

M. S. Nusbaum

for


National Institute of Occupational
Safety and Health (NIOSH)
1014 Broadway
Cincinnati, Ohio 45202

and

Aluminum Association
750 Third Avenue
New York, N.Y. 10017

IIT RESEARCH INSTITUTE

REPRODUCED BY:
U.S. Department of Commerce **NTIS**
National Technical Information Service
Springfield, Virginia 22161



Advanced concepts are being used by IIT Research Institute to solve research, development, and design problems for industry and government through contract research. Our services encompass virtually all of the physical and biological sciences. Principal areas are: chemistry, computer sciences, electronics, engineering mechanics, life sciences, mechanics of materials, medical engineering, metals, and management and social science research.

The interdisciplinary approach at IITRI brings the latest technology to bear upon the problem-solving process.

Principal office:

10 West 35th Street
Chicago, Illinois 60616

i

BIBLIOGRAPHIC DATA SHEET		1. Report No. d-HSM-95-73-27	2.	3. Recipient's Accession No. PB 80 191794
4. Title and Subtitle Molten Aluminum-Water Explosion Initiation Mechanism Study (Final Report)			5. Report Date 09/00/75	
7. Author(s) Nusbaum, M. S.			8. Performing Organization Rept. No.	
9. Performing Organization Name and Address NIOSH, Cincinnati, Ohio			10. Project/Task/Work Unit No.	
			11. Contract/Grant No.	
12. Sponsoring Organization Name and Address Same			13. Type of Report & Period Covered	
			14.	
15. Supplementary Notes 00092023				
16. Abstracts <p>ABSTRACT: Mechanisms for initiation of molten aluminum and water explosions were evaluated using bleed out simulations, chemical assessment of initiation, and mechanical, thermodynamic, and other potential initiation mechanism studies. Spontaneous nucleation of liquid quench water contained in quench pit surface capillaries was identified as the most probable initiation mechanism. An impact generated shock from aluminum flow over the quench pit surface was the most probable and frequent triggering mechanism for collapsing the vapor film which separates the molten aluminum and liquid water. Vapor film thickness reduction correlated with the time that the aluminum flow impacts quench tank side surfaces. The author concludes that the aluminum industry's current safety practices, which emphasize the elimination of the surface cavities which trap the liquid water required for initiation of the explosion, are a step in the right direction.</p> <p>KEYWORDS: NIOSH-Publication, NIOSH-Contract, Contract-95-73-27, Aluminum-production, Industrial-factory-workers, Industrial-processes, Explosiveness, Thermodynamic-reactions, Phase-transformations, Safety-measures</p>				
17b. Identifiers/Open-Ended Terms				
17c. COSATI Field/Group				
18. Availability Statement Available to the Public			19. Security Class (This Report) UNCLASSIFIED	21. No. of Pages
			20. Security Class (This Page) UNCLASSIFIED	22. Price

ABSTRACT

This is the final report on the "Molten Aluminum - Water Explosion Initiation Mechanism Study." The study was focused on molten aluminum bleed-outs occurring during direct chill (DC) operations. These bleed-outs result in aluminum flowing into the quenching water used in the chill process. On occasion these interactions lead to explosions having various degrees of severity.

The aspects of the interaction which lead to explosions were studied to identify initiation mechanisms which were consistent with commercial experience, operations and would account for the randomness that explosions occurred and the varying degree of severity. This report documents the program results and identifies the operational conditions found to be pertinent. The most probable initiation mechanism has been identified as spontaneous nucleation of liquid quench water contained in quench pit surface capillaries. The molten aluminum is separated from this liquid water by a vapor film which must be collapsed to provide intimate contact between molten aluminum and liquid water. The most probable and most frequent trigger mechanism producing the required contact has been identified as an impact generated shock. The aluminum flow over quench pit surface produces this shock.

These program findings have been based upon: experimental work conducted in this program and by other investigators; analysis of experiments and reports on commercial operations; and to some degree deduction applied to circumstantial evidence. A significant aspect of the program was devoted to determining those mechanisms which did not apply to DC operations. In determining what mechanisms did not apply and the conditions which were present during simulations of DC bleed-outs, the initiation mechanism was identified. This led to defining a culminating experimental program which provided direct evidence on some aspects of the mechanism and circumstantial evidence on others. Direct evidence proved that molten aluminum was present during simulation bleed-out capable of producing spontaneous nucleation of liquid water;

that liquid water was present in the quench tank surfaces; and photomicrographs of quench tank surfaces showed that capillaries were present in surfaces of the type on which explosions had been obtained. Circumstantial evidence was obtained which established that an impact shock was the trigger for collapsing the vapor film separating the two liquids. Molten aluminum flow speeds were calculated (indirectly) and shown to be capable of producing shock pressures on the order of several thousand pounds per square inch. Vapor film thickness reduction was shown to correlate closely with the time the aluminum flow impacts quench tank side surfaces.

A firm basis has been established for continued investigation of the molten aluminum - water explosion phenomena. The current safety practices followed by the aluminum industry are in the right direction. They emphasize the elimination of the surface cavities which trap the liquid water required for initiation of the explosion.

FOREWORD

The IIT Research Institute (IITRI), under contract HSM 99-73-27 with the National Institute for Occupational Safety and Health (NIOSH) and the Aluminum Association (AA), has performed a "Molten Aluminum - Water Explosion Initiation Mechanism Study." The contract effective date was 15 May 1973 and expiration date was 18 September 1975. The program technical monitors for NIOSH were Mr. Nelson Leidel and Dr. Lloyd Stettler; and for the AA were Mr. Seymour Epstein and the AA Task Group on Molten Metal Explosions, chaired by Mr. K. J. Brondyke. Eight review meetings were held during the program which were attended by the technical monitors and the task group. The program was established as IITRI Project J6309 in the Engineering Mechanics Division under the overall supervision of Dr. K. E. McKee, Director. The actual day-to-day operations of the program was carried out in the Systems Research Section, whose line manager is Mr. E. P. Bergmann. The IITRI project staff during the first 13 months of the program included: Mr. C. J. Dahn, Project Engineer; Dr. E. Raisen, Project Leader for Chemistry Studies; Dr. A. Snelson performed the Matrix Isolation Studies; Dr. R. O'Shay and Mr. T. Watmough provided metalurgical Support; and Mr. Frazier and Mr. Wanda conducted the Electrostatic Charge Investigation. The final portion of the program was conducted by Mr. M. S. Nusbaum who became the Project Engineer in June 1974. Technical support was supplied throughout the program by IITRI staff and of particularly significance was that provided by Mr. A. H. Weidemann, Scientific Advisor in the Fire and Safety Research Section.

The program encompassed experimental and analytical aspects with the greatest emphasis placed upon experimental activities. The initial program investigation follow four parallel studies:

- 50 pound bleed-out simulations
- Reaction species identification
- Potential initiation mechanism determination

• Literature review

The next portion of the program focused on the role of electrostatic charge developed during the molten aluminum - water interaction and on small scale simulations. The final portion of the program encompassed: a reevaluation of the literature and program activities; determined, by process of elimination, a most probable initiation mechanism; and was completed by performing large scale bleed-out simulations to demonstrate that the most probable initiation mechanism is spontaneous nucleation (vapor explosion) of liquid quench water triggered by an impact shock resulting from molten aluminum flow.

This is the final report of the program. The findings and results of the studies performed are presented. The assistance and support provided by NIOSH, AA and IITRI staff are acknowledged as having been of significant help in the conduct of the program.

Respectfully Submitted,
IIT Research Institute

M S Nusbaum
M. S. Nusbaum
Senior Research Engineer

APPROVED:

E. P. Bergmann

E. P. Bergmann
Manager, Systems Research

TABLE OF CONTENTS

	<u>Page</u>
1. INTRODUCTION	1-1
1.1 Program Objectives	1-1
1.2 Program Scope	1-1
1.3 Plan of Attack	1-2
1.4 Revised Plan	1-3
1.5 Program Emphasis	1-4
2. SUMMARY AND RECOMMENDATIONS	2-1
2.1 Most Probable Initiation Mechanism	2-1
2.2 Recommendations	2-2
3. PROGRAM ACCOMPLISHMENTS	3-1
3.1 Facilities	3-1
3.2 Chemistry Studies	3-1
3.3 Gross Experiments (50 pound simulations)	3-1
3.4 Electrostatic Studies	3-2
3.5 Small Scale Experiments	3-2
3.6 Initiation Mode Definitions	3-2
3.7 Experimental Investigation of the Most Probable Initiation Mechanisms	3-3
4. MOLTEN ALUMINUM-WATER REACTION PARAMETERS	4-1
4.1 Reaction Parameters	4-1
4.2 Reaction Parameter Discussion	4-1
4.2.1 Aluminum Parameters	4-1
4.2.2 Water Parameters	4-4
4.2.3 Impact Surface Parameters	4-5
4.2.4 Drop Distance Parameters	4-6
4.2.5 Flow Dividers	4-7
4.2.6 Quench Tank Crossectional Area	4-7
4.2.7 Reaction Time Parameter	4-7
5. TYPICAL MOLTEN ALUMINUM-WATER INTERACTION CHARACTERISTICS	5-1
5.1 Overall	5-1
5.2 Temperature Profiles	5-3
5.3 Heat Transfer	5-6

TABLE OF CONTENTS (Continued)

	<u>Page</u>
5.4 Aluminum Flow	5-14
5.4.1 Initial Aluminum Speed	5-14
5.4.2 Air Flow	5-14
5.4.3 Initial Flow through Water	5-15
5.4.4 Initial Aluminum Surface Flow	5-19
5.4.5 Final Flow	5-27
6. BASIC INTERACTION SCENARIO	6-1
6.1 Induction	6-1
6.2 Trigger	6-2
6.3 Propagation	6-4
6.4 Final Reaction	6-7
7. CANDIDATE INITIATION MECHANISMS	7-1
8. CHEMISTRY STUDIES	8-1
8.1 Matrix Isolation Study	8-3
8.2 Aluminum Reactions	8-4
8.3 Active Site Study	8-6
8.4 Ignition and Propagation Study	8-7
8.5 Thermite Reaction Study	8-8
8.6 Debris Examination	8-8
9. LARGE SCALE SIMULATIONS	9-1
9.1 Overview	9-1
9.2 Facility Preparation	9-2
9.3 Instrumentation	9-6
9.4 Experiment Results and Discussion	9-7
9.5 Summation	9-10
9.6 Conclusions	9-12
10. ELECTROSTATIC CHARGE STUDY	10-1
10.1 Gross Experiments	10-1
10.2 Laboratory Experiments	10-3
10.3 Conclusion Regarding Electrostatic Discharge	10-7
10.4 Surface Tension Effect	10-7
10.5 Role of Electrical Phenomena	10-10
10.6 Summation and Conclusion	10-11

IIT RESEARCH INSTITUTE

TABLE OF CONTENTS (Continued)

	<u>Page</u>
11. SMALL SCALE EXPERIMENTS	11-1
11.1 Overview	11-1
11.2 Equipment Description	11-2
11.3 Results	11-3
11.4 Conclusions	11-4
12. INITIATION MECHANISM DEFINITION	12-1
13. INITIATION MECHANISM EXPERIMENTS	13-1
13.1 Overview	13-1
13.2 Tangential Flow Impact Generated Shock	13-2
13.3 "Free Standing" Vertical Flow	13-7
13.4 Conclusions	13-7
14. SIMULATION EQUIPMENT DESIGN	14-1
15. STUDY APPLICABILITY TO FURNACE CHARGING	15-1
15.1 Experimental Data	15-1
15.2 Discussion	15-2
15.3 Initiation Mechanism	15-5
15.4 Conclusion	15-7
16. CONCLUSIONS	16-1
17. RECOMMENDATION	17-1
17.1 Initiation Characterization and Prevention Concept Formulation	17-1
17.1.1 Equipment Development	17-2
17.1.2 Supporting Studies	17-3
17.1.3 Response Equation Validation	17-3
17.1.4 Explosive Parametric Study	17-3
17.2 Implementation of Prevention Measures	17-4
APPENDIX A	A-1
APPENDIX B	B-1
APPENDIX C	C-1
APPENDIX D	D-1
DISTRIBUTION LIST	DL-1

LIST OF ILLUSTRATIONS

<u>Figure</u>		<u>Page</u>
5.1	Characterization of a 50 pound Aluminum Bleed-out from 18 Inches into 6 Inches of Water	5-2
5.2	Typical Generalized Temperature Near the Bottom (About 1/4 inch) of the Quench Tank	5-5
5.3	Water Temperature Profile and Heat Flux Versus Time For Molten Aluminum Stream Flowing Through Water	5-7
5.4	Position of Initial Aluminum Temperature from Water Interface Versus Time (One Dimension Heat Transfer Initial Water Temperature 40°C)	5-8
5.5	Quenching Curve (Norm Cochran's Data, Alcoa) Reported	5-10
5.6	Aluminum Temperature Versus Quench Time	5-12
5.7	Heat Flux Versus Time to Heat Water to Limit of Superheat for Three Cavity Depths	5-13
5.8	Aluminum Surface Profile Characterization (Ideal) as a Function of Air Drop Distance	5-17
5.9	Cavity Volume Versus Air Drop Distance	5-18
5.10	Time for Flow Field and Surface Cavity Formation Versus Air Drop Distance with Time Aluminum in Water at Four Depths	5-20
5.11	Shock Pressure Versus Molten Aluminum Impact Speed	5-21
5.12	Idealized Initial Aluminum Over the Bottom of a 12 inch Square Quench Tank	5-23
5.13	Height and Surface Area Versus Initial Flow Radius of Molten ALuminum on Quench Tank Bottom Surface	5-26
6.1	Schematic of Trigger Mechanism	6-3
6.2	Molten Aluminum-Water Interaction Events	
9.1	Plan View of Melt/Detonation Facility at Burning Area Unit Y-8, Kingsbury Ordnance Plant	9-3
9.2	Base Line Configuration, Molten Aluminum Water Explosion, Initiation Study	9-5
10.1	Ignition Energy Versus Aluminum-Water Ratio	10-6
10.2	Bubble Destabilizing Voltage Versus Water Vapor Temperature	10-9

IIT RESEARCH INSTITUTE

LIST OF ILLUSTRATIONS (Concl)

<u>Figure</u>		<u>Page</u>
11.1	Test Number 41: 1/2 pound; 3/8 inch diameter 1600°F aluminum stream dropped 18 inches into 2 inches of distilled and boiled water	11-5
11.2	Test No. 43: 1/2 pound, 3/8 inch diameter 1600°F aluminum stream dropped 18 inches into 2 inches of tap water with 1 percent liquid soap added	11-6
11.3	Test No. 31: 1/2 pound, 3/8 inch diameter 1600°F aluminum stream dropped 18 inches into 21 inches of distilled water with 2 percent aluminum sulphate added	11-7
11.4	Test No. 32: 1/2 pound, 3/8 inch diameter 1600°F aluminum stream dropped 18 inches into 2 inches of distilled water with 2 percent sodium bicarbonate added	11-8
13.1	Flow Profile on Quench Tank Side Walls (Schematic)	13-5
13.2	Approximate Tangential Flow Impact Condition	13-6

LIST OF TABLES

<u>Table</u>		<u>Page</u>
4.1	Molten Aluminum-Water Reaction Parameters	4-2
5.1	Molten Aluminum Stream Breakup Time	5-15
9.1	Gross Experiment Data Summary	9-8
10.1	Number of Tests without Additives	10-4
10.2	Number of Tests with Additives	10-4
11.1	Small Scale Bleed-out Simulation Experimental Variables	11-1
11.2	One Half Pound Three Eights inch Diameter Bleed-out Simulations (April through June, 1974)	11-3

1. INTRODUCTION

The Aluminum Industry has been cognizant of the potential serious problems which can arise when molten aluminum and water accidentally come in contact during handling and processing operations. Documented case histories covering all types of molten metal-water accidents during the period of 1944 through 1971, included 59 incidents of which 55 were catastrophic or violent. Since 1967, when the Aluminum Association started gathering data on accidents, 33 incidents of varying degree have been reported. Considerable effort has been expended by the Aluminum Industry in the investigation of this problem and preventive measures have been established based upon simulation experiments.

The initiation mechanism for molten aluminum-water explosions has eluded definition even though the prevention measures employed appear to be effective. The effort expended in defining these measures has been largely directed toward the engineering aspects of the safety problem. As a result of these factors, a margin of safety can not be assigned, with any degree of confidence, to the safety measures being practiced. This situation provides the basis for establishing the objectives of the program.

1.1 Program Objectives

The overall objective of the program was to establish personnel safety in all expected molten aluminum-water encounters. This objective was to be achieved by systematically defining and characterizing the mechanisms which comprise initiation of molten aluminum-water explosions. The procedures was to establish the parameters of initiation so that preventive measures may be identified and then evaluated for their effectiveness in preventing explosions.

1.2 Program Scope

The scope of work includes three phases:

- Phase I - Explosion Initiation Mechanism Study.
- Phase II - Explosive Initiation Characterization and Preventive Measures Formulation.

- Phase III - Preventive Measures Implementation

The basic nature of this work requires the combination of experimental, diagnostic and analytical efforts. The analytical effort was oriented toward explaining the initiation phenomena and establishing experimental designs.

Phase I, Explosion Initiation Mechanism Study, was the only effort funded and was to identify and define initiation mechanisms which govern the onset of molten aluminum-water explosions. The following specific tasks have been included in the scope of work:

- Gross Characterization of Initiation
- Initiation Mechanism Isolation
- Refined Initiation Study
- Program Review Meetings, Bimonthly Progress Reports and Phase I Final Report

1.3 Plan of Attack

In essence, the program was planned to proceed along three basic parallel efforts initially:

- bleed-out simulations made with 50 pounds of molten aluminum
- chemistry studies to assess this aspect of initiation
- mechanical, thermodynamic and other potential initiation mechanism studies

Simulations conducted in prior research efforts had been unsuccessful in obtaining high speed photographs of an initiation. The initial simulations were planned with the expectation that framing rates used previously, 1000 to 5000 pictures per second (pps), were too low and that rates of 40,000 pps would be sufficient to provide photographic evidence. This data was expected to provide direction for the selection and application of more sophisticated or innovative instrumentation.

Background studies performed during the process of defining this program lead IITRI staff to believe that the explosions could encompass chemical chain reactions. IITRI prior experience

included analogous situations in which chain reactions were broken by the use of small amounts of "poison". Pursuit of this aspect of molten aluminum-water explosion constituted the second major parallel effort. This effort was planned to be started by performing matrix isolation studies which would identify potential chemical species in a chain reaction (if present).

The study of mechanical, thermodynamic and other mechanisms to establish their potential for initiation was to be carried out in parallel with the two above studies. The results of these three separate studies were planned to provide specific guidance and direction for the balance of the program. The photographic evidence would either provide new directions for defining mechanisms or confirm the indications provided by the other studies.

The most promising mechanisms identified by the combined results of the initial three studies would be evaluated using 50 pound simulations, small scale laboratory experiments and further analysis. This second major effort of the program was planned to lead to a study which would refine the most promising initiation mechanism(s).

1.4 Revised Plan

Unfortunately, the high speed films of the explosions (40,000 pps) were not fast enough to provide data on the reactions and the matrix isolation studies did not identify chemical species which could be attributed to a chain reaction. The other initiation mechanism isolation studies did indicate the possibility that a significant electrostatic charge could be developed and its discharge could constitute an initiation mechanism or make a significant contribution to the initiation. This mechanism was studied by means of 50 pound simulations and laboratory experiments.

Because of the lack of specific information obtained in the initial part of the program, the plan was revised and small scale simulations were made to provide additional insight to the phenomena. In addition, an intensive review of the literature

and information made available by the Aluminum Associate Task Group for Molten Aluminum-Water Explosions was performed again. These three activities:

- electrostatic charge study;
- small scale study;
- literature review and analysis,

lead to the final task, Refined Initiation Study, which culminated in a series of experiments.

1.5 Program Emphasis

There are two commercial operations which encompass the majority of accidental molten aluminum and water encounters:

- Direct Chill (DC) Operations
- Furnace Charging

The major thrust of the program has been the study of initiation mechanisms in DC operations. This has been acknowledged in the program review meetings and the bi-monthly progress reports. Significantly, DC operations require water, where as furnace charging does not.

Furnace charging safety operational procedures establish that charged material should be free of water. The scope of the program, in regard to furnace charging, was to assess the research performed to identify information and initiation mechanisms involved in DC operations for their applicability to furnace charging operations. Section 15 addresses this aspect of the scope.

2. SUMMARY AND RECOMMENDATIONS

The program proceeded as it was originally proposed for the initial seven months. The activities performed had not provided the expected definition of initiation mechanisms and the program plan was revised. Emphasis was shifted from 50 pound simulations, balanced with chemistry studies, to a series of investigative studies including small scale simulations. These studies were viewed as probing for basic data which would enhance initiation mechanism isolation/definition. The program, as performed encompassed seven major activities:

- Literature Survey
- Chemistry Studies
- Gross Experiments (50 pound field simulation)
- Electrostatic Studies
- Small Scale Experiments
- Initiation Mode Definition
- Experimental Investigation of Most Probable Initiation Mechanism

2.1 Most Probable Initiation Mechanism

The most probable molten aluminum-water explosion initiation mechanism taking place in direction chill (DC) operations is spontaneous nucleation (vapor explosion) of liquid quench water. This initiation mechanism is most frequently triggered by an impact generated shock which collapses the vapor film between the liquid aluminum and liquid water. The shock is produced by molten aluminum flow on or at the quench pit surfaces. The liquid water is contained in capillaries in the quench pit surfaces.

This initiation mechanism definition is based upon logic and limited experimental data. The limits on the conditions under which this mechanism will be operative are not well defined or are the parameters bounded. The mechanism satisfies the majority of the data and information available and no other mechanisms has been identified which meets these criteria as well. The major flaw in the initiation mechanism is the trigger and is related to

the time frame in which an aluminum flow impact shock can be predicted. This time frame covers the period from the start of a bleed-out or simulation to the time when the entire bottom surface of the casting pit or quench tank is completely covered with molten aluminum. It is possible that flow conditions thereafter could result in an impact shock, but this is considered not to be readily predicted and therefore a random event. Limited simulation data indicates that explosions have taken place after the time period in which an impact shock can be predicted.

2.2 Recommendations

It is recommended that additional work be performed to resolve the time frame limits which are assumed to operate on the impact shock trigger mechanism in the initiation mechanism identified. In addition, the operational parameters which bound the occurrence of the vapor explosion and the forcing function required to obtain liquid-liquid contact to produce the initiation should be defined. The definition of the forcing function requirements should provide a sound method for assessing the potential of an impact shock to trigger the vapor explosion and make it possible to examine other potential trigger mechanisms inherent in the overall interaction. This effort should include evaluation of the impact shock strength and dissipation characteristics to complete the assessment of the trigger mechanism.

Coupled with the above work is the need for equipment design and development. Better control of the simulated bleed-out stream geometry and aluminum temperature are required. More reliable and economic sensors are needed to describe the aluminum flow on/in the quench tank. Equipment needs to be designed and experiments conducted to: characterize the impact shock wave potential for collapsing vapor films; and investigate initiations which occur at "late" times to identify trigger mechanisms.

3. PROGRAM ACCOMPLISHMENTS

An extensive literature survey was performed during the program. The documents are listed to Appendix A and encompasses 315 references divided into 11 categories. This activity was very important in establishing: background, potential initiation mechanisms, pertinent experimental data and initiation parameters.

3.1 Facilities

Three facilities were constructed during the program. The major facility was that for performing the gross experiments, 50 pound bleed-out simulations. The physical modification cost was absorbed by IITRI. In addition to this facility, a small-scale physics facility was assembled which had a weight limit of 1 pound. It was used to perform 1/2 pound bleed-out simulations and multiple flash x-rays and a fastex camera constituted the instrumentation. Equipment capability was designed, assembled and employed to: detect and measure; and simulate electrostatic charge phenomena. This equipment was used in bleed-out simulations and laboratory investigations.

3.2 Chemistry Studies

These activities encompassed matrix isolation and active site investigations. No significant species were detected in the isolation study which participate in initiation reactions. This work is summarized and presented as Appendix B. The active site work was not pursued far enough to demonstrate potential for consideration in the initiation reaction. Based upon the overall results of the chemistry studies, it was concluded highly unlikely that chemical reactions are a primary factor in initiation.

3.3 Gross Experiments (50 pound simulations)

Fifteen gross experiments were performed: to develop photographic data on initiations and explosions; and in support of electrostatic charge studies. IITRI purchased a 44,000 pps hycam camera for this work. It was established that the reactions could not be photographed at this framing rate, e.g., it took place in

less than 25 microseconds. Despite the use of glass quench tanks, the important events in initiation were not visible or occurred too fast to be photographed.

3.4 Electrostatic Studies

These studies were performed in three stages: analytical, simulation experiments and laboratory micro-scale experiments. The analysis established that there was a significant potential for electrostatic charge development. The simulation experiments demonstrated that a significant electrostatic charge was developed and the laboratory experiments established energy thresholds for electrical initiation of aluminum and water reactions. It was concluded that the electrostatic charge phenomena was not a primary factor in the initiation mechanism but could have an effect such as reducing the surface tension of the water and thereby reducing the stability of the film in film boiling.

3.5 Small Scale Experiments

This study complimented the large scale bleed-out simulations by showing details of the interaction between molten aluminum and water. Of particular importance was the demonstration that various initiation mechanism postulated in the literature were not applicable. In particular, the following mechanisms were eliminated from serious consideration: bubble collapse, encapsulation, violent boiling, shell theory, and the Webber Number Effect. The experiments illuminated the following aspects of the interaction between molten aluminum and water: stream breakup, stream size in relation to quench tank size, and the volume of steam produced in relationship to the aluminum stream size. The effect of additives to the water and the temperature of water were investigated.

3.6 Initiation Mode Definition

This effort corresponds to the "Refined Initiative Study" which was embarked upon after the initial program activities did not converge to provide specific data which would identify realistic initiation mechanisms. A comprehensive review of the pertinent portions of the acquired literature was performed against the background of the work accomplished in the program. Realistic

pertinent portions of the acquired literature was performed against the background of the work accomplished in the program. Realistic parameters and their relationship to initiation were established. An additional candidate initiation mechanism was formulated and an analytical evaluation of initiation mechanisms made. These activities resulted in postulating the most probable initiation mechanism, the vapor explosion.

3.7 Experimental Investigation of the Most Probable Initiation Mechanisms

A series of 6 experiments were planned to obtain data for substantiating the vapor explosion as the most probable initiation mechanism. The evaluation focused on quench tank surface conditions (rough and smooth) and a determination of temperature profiles and aluminum flow parameters. A new drop crucible, with external sealing, was designed and fabricated for use in the experiments. Analysis was performed to establish interaction parameters and to specify the instrumentation. The new drop crucible did not function properly, so that the conventional equipment which was used in the gross experiments was substituted. Seven data points were obtained and one of them was a mild steam explosion. The experiments are presented in Appendix C. It was concluded that a vapor explosion triggered by an impact shock, produced by aluminum flow, is the most probable initiation mechanism. It was demonstrated that the most likely source of liquid water, which is spontaneously nucleated, is in the capillaries in rough quench tank surfaces.

4. MOLTEN ALUMINUM-WATER REACTION PARAMETERS

4.1 Reaction Parameters

A compilation of operational and environmental parameters has been made based upon industrial experience in direct chill (DC) aluminum process and experimental simulation of DC "bleed-outs". The parameters are largely based upon: Alcoa reports: No. 2-50-33 (known as Long's work), No. 7-68-BE21 and supplement (Brondyke and Hess); Reynolds Report dated 8 June 1961 (Raschke); IITRI and Battelle programs on Molten Aluminum-Water Explosions; and information provided by members of the Aluminum Association Task Group for Molten Metal Explosions. Table 4.1 summarizes the reaction parameters.

4.2 Reaction Parameter Discussion

4.2.1 Aluminum Parameters

The stream diameter (at a given initial temperature) clearly plays three important roles in the overall reaction characterizing: the heat sink, rate of heat added and rate of aluminum added. In addition, there are two other potential factors which may be important. The diameter corresponds to an area on the impact surface which has elevated pressure (static and dynamic head) and an optimum path for conducting a shock pulse from the initiation site to the bulk mixture of aluminum and water. In the latter case, the sonic shock will travel faster through liquid aluminum than through the mixture and the shock energy will be dissipated less. The higher pressure which could exist between the impact surface and flow may be important in the development of a pressure sensitive chemical reaction and/or in the control of a vapor explosion. In relation to a vapor explosion, the loss of the aluminum head over heated water could reduce the pressure to "induce" superheated water. There is a strong dependence on the combined conditions of stream diameter and drop height. Three-eighths inch diameter streams dropped from five inches to 28-1/2 inches (not limiting values) breakup into segments. Aluminum streams 3-1/4 inches

TABLE 4.1

MOLTEN ALUMINUM-WATER REACTION PARAMETERS

Parameter	Value	Reaction
● Aluminum		
- Stream diameter, D, inches	$D > 2.75$	Yes
	$D \leq 2.50$	No
- Temperature, T, °F	$T > 1382$	Yes
	$T = 1238$	No/Yes ¹
- Weight, W, pounds	$w \geq 10$ ²	Yes
● Water		
- Depth, d, inches	$0 \leq d \leq 10$ ³	Yes
- Temperature, T, °F	$T \leq 130$	Yes
	$T \geq 140$	No
- Additives	Soluable oil, wetting agents (0.01%)	No
	NaCl @ 15% @ 172°F	Yes
- Chemistry (Natural)	No data available	-
● Impact Surface		
- Material	Concrete & Steel ⁴	Yes
	Glass, Aluminum (535) & Stainless Steel (302)	No
- Surface Finish	Rough	Yes
	Smooth	No
- Coating	None	Yes
	Tarset, paint, oil, Grease, etc.	No
	Lime, gypsum, rust, aluminum and calcium hydroxide	Yes
	Lime over painted steel	Yes
- Coating Thickness	Not important	No

¹ At 1238°F and an 18 inch drop, there is no reaction with 10 inches of water and with 8 inches there is one.

² Reactions have been obtained with 10 pounds of aluminum. Data is not available on lesser weights, e.g., they were not made under conditions that would otherwise have produced a reaction.

³ Reactions have been obtained in simulation experiments with as little as 3 inches of water. It is reported, verbally, that aluminum dropped on "damp" concrete "pops".

⁴ Steel surfaces specially prepared (by furnace conditioning).

TABLE 4,1 (Concl)

Parameter	Value	Reaction
(Impact Surface Continued)		
- Taret Coating	6 inch square	1 of 2
- bare spots	4 inch square	2 of 2
	2 inch square	0 of 5
- Orientation	Horizontal, vertical	Yes
- Presents of objects	Aluminum kelp, steel balls, iron oxide	Yes
● Drop Distance		
- Air, H, inches	$8 \underline{1} \leq H \leq 42$	Yes
- Air/water, inches	8/10; 14/4; 15/3; 36/6; 42/6;	Yes
	8/10(1238°F); 12/20; 22/20; 90/30; 100/20; 108/12; 112/8; 114/6; 116/4; 117/3; 118.5/1.5 <u>2</u>	No
● Flow Divider	1/8 inch by 1 inch mild steel bars forming 1 inch square openings	No
● Quench tank Crossec-tional area, A, square inches	$42 < A < 576$ $A \geq 230 \underline{4}$	Yes Mild
● Explosive Reaction Time		
- Instantaneously, Microseconds	5 to 1000 (1 msec)	?
- Normal, milliseconds	1 to 1000 (1 sec) <u>3</u>	Yes

1 Eight inches is the lowest drop distance used under conditions that would have otherwise produced a reaction.

2 Drop heights, the sum of the air and water distance, equal to 120 feet representing the conditions in which the 3-1/4 inch diameter aluminum stream broke up into segments.

3 Long reports reactions taking place after 15 seconds from the start of aluminum flow.

in diameter breakup into segments when dropped 120 inches, while they do not when dropped from 18 inches. The heat sink characteristics of a stream segment will be much different than an integral stream (it will cool faster).

The initial temperature of the molten aluminum (of a stream of a given diameter) also plays an obvious significant role in the reaction. It determines the: potential thermal energy which can be transferred to the water; the magnitude of the time until the phase change (solid at 1220°F) can occur; and the initial "position" on the quenching boiling curve (which also depends upon the water temperature and flow speed) which relates to the heat flux time characteristics. The degree of cooling, when the flow reaches a surface (which also depends upon the water depth and cooling time history), also depends upon the initial temperature.

The weight of aluminum, beside being related to the total potential for heat energy, may enter the reaction in terms of the amount of aluminum that has been added to the water, and mixed with it, before an explosion. This weight depends upon a number of other parameters, but is limited by the time from the start of flow to the reaction. The initial weight (really the head) under a specific set of "drop" conditions or the amount of aluminum above the site of a billet bleed-out, will determine the initial efflux speed of the flow. The flow speed time curve (a function of the head remaining) and the maximum time which the flow can persist will be determined by this weight.

4.2.2 Water Parameters

The quenching water may enter the reaction as a coolant, a working fluid (for mechanical explosion), as an oxidizer and hence as a source for hydrogen (chemical reaction). The water temperature and chemistry (including additives) have a pronounced effect on the rate of heat transferred from the aluminum (to the water).

Additives which stabilize film boiling, e.g., hold off transition and nucleate boiling which transfers heat much faster, effect the occurrence of a reaction. High water temperature (140°F and over) acts the same way. The opposite is also true, additives which promote transition and nucleate boiling (and low water temperature, below 130°F) enhance reactions. Water depth, for a given drop height corresponds to an initial quench time for cooling the stream leading edge (until it impacts a surface). This can apparently be a crucial factor, for in the case of 1238°F aluminum dropped 18 inches, a reaction will occur when the depth is six inches but not when it is ten inches. These factors effect the vapor film thickness as well as its stability. The depth also establishes the local pressure (head of water).

The United Kingdom is conducting a program, "Explosive Risk in Continuous Casting", at the University of Aston in Birmingham, Departments of Chemistry and Metallurgy. In their research progress report for January through May, 1974, some effects of water additives on water surface tension, the boiling process and heat flux are discussed. It was noted that cationic and anionic surfactants, which both elevate the temperature limit of molten tin-water fragmentations, have opposite effects on water surface tension. Work was cited which indicates that reduced water vapor surface tension changes the nature of the boiling process. In addition, these surfactants decreased the heat flux even though the reaction temperature limit was elevated. It was concluded that the increase in the threshold temperature is not necessarily caused by the effect of additives on heat transfer but by the effect on the boiling mechanism and extent of liquid-liquid interaction.

4.2.3 Impact Surface Parameters

The impact surface appears to have the potential for entering the reaction in several different aspects. Aside from the contribution of the surface to initiation, restraint is provided by the impact surface for initiation, the impact surface and adjacent "bounding" surfaces promote mixing molten aluminum and water, and

provide the means for building up a mass of material to accept initiation energy and become the reactants in the major portion of the interaction. In addition, as indicated in 4.2.1, the surface may act as a boundary which permits the development of a pressure greater than that established by the head of water. Other potential attributes of the surface are its: chemical and thermal properties, roughness and cavities for water entrapment.

Surface coatings which prevent reactions would tend to modify these attributes. It is interesting to compare the areas corresponding to the stream diameters which represent "go" and "no-go" conditions and the basic area-reaction data for tarset. The "no-go" diameter of 2-1/2 inches corresponds to 4.9 square inches, the "go" diameter of 2-3/4 inches corresponds to 5.9 square inches, and the 3-1/4 inch diameter which provides reactions two out of three times is 8.3 square inches. As indicated in Table 4.1, a six square inch bare area causes one reaction out of two tries, not quite as many as the 3-1/4 inch diameter stream, and possibly on the order of what would be expected for a 2-3/4 inch diameter stream. The two out of two reactions obtained with a four square inch bare area, the number of trials were quite low and it is difficult to assess any correlation. More clearly, the five trials with two square inch bare area produced no reactions. Since the area is over 50 percent less than the 2-1/2 inch diameter stream, it would seem reasonable to postulate a correlation between these results and indicate the importance of direct surface contact area.

4.2.4 Drop Distance Parameters

The drop distance parameters may be viewed in two ways: the distance dropped through air, corresponding to the major acceleration period and the ratio of air drop distance to water depth, which is related to the time the aluminum leading edge is cooled before surface impact. This is also the quenching period for all of the molten metal. It appears that if the quenching process reduces the aluminum surface temperature to a value which provides a stable or thick vapor film, no reaction will take place.

4.2.5 Flow Dividers

Flow dividers were used by Long in 13 experiments, with water depths varying from two inches to ten inches, no reactions were produced. It is reasonable to assume that the divider produced approximately one square inch streams (equivalent diameter is about 1-1/8 inch) which were cooled too much to produce a reaction. The effect corresponds to too small a diameter stream and too stable or too thick vapor films.

4.2.6 Quench Tank Crossectional Area

Long investigated the effect of container size which really was an examination of the effect of the crossectional area. Little difference was noted with 6-1/2, 12 and 24 inch square crossections. However, under similar conditions a 48 inch square crossection appeared to make the reaction milder. This then would seem to be related to coupling the initiation energy to the bulk mixture of aluminum and water. The depth of the mixture at any given time would be less with the larger crossectional area container which could be expected to have a different interaction with a bottom central surface initiation. For the same initiation pulse, the greater the depth of the reactants, the greater would be the energy coupling and hence the more vigorous the final reaction. In addition, side wall impact generated shocks which could collapse vapor films separating the aluminum and liquid water in surface cavities would have their energy dissipated to a greater degree.

4.2.7 Reaction Time Parameter

The time for a reaction to take place, after the start of a simulated bleed-out, has been reported by Long¹ as "The explosion may occur any time after the start of the metal pour and up to 15 seconds ...". Data has been obtained from 18 experiments, six from Battelle, eight from IITRI and four from Alcoa, which used

¹ Alcoa Report No. 2-49-23, page 8.

aluminum at temperatures from 1470°F through 1930°F. These experiments covered a time range of 0.20 second through 0.82 second. The aluminum temperature did not seem to have a significant effect. The median time was 0.30 second, the average 0.34 second and 11 times were between 0.25 and 0.34 second. An 18 inch drop, including six inches of water, requires about 0.16 second for the initial aluminum to reach the impact surface. Thus the average reaction time, after surface contact, is on the order of 0.18 second and the mean about 0.14 second.

Long indicated that the most violent reactions came in the shorter times whereas the more recent Alcoa work indicated that the reaction which came at 0.82 second was the worst they had (in comparison to 0.20 to 0.25 second). It is reasonable to assume that Long meant "short" to be on the order of two seconds or less, as compared to 15 seconds. Fifty pounds of aluminum dropped 18 inches, or there about, will all be in the quench tank within about two seconds. Thus the dynamics of the pour will have been completed "early" in relation to 15 seconds and it could be inferred that any reaction which takes place after the pour, and hence "bleed-out", is over will be less severe than those which take place before. This may mean that the "initiation" did not take place in sufficient strength to significantly increase the heat transfer rate or initiate a subsequent chemical reaction.

The point of this discussion is to establish the possibility that there may be a finite time period in which a serious reaction can take place. This does seem plausible based upon the above discussion and even more so if it is assumed that the initiation is directly related to a surface. The point is pedantic on a nonhorizontal surface which retains no aluminum. As soon as the aluminum flow has stopped, the interaction with the surface will be over. The conditions on a horizontal surface, or one which retains aluminum are different, as the time of interaction goes on, aluminum builds up over the surface until the flow is over. Thereafter the conditions providing the maximum potential for an

initiation should have been reached. Whatever the initiation mechanisms may be, the likelihood of an initiation should go down at some point in time after the flow has stopped. As an example, if the initiation mechanism is a superheated water vapor explosion, after some point in time the vapor explosion will take place and initiation a reaction or all the water which could potentially spontaneous nucleate will have been vaporized. Later on, the aluminum will cool so that the potential for superheating is diminished and finally no longer exists.

5. TYPICAL MOLTEN ALUMINUM-WATER INTERACTION CHARACTERISTICS

The bleed-out of molten aluminum encompasses multiple physical processes and potentially multiple chemical reactions. An understanding of the interactions taking place is important in establishing initiation mechanisms. An evaluation of the interaction in terms of the reaction parameters is an important step in establishing potential initiation mechanisms. The available information on bleed-out simulation experiments (made with 50 pounds of metal) indicates that a 3-1/4 inch diameter stream of 1400°F molten aluminum dropped 18 inches, with the last six inches being water 50 to 80°F, (impacting a bare rough steel surface) will produce a reaction two out of three times from a sample of about 50. Thus, it appears reasonable that the establishment of "nominal" conditions involved in this type of experiment should illustrate potential initiation mechanisms.

Analysis has been performed to aid in characterizing the normal or average conditions which may be expected. This material is presented and establishes background for evaluation of potential initiation mechanisms. While it is certainly possible that there is no one "initiation mechanism," it will be significant if one most probable or one "most likely" to take place can be established.

5.1 Overall

Figure 5.1 characterizes some broad aspects of the "typical" interaction leading to an explosion. As indicated at the start of the bleed-out simulation, the efflux speed of the molten aluminum, at the opening of the drop crucible, depends upon the head of aluminum. As the flow continues, the head decreases, proportionately to the opening area and crucible internal cross-section, until all the metal is discharged. The efflux speed reduces proportionally to the head until the speed is zero. In the typical simulation, illustrated in Figure 5.1, the initial speed is about 82 ips and the emptying time is on the order of 1 second.

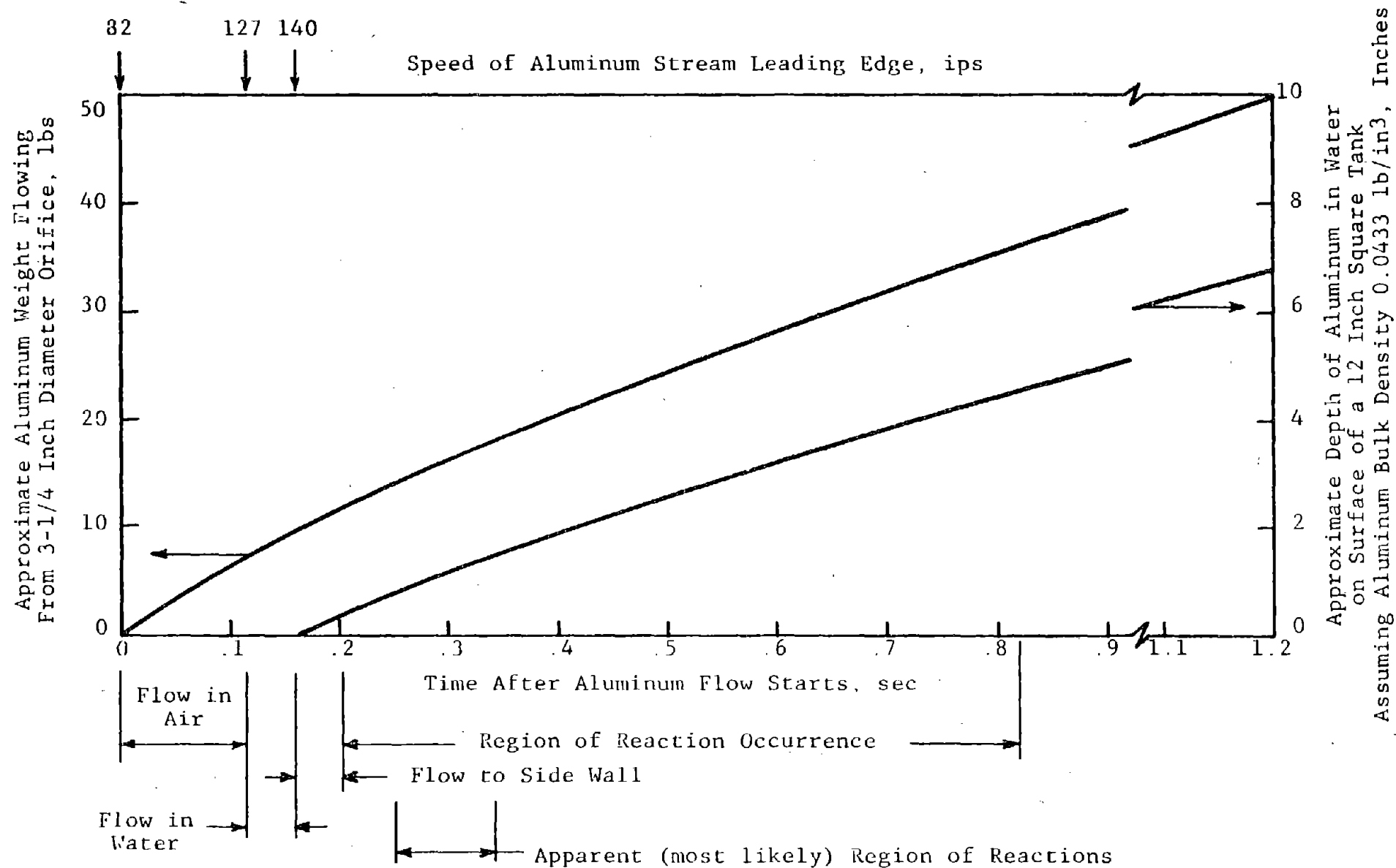


Figure 5.1 Characterization of a 50 Pound Aluminum Bleed-Out From 18 Inches into 6 Inches of Water

The leading edge of the molten stream will accelerate (due to gravity and assuming no drag) to about 127 ips in about .115 seconds during its fall through 12 inches in air to the surface of the water. Thereafter the stream, ideally, will accelerate only to 140 ips because of the water drag and impact with the bottom will occur at about 0.16 second. If this flow speed is not reduced by drag on the impact surface or accelerated by the stagnation pressure existing at the impact point, aluminum will reach a quench tank wall at about 0.20 second.

Soon after the first metal reaches the interior wall surfaces, build up on the bottom will develop. The approximate depth of aluminum in water has been noted in Figure 5.1 to indicate the time relationship. It is assumed that the aluminum density on the bottom surface is half of its nominal liquid density. As indicated in the figure, many of the reactions obtained in simulations take place when this layer is on the order of one to two inches thick. The most violent reaction reported (by Alcoa), for which time was recorded, took place when the aluminum-water mixture was on the order of five inches thick.

In the final experiments made, reported in Appendix C, this build up of aluminum in the quench tank did not take place. When the flow over the bottom surface reached the side walls (of the circular tank) it was deflected up the walls. The glass tanks broke before this aluminum could reverse direction and build up on the bottom surface. This type of flow pattern had not been essentially accumulated on the bottom of the quench tank as referred to above.

5.2 Temperature Profiles

Limited thermocouple data was obtained by Alcoa (five tests) and Battelle (three tests) and it appears that an overall generalization of this data may be useful. Data from both organizations generally indicates that the aluminum in the center of the quench

tank (near the initial impact point) suffers a temperature drop on the order of 200°F. Temperatures two or three inches from this point seem to be about the same. At or near the sides of the quench tank the temperature is 300 to 500°F lower. Temperatures at (on/in) the bottom surface near the initial impact point range from the initial water temperature, to within 200°F of the incoming metal temperature. Figure 5.2 illustrates the nominal temperature profile near the bottom surface of the quench tank.

It would appear that the temperature measured at the bottom surface depends upon the thermocouple vertical position (in surface, on surface, just above surface), and the dynamic conditions at the surface. It seems reasonable to envision that the bottom surface is generally blanketed with a steam layer. This steam layer may be collapsed under the dynamics of the interaction so that the thermocouple may measure the metal temperature. If there is no water at the thermocouple to vaporize and the flow does not disturb this condition, the thermocouple will stay in contact with the metal. On the other hand the film thickness between molten metal and liquid water will determine the temperature of the steam layer in contact with the thermocouple. Then the thermocouple may remain in contact with steam. The thermocouple may remain surrounded by water which has a steam layer between it and the metal and sense the liquid water temperature for "quite some time" before "seeing" a temperature rise.

After all of the aluminum has emptied from the crucible a "stagnant" layer of aluminum will cover the quench tank bottom. The variation in the temperature response of the thermocouples should then depend upon the interaction between: the steam layer, the stagnant aluminum layer, the heat transferred from the aluminum overburden and the heat transfer into the bottom surface. Thus, local temperature variations could still exist.

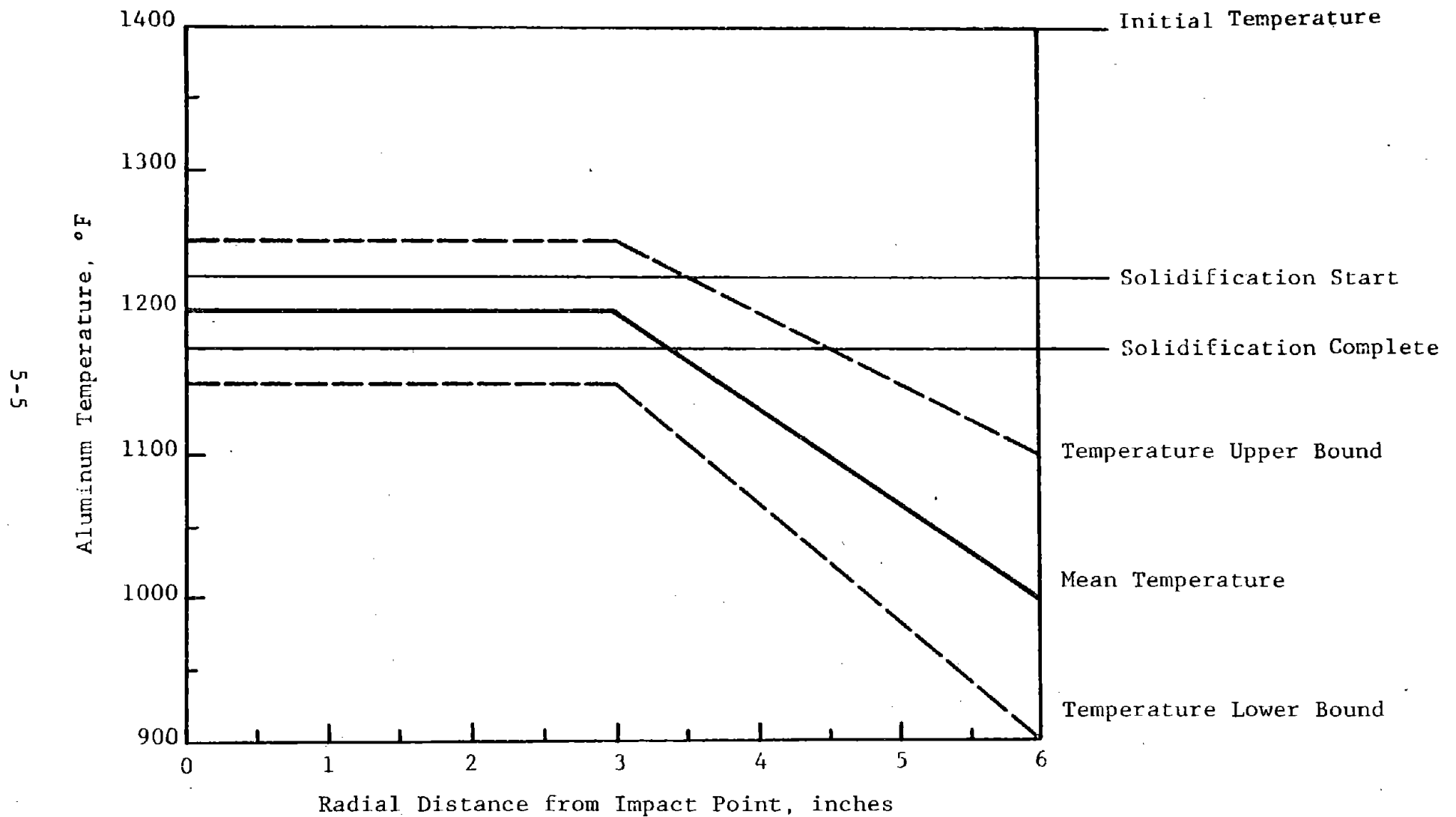


Figure 5.2 Typical Generalized Temperature Near the Bottom (About 1/4 inch) of the Quench Tank

Data obtained at IITRI shows that the aluminum will be liquid during the entire pouring period. Thus one condition for superheating water to its limit is present, molten aluminum. The instantaneous interfacial temperature (IIT) resulting from 1220°F liquid aluminum and liquid water ranges from 1105°F, for 32°F water to 1115°F for 130°F water. The limit of superheat for water is on the order of 512 to 572°F. Therefore, neglecting other influencing factors, liquid-liquid contact between molten aluminum and liquid water should be capable of superheating water to the limit.

5.3 Heat Transfer

Three aspects of the conductive heat transfer are considered in this section. These are: the transfer of heat from aluminum to the quench water during the initial motion to the quench tank surface; typical quenching-boiling data representing the heat transfer potential of the molten aluminum; and heating of water trapped in cavities in the impact surface.

Figure 5.3 presents the temperature profile in water predicted by a one-dimensional infinite cylinder model. The instantaneous temperature which is obtained upon contact between the aluminum and water is 666°C (1230°F). In one millisecond, the steam layer extends 0.002 inch to a temperature of 267°C (approximate limit of superheated water) or to approximately .003 inch to water at the boiling temperature. The unheated water layer is about 0.009 inch from the aluminum. The heat flux going into the water under these conditions (assuming the steam layer properties are the same as liquid water) is 4.5 million Btu/hr-ft². The aluminum should reach the bottom surface in 45 milliseconds, at which time the heat flux is 600,000 Btu/hr-ft² and the distance from the aluminum to unheated water is about 0.060 inch.

The one dimensional model predicts that the aluminum-water interface temperature stays at 666°C and as time passes the location of the initial 750°F aluminum temperature recedes. Figure 5.4 illustrates the position-time relationship for the 750°F

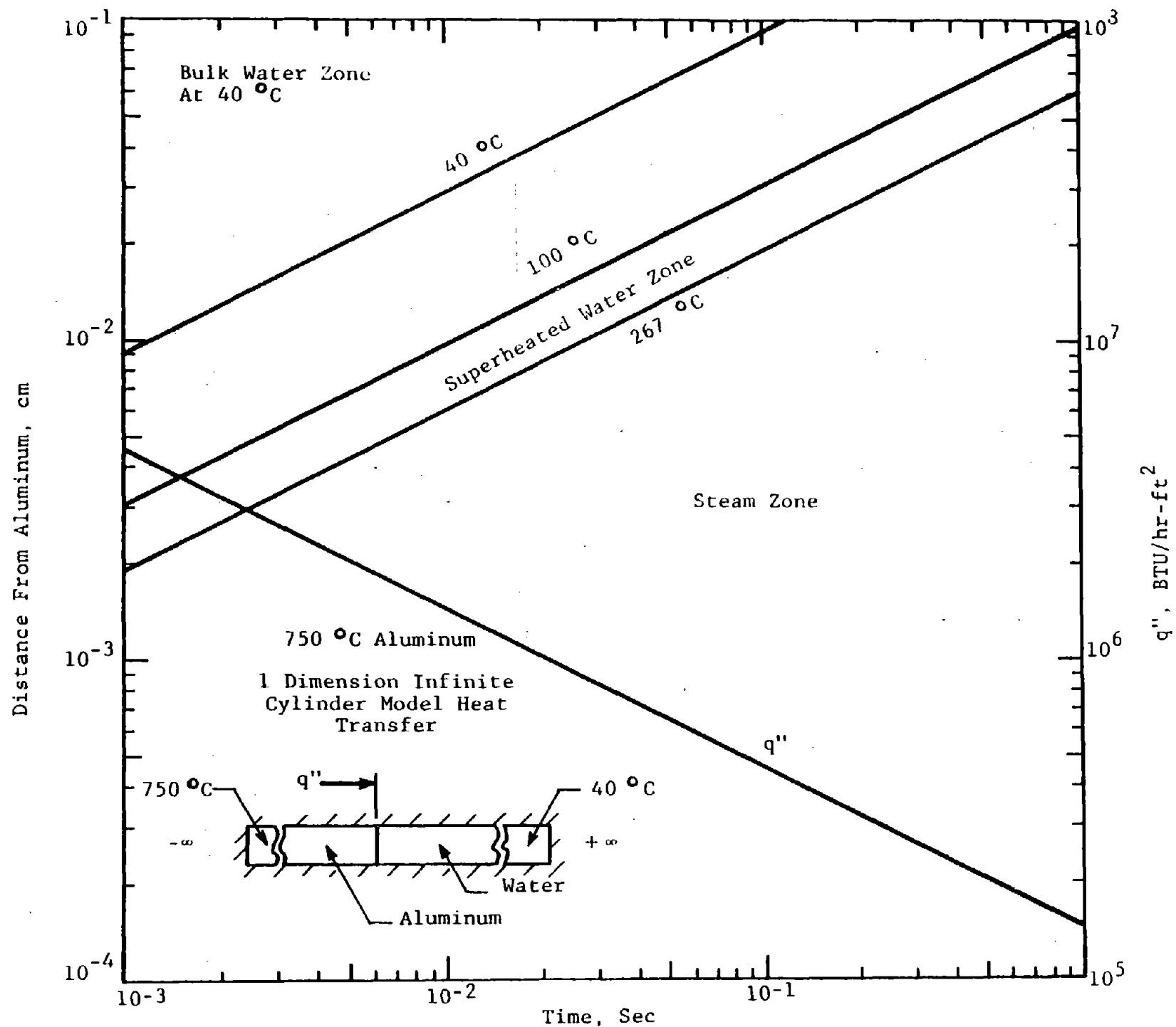


Figure 5.3 Water Temperature Profile and Heat Flux Versus Time for Molten Aluminum Stream Flowing Through Water

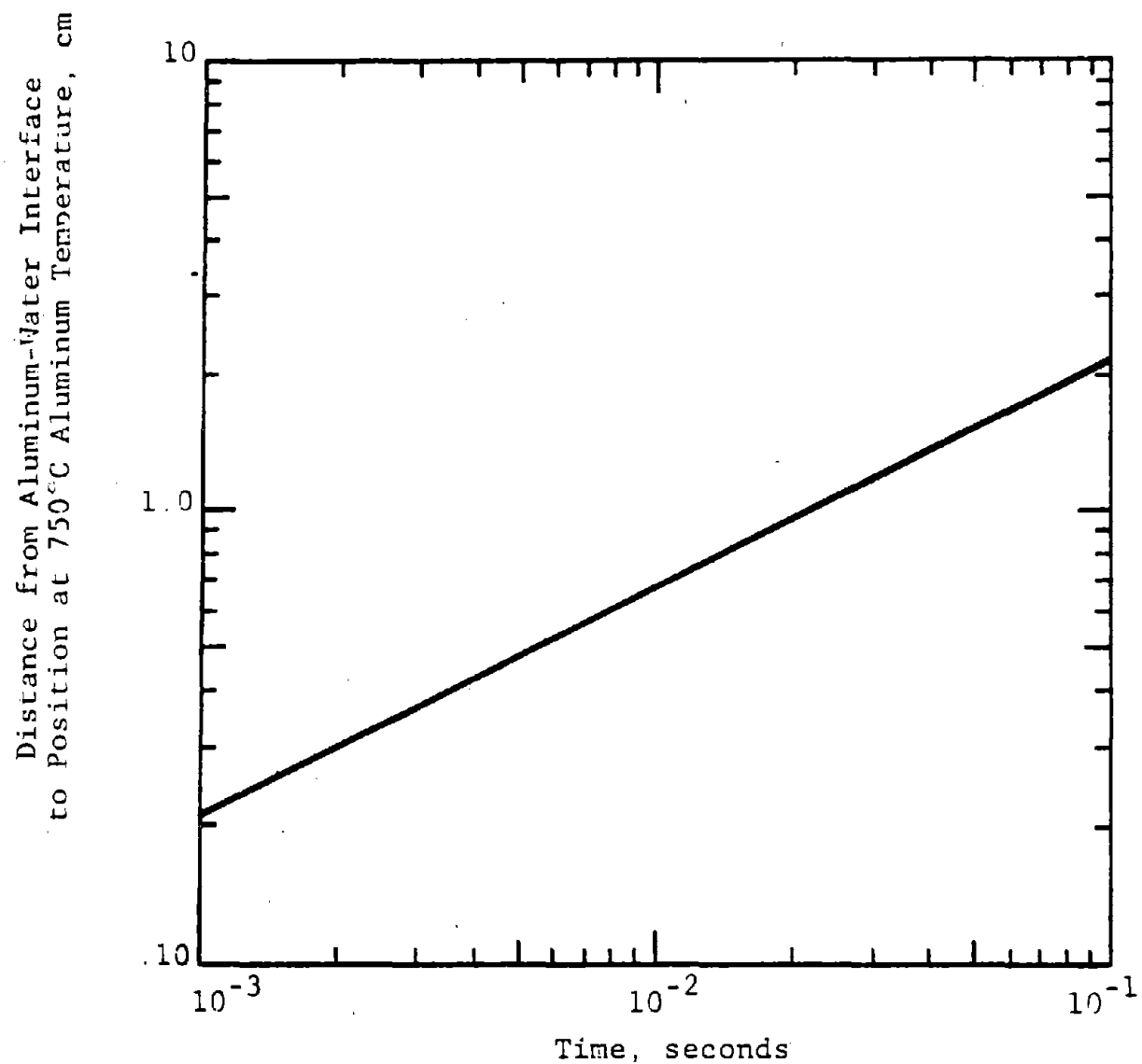


Figure 5.4 Position of Initial Aluminum Temperature from Water Interface Versus Time (One Dimension Heat Transfer Initial Water Temperature 40°C)

aluminum temperature. As shown, the 750°F temperature will be about 1.5 cm (about 0.6 inch) back from the aluminum-water interface at impact (about 0.45 sec). The predicted aluminum surface temperature of 1230°F roughly agrees with the available data reported in Section 5.2. If the initial aluminum temperature had been 1238°F, this model predicts the interface temperature to be about 1100°F which would indicate that the metal had solidified.

Alcoa conducted quenching tests using aluminum heated to just below its melting point. Four sets of data were smoothed, extrapolated and replotted as shown in Figure 5.5. The upper three curves represent conditions under which explosions are obtained and the bottom curve represent a condition in which they are not obtained. From this data, it appears that the heat flux is on the order of 400,000 to 700,000 Btu/hr-ft² at about 1220°F when explosions occur and that when the flux drops below 70,000 Btu/hr-ft², no explosion takes place. Data obtained for water at 140°F and 180°F (when no explosion results) correspond almost exactly to the 140°F water with 1 percent soluble oil flux at 1000°F. The high temperature water appears to have a heat flux of about 40,000 to 50,000 Btu/hr-ft² at 1100°F, whereas the flux from the 140°F water with oil rises to about 100,000 Btu/hr-ft².

The magnitude of the heat flux may not be the significant aspect of the interaction. The stable film boiling temperature and the length of time which it persists may be the significant aspect of the heat transfer in the interaction. In examining the physical conditions necessary for heating water (rather than reducing pressure) to the limit of superheat, liquid liquid contact between molten aluminum and water is required. In the general time frame of the explosion, it is almost certain that these two fluids are separated by a film of steam. In examining Alcoa quench data, although obtained with aluminum just below the melting temperature (about 600°C), it seems to be indicated that film boiling will be the boiling mode (rather than nucleate) at the temperature of molten aluminum.

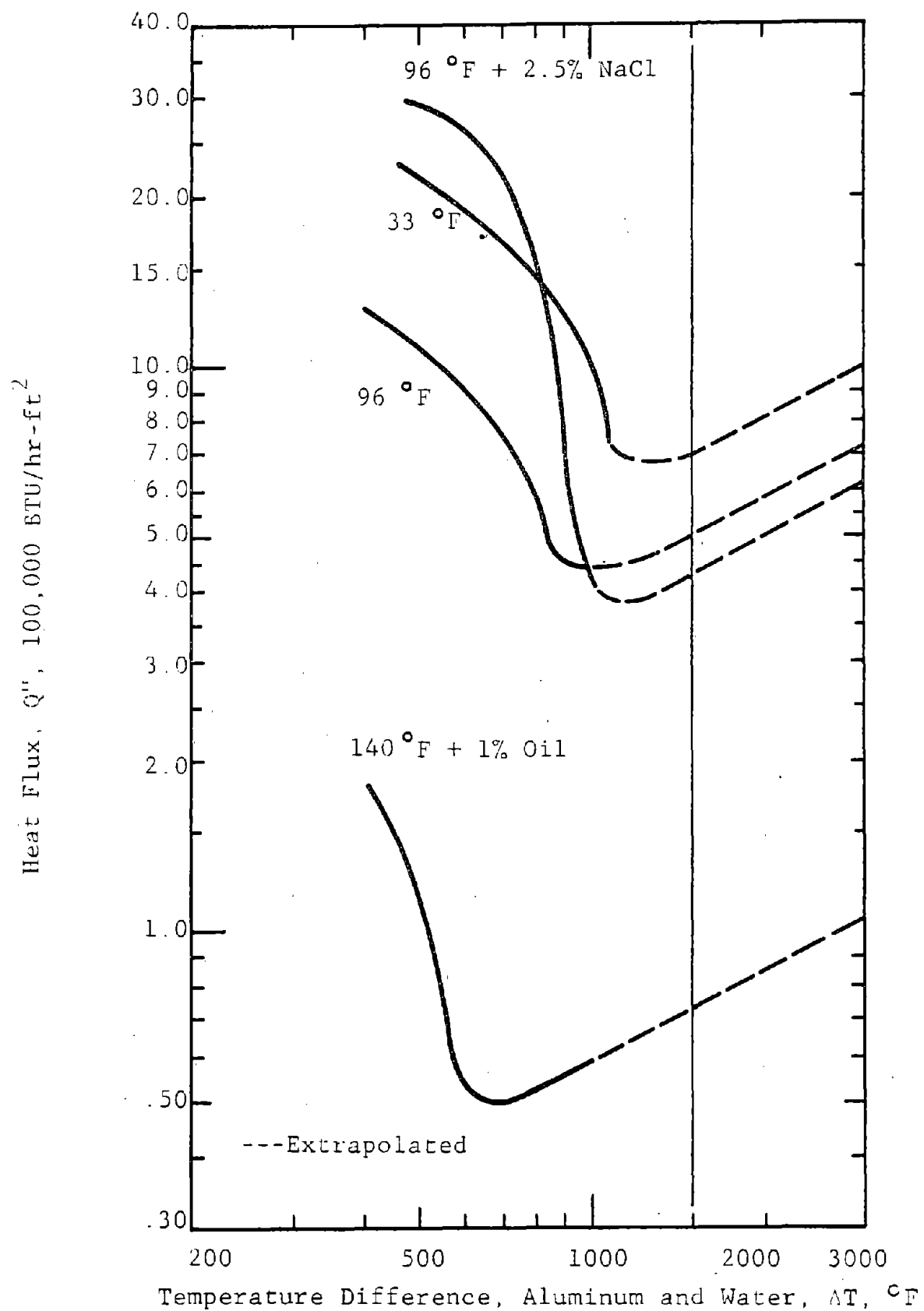


Figure 5.5 Quenching Curve (Norm Cochran's Data, Alcoa) Replotted

High speed films of gross experiments (at Battelle and IITRI) and small scale experiments (IITRI) as well as IITRI flash x-ray radiographs of small scale experiments reinforced this point. Then, if the relative stability of the film is considered, the less stable the film, the easier it will be to collapse it to obtain liquid-liquid contact and achieve spontaneous nucleation. In order to emphasize this point and provide relevant data, Alcoa quench data relating the aluminum temperature drop as a function of time was smoothed and replotted. Figure 5.6 shows these data with the apparent transition points from film to nucleate boiling indicated. The transition point for 33°F quench water does not show as it appears that the boiling goes into nucleate boiling very fast. The actual data started at about 600°C, but was extrapolated to 750°C (1382°F), the typical operational temperature. It is postulated that the stability of the film is proportional to the time it takes for the film boiling to go to nucleate boiling. The three curves forming the left group represent conditions in which explosions do occur and the three curves forming the right group represent conditions in which explosions do not occur. There is a rather dramatic difference which may indicate the "relative" stability of the films under the various conditions.

Heat fluxes in the general range of interest were used to estimate heating times for different arbitrary impact surface cavity depths. A two layer semi-infinite model, with constant heat flux, was used to calculate the time it would take to heat water to 267°C (assumed limit of superheat for water). This calculation assumes that the water in the cavity is all at the same temperature and that there is no steam interface on the heating surface (pure conduction). These calculations are summarized in Figure 5.7. It indicates the effect of heat flux and cavity depth on the time required to reach the limit of superheat. The purpose of these estimates is to illustrate that under the condition of conduction, the flux level and cavity depth could account for the time lag between initial surface contact (by the molten aluminum) and reaction.

IIT RESEARCH INSTITUTE

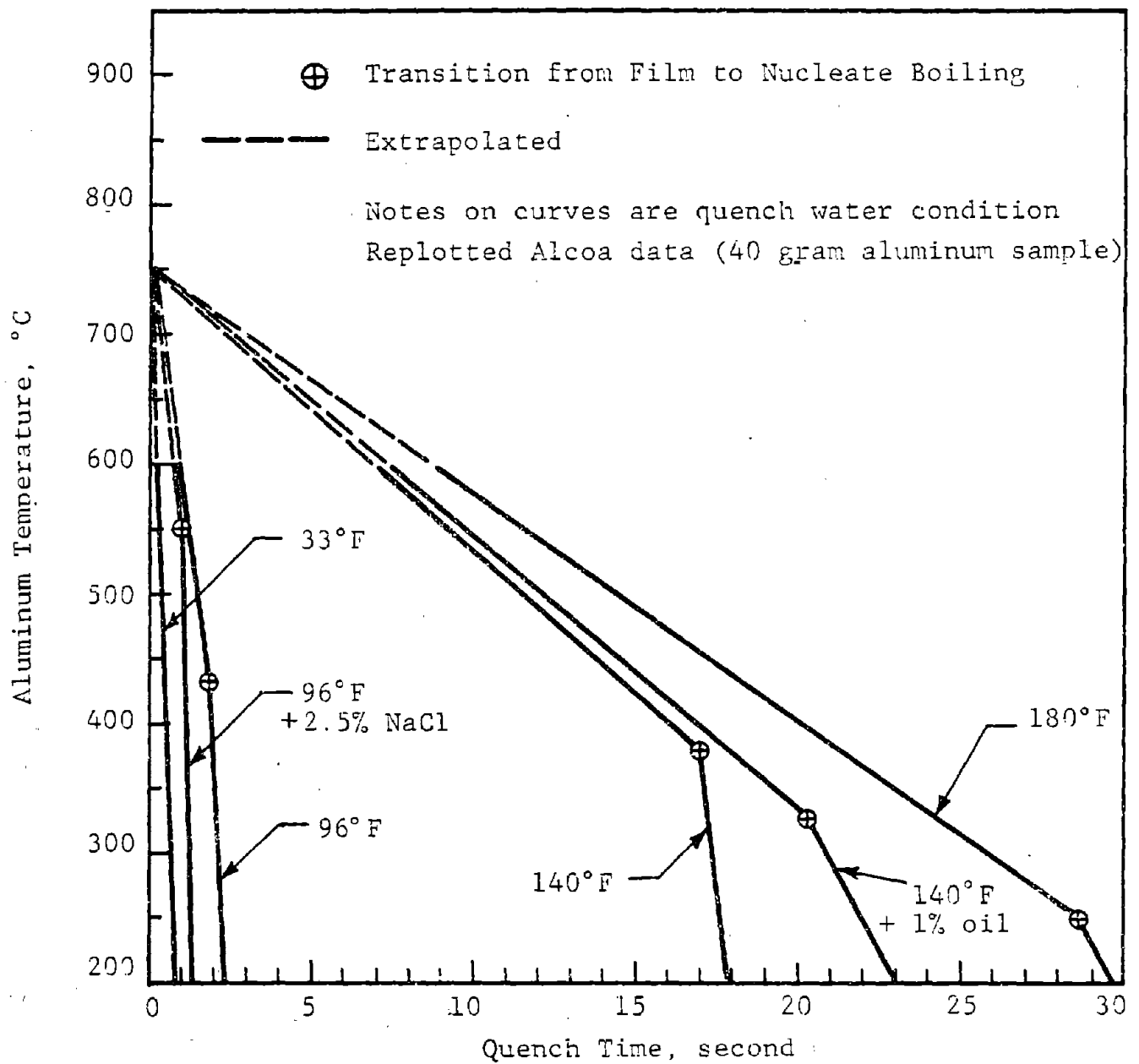


Figure 5.6 Aluminum Temperature Versus Quench Time

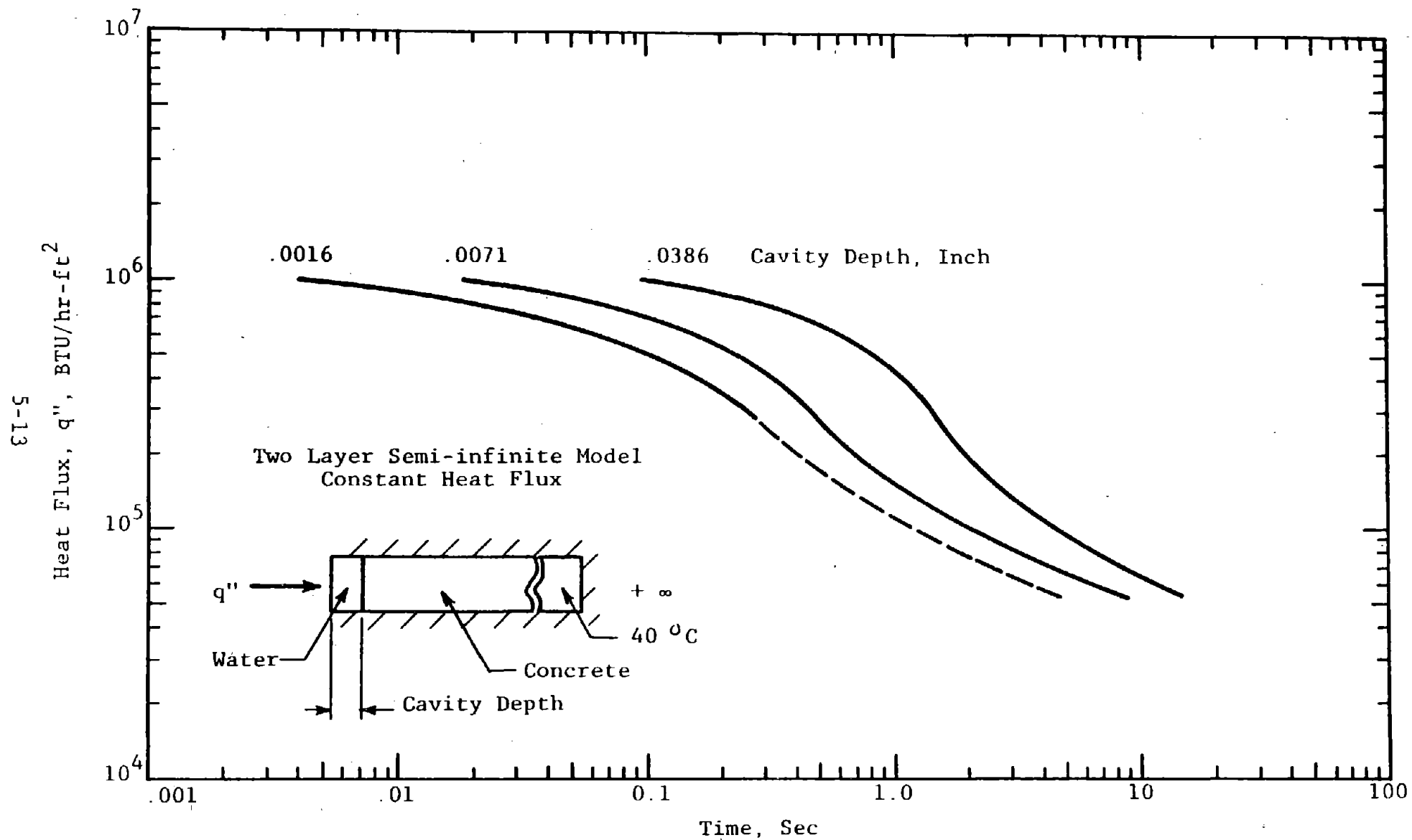


Figure 5.7 Heat Flux Versus Time to Heat Water to Limit of Superheat For Three Cavity Depths

5.4 Aluminum Flow

The flow of aluminum may be considered in four parts: that from the drop crucible (or billet) in air; initial flow through the quench water until it just impacts a surface; the next flow period is that which takes place between the impact surface and some second surface; and the final period which encompasses all the ensuing flow.

5.4.1 Initial Aluminum Speed

The head of aluminum, above the flow opening, corresponds to the aluminum efflux speed. The rate of change in the head depends upon the flow opening area and the internal geometry of the crucible or billet. In the case of a 50 pound bleed-out simulation, the initial efflux speed is about 82 ips and, for a 3-1/4 inch diameter bleed-hole, the emptying time is on the order of 1 second. During this time the efflux speed drops to zero.

5.4.2 Air Flow

The aluminum accelerates considerably more during its flow through air than in water. For example, with an initial efflux speed of 82 ips, flow through 12 inches of air increases the speed to 127 ips and the flow through six inches of water increases to 140 ips. The respective speed changes are 45 ips and 13 ips so that the air flow (double the path of that in the water) provides over three times the speed increment.

Flow through air may also be related to stream breakup. The time for stream breakup may be estimated from natural frequency conditions (after J. O. Hinze):

$$t = 0.8 \pi [\rho R^3 / 8\sigma]^{0.5}$$

where:

- t = breakup time
- ρ = liquid density
- R = spherical radius
- σ = surface tension

If we use this relationship to predict the breakup of a stream with a radius R into spheres with the same radius, we may estimate the aluminum flow stream breakup time and relate it to an air fall distance.

Table 5.1, below, was prepared to provide such predictions based upon an initial aluminum speed of 82 ips.

Table 5.1
MOLTEN ALUMINUM STREAM BREAKUP TIME
(82 ips Initial Aluminum Speed)

Stream Diameter (inch)	Breakup Time (seconds)	Air Drop Distance (inches)
0.375	0.015	1.3
0.5	0.023	2.0
1.0	0.046	4.2
1.5	0.120	12.6
2.0	0.185	21.8
2.5	0.259	34.2
2.75	0.298	41.6
3.25	0.383	59.7
4.0	0.523	95.7

The predictions in Table 5.1 seems to be on the right order. The small scale tests made at IITRI with 3/8 inch diameter streams always broke up. It has been reported that the 3-1/4 inch stream dropped from 120 inches into various water depths broke up. However, this diameter stream does not break at a drop of 20 inches or less (IITRI results) and presumably does not from drops as high as 48 inches.

5.4.3 Initial Flow Through Water

The aluminum may be hot enough to vaporize the water before initial contact can be made as it approaches the water surface. If not, immediately upon contact, steam at 1230°F (for

aluminum at 1382°F and water at 104°F) will be formed. The steam layer will most likely be a stable film on the order of a 10,000th of an inch thick after one millisecond and grow to about .01 inch at the time of bottom surface impact (refer to Figure 5.3). The initial "contact" of the metal and water will result in the formation of a shock. The shock pressure (in the aluminum, steam and water) will depend upon the impact velocity. In the case of an air drop through 12 inches with an initial aluminum efflux speed of 82 ips, and an impact speed of 127 ips, the shock pressure will be about 600 psi. The acoustic shock will travel about 185,000 ips in aluminum and 58,900 ips in water. Thus, the shock wave will dissipate rapidly, 65 microseconds in aluminum and 100 microseconds in water. The motion of the molten metal in the water produces a dynamic pressure ($1/2 \rho v^2$) of $3/4$ psig initially and when it arrives at the bottom, after passing through six inches of water, it will be almost one psig.

During the flow through the water, the Reynolds number will be on the order of 130,000. We may consider the flow in two ways: that of the aluminum flowing into water; and the water flowing into aluminum. Using the stable Welber number criteria of ten, the maximum stable radius of spheres can be calculated and interpreted to mean the radius of a concave hemispherical cavity formed in aluminum (due to water flowing into aluminum) separated by a convex surface (due to aluminum flow into water). The cavity in aluminum will have a radius of about 1/64 inch and the convex surface will have a radius of about 1/32 inch. Some aluminum samples recovered from small scale tests (1/2 pound of aluminum dropped with a 3/8 inch diameter stream) had surface cavities of this size spaced more or less in this manner. Figure 5.8 presents the results of calculations made for various air drop heights. Considering the combined diameter of the two surfaces, a hexpack distribution may be used to estimate the number of hemispherical cavities which might be produced in a given surface. Figure 5.9 summarizes these calculations for four stream diameters. Time bounds for

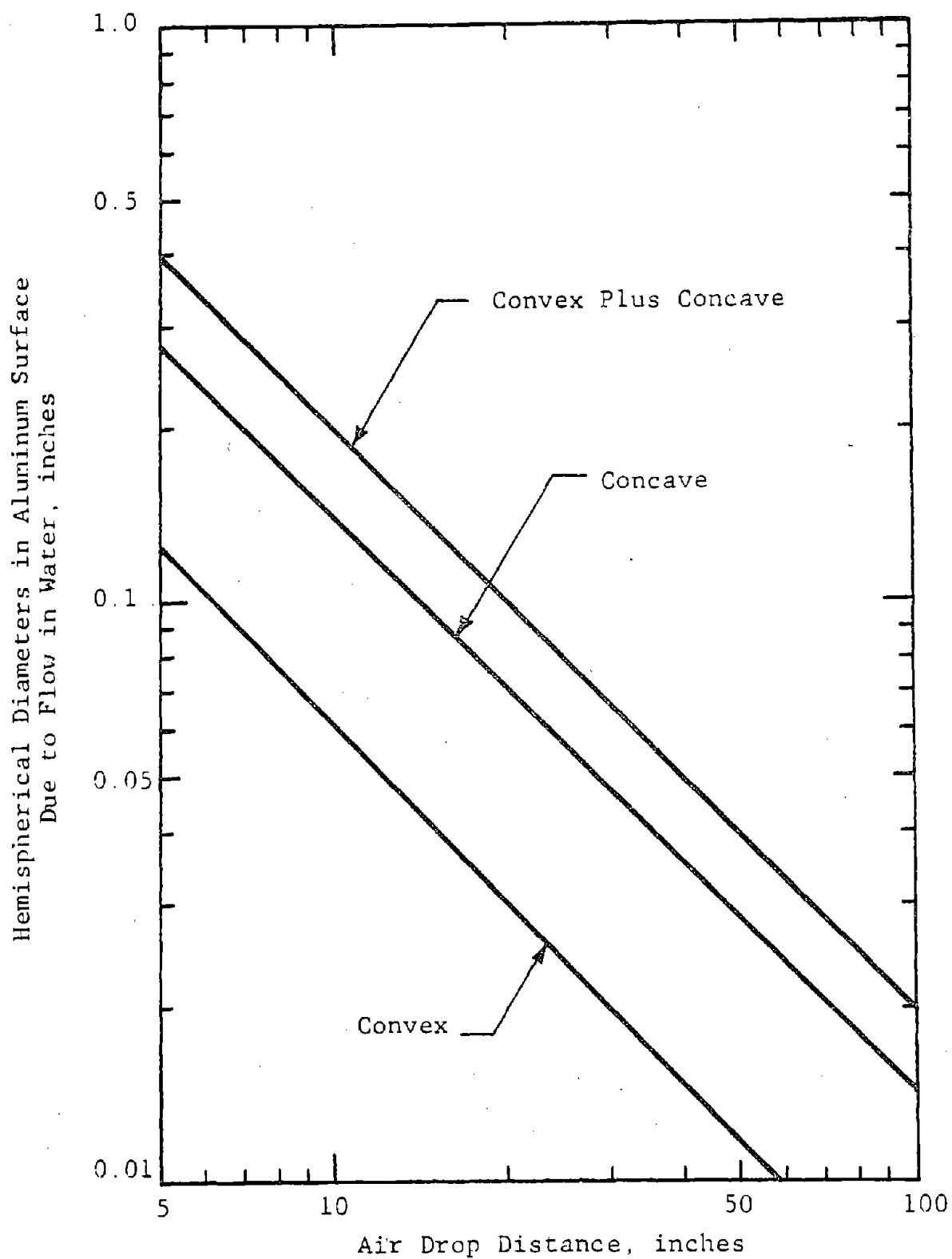


Figure 5.8 Aluminum Surface Profile Characterization (Ideal) as a Function of Air Drop Distance

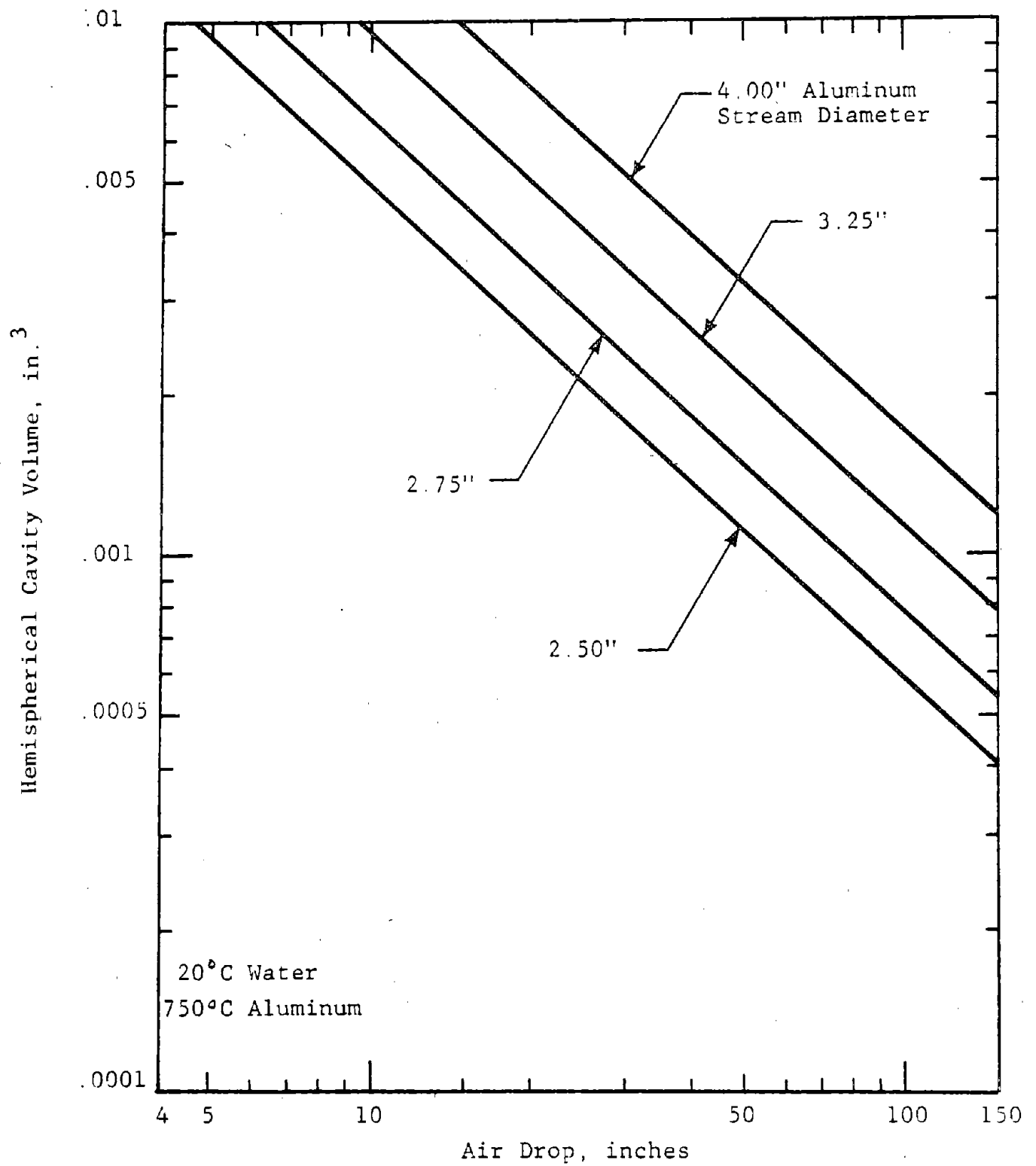


Figure 5.9 Cavity Volume Versus Air Drop Distance

the formation of the cavity volume (shown in Figure 5.9) are shown in Figure 5.10. The time bounds are based on the cavity formation time and the time for the flow field to be established prior to the cavity formation. The time for establishing the flow field is calculated on the basis of upper and lower bounds which is the reason for the time range shown in Figure 5.10. The order of magnitude of the time the aluminum flows through the water is indicated for four water depths as a function of air drop distance. It is assumed the speed in water is just that resulting from gravitational acceleration. Cavity formation will not be completed during flow through the six inches of water, but will be for 30 inches and for 20 inches. Cavity formation should be considerably more complete for ten inches of water than for six inches.

Although it is not clear that such cavities form and what part they play in the interaction process, one possible role may be advanced. The cavities may provide a reservoir of high temperature vapor. Upon surface impact, some of the vapor may be forced out from between the two surfaces, but that in the cavities may flow into the interface afterward, forming a thin layer between the hot aluminum and cool quench tank surface. If this is the case, a significant effect at the bottom interaction would be established.

5.4.4 Initial Aluminum Surface Flow

The initial contact between the molten aluminum stream and a surface may reduce the vapor film thickness due to the impact. Shock pressures on the order of 2500 to 4000 psi may be generated with a speed of 140 ips, depending upon the surface material. Figure 5.11 shows the functional relationship between shock pressure and impact speed for: steel, solid aluminum, glass and concrete. The shock wave will be dissipated at the speed of sound in the materials in a time on the order of 50 microseconds.

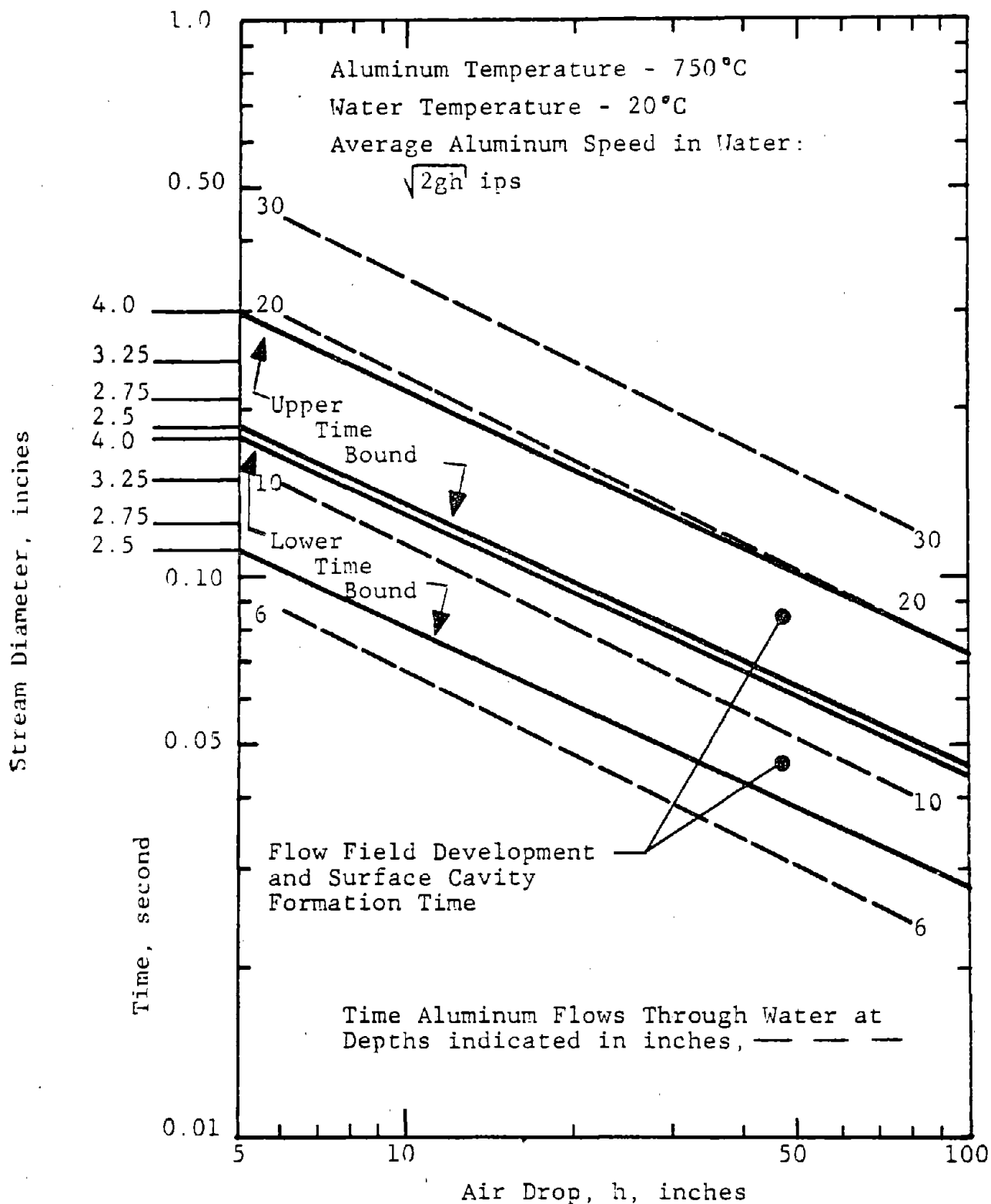


Figure 5.10 Time for Flow Field and Surface Cavity Formation Versus Air Drop Distance with Time Aluminum in Water at Four Depths

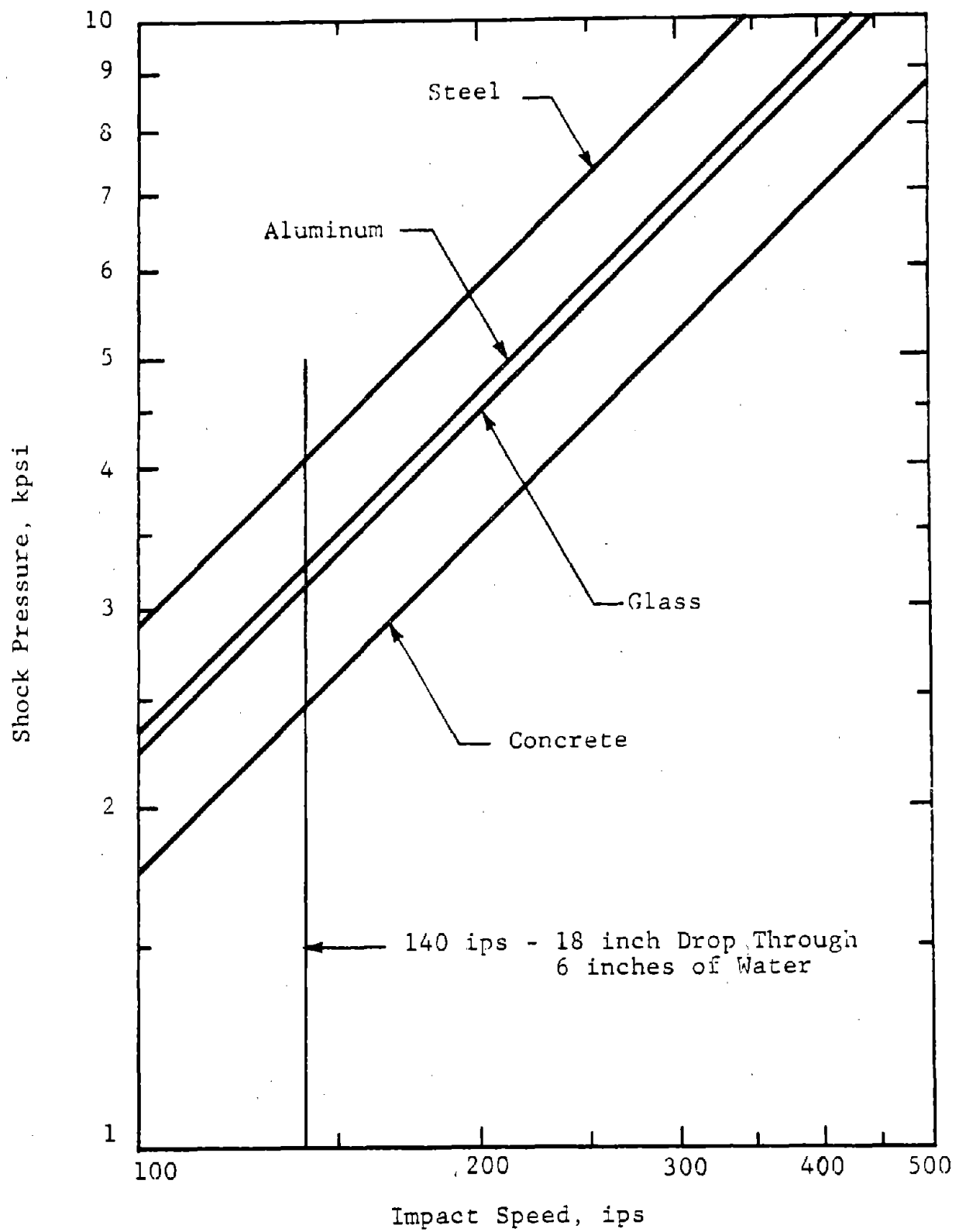


Figure 5.11 Shock Pressure Versus Molten Aluminum Impact Speed

The aluminum flow speed and the 18 inch column (head) will establish a total stagnation pressure of about 3.7 psig under the axis of the stream. The pressure surrounding the aluminum will be about 0.2 psig due to the six inches of water. The aluminum will flow radially along the surface due to the difference in pressure. The viscosity of molten aluminum is very low so that, if there were no steam layer (or where there is no steam layer), the boundary layer will be quite thin, about 0.01 inch at 1220°F (liquid) and thinner at higher temperatures. The absolute viscosity of 1220°F aluminum is about the same as 68° water and its kinematic viscosity is about half that of water.

The ideal flow over a horizontal bottom surface may be approximated by conservation of mass considerations and an estimate of the time it takes the flow to reach a side wall of the quench tank (from simulation experiments). Data obtained from IITRI experiments indicate that this time is about 0.045 seconds. This corresponds to an average speed of 97 ips for flow from a 3-1/4 inch diameter stream at the center of a 12 inch square tank (to the nearest surface). With the assumption of a constant acceleration from the stream diameter to the wall, the impact speed will be 194 ips. Figure 5.12 shows this linear speed relationship as well as the position time of the aluminum flow and the thickness of the leading edge. The plots are extended to indicate these parameters when the flow reaches the corner of the square tank, a radial distance of just under 8-1/2 inches. The leading edge of the flow is about 0.2 inch thick at the side and 0.1 inch at the corner.

The radial flow speed is great enough to produce an impact shock at the side wall similar to that which occurs when the stream initially impacts the bottom surface. As indicated in Figure 5.11, 190 ips impact on concrete would provide a shock pressure about 3400 psi and 5600 psi on a steel surface. It has been reported (by the United Kingdom subcommittee) that experimental work at Aston has shown that a shock at the interface of

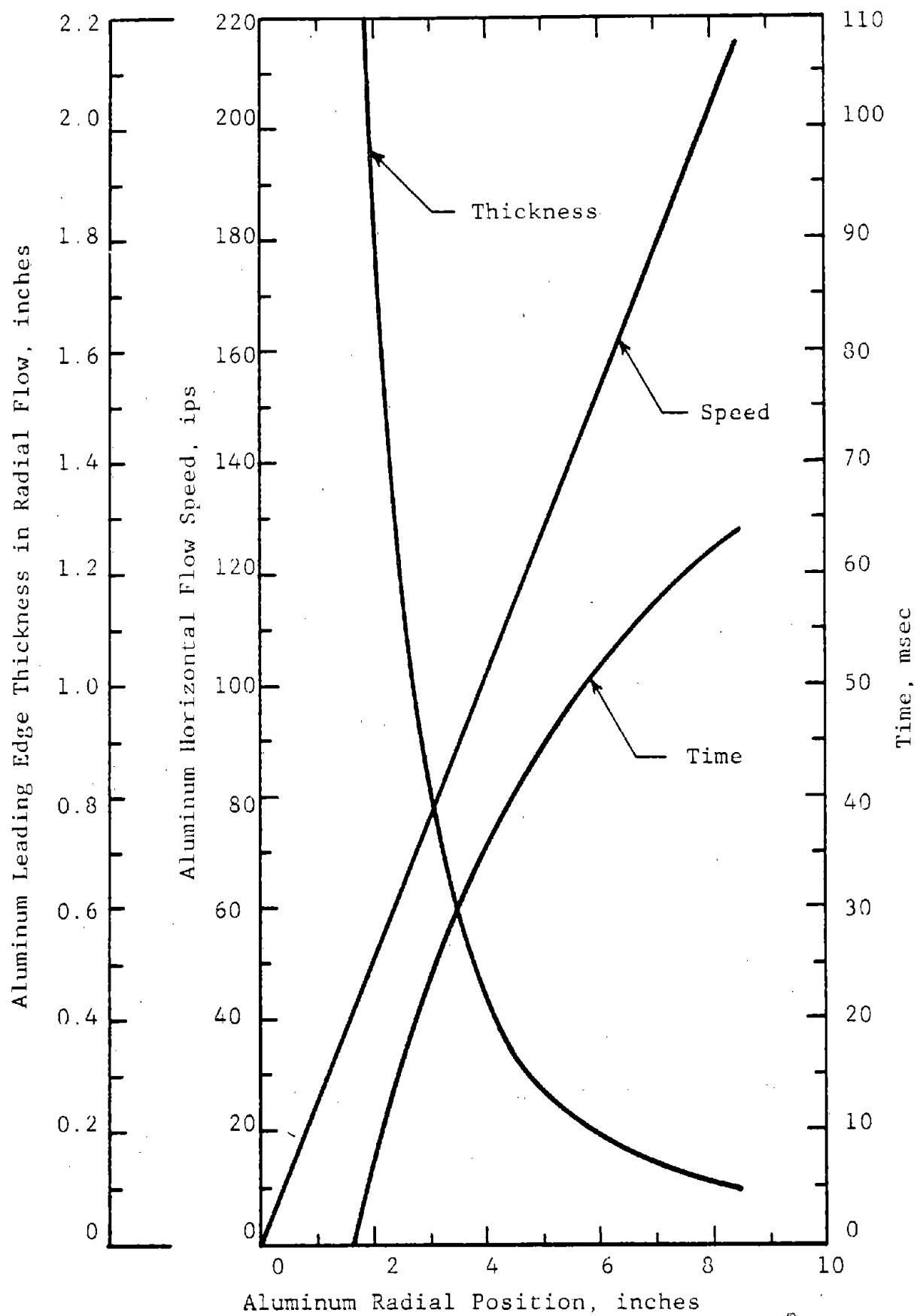


Figure 5.12 Idealized Initial Aluminum Flow Over the Bottom of a 12 inch Square Quench Tank

the surface of steam (under water) over liquid tin will collapse the steam film layer. Thus it may be reasoned the shock the molten aluminum flow impact produces on a side surface will propagate back along the aluminum-steam-bottom interface and collapse the film. If this occurs with molten metal over a bottom surface with cavities containing liquid water, an instantaneous vapor explosion could take place. The shock will travel through 12 inches of steel, aluminum, glass or concrete in 65 to 100 microseconds and through steam (100°C) in about 750 microseconds. The passage of this pressure wave may collapse the steam layer between the aluminum and tank surface if the pressure pulse is "strong" enough in relation to the "stability" of the layer. The rate of steam layer collapse will be proportionate to the aluminum flow speed. Obviously the time for film collapse will depend upon its thickness. It is estimated that the steam layer could be between 0.03 inch (Figure 5.3, distance to 100°C water at 0.1 second) and .001 inch (Figure 5.9, considering the hemispherical volume from a 12 inch air drop of a 3-1/4 inch diameter stream distributed over the stream surface area). If the collapse rate lies between 20 ips and 200 ips, the collapse time lies between 1.5 millisecond and five microseconds.

In order to obtain another bound on the time which might be related to the collapse of the steam film, which could provide liquid aluminum and liquid water contact, Battelle film records were examined. Explosive driven pressure bars were used in their run Nos. C-37 and C-42. A visible pulse traversed 12 inches in .001 second (12,000 ips) in run No. C-37 and in .002 second (6,000 ips) in run No. C-42. Both of these runs resulted in catastrophic reactions. The speeds calculated are too slow to be acoustic and too fast to be particle motion. Thus it seems that the vapor film collapse time may be characterized as a millisecond event rather than a microsecond one. Since the pressure bar would provide a stronger pulse than the aluminum flow impact on a side tank wall, the film collapse time could be greater and might be on the order of five milliseconds.

The incoming molten aluminum stream has its surface area changed when it contacts the bottom surface of the quench tank. The stream is spread over the surface and the area of the stream is increased as it flows to the quench tank side walls. Figure 5.13 shows a profile of the flow and the total surface area as a function of the radial position of the flow. The surface area is hardly effected until the flow has reached a radius of 3-1/4 inches (starting from 1-5/8 inches). It takes about 0.023 second for the area to increase from about 70 square inches to about 225 square inches. If the fresh area oxidizes a 50 Å* thick layer, $1.3(10^{-6})$ pound of aluminum will have reacted. This will release 0.005 Btu corresponding to a heating rate of 0.2 Btu/second. In more conventional terms, the heat flux will have been 675 Btu/hr-ft². If the oxidized layer is 5000 Å, the heating rate would be 67,500 Btu/hr-ft². This heat transfer rate corresponds to values shown in Figure 5.5, for which explosions do not take place.

If the aluminum flows over the bottom surface on a layer of steam, there will be no shear force developed. If there is no steam layer, then the shear force will be on the order of the product of the absolute viscosity of the aluminum [$2(10^{-7})$ lb-sec in²] and the average flow speed (100 ips) divided by the boundary layer thickness (0.01 inch) which is 0.002 psi. This is hardly significant.

The two mechanisms described above produce oxidation of fresh aluminum surfaces which releases hydrogen. Hydrogen atoms are 17 times more soluble in aluminum when it is liquid as compared to when it is solid. It could be expected that upon solidification of the aluminum surface, some hydrogen atoms would be driven out of solution and form molecular hydrogen, releasing heat. This action may provide a basis for defining an initiation mechanism.

* $1 \text{ Å} = 10^{-8} \text{ cm.}$

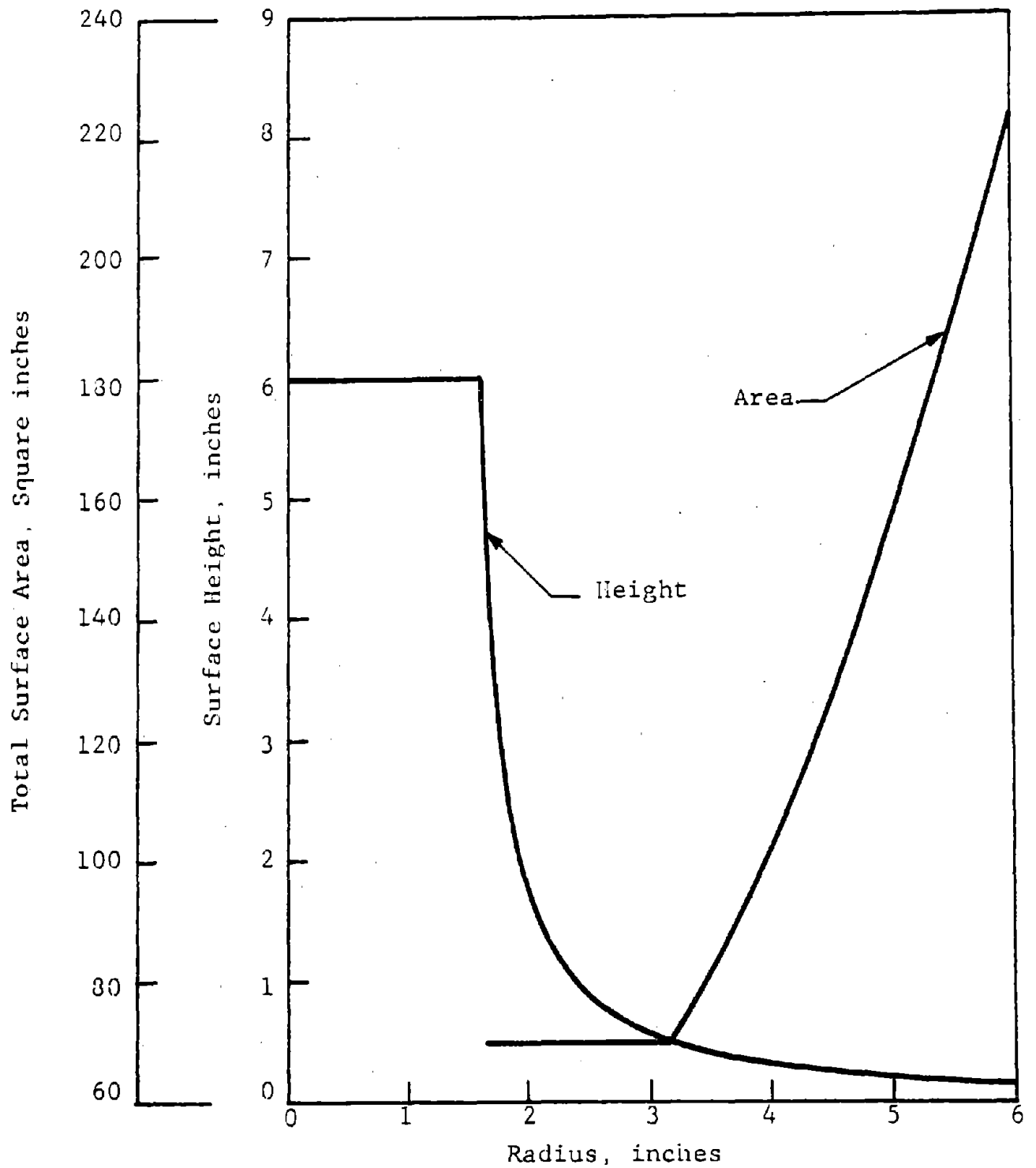


Figure 5.13 Height and Surface Area Versus Initial Flow Radius of Molten Aluminum on Quench Tank Bottom Surface

5.4.5 Final Flow

All of the flow taking place after contact with the quench tank side walls may be lumped into a period dubbed "final flow". Two general characteristics of the period have been identified.

The amount of aluminum which has accumulated in the quench tank should be an important parameter in the potential for the destructive capability of a violent reaction. Given an initiation, the more aluminum mixed with water, the greater will be the "potential" chemical and/or heat energy which can enter the overall reaction. In other words, complete oxidation of five pounds of aluminum will release more energy than one pound and can potentially produce more damage.

The other important aspect of this flow period is that the continued aluminum flow can supply heat to the aluminum previously cooled down. This is especially important in considering one of the requirements for the vapor explosion. In order to obtain spontaneous nucleation of water, liquid aluminum and liquid water must come into contact. At a minimum, the continuing aluminum flow should aid in maintaining the aluminum liquid under the flow impingement area.

6. BASIC INTERACTION SCENARIO

The relevant operational and environmental aspects of the interaction of molten aluminum and water (in the direct chill process) have been combined to form an interaction scenario. The scenario is in a basic form which postulates the simplest set of events which form an interaction that may lead to a catastrophic explosion. This scenario encompasses the envelope of "environmental" effects determined by various experimental programs. The central hypothesis in the formulation is that rapid oxidation of aluminum is required to produce a catastrophic explosion. This contention is based upon specific energy considerations. The specific energy available from the oxidation of aluminum and water is much greater than that from the expansion of superheated water vapor (steam) which could be obtained under atmospheric conditions. The specific energy available from the chemical reaction is on the order of 2000 calories per gram of reactants (about 0.5 gram each of water and aluminum). The specific energy released when steam heated to 300°C at atmospheric pressure expands to drop the temperature to 100°C at 1 atmosphere (saturation conditions) is on the order of 100 calories per gram of water. The ratio of specific energies of the oxidation reaction to that for the expansion of superheated steam is 20:1.

It appears that rapid oxidation of aluminum will take place at the melting temperature of aluminum oxide, about 2000°C. Since this is about three times as high as the initial temperature of the incoming molten aluminum, some mechanism must be present to provide this large change. This is construed to be the initiation mechanism.

The basic interaction of molten aluminum and water may be divided into four parts: induction, trigger, propagation and final reaction. These are described in the following sections.

6.1 Induction

This part includes all events starting with the molten aluminum "bleed-out" up to the propagation period. Chronologically, it encompasses the trigger. The main events of this period are: acceleration of the aluminum (due to gravity); heat transfer from aluminum to

water and the water vapor film "attached" to the hot aluminum: and bulk mixing of aluminum and water, accompanied by water heating. These events are dependent upon: drop height; the amount of aluminum, its temperature and stream diameter; and water temperature, depth and chemistry.

This scenario includes a special condition in which there is no trigger event. In this case a very mild steam explosion could be the result. Induction and propagation are one and the same in this situation. The aluminum flow continues until sufficient heat is transferred into the water to form water vapor at a pressure high enough to vent through the overburden of water and aluminum. If the vapor reaches a superheat state, the resulting explosion will be more severe, if not the results may not be only a "pop".

6.2 Trigger

This event starts with the impact of the aluminum stream on a surface and stops at the start of the propagation stage. The trigger includes a series of events which start when an aluminum impact which produces a shock that in turn collapses the water vapor film between the aluminum and a surface. This results in spontaneous nucleation of the water.

The important parameters in this event are: aluminum temperature, speed and stream diameter; impact surface physical properties; surface capillary size; and vapor state (temperature, density and pressure). The nature of the bulk aluminum flow and mixing during the last part of the induction, taking place during the trigger phase, is also significant in the propagation period. The state of the bulk aluminum and water mixture relates directly to the extent of the propagation of the trigger and the final reaction.

Figure 6.1 illustrates induction and triggering as described. The large center view represents the condition which exists after the impact shock has collapsed the vapor layer separating liquid aluminum and liquid water. This action will precipitate spontaneous nucleation of the liquid water in the quench tank surface cavities constituting the generation of a shock wave which provides the initiation energy.

IIT RESEARCH INSTITUTE

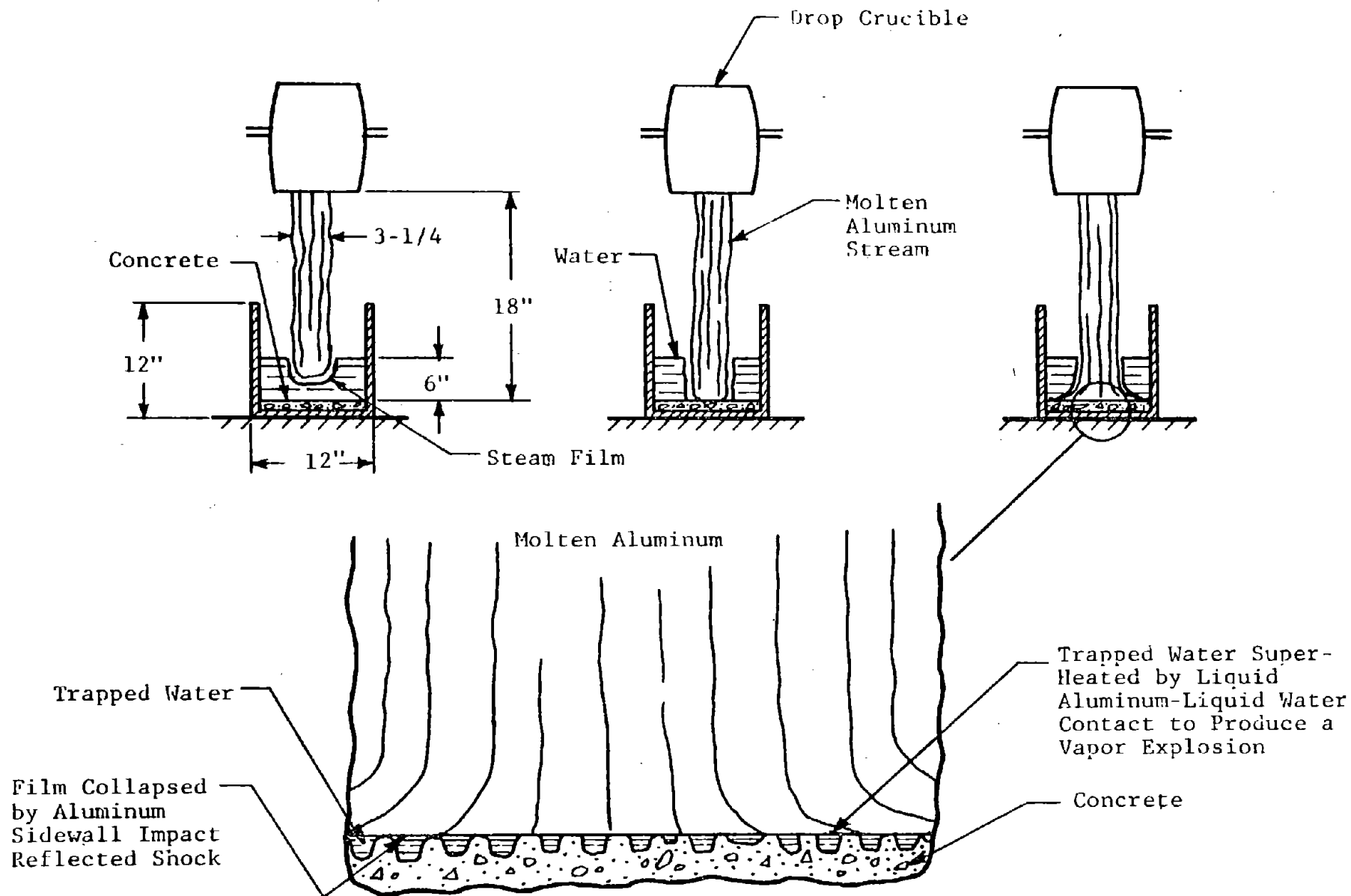


Figure 6.1 Schematic of Trigger Mechanism

6.3 Propagation

This period starts with the end of the trigger action and lasts until the final reaction, the explosion takes place. The propagation phase is considered a transition period during which the triggering energy is amplified and the bulk of the aluminum and water is conditioned to support a stable reaction. The propagation phase is considered completed when the stable reaction has been achieved. The portion of the induction phase, the bulk mixing of molten aluminum and water, which takes place during triggering, is considered completed at the start of propagation. The events which take place during propagation depend upon the strength and nature of the trigger and upon the conditions in the bulk of the aluminum and water. The violence of the final reaction depends upon the results of propagation. Figure 6.2 illustrates propagation and reaction following a trigger event.

The energy provided by the trigger event is propagated throughout the bulk of the mixture of the molten aluminum, water vapor and water. The effect of the propagation will depend upon the strength (and perhaps subsequent enhancement by further oxidation) of the trigger, the nature of the mixture of the bulk of the aluminum and water and the temperature of the water vapor in this mixture. The propagation of the trigger combines two modes: heat transfer and chemical reaction, e.g., aluminum oxidation. The propagating energy breaks up molten aluminum into particles with unreacted surfaces. Both heat transfer and oxidation are proportionate to the amount of fresh surface area generated. Small size particles (probably below 100 microns) and high water vapor temperature (above the transition temperature for nucleate boiling) promote the chemical reaction phase. If the particles are large in size (probably over 100 microns) and the water vapor temperature is in the nucleate boiling region, the heat transfer mode may be predominate. It may be possible for the heat transfer mode to go into the chemical reaction mode under some combination of conditions.

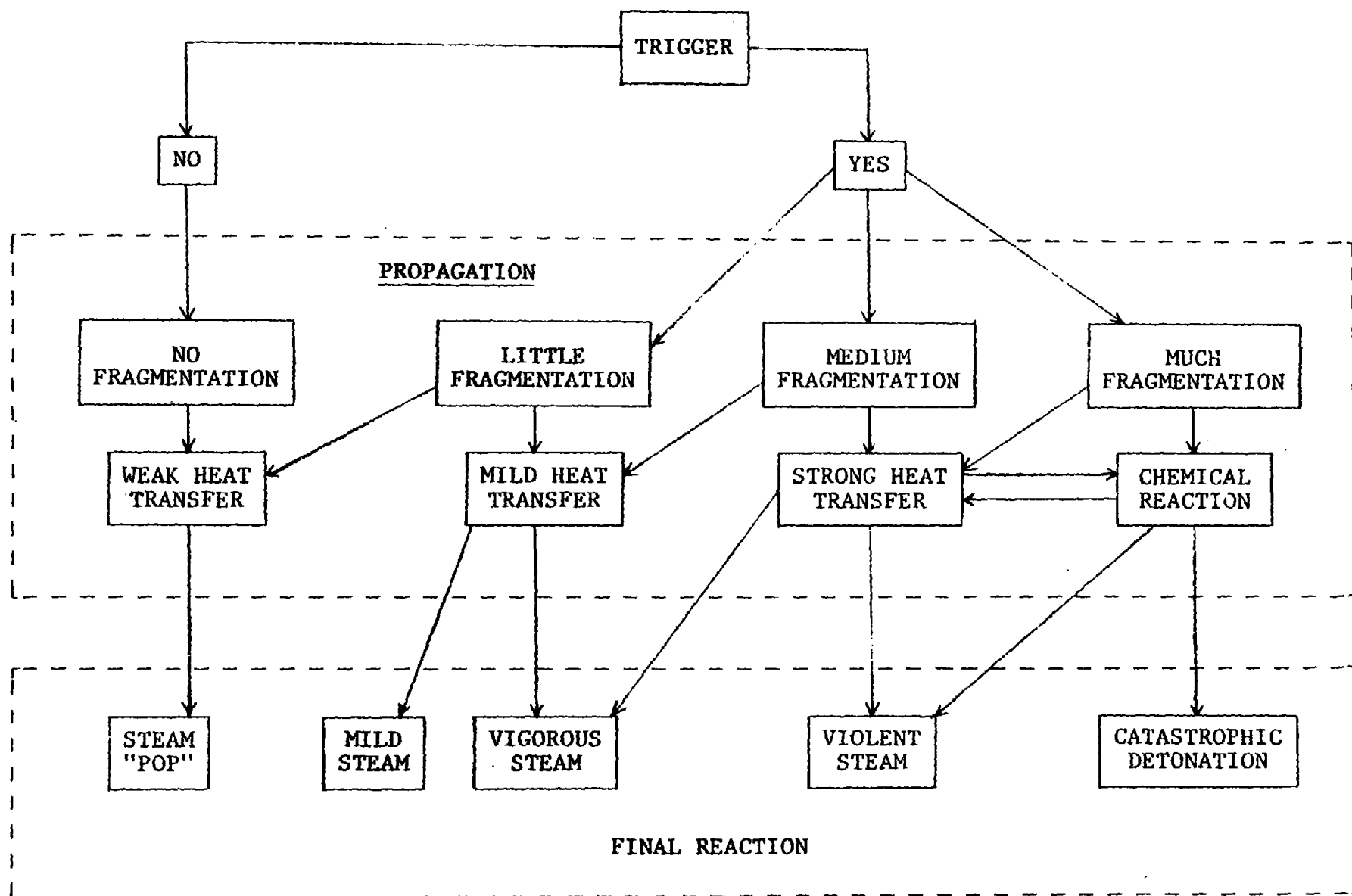


Figure 5.2 Molten Aluminum-Water Interaction Events

7. CANDIDATE INITIATION MECHANISMS

The literature is resplendent with interesting mechanisms involving liquid metals and coolants. A large number of these mechanisms are concerned with metal fragmentation which produce large surface areas. The large surface area is considered necessary for rapid heat transfer which can provide a vigorous mechanical explosion. Many of these mechanisms do not appear applicable because they do not seem to have a potential for a chemical explosion. The final size of the fragments is too large to account for the energy released in catastrophic explosions. In this type of explosion it would appear that quite small particles, approaching 13 microns would be required. Particles this small will react spontaneously with water at a temperature of about 1400°F. However, large micron size particles would provide large amounts of unoxidized aluminum which can react with water and its vapor, releasing a significant amount of energy.

The fragmentation of molten metals by "entrapment" of liquid water against a solid surface is based upon the hypothesis that the water is heated to a high enough pressure to blow apart the metal and thereby producing small fragments providing a large surface area. Such a process is relatively slow and would depend upon the liquid metal overburden to provide confinement during pressure build-up. The maximum head available during bleed-out simulation is less than 5 psi and the seal between the molten aluminum and restraining surface is not likely to be good enough to maintain significant pressure.

Mechanisms for obtaining fragmentation without a restraining boundary include: violent boiling theory, shell theory and the Webber Number effect. The violent boiling theory notes that the "stable film" existing during film boiling is not stable, but collapses and reforms. Presumably in transition boiling this process could provide a violent force, overcome the liquid metal surface tension and produce metal fragmentation. There are two shell theories: one postulates that liquid water is entrapped by the molten metal and rapid vaporization tears the metal apart;

the other theory is based upon the concept that the solidifying molten metal becomes internally pressurized and that this pressure exceeds the strength of the solidifying shell, producing fragmentation. Neither of these concepts appear to apply to the rather massive aluminum streams involved in bleed-outs and their simulations. The extent of entrapment which could be obtained by fluid-fluid instability would not seem to be significant. The internally developed pressure theory suffers from the same problem, the size scale is inappropriate. In addition, analysis has shown that in order for extensive fragmentation to occur, the metal must be liquid which would make the solidified requirements to buildup the internal pressure inapplicable. This mechanism is quite close in concept to the thermal stress theory. It postulates that differential cooling of the metal gives rise to thermal stresses which exceed the strength of the solidified metal and fragmentation results.

The Webber Number effect has been proposed as an important fragmentation mechanism and has been demonstrated experimentally. The Webber Number is the ratio of two forces acting on a molten metal sample flowing through water. It is the ratio of the sample inertial forces and surface tension forces. When the inertia force becomes significantly large, the surface tension of the liquid metal cannot hold it together and fragmentation results. The critical value for this ratio lies between 10 and 20. This theory does not seem to apply to the bleed-out condition which produces a rather large liquid metal stream. It is postulated that the Webber Number effect in this case produces an undulated surface on the aluminum stream. The characteristics of this phenomenon were presented in Section 5.4.3.

In addition to these mechanisms which do not seem applicable to D.C. operations, there is another more germane group. Some of these are contained in the literature and others were postulated by the Aluminum Association Task Group on Molten Aluminum and Water Explosions, and by IITRI.

- a. Bubble Collapse and Rebound Driven by Heat Exchange Between the Hot Aluminum and Encapsulated Water: This model was provided by Battelle for the Aluminum Association and was applied to the SMELT water problem.
- b. Bubble Collapse Producing a Jet of Water or Water Vapor Which Penetrates the Surrounding Molten Aluminum: As in the case of the first candidate, this mechanism is driven by heat transfer and differs in that a jet emanates from the bubble. This model was developed by O. J. Buchanan (Culham Laboratory).
- c. Cavity Collapse Induced by an Impact Generated Shock Wave: This model has been prepared and used by IITRI staff in analysis of propellant and explosive sensitivity determinations. The cavity heats up drastically during collapse which is driven by the energy from the impact. The cavity collapses assymmetrically producing a steam jet which penetrates the surrounding molten aluminum and precipitates oxidation of aluminum. It applies at the time the aluminum steam initially impacts a surface of the quench tank.
- d. Electrostatic Initiation Produced by Discharge of an Electrostatic Charge: IITRI studies made during gross experiments in this program showed that the molten aluminum flow into the quench water developed a large bulk electrostatic charge. Separate small-scale studies showed that an electrostatic discharge into small aluminum particles, in water, produces a rapid reaction. The driving force is the electrostatic charge produced by the aluminum flow.
- e. Oxidation Produced by Steam Surface Increase During Flow Over Bottom Surface: This mechanism was suggested by the Aluminum Associated Task Group. It was discussed at the end of Section 5.4.4. The incoming cylindrical steam is reshaped upon contact with the bottom surface of the quench tank during radial flow. The surface area increases by a factor of three to four providing fresh, unoxidized aluminum surfaces which can react and release heat.

- f. Hydrogen Molecular Recombination: This mechanism was suggested by the Aluminum Associated Task Group. During the entire flow aluminum period, fresh surfaces of aluminum are produced, as in "e" above, which result in the formation of hydrogen. It is dissolved in the liquid aluminum, near its exposed surface, as atomic hydrogen. The solubility of hydrogen is reduced significantly upon solidification of aluminum. Thus, hydrogen atoms would be "rejected" and could reform molecular hydrogen releasing heat.
- g. Spontaneous Nucleation: This mechanism is treated in the literature and has been accepted by IITRI as the initiation mechanism which most probably causes the explosion in D.C. operations. Intimate contact of two liquids which results in an instantaneous interfacial temperature at or above the limit of superheat for the cold liquid produces a vapor explosion. This is a microsecond event giving rise to a shock. The shock propagates through the aluminum-water mixture, producing micronsize fresh surface aluminum particles. These oxidize and transfer heat to produce the major explosion.

Mechanism "a" and "b" do not seem applicable to D.C. operations. These are quite like the entrapment theory presented earlier. The sizes considered relative to the bleed-out stream indicate that these mechanisms would not hold during the time period when most of the simulations produced explosions. They could apply at later times and may be applicable in furnace charging operations. They also may constitute mechanisms which are involved during propagation of the initiation and the final explosion.

Mechanism "c" is analysed in greater detail in Appendix D. The major drawbacks to the applicability of this model are the time frame in which it can take place and the fact that the incoming stream of aluminum does not appear to contact the quench tank bottom surface upon first approach. This mechanism could only apply during the first millisecond after "initial" contact.

Mechanism "d" was conceived and explored during the program. It is considered a significant mechanism in the interaction of aluminum and water. The work performed and results obtained are presented in Section 10. It was not shown conclusively that this energy source was responsible for initiation.

Mechanisms "e" and "f" are certainly present during the interaction. The amount of energy released by them is the key to their importance as being initiation mechanisms or contributing to initiation. Analysis indicates that their contribution is relatively small or the relative rate is low compared to the spontaneous nucleation mechanism g. As indicated in Section 2.2, this mechanism is considered the most probable one. It is triggered by an impact shock arising from aluminum flow in the quenching pit or tank. Sections 12 and 13, and Appendix C provide greater detail.

8. CHEMISTRY STUDIES

These studies encompassed five activities of varying effort levels:

- Matrix Isolation
- Aluminum Reactions
- Active Sites
- Thermite Reaction Studies
- Debris Examination

These activities were oriented toward studying the chemical basis of the explosion with the ultimate goal of developing relatively simple and inexpensive ways to prevent explosions. The nature of the planned and unplanned explosions that have occurred in the past appears to implicate a branching chain chemical mechanism as being responsible for the extremely rapid release of large amounts of energy. This is reinforced by the unpredictability with which the explosions occur, and the sensitivity of their occurrence to minor variations in the conditions. For instance, rust surfaces appear to induce explosions and tarset coatings appear to inhibit them.

It was assumed that in the physical process, once the molten aluminum starts falling toward the water, many different paths may be taken to the end of the process. Some of the paths will lead to inconsequential events, some to a steam explosion, and some to a chemical explosion. Each event may result from many different pathways; however, all the possible paths that lead to the chemical explosion must meet at the initiation and propagation steps of the chain branching reactions. For instance, the explosion reaction might be initiated by friction, pressure, a shock wave, a thermal pulse, an electrical pulse, etc.

One possible mechanism, that is supported by data reported in the literature, may consist of the following: mechanical atomization of the molten aluminum to small particles; dispersion in the water vapor; and the input of a high pressure pulse to the small particles.

IIT RESEARCH INSTITUTE

The ignition temperature of aluminum particles in water vapor is strongly dependent on the particle size. Gurewich (Ref. 1) found an ignition temperature of 1400°F for 13 μm dia. particles and predicted, theoretically, an ignition temperature of 3600°F for particles larger than 60 μm . Wilson's (Ref. 2) work agrees with this trend experimentally. He found an "instantaneous" ignition temperature of 3200°F for 8 μm particles. Sebald and Krschfield (Ref. 3) showed that the speed of combustion of aluminum wire in oxygen is a very complex function below 22 atm, but increases monotonically very rapidly from 22 atm up to at least 100 atm pressure. This type of behavior is characteristic for reactions that lead into explosive rates at higher pressures. It is assumed that the Al-H₂O reaction should behave similarly but at the higher pressures.

These experiments were done at constant pressure. In an Al-H₂O mixing event, a feedback mechanism is present that, combined with the rapid increases of burning rate with pressure, could conceivably lead to the explosive reactions. The increase in pressure increases the burning rate, which in turn increases the pressure (because it's in a relatively confined system), which increases the burning rate, etc. The required pressures are rapidly attainable in these mixing situations. For instance, a pressure of 320 atm with rise time of 100 sec, by a supersonic shockwave, has been reported (Ref. 3) when water was dropped into molten aluminum. The combination of these events could then lead to an explosion in the following manner:

-
1. Gurewich, M.S., et al, Heterogeneous Ignition of an Aluminum Particles in Oxygen and Water Vapor, Combustion, Explosion and Shockwaves, 6(3), p. 291-297, March 1973.
 2. Wilson, R.E., Reactor Safety II, p. 102.
 3. AEC Report, STL 372-50, December 1966.

- (1) molten aluminum temperature $\sim 1400^{\circ}\text{F}$ drops into the water;
- (2) mechanical breakup to aluminum droplets $\sim 13\text{ }\mu\text{m}$ diam occurs;
- (3) ignition of the droplets occurs (i.e., an incandescent self-sustaining reaction of aluminum with H_2O producing very high local temperatures $\sim 5500^{\circ}\text{F}$);
- (4) ignition of larger droplets near the small burning ones by the high temperatures produced by the small ones;
- (5) impact of a pressure pulse on the burning droplets (this increases the burning rate, which increases the temperature and pressure and leads to the feedback mechanism that leads to the explosion).

All these events must occur for the chemical explosion to take place. The chemical initiation and propagation reactions must then proceed very rapidly.

Therefore, the main objective of the chemical studies was to determine the important species involved in the initiation and propagation steps of the branching chain reactions, and ultimately, to determine "poisons" that will combine with the critical species and prevent the initiation and/or propagation steps from occurring. Several approaches were taken to determine these species.

8.1 Matrix Isolation Study

IITRI matrix isolation equipment was modified for the planned experiments. A sample cell of aluminum oxide inside a tantalum receptor was fabricated. The tantalum is heated by a RF coil which melts the aluminum sample inside the alumina boat. An inlet for the water vapor was installed. The aluminum is melted and held at temperatures near 1300°F . The water vapor is allowed to flow over the molten aluminum and react with it. The reaction products diffuse through a small orifice, and mix with an inert gas. This mixture impinges on a KBr plate that is maintained at 4°K , and solidifies on it. The solid layer of inert gas, with the reaction

species embedded, are then examined in an IR spectrometer. The spectral curves are used to determine the nature of the species, and eventually can be used to determine their thermodynamic constants.

A total of 38 experiments were run. The reactions between water vapor at low pressure ($\approx 10^{-4}$ atm) and molten aluminum at temperatures from 1350 to 2460°F were studied. In this experimental arrangement the water reacted completely above 2300°F (very little at lower temperatures) and generated the known species Al_2O . Some evidence was found for AlOH being formed. The presence of Fe_2O_3 in contact with the molten aluminum did not produce any new species. Additional matrix isolation studies were planned if the results of the species studies in the ignition and propagation experiments indicate the need; they did not. The details of the matrix isolation studies are given in Appendix B.

8.2 Aluminum Reactions

The literature was reviewed very carefully for corroborative information to help in establishing a reaction mechanism for the explosion. The reported mechanisms for other explosive reactions were examined to determine what possible analysis and extrapolations exist between them and the $\text{Al-H}_2\text{O}$ explosion reaction. This also included reports on inducement and inhibition of explosive reactions which might have provided clues to understanding the $\text{Al-H}_2\text{O}$ explosion.

There are essentially no reports in the literature on the chemistry of the aluminum-water explosion. Studies have been made of the oxidation of aluminum by air and oxygen at a variety of temperatures and pressures. Corrosion type studies were usually done at relatively low temperatures (a few hundred degrees centigrade) and pressures (subatmospheric to slightly above atmospheric). Atmospheres of air or various concentrations of oxygen and sometimes water vapor were used. The oxidation rates are slow due to

the coherent oxide layer, and are usually expressed in the form of a parabolic rate law. Combustion type studies have been done with different physical forms of aluminum (bulk metal, wires, particles, liquid, vapor) usually at atmospheric and higher pressures (using air, or various concentrations of oxygen and sometimes water vapor). A few studies have been reported on the vapor phase reaction of aluminum and oxygen.

Because it seems likely that a chain branching mechanism is involved in the final stages of the chemical reactions during the explosion, the literature was examined for reactions that are similar to, or can be related to those in the $\text{Al-H}_2\text{O}$ explosion. Special attention was given to the $\text{H}_2\text{-O}_2$ explosion reaction, since this system is the best understood today, and about which the most information exists. Many materials are known that either catalyze or inhibit this explosion. It was hoped that this system would serve as a model for the $\text{Al-H}_2\text{O}$ system, and that by establishing similarities in species and in mechanism, and building upon this system, we would be able to determine enough about the $\text{Al-H}_2\text{O}$ system to control it. This was not the case and similarities could not be established.

Other things that help induce explosions are gas bubbles (in a solid, if we start with solid aluminum wire for instance) or the presence of various additives such as mercury, copper and flourine. Halogens such as bromine and iodine may inhibit the explosion. Other conditions, such as large surface to volume ratios in the apparatus and large particle size may inhibit the reaction. Even with all conditions adjusted properly, it may be impossible to produce explosions because of the "critical size" limitation. Almost all explosives require a minimum amount of material to detonate even when all other conditions are favorable. This is related to all the parameters mentioned, and to the shock wave phenomena in the explosive.

The initial experimental work planned has been oriented toward determining if an explosion could be produced in the lab. Subsequent work would be done to determine the species formed during the explosion and rapid reactions using optical and mass spectroscopy and other techniques such as gas chromatography. This line of research was not pursued as it was believed that the likelihood of obtaining explosions was too low. Further, the equivalent effort could be used more profitably in other aspects of the program.

8.3 Active Site Study

Activities were conducted to establish unknown chemical reactions and their contribution to initiation. Reaction site studies were conducted at high temperature (2000°C) and room temperature (under rapid oxidation conditions). Conditions which enhance reaction rates and lower initiation temperatures were identified.

The experimental arrangement consisted of heating 16 gauge diameter aluminum wire within an oxygen/methane flame (about 2000°C) enveloped in a prescribed environment. The environments were O₂, H₂O vapor and air. Indium and zinc fluxes; aluminum particles; and a sodium hydroxide surface treatment enhanced the formation of active sites at high temperatures. A gelatinous and amorphous Boehmite oxide type was formed at ambient temperatures; whereas at high temperature, alpha aluminum oxide (Al₂O₃) was formed. The oxides formed were evaluated using the scanning electron microscope (SEM) and by determination of refraction indexes.

One thousand phase diagrams of various materials and aluminum oxides were reviewed to identify those which have the potential for significantly lowering the melting temperature of aluminum oxide. A reduction in melting temperature could correspond to reduction in the protection the oxide provides the base metal from further oxidation. The following materials, in various combinations, did lower the melting point: K₂O, SiO₂, Na₂O, CaO, Li₂O.

This line of investigation was terminated after the above work was performed. The development of equipment to permit these studies to be made in the temperature range from 600 to 800°C appeared to be more costly than appropriate; that is, the funds which would be available to evaluate positive results in simulated bleed-outs, would not be available.

8.4 Ignition and Propagation Study

Calibration experiments were made to develop the data necessary for designing controlled experiments to study ignition and propagation. Most of the experiments were done with aluminum wires because the experimental procedure is more controllable and theoretical interpretations are more direct. Wire of 1.63 mm diameter was used for the preliminary tests. Wires with diameters about 130 μ and aluminum foil 2.5 to 250 μ were planned to be used in evaluations.

Test parameters variations included the effects of water depth, diameter, pH and temperature on ignition and propagation. Different methods of heating the aluminum such as flame, electrical resistance, RF, RF with levitation and radiation were planned as well as pretreatment of the aluminum surface (abrasive, mercury, acid, base). The spectrographic and photographic exposures had to be determined for the conditions used.

Initial calibration experiments were performed in which aluminum was burned in water vapor and under liquid water. It was found that the aluminum burning rate and temperature accelerated significantly when the burning environment was changed from air to water vapor. More calibration experiments would have had to be made to complete the required definition of experimental conditions.

This study was discontinued as the effort required to define the experiment was judged greater than the potential benefits and because it paralleled Gurevich's work to some degree.

8.5 Thermite Reaction Study

The object of this study was to determine metal-metal oxide conditions conducive to low initiation temperatures. If the results indicated a strong probability for initiation at low temperatures, studies would be conducted in water vapor environments. The reaction between molten aluminum and iron oxide could have been significant in the initiation of a catastrophic aluminum-water explosion. Aluminum powder (solid propellant rocket grade) and ferric oxide (Fe_2O_3) were reacted in differential thermal analysis (DTA) laboratory equipment. The differential thermal analysis was conducted on mixtures of atomized Al (reported 13 μm size) with different iron oxides, Fe_2O_3 and Fe_3O_4 , and with a black iron oxide scale obtained from one of the steel plates used in the gross experiments.

The DTA curves exhibited a sharp endotherm when the Al melted, and a broader exotherm, when the thermal reaction took place. The exotherm initiated at about 1400, 1500 and 1650°F for the three oxides respectively. These results did not indicate that thermite reactions had the potential for lowering the initiation temperature and the study was terminated.

8.6 Debris Examination

Scanning electron microscope (SEM) and index of refraction analysis were made on debris samples from gross experiments. Scanning electron microscope analysis of explosion debris showed fine particle aluminum ($\sim 10\mu$) to be present. Holes and pits were observed on aluminum sections. The specimens were viewed from 20X to over 30,000X magnification.

Index of refraction measurements were made on the specimens. Half the specimens had indexes in the range from 1.745 to 1.765 and half in the range of 1.626 to 1.554. The higher range corresponds to α - alumina (index = 1.765) with a slight amount of water absorbed or chemically combined, accounting for the slightly low index values. The lower range of indexes is below that for

aluminum hydroxide ($1.556 \leq \text{index} \leq 1.587$). These samples had a considerable amount of water in them and appeared to be fibrous.

The examination did not provide information which was useful in establishing initiation mechanisms. For this reason, further examinations were not made.

2

9. LARGE SCALE SIMULATIONS

Research on molten aluminum-water initiation has been conducted on the basis of simulating commercial DC bleed-outs by means of large scale experiments. The majority of the work has been accomplished using 50 pounds of molten aluminum "dropped" from number 60 crucibles which incorporated 3-1/4 inch diameter flow ports. This experimental procedure has been referred to as "Gross Experiments." These types of experiments have provided controlled explosions which occur on the order 2 out of 3 attempts. A modification to this technique has been used to obtain a higher incidence of initiation. The modification is the addition of an explosive source. It is believed that this procedure provides an "artificial" initiation, in comparison to a "natural" initiation. This technique was not implemented in the work conducted by IITRI.

9.1 Overview

The gross experiments were expected to fulfill several roles in the program. These roles were to change as progress was made in understanding the fundamentals of the initiation mechanism. Initially, the experiments were to provide photographic data which would be used to aid in selecting more sophisticated instrumentation. Thereafter the data would be used in conjunction with the other program studies to guide the investigation. The gross experiments were then to be used to verify the various aspects of the mechanisms identified or postulated. Finally, this evaluation method would be used to refine and validate the initiation model. A total of 15 experiments were performed with 10 of these producing reactions. The reactions ranged from mild steam "pops" to an "extremely violent explosion" but did not include a catastrophic event. The most significant data obtained from the gross experiments was related to the development of electrostatic charge buildup during the interaction of molten aluminum and water. It had been predicted (theoretically) that significant bulk charge could be developed during the flow period which might discharge

and initiation chemical reaction. Special electrostatic charge detection instrumentation was designed and used to verify and characterize the bulk charge.

As indicated in sections 1.3 and 1.4, the 40,000 pictures per second (pps) framing rate was too slow to obtain multiple pictures of an explosion. This established that the initiation takes place in less than 25 microseconds (μ s). Thus the high speed photography was not able to aid significantly in understanding the initiation mechanism by providing fundamental data. Consequently this basis for selecting/applying more sophisticated instrumentation did not develop, except for the obvious use of photographic equipment which would provide a higher number of pps. This could not be done practically because equipment with this capability requires exact time sequencing with the initiation. The exact time of initiation could not be predicted and precursor signals were either non-existent or not identified.

Because of the above problem, this activity was stopped after 15 gross experiments were performed. This experimental method had become marginal as to the information obtained in comparison to the cost. Small scale experiments were used to continue this investigative effort which reduced the cost and were more amenable to high resolution photography. The small scale effort is reported in Section 11, the large scale facility and experiments are described in the following sections.

9.2 Facility Preparation

The melt-detonation facility site was constructed at IITRI Explosive Research Laboratory, Kingsbury Ordnance Plant (KOP), Kingsbury, Indiana (near LaPorte) on the north range. A plan view of the facility is shown in Figure 9.1. The bunker was sized to protect the building from direct fragment impact and to provide orthogonal camera observation tunnels. This arrangement was compatible with the location of the Hycam Camera which was about 50 feet south of the tunnel center lines intersection.

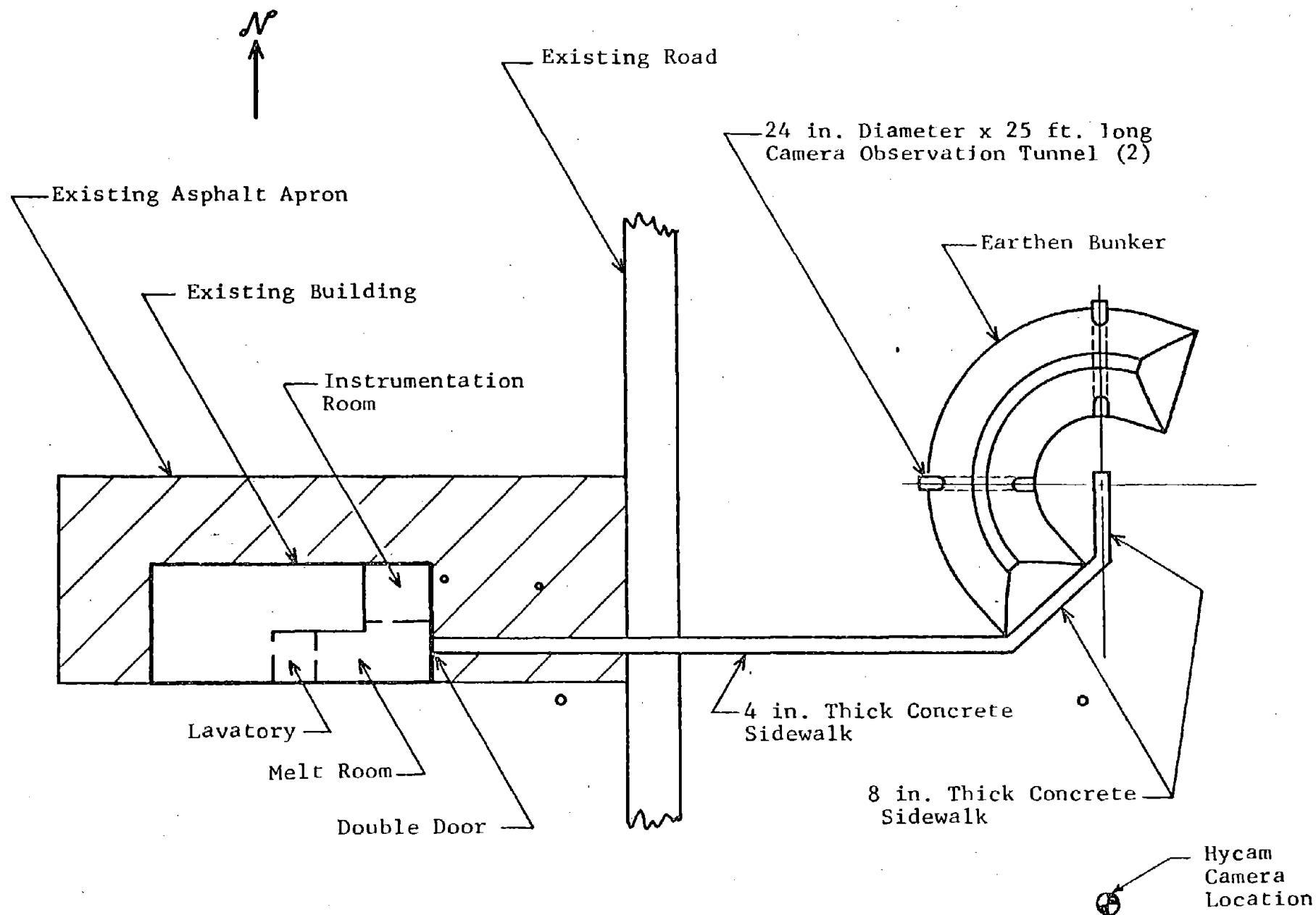


Figure 9.1 Plan View of Melt/Detonation Facility at Burning Area Unit Y-8, Kingsbury Ordnance Plant.

These locations and the bunker design depend upon the elevation of the initiation location and camera field of view. Figure 9.2 shows the base line configuration used in the large-scale gross characterization experiments.

The bunker protects the building from direct fragment impacts. The ceiling over the instrumentation room and the front of the building, facing the detonation site, were protected from ballistic fragment impact. The instrumentation room housed the communication equipment, operational and safety controls. Operations personnel inhabit the instrumentation room during the conduct of experiments.¹

The furnace was planned to be located close to the double doors in the melt room (Fig. 9.1) and to be serviced by chain fall for removing the melt crucible from the furnace and placing it on a four wheel cart. The double doors permit the cart to be brought into the building. A 3-foot wide concrete walk was provided for safe transportation of the aluminum to the experimental site. A separate furnace was planned to be used to preheat the crucible provided with the remotely removable plug.

The furnace was actually located outside of the melt room double doors just south of the sidewalk and adjacent to the building. The preheat furnace for the drop crucible did not work out as the crucible cooled too fast. The drop crucible was insulated and placed in position at the drop site and preheated with a bull torch. The bull torch was removed just before the aluminum was transferred from the melt crucible to the drop crucible. Photographic and descriptive material on the experimental site and operation are presented in Appendix C.

¹ The facility construction was funded by IITRI.

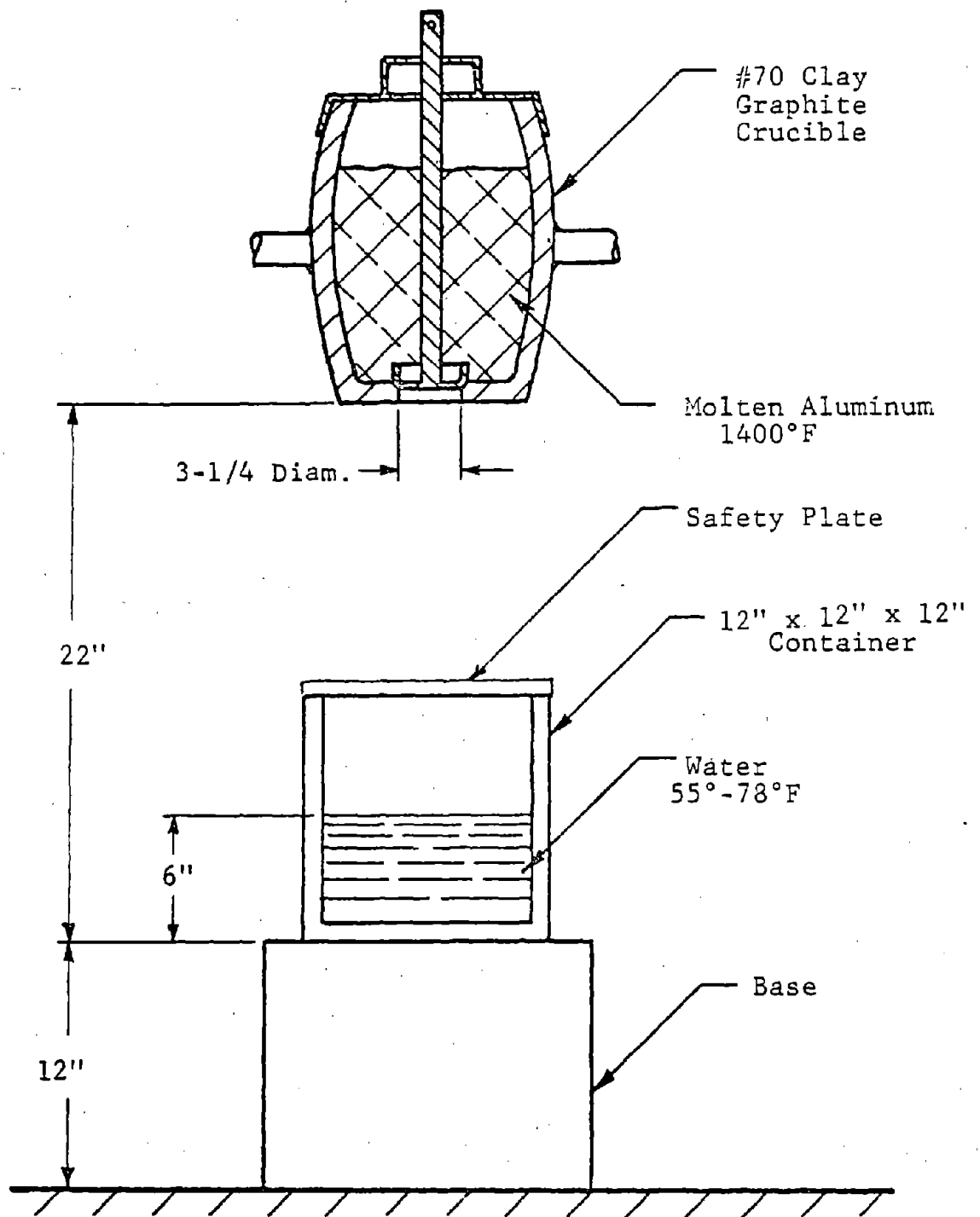


Figure 9.2 Base Line Configuration, Molten Aluminum Water Explosion, Initiation Study

9.3 Instrumentation

The primary instrumentation used in the gross experiments was photographic. Overall documentation was obtained with a Bell and Howell 16 mm camera operated at 64 pps. Intermediate data was obtained with a fastex camera operated at about 4000 pps. The primary photographic data source was a 400 foot reel capacity hycam camera¹ operated at framing rate of up to 44,000 pps. Most of the useful portion of the hycam data was taken at 40,000 pps. The higher rate is the peak value which is attained near the end of the reel.

Color film was used in all of the cameras throughout the 15 experiments. Infrared film was used in the fastex camera for experiments Nos. 14 and 15. This film type did not provide any usable visible data. A diffraction grating was used in experiment 5, with color film in the fastex camera. It did not reveal any helpful spectral information and obscured details of the interaction. Therefore, the diffraction grating was not used again.

An attempt was made at obtaining air blast over pressure during experiments Nos. 10, 11 and 12. The signal to noise ratio was not great enough to provide useful data. It would have required an expenditure of funds, which was not considered commensurate with information which could be obtained, to acquire this data. Therefore, this instrumentation was discontinued.

Two types of sensors (see Section 10) were designed and used to detect bulk electrostatic charge developing during the interaction. This type of instrumentation was used in experiment Nos. 4, 5, 6, 12, 13 and 14 and provided data characterizing the electrostatic charge developed.

¹ IITRI Scientific equipment funds were used to purchase this camera specifically for use in the program.

9.4 Experiment Results and Discussion

Fifteen gross experiments were performed of which 13 were expected to produce reactions and 10 of these did. This is slightly greater than the average proportion of events normally expected; however, no catastrophic explosions were obtained. Two basic aspects of the interaction were identified. The interaction produces a significant electrostatic charge and the initiation mechanism is triggered and propagates in less than 25 μ s.

The data for the experiments is summarized in Table 9.1. The majority of the experiments were conducted using: 12 inch square by 12 inches deep quench tanks; tap water at a depth of 6 inches; with temperatures between 60 and 70 °F, an air drop distance of 16 inches; and molten aluminum in the temperature range of 1450 to 1500 °F. The time from water contact to reaction was determined for 7 experiments and was quite constant. It ranged from 151 msec to 199 msec with an average of 177 ± 13 msec. However, two of the experiments, for which time to reaction data was determined, were made in circular tanks and should be considered separately from the square tanks. These two times were 168 msec (No. 12) and 199 msec (No. 6). Excluding these data, the time ranged between 151 and 187 msec with an average of 174 ± 16 msec. The difference is not significant. The time for aluminum to flow through the water to the quench tank bottom surface was determined in 6 instances and was 85 ± 17 msec. The variation in this initial flow period was undoubtedly effected considerably by the wide range of geometries which the leading edges of the aluminum stream developed. The aluminum stream speed, as it approached the quench tank water surface, was determined in 5 cases and had an average value of 99 ± 3 ips. This is quite consistent and using the average and standard deviation to estimate flow through 6 inches of water indicates that the average time would be on the order of 61 ± 2 msec. Thus the longer time period and variation obtained for the direct measurement may be attributed to the stream geometry. Since the standard deviation

IIT RESEARCH INSTITUTE

Table 9.1
CROSS EXPERIMENT DATA SUMMARY 11

Experiment Number	1	2	3	4	5	6	7	8	9	10	11	12	13	14	15
Date, 1973	9/23	9/26	10/2	10/10	10/17	10/23	10/23	10/20	10/26	11/1	11/1	11/8	11/8	11/20	11/20
Ambient Temperature, °F	66	75	75	85	63	70	72	60	60	50	60	38	35	52	54
Quench Tank:															
Depth, in.	12	12	12	12	12	12	12	12	12	12	12	12	12	12	9
Crosssection, in.	12x12	12x12 ²	12x12	12x12	12x12	12 dia.	12x12	12x12	12x12	12x12	12x12	12 dia	12x12	12 dia.	9-1/2 dia.
Bottom surface															
Material	Steel	Steel	Steel	Steel	Steel	Steel	Steel	Steel	Steel	Steel	Steel	Steel	Glass	Steel	Steel
Surface Cavities	yes	yes	yes	yes	yes	yes	yes	yes	yes	no	yes	yes	no	yes	yes
Quench Water:															
Type	tap	tap	tap	tap	tap	tap	tap	tap	tap	Dis-tilled	tap	Dis-tilled	Dis-tilled	Dis-tilled	Dis-tilled
Depth, in.	6	6	6	6	6	6	6	6	6	6	4	6	6	6	6
Temperature, °F	66	75	70	75	NR ⁴	70	72	60	60	58	49	55	50	55	60
10 gm CaOH added	no	no	no	no	no	no	no	no	no	no	no	no	no	yes	yes
Ph	NR	7.92	NR	8.38	NR	NR	NR	8.25	8.25	7.31	8.37	7.30	8.50	12.05	12.2
Resistivity, ohms/cm	NR	2540	NR	2710	NR	NR	NR	2640	2640	27,300	3030	27,000	27,000	184	125
Drop Conditions:															
Distance port to tank bottom, in.	22	22	22	22	24	24-1/2	22	24-1/2	24-1/2	22	22	23-1/2	24	22	22
Port opening time, msec.	21	21	21	21	21	21	21	21	21	21	21	21	21	26	21
Aluminum temperature, °F	1450	1470	1475	1525	1475	1470	1470	1475	1475	1350	1575	1650	1620	1500	1520
Results:															
Reaction expected	yes	yes	yes	yes	yes	yes	yes	yes	yes	no	yes	yes	no	yes	yes
Stream Explosion Type	none	mild	violent	very violent	none	violent	none	mild	pop	none	violent	very violent	none	big thump	2 pops
Event time (t=0 @ H ₂ O surface), msec															
Bottom	NR	NR	NR	65	110	84	NR	72	74	NR	NR	104	NR	NR	NR
Side	NR	NR	NR	NR	153	119	NR	117	129	NR	NR	NR	NR	NR	NR
Reaction	NR	151	NR	175	NA ⁵	199	NR	187	181	NR	175	168	NR	NR	NR
Initial aluminum flow speed, ips	NR	92	NR	96	NR	100	NR	98	108 ⁶	NR	NR	NR	NR	NR	NR
At time of reaction:															
Pounds aluminum in water	NR	11	NR	14	NR	17	NR	16	17	NR	NR	NR	NR	NR	NR
Stream volume, cu. in.	NR	184	NR	180	NR	347	NR	417	236	NR	NR	NR	NR	NR	NR

50 pounds of aluminum from a number 70 clay-graphite crucible through an internally plugged 3-1/4 inch diameter port
 Square crosssection.
 Circular crosssection.
 NR means no record.
 NA means not applicable.
 Aluminum stream located 2 inches off center of quench tank

of the time period from initial water contact to reaction is about the same as that for the flow through the quench water to the tank bottom, the major portion of the reaction time variation may be attributed that incurred during the downward aluminum flow through the quench water.

The time from aluminum impact on the quench tank bottom to the tank sides and to a reaction may be obtained from Table 9.1. In 4 cases the time to the sides was determined as ranging from 35 to 55 msec with an average of 45 ± 10 msec. In this case the round tank data is applicable. The time period from first contact with the quench tank bottom and reaction was determined in 5 cases and ranged from 64 to 115 msec with an average of 102 ± 21 msec. If the times for the round tank (nos. 6 and 12), 64 and 110 are eliminated, the times are: 107, 115 and 115 msec with an average 112 ± 5 msec. This would seem to indicate two different regimes of reaction time. The 64 msec time to reaction seems more closely associated with the side impact time which averages 45 ± 10 msec and which will range up to 75 msec. The average radial flow speed (for round or square tank) is 97 ips $[(6-3.35/2)/.045]$ with a standard deviation of 17 ips. The average time for the radial flow to each a corner (square tank only) would be 70 msec $[(6\sqrt{2} - 3.25/2)/97]$ with a standard deviation of 15 msec. Thus, the longest time would be 115 msec which includes the time period for the late reactions cited above.

In five experiments, numbers 2, 4, 6, 8 and 9, the following data was obtained:

- incoming aluminum speed
- weight of aluminum in quench tank
- stream volume present at reaction
- reaction time

There is no obvious correlation with the reaction strength. Experiment numbers 11 and 12 had reaction times determined and they do not correlate with reaction strength. Very violent reactions took place at 160 and 175 msec; violent ones at 175 and 199 msec; mild at 151 and 187 msec; and a "pop" at 181 msec.

In the limited cases where; water and resistivity data are available, no correlation appears evident to reaction occurrence or strength. At best, the results of experiments 14 and 15 in which 10 grams of calcium hydroxide (CaOH) was added to the quench water, which had high Ph and low resistance, the reaction strength was reduced. It would seem more likely that the C_aOH stabilized film boiling rather than that the Ph or resistance were important. Distilled water, which has a high resistivity, was used in experiments 10, 12 and 13. Experiment 10 had a furnace oxidize steel plate which had not been sand blasted and is assessed, therefore, not to have surface cavities so it could not react. Experiment 13 was made with a glass quench tank bottom surface and so it would not be expected that a reaction could take place. Thus only experiment 12, which had a violent steam explosion, of the 3 which had distilled quench water (with very high resistance) could react and did violently. Since high resistivity would reduce the tendency for the electrostatic charge to discharge, the main cause and effect relationship which could be postulated would be a reduced surface tension effect on the quench water. This is interpreted to have destabilized the film between the molten aluminum and water and thus enhancing spontaneous nucleation of the water.

9.5 Summation

The gross experiments provided two types of results: those which are demonstrated and those which are of a circumstantial nature. The results stated in Section 9.1, Overview, are of the first type while those indicated by Section 9.4 and presented in this section are of the second type.

One interesting tentative result arises from experiment no. 10. The aspect referred to is that the steel plate forming the quench tank bottom surfaces was not sand blasted; it was furnace oxidized. At the time the experiment was made, experiments on the quench tank surface type were related to the type of oxide present and how it was generated rather than the presence

of surfaces cavities or lack of surface cavities. This comparison has been changed in presenting the data now (as is evident in Table 9.1). The lack of a reaction in experiment 10 may be used to support the contention that surface cavities must be present to have a reaction. This claim is weakened by the fact that only about 77 percent of the expected reactions were obtained so that the lack of a reaction could be attributed to this experiment falling in the 23 percent that are unexplained. However, this does suggest an interesting experimental condition, the use of a nonoxidized sand blasted quench tank bottom surface.

Other circumstantial results rest on the lack of apparent correlation with the experimental variables noted at the end of the Section 9.4. This directs the meaning of the experimental results toward the initiation mechanism defined as spontaneous nucleation triggered by an impact shock.

The mild reaction obtained for experiment 15 might well be caused by the smaller diameter tank used. The aluminum surface radial flow speed would be lower because the potential flow would not have accelerated to as high a speed as it would with larger crosssection tanks. The lower flow speed would correspond to a weaker impact shock and hence less water would be spontaneously nucleated. The eccentric position of the impact point of the aluminum stream in experiment 9 should provide an early or late reaction time. Early because the first surface impact would come sooner due to the eccentricity and late because the radial flow would reach the farthest corner later. The reaction time was at 187 msec which was 115 msec after first bottom contact which is late. As the limited data show, the three experiments made in square tanks, for which reaction time was available, had initiations associated with the time for flow to a corner rather than a side. Initiation time data for 2 of the round quench tanks show the time to be 115 msec (No. 67) and 64 msec (No. 12). The shorter time is associated with the radial flow to the diameter where as the larger time would have to be associated with

with another condition. As indicated in Appendix C, this would be associated with tangential flow resulting from impact eccentricity. The tangential flow condition is presented and discussed in Section 12.

Finally the role of electrostatic charge may be inferred from the results of experiments 10, 12, 13, 14 and 15. In the first three cases the quench water was distilled which has a resistivity an order of magnitude higher than the tap water used in the other experiments. High resistivity is associated with the development of higher electrostatic charge. That is, the charge developed does not leak off or discharge as easily. In experiments 10 and 12, no reaction was expected because the surfaces were smooth. If the electrostatic charge were the initiation mechanism, it could have been expected that these experiments would have had reactions. In contrast, it may be argued that high resistivity water prevents electrostatic discharge and hence this initiation mechanism is inhibited. Experiments 14 and 15 had quench water with resistivity two orders of magnitude lower than the distilled water and one lower than tap water. Then, if low resistivity was the key to effective electrostatic discharge initiation, these two experiments should have had reaction as strong or stronger than any encountered. This was not the case at all, but the opposite, the reactions were among the weakest obtained. Experiment 13 was one of the 2 most violent (the other was No. 4). The role which the higher electrostatic charge may play is that it reduces the water surface tension making the film in film boiling less stable and hence easier to collapse.

9.6 Conclusions

Two kinds of results have been claimed for the gross experiments: demonstrated and circumstantial. The demonstrated ones were that: the initiations takes place in 25 μ s or less because it takes place between pictures on 40,000 pps film records; and that an electrostatic charge is developed during the interaction

between molten aluminum and water. The circumstantial evidence is that: the role of the electrostatic charge is to destabilize the film in film boiling and does not constitute an initiation mechanism (by discharge initiation of a chemical reaction); the initiation mechanism is spontaneous nucleation of quench water; and an impact shock generated by aluminum flow over the bottom surface of the quench tank is the trigger mechanism for spontaneous nucleation. In addition, the most likely position for the flow to produce the impact shock is associated with a corner of the square quench tank.

10. ELECTROSTATIC CHARGE STUDY

This study was initiated early in the program by performing analysis which indicated that there was a significant possibility that electrostatic charge phenomena could play an important role in the interaction between molten aluminum and water. The flow of molten aluminum into water produces electrostatic charges in the water. The electrical energy may enter the interaction by discharging (as a condenser) and/or by destabilization of the water vapor film (same effect as reduced surface tension). This section presents a description of the gross and laboratory investigations and a preliminary conclusion that electrostatic discharge does not enter the reaction. In addition, discussion of the role electrostatic charge may have, through the effect on surface tension, is presented.

10.1 Gross Experiments

Experimental determinations have been made of the electrical phenomenon taking place during bleed-out simulations made with 50 pounds of aluminum. Voltage buildup has been measured by inserting electrodes in the quench tank. Bulk currents have been measured by placing solenoid coils around the quench tank.

The experimental method using inserted electrodes depends upon measuring a voltage across two electrodes and knowing the resistance between them. This voltage and resistance are used to define a leakage current which in turn are used, with bulk resistance of the quench water, to determine the bulk voltage developed. The uncertainty in this method lies in knowing the actual resistance between the inserted electrodes during the aluminum flow period. The resistance could be significantly lower than that measured before the start of the pour. Electrode voltages measured ranged from one to 2.3 volts, which when considered flowing through 700 ohms of water resistance corresponds to 1.4 to 3.3 milliamperes. The bulk resistance of tap water is 3000 ohms which means that the bulk voltage present

ranged from 4.2 to 9.9 volts. In distilled water the bulk resistance is greater by a factor of ten, so that the bulk voltage could be as great as 99 volts. However, it is not unreasonable to suggest that the resistance between electrodes could have been lower by a factor of as much as 700 which could make the current 2.3 amps and the bulk voltage as great as 69,000 volts.

The experiments made using the solenoid technique, to determine bulk current, voltage and energy, indicated much greater transient electrical phenomena. The voltage induced in the solenoid coil by the aluminum flow through the water is integrated with respect time to determine the bulk current. The current is multiplied by the bulk water resistance to obtain the bulk voltage. The product of the bulk current, voltage and time yield the instantaneous energy. IITRI experiments 12 and 14, which resulted in violent explosions, exhibited the following bulk values during these experiments: current - 98 and 59 amperes; voltage - 294 KV and 176 KV; and energy - 144,000 and 51,900 joules. Experiment 13 did not result in an explosion and the following maximum bulk values were obtained: 9.8 amperes, 29 KV and 1,440 joules. Similar values to these were obtained early in experiment 14.

Reconstructing the time history for experiment 14, it appears that there was an immediate indication of electrical phenomenon which persisted for approximately 200 milliseconds after the aluminum flow initiated the recording circuit (at water entry) until the explosion. The explosion occurred about 70 milliseconds after impacting a side wall of the 12 inch diameter glass quench tank indicating an induced voltage of 60 mv (and went off scope) in about five milliseconds. The entire time from the start of pour to the explosion was about 0.3 second. The voltage trace exhibited a basic amplitude of about eight millivolts, + 4 mv to - 4 mv. The frequency of the solenoid voltage appears to be 400 ± 100 cps. There were voltage excursions to peak values ± 10 mv during the first 50 msec, none during the second 50 msec, two in the third 50 msec to ± 14 mv and at the explosion, the trace went

off scale at 60 mv in five msec or less. This last excursion corresponds to bulk values of 50 amps, 176 KV and 51,900 joules reported above. The 10 mv in the coil corresponds to the bulk value report for experiment 13.

Interpretation of the limited data is difficult. The 13th experiment was made with a glass bottom tank, whereas the others were steel. Thus, it is ventured that this electrical phenomenon is indicative of flow generated effects, whereas those of larger magnitude reflect the effects produced by the explosion. The question then remains as to the effect of electrical phenomena characterized by the development of the following minimal values: 10 amps, 30 KV and 1500 joules. The condition, in the molten aluminum interaction, is water separated from aluminum by a layer of steam insulating the electrostatic charge built up in the aluminum. It would appear, from the gross experiments using the solenoid coil, that the bulk electric charge arises from a current flow from the aluminum to the water as a result of periodic steam film collapse. The resistance of the aluminum oxide layer, 50 Å [5(10⁻⁷)cm] thick on the aluminum is 10¹⁴ ohms/cm which amounts to 50 million ohms. The arcing voltage required is 500 million volts [$V = I \cdot R = 10(5)(10^7)$] which is four orders of magnitude greater than the 30 KV measured when there is no explosion (Experiment 13) and the maximum voltage measured during an explosion is three orders of magnitude less. It seems clear that the electrical phenomena measured in the 13th experiment provided criteria that it was insufficient to cause an explosion (none took place). Thirty KV will not arc through the oxide layer.

10.2 Laboratory Experiments

The experimental determination of the large amount of available electrostatic energy (in gross experiments) provided the stimulus for a laboratory investigation of the initiation characteristics of aluminum particles mixed with water. Approximately 200 small scale evaluations were made; Tables 10.1 and 10.2

Table 10.1
NUMBER OF TESTS WITHOUT ADDITIVES

Particle Size (ft)	Mixture Weight Ratio Aluminum/Water					Water Only
	Only Metal	0.25	0.50	1.0	2.0	
Water	-	-	-	-	-	1
13	1	7	29	27	13	-
300	-	-	15	10	16	-
830	-	-	7	-	-	-

Table 10.2
NUMBER OF TESTS WITH ADDITIVES

Particle Size (U)	Weigh Ratio Aluminum to Water	Additive		Number of Tests
		Weight (%)	Material	
None	Only Water	20	Sackrete	3
13	0.5	20	Sackrete	12
13	0.5	10	Fine Al_2O_3	4
300	0.5	10	Fine C_aCO_2	11
300	0.5	10	Sackrete	12
300	0.5	20	Sackrete	9
300	0.5	30	Sackrete	9
300	0.5	?	Fe_2O_3	4
830	0.5	?	Fine Concrete Chips	7

summarize the experimental variables. The experimental procedure was to subject about 0.5 cc of the aluminum-water mixture to the axial discharge of a 0.04 microfarad condensor through the mixture. The sample was placed within a length of 1/16 inch inside diameter tygon tubing which was forced over the electrodes forming a seal. The capacitor was charged and discharged to increasing voltages until the sample was initiated (quite often a significant "fire ball" was obtained). After achieving an initiation, the voltage level was increase or decreased in a manner similar to a Bruceton technique to determine the required initiation energy level. Statistical significant levels were not established as the total effort would have been too great. The basic experiments were performed using 13 and 300 micron size particles with weight ratios (to water) of: .05, 1.0 and 2.0. Figure 10.1 summarizes the basic data and includes two additional conditions: 13 micron particles at a weight ratio of 0.25 and 830 micron particles at a weight ratio of 0.5.

Initiation energies ($1/2 CV^2$), based upon the 0.04 μf capacitor and charged voltage ranged from 1/2 to 40-1/2 joules. The data shown for 300 micron particles at a 0.5 weight ratio reflects three separate series and for 13 microns at a weight ratio of one for two series. A general trend may be ascribed to these results which indicates that the initiation energy required increased with particle size and metal weight.

The effect of distilled and dionized water used with 300 micron particles, in comparison to tap water (data in Figure 10.1) was not discernable. The initiation energy levels were 4.5 to 8 joules for both, which is in the mid range of energy for tap water. The same weight ratio and metal size was used to evaluate other additives. Additives of 10, 20 and 30 percent sackrete (concrete ready mix) and ten percent of iron oxide (Fe_2O_3) had no significant effect. The addition of ten percent of calcium carbonate did indicate an increase in energy required; the range was 12.5 to 24.5 joules. The small aluminum particles were mixed with 10

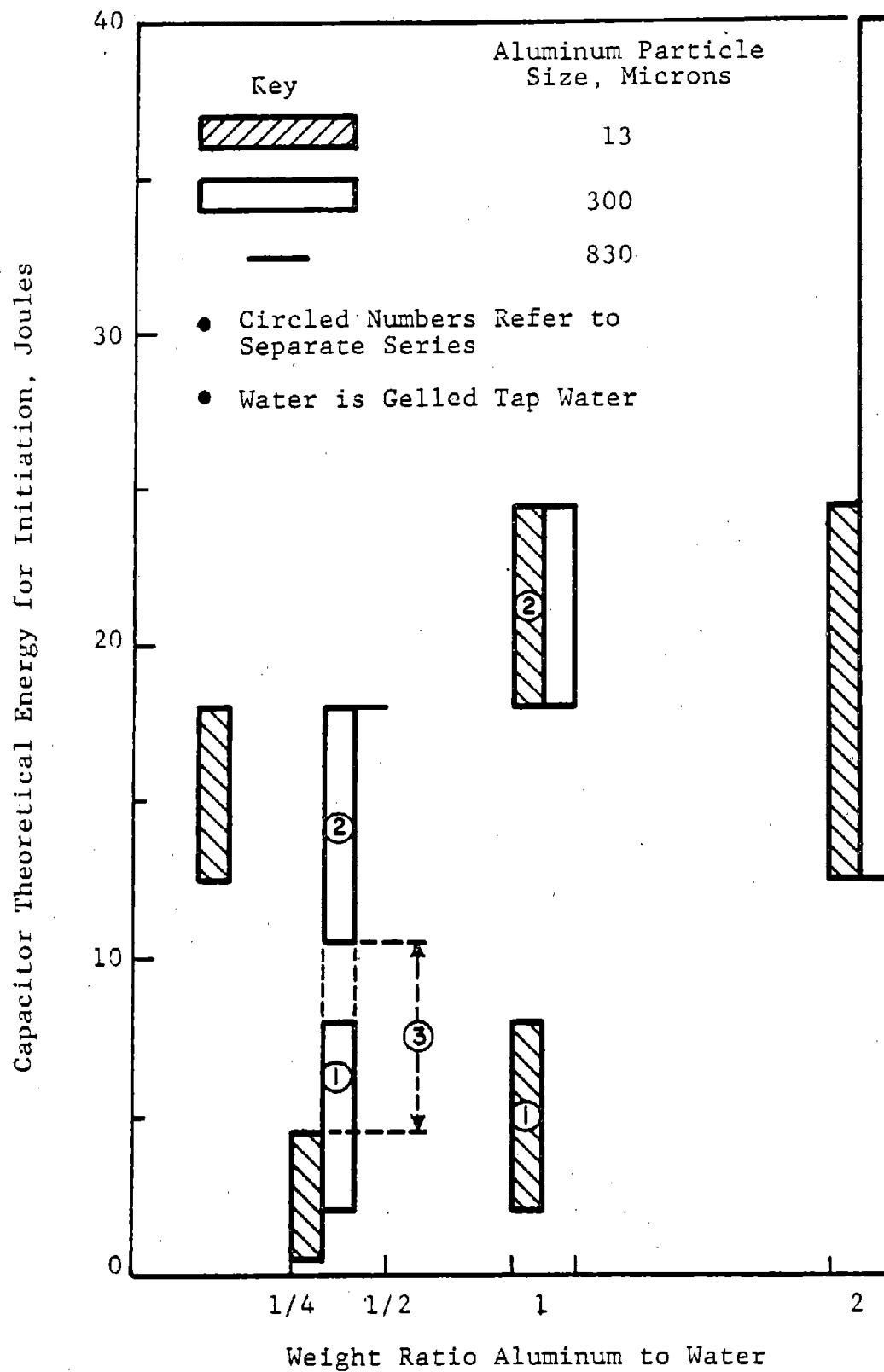


Figure 10.1 Ignition Energy Versus Aluminum-Water Ratio

IIT RESEARCH INSTITUTE

percent sackrete and required: 8 joules at a weight ratio of 0.25 and 4.5 joules at a 0.50 weight ratio. These particles without water, could not be initiated with 32 joules. The addition of fine chips of concrete to 830 micron size particles, at a 0.5 weight ratio with water, reduced the initiation energy to 4.5 to 8 joules (from 18 joules).

10.3 Conclusion Regarding Electrostatic Discharge

Although the above data are not "precise", the fact that 1500 joules of energy were presumably available in gross experiments, when explosion did not take place, would seem to have some significance. Since there would have been almost 40 times as much energy available, as necessary to initiate a highly visible trigger (fire ball in laboratory experiments), it could be concluded that there were very few aluminum particles (in the gross experiment) at or below 830 micron. More generally, it is indicated that:

- Aluminum particles are not present in significant number in the simulations
- The mixture ratio in simulations corresponds to a high concentration of aluminum in the neighborhood of a discharge, if one took place.
- The water-aluminum "capacitor" did not discharge.
- The electrostatic charges built up do not play a major role, but at best a synergistic role in the initiation.

10.4 Surface Tension Effect

Droplets or bubbles become unstable when they become electrically charged. The criteria for destabilization, according to Lord Rayleigh, is:

$$\sigma < Q^2 / [16 \pi r^3]$$

where:

σ = surface tension

Q = electrical charge

r = spherical radius

IIT RESEARCH INSTITUTE

Thus the destabilizing criteria becomes:

$$\sigma < V^2/16 \pi r$$

The stability criteria for vapor bubbles is:

$$P_v \leq P_a + 2\sigma/r$$

where:

P_v is the vapor pressure

P_a is the surrounding pressure assumed atmospheric.

Rearranging this equation to define the radius:

$$r = 2\sigma/[P_v - P_a]$$

and solving the electrical instability criteria for voltage and substituting the above value for the radius,

$$V > 4\sigma[2\pi/(P_v - P_a)]^{1/2}$$

The surface tension of water is assumed unchanged by temperature (it decreases) and the P_a is assumed to be atmospheric and P_v is assumed to correspond to a water temperature. Figure 10.2 was prepared under these assumptions and indicates that at 100°C a charge corresponding to the bulk water voltage of two volts could trigger spontaneous nucleation of any vapor bubbles present. It is noted that at the limit of superheat, assumed 267°C, no electrification should be required, even though Figure 10.2 indicates 0.11 volts would be required. The curve would pass through zero volts at 300°C which is often taken as the superheat limit.

Thus, it would seem that the development of bulk voltage could trigger a vapor explosion. The experimentally determined bulk voltages (in 50 pound drops) were considerably in excess of two volts, on the order of 29,000 volts. Using the electrical destabilization criteria to estimate the bubble radius which could be destabilized by this voltage, it would be less than:

$$r > V^2/16$$

$$r > (29,000)^2/16 \quad 81$$

$$r > 200,000 \text{ cm}$$

IIT RESEARCH INSTITUTE

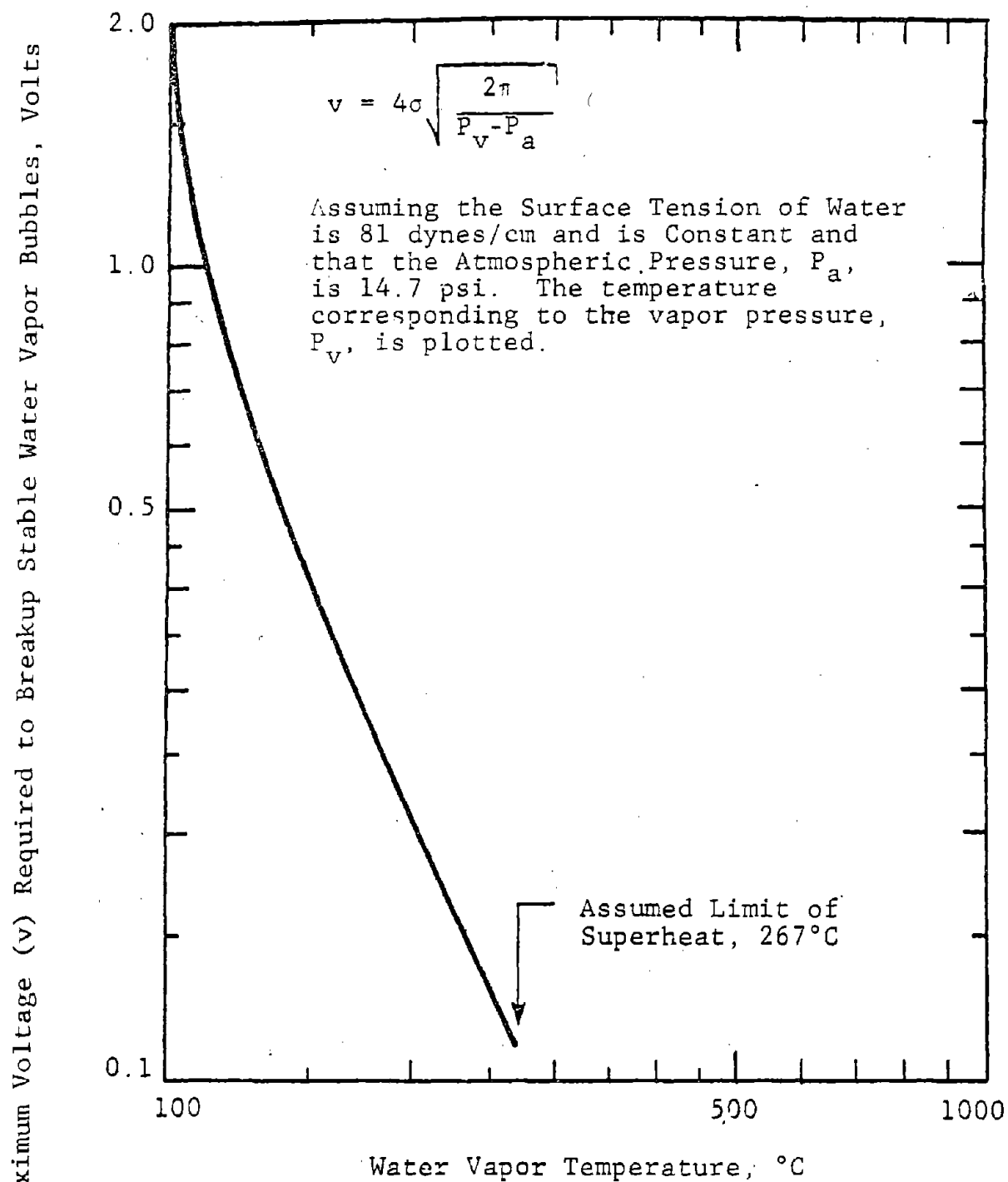


Figure 10.2 Bubble Destabilizing Voltage Versus Water Vapor Temperature

This does appear ridiculous but could indicate that any size vapor bubble present would become unstable. As may be seen from the above radius stability criteria, the smaller the bubble (or nucleus) the less the destabilizing voltage required: e.g., very small bubbles require very small voltages to destabilize them, e.g., 0.2 volt will destabilize a bubble with a ten micron radius. A better way of viewing the effect of electrification is that it may destabilize the vapor film (steam) between the molten aluminum and liquid water. This action would "help" the impact shock (produced by an aluminum impact) collapse the film and provide liquid-liquid contact. The steam film may be considered a sphere with an infinite radius, e.g., 200,000 cm.

10.5 Role of Electrical Phenomena

A role which the electrical phenomena may play, is postulated in this section. In presenting it, an observation made by project staff from our Electronics Division is presented as well as some discussion of the implication. In describing the electrical signal recorded during 50 pound drop tests, made with the inserted electrode device, it was reported "... from 120 to 200 millisecond is the recording of voltage buildup as charged molecules are in the aligning process ...". The 120 millisecond referred to is the time at which the aluminum stream contacted the quench tank bottom surface and the zero time was associated at a location about six inches above at the air water interface.

The point of recounting this is, that although the electrostatic charge starts building up during the initial flow, some time is required to align the charges and develop the voltage. In the inserted electrode experiments, the electrodes were shorted out when the aluminum arrived at and filled the space between them. Thus it is reasoned that the time frame reported may be dependent on the measuring technique. In that particular experiment, the explosion came at about 600 milliseconds which is 400 milliseconds after the reported voltage buildup (which was about 2 volts). This 400 millisecond period would be considered an

induction time for the voltage to "take effect" or rather for there to be sufficient nuclei available for the voltage to destabilize and/or to destabilize the steam film in conjunction with the impact shock.

In relation to the availability of bubbles or a film available to destabilize, the results obtained with the 13th gross experiment are cited. This experiment was made using an all glass (including glass bottom) quench tank. The bulk voltage, calculated from measurement of induced solenoid voltage, was 29,000 volts and yet no explosion occurred. In presenting the role of electrification, the reason for no explosion would be that there was no water and little or no steam between the glass and aluminum. The glass bottom contained no liquid water to form bubbles which could be triggered to affect spontaneous nucleation. Therefore there was nothing available to form a trigger. This reasoning precludes the bulk mixture (away from the bottom surface) from entering a trigger action.

10.6 Summation and Conclusion

The incoming flow of aluminum develops an electrostatic charge. The impact of the aluminum on a surface, which has very small water containing cavities, creates a thin steam film between the aluminum and bottom surface, effectively insulating the water in the cavities from the molten aluminum. The flow of the aluminum to the side walls of the quench tank aligns the charged molecules establishing the bulk voltage. An aluminum impact collapses the steam film (the electrostatic charge may reduce the stability of the film) permitting liquid aluminum-liquid water contact and the electrification of the liquid water. These processes are considered related to: the size of the surface cavities containing liquid water, the distribution of these cavities and location of this distribution with respect to the liquid aluminum. The electrical charge is envisioned as amplifying the effects of the vapor explosion caused by liquid metal-liquid water contact.

The vapor explosion provides a shock pulse which is propagated through the aluminum-water mixture. The strength of the trigger and the nature of the mixture in the vicinity of the initiation shock may have a significant effect on the propagation. The electrostatic charge in the water may well play a part in the propagation phase of the interaction. Given a trigger (vapor explosion) the effect of the electrostatic charge may be to drive the propagation toward a more violent final reaction. The reduction in water surface tension could promote repeated vapor explosions, induced by shock collapse of vapor. The steam film surrounding the molten aluminum could be less stable than otherwise, because of the electrostatic charge.

11. SMALL SCALE EXPERIMENTS

Qualitative data describing the interaction of molten aluminum and water which illuminated initiation parameters were not obtained from the gross experiments. A small scale drop facility was designed and put into operation which could accommodate 1 pound of molten aluminum. The size of this equipment reduced the cost of operation and facilitated the use of diagnostic instrumentation which was not practical to use in 50 pound simulation experiments. Fifty one experiments were performed.

11.1 Overview

The study included six interaction variables; the basic parameters held constant were: 1/2 pound of aluminum; 3/8 inch diameter aluminum stream size; 2 pound drop opening weight; and the combined melt/drop crucible. The parameters varied and their values are summarized in Table 11.1.

Table 11.1
SMALL SCALE BLEED-OUT SIMULATION EXPERIMENTAL VARIABLES

Line No.	Parameter	Parameter
1	Drop height, inches	5, 18 and 23-1/2
2	Water depth, inches	2, 5, 7 and 8
3	Quench tank: volume, ml diameter, inches	250, 500, 1000 and 2500 2-1/2 and 5-1/2
4	Water: Type Temperature, °F Additives (1-2% by volume)	Tap, boiled and distilled 33, room (50 to 70) and 150 Aluminum sulfate, sodium bicarbonate, water soluble oil, liquid soap and tarsol coated bottom surface
7	Aluminum Temperature, °F	1450, 1500, 1650, 1750 and 1850

The experimental series was planned to obtain qualitative information regarding: encapsulation, bubble collapse, interaction generated shock waves and motion of aluminum and water. The major drawback in the experimental setup was that the 3/8 inch diameter stream broke into segments which did not represent the heat sink characteristics of the large scale experiments. It became clear that many of the postulated fragmentation phenomena described in the literature did not apply to initiation resulting from DC bleed-outs.

11.2 Equipment Description

The experimental equipment was quite similar to that for the 50 pound simulations. However, since explosions were not expected, the aluminum was melted and dropped from the same crucible. An electric furnace containing the melt/drop crucible was positioned 30 inches above a rigid surface on a steel frame over the quench tank. The crucible plunger weight opening arrangement was similar to that used for the 50 pound drops. The drop height was adjusted by placing the quench tank on various height blocks. The furnace support frame was made wide enough to provide an unobscured view.

The basic data was obtained photographically. Overall documentation was obtained with a 16 mm camera operating at 64 pps and interaction details were obtained with a 16 mm fastex camera operated at 2000 to 3000 pps. Flash x-ray equipment was used in over half of the experiments. In many instances 2 x-ray heads were used and in several experiments 3 x-ray heads were employed.

11.3 Results

A summary of the test conditions used in this study is presented in Table 11.2. The effect of changing the variables was to produce changes in the steam developed by the molten aluminum and the geometry of the aluminum stream segments as they passed through the quench water or steam formed by the previous segment. The effect of the applied electric field was to cause earlier and greater stream segment breakup. The results may be illustrated best by the radio-photographs from selected tests. Figures 11.1 through 11.4 show

MIT RESEARCH INSTITUTE

Table 11.2

ONE HALF POUND THREE EIGHTS INCH DIAMETER BLEED-OUT SIMULATIONS (April through June, 1974)

Test No.	Aluminum Temperature (°F)	Drop Height (in.)	Quench Tank		Quench Water			Special	
			Volume (ML)	Type (-)	Depth (in.)	Type (-)	Additive (-)	Instru-mentation	Conditions
1	1600	28-1/2	200	Beaker	1-1/2	Tap	-	-	-
2	1600	28-1/2	200	Beaker	1-1/2	Tap	-	-	-
3	1600	28-1/2	200	Beaker	2	Tap	-	-	-
4	1600	28-1/2	250	Graduate	8	Tap	-	-	-
5	1600	28-1/2	250	Graduate	8	D&B ¹	-	-	-
6	1700	28-1/2	100	Beaker	1	D&B	30 °C	-	-
7	1800	28-1/2	100	Beaker	1	D&B	1/2 in. ²	-	-
8	1600	28-1/2	250	Graduate	8	Tap	-	-	A.E.F. ³
9	1600	18	100	Beaker	1-1/2	Tap	-	-	A.E.F.
10	1600	18	250	Graduate	8	Tap	-	-	-
11	1600	18	250	Graduate	8	Tap	-	-	-
12	1600	18	150	Beaker	2-1/4	D&B	-	-	-
13	1600	18	150	Beaker	1-1/2	Tap	NaCl	-	-
14	1600	18	100	Beaker	1-1/2	Tap	NaCl/mm	-	-
15	1600	18	600	Beaker	1-1/2	Tap	NaCl/ice	-	-
16	1600	18	600	Beaker	1-1/2	Tap	130 °F	-	-
17	1600	18	600	Beaker	3	Tap	NaCl/-4 °C	-	-
18	1600	18	2500	Beaker	5	Tap	180 °F	-	-
19	1600	28-1/2	600	Beaker	3	Tap	1% Oil	-	-
20	1600	28-1/2	250	Beaker	2	Tap	-	-	-
21	1600	18	250	Beaker	2	Tap	-	-	-
22	1600	18	250	Beaker	2	Tap	-	-	-
23	1600	18	250	Beaker	2	Tap	-	-	-
24	1600	18	250	Beaker	2	Tap	-	-	-
25	1600	18	250	Beaker	2	Boiled	-	-	-
26	1600	18	250	Beaker	2	Boiled	-	-	-
27	1600	18	250	Beaker	2	Distilled	-	-	-
28	1600	18	250	Beaker	2	Distilled	-	-	-
29	1600	18	250	Beaker	2	Distilled	-	-	-
30	1600	18	250	Beaker	2	Tap	-	-	Mercury
31	1600	18	250	Beaker	2	Distilled 2% AlSO ₄	-	1 x-ray	-
32	1600	18	250	Beaker	2	Distilled 2% NaCO ₄	-	1 x-ray	-
33	1600	18	250	Beaker	2	Distilled 2% NaCO ₄	-	1 x-ray	-
34	1600	18	250	Beaker	-	Test Aborted ⁴	-	-	-
35	1600	18	250	Beaker	2	Tap	-	-	-
36	1600	18	250	Beaker	2	Tap	-	2 x-rays	-
37	1600	18	250	Beaker	-	Aluminum Solidified	-	Test Aborted	-
38	1600	18	250	Beaker	-	Distilled 2% AlSO ₄	-	2 x-rays	-
39	1450	18	250	Beaker	-	Distilled 2% NaCO ₄	-	2 x-rays	-
40	1600	18	250	Beaker	2	Tap	2% Oil ⁴	2 x-rays	-
41	1600	18	250	Beaker	2	D&B	-	2 x-rays	-
42	1600	18	250	Beaker	2	Tap	150 °F	-	-
43	1600	18	250	Beaker	2	Tap	1% liq soap	2 x-rays	-
44	1600	18	250	Beaker	-	Furnace Malfunctional	-	Test Aborted	-
45	1600	18	2500	Beaker	8	Tap	-	-	A.E.F.
46	1600	18	2500	Beaker	8	Tap	-	-	A.E.F.
47	1600	18	2500	Beaker	6	Tap	Target	2 x-rays	-
48	1500	18	250	Beaker	2	Tap	-	-	-
49	1600	5	1000	Beaker	7	Tap	-	2 x-rays	-
50	1600	5	1000	Beaker	7	Tap	-	2 x-rays	-
51	1600	5	1000	Beaker	7	Tap	-	2 x-rays	-
52	1600	18	1000	Beaker	7	Tap	-	1 x-ray	-
53	1600	28	250	Beaker	7	Tap	-	2 x-rays	-
54	1600	18	1000	Beaker	6-1/2	Tap	2% Sol. Oil	2 x-rays	-
55	1600	18	1000	Beaker	6-1/2	Distilled 2% NaSO ₄	-	2 x-rays	-
56	1600	18	250	Beaker	-	Test Aborted	-	-	-
57	1600	18	250	Beaker	2	Tap	33 °F	2 x-rays	-
58	1600	18	1000	Beaker	5-1/2	Tap	Liquid Soap	1 x-ray	-
59	1600	18	1000	Beaker	5-1/2	Tap	150 °F	1 x-ray	-

¹ D&B = Distilled and Boiled; ² mm = morthar mix; ³ AEF = Applied Electric Field

incoming stream segments and segment geometries in the quench water. All of these drops were made with 1/2 pound of 1600°F aluminum free falling 18 inches into 250 ml breakers with water depths of 2 inches. The quench water was the only variable changed in each of the tests. Figure 11.1 shows the interaction for distilled and boiled quench water; Figure 11.2; tap water with 1 percent (by volume) of liquid soap; Figure 11.3; distilled water with 2 percent of aluminum sulphate; and Figure 11.4; distilled water with 2 percent of sodium bicarbonate. The effect of aluminum sulphate, (Figure 11.3) as compared to plain distilled and boiled water (Figure 11.1) appears to be insignificant. Liquid soap (Figure 11.2) and sodium bicarbonate (Figure 11.4) produced similar results, but an aluminum segment has completely formed into a "cup" like shape where as the previous two conditions did not result in as much aluminum distortion. The cup shape obtained with the liquid soap additive appears to be smaller and less uniform than that produced when sodium bicarbonate was the additive. The difference between the geometries does not really appear to be significant. The tests in which second radiographs were obtained showed that the cup shape appeared to have closed over, trapping vapor or vapor and liquid.

Drop height appeared to have no significant effect. Water depth effects, except for the longer falling distance, indicated no particular differences. Segments "falling" through the vapor formed by a previous segment did not deform as much and as a result had different shapes. This would be expected as the resistance force is reduced considerably in the absence of liquid water.

11.4 Conclusions

This study was especially significant because it demonstrated that the majority of fragmentation and encapsulation mechanisms do not apply to the DC bleed-out interactions. Comparing the stream geometry in Figures 11.1, 11.2, 11.3 and 11.4 to those in Appendix C, Figures C.30 and C.31, makes this quite clear. The 3/8 inch diameter streams breakup whereas the 3-1/4 inch

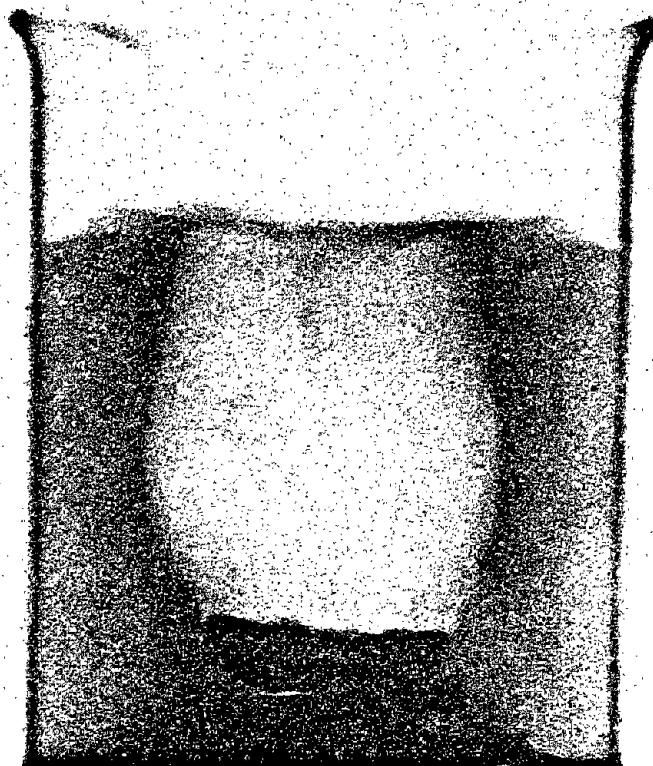


Reproduced from
best available copy.



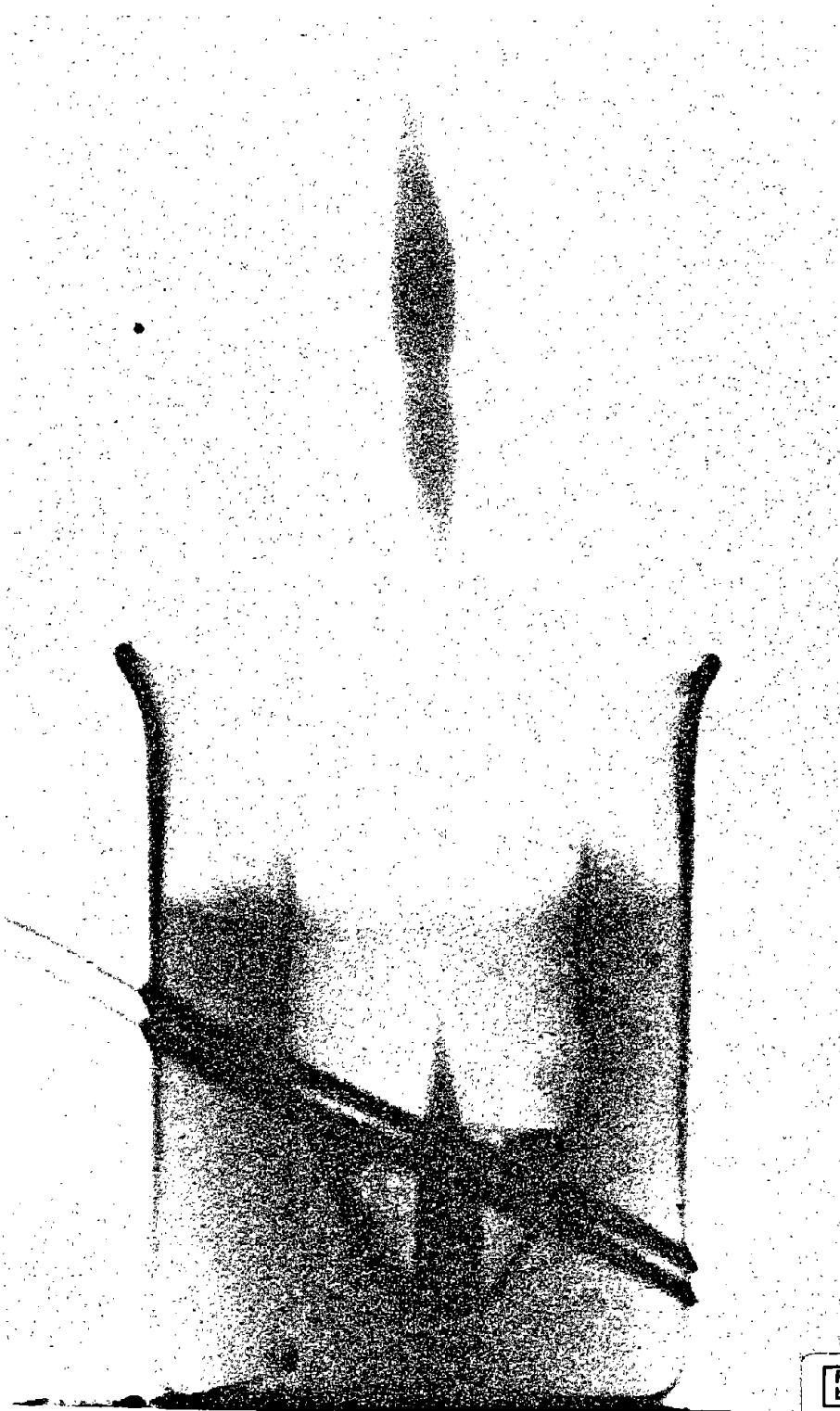
Figure 11.1 Test Number 41: 1/2 pound; 3/8 inch diameter
1600°F aluminum stream dropped 18 inches into
2 inches of distilled and boiled water.

IIT RESEARCH INSTITUTE



Reproduced from
best available copy.

Figure 11.2 Test No. 43: 1/2 pound, 3/8 inch diameter 1600°F aluminum stream dropped 18 inches into 2 inches of tap water with 1 percent liquid soap added.



Reproduced from
best available copy.



Figure 11.3 Test No. 31: 1/2 pound, 3/8 inch diameter 1600°F aluminum stream dropped 18 inches into 2 inches of distilled water with 2 percent aluminum sulphate added.

IIT RESEARCH INSTITUTE

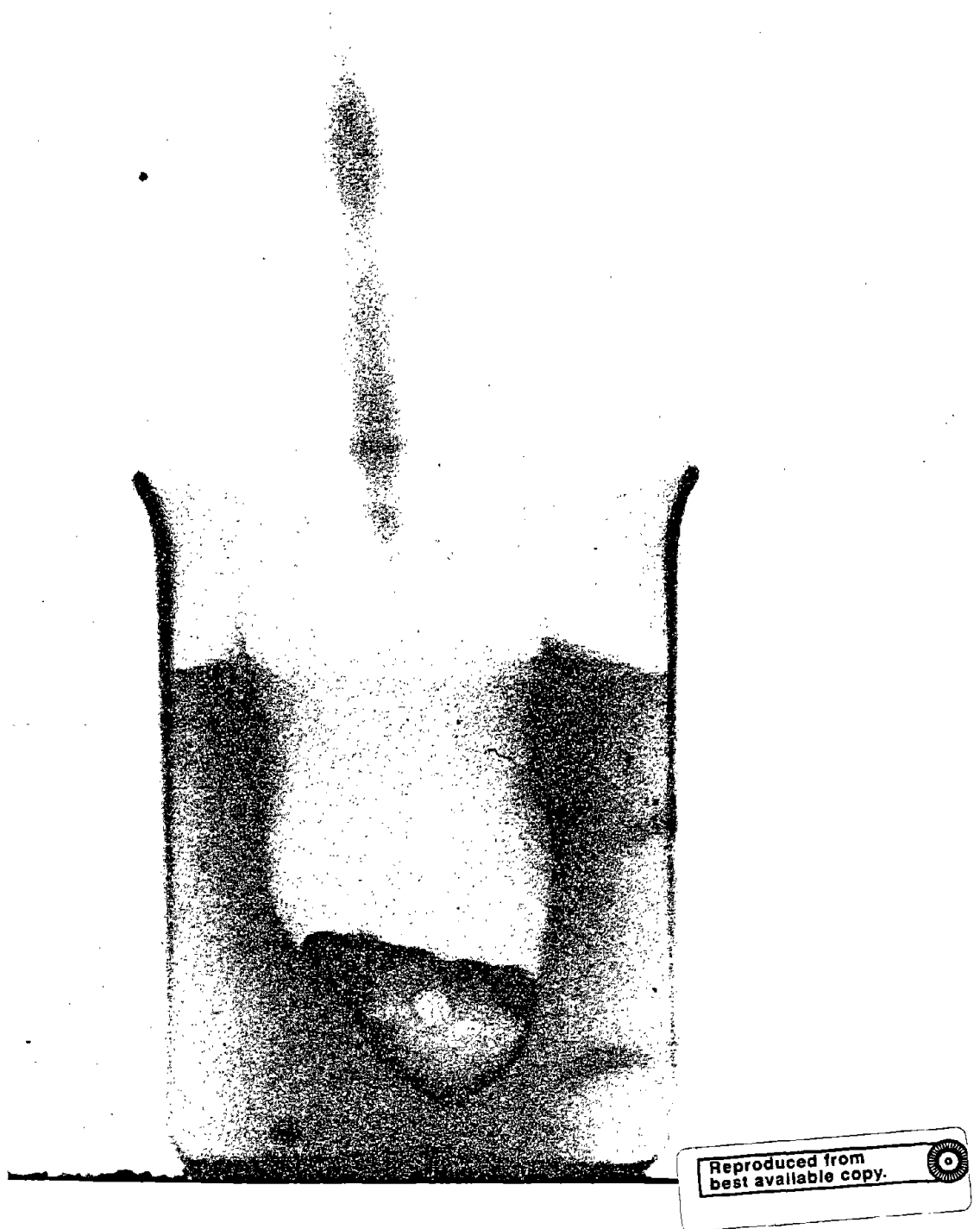


Figure 11.4 Test No. 32: 1/2 pound, 3/8 inch diameter
1600°F aluminum stream dropped 18 inches
into 2 inches of distilled water with 2
percent sodium bicarbonate added.

IIT RESEARCH INSTITUTE

diameter streams do not. The larger diameter stream does not form the shapes that the smaller ones do. The small stream loses heat rapidly (no vapor is attached to the deformed streams in Figure 11.1 through 11.4) whereas there is considerable steam "attached" to the larger streams (Figures C.30 and C.31). This investigation, by eliminating potential initiation mechanism candidates, aided significantly in deducing the most probable initiation mechanism.

12. INITIATION MECHANISM DEFINITION

This program activity was initiated at the conclusion of the small scale experimental study. The other studies, Literature Search, Chemistry, Gross Experiments, and Electrostatic charge, had been completed previously. The state of knowledge relevant to initiation mechanisms was primarily that most candidates were not applicable.

This study was performed by conducting six subtasks which provided the following:

- review of program results and relevant literature
- molten aluminum-water reaction parameters (Section 4)
- typical molten aluminum-water interaction characteristics (Section 5)
- basic interaction model (Section 6)
- impact shock cavity collapse initiation mechanism (Appendix D)
- candidate initiation mechanism evaluation (Section 7)

In accomplishing these subtasks, the "most probable initiation mechanism" was defined. This mechanism is the spontaneous nucleation of liquid water. Of the many possible energy release mechanisms, this is the most likely one which conceptually could provide the range of explosion types noted in DC simulations and is consistent with the reaction parameters (Section 4). The action time for a "vapor explosion" (spontaneous nucleation) is reported to be a microsecond event, on the order of 5 μ s, which is consistent with the gross experimental results (less than 25 μ s). The range of reactions described by Figure 6.2 may be directly related to the amount of liquid water which enters the vapor explosion. There are four key requirements for a vapor explosion to take place:

- liquid heat source

- liquid cold working fluid
- contact between the liquids
- instantaneous interfacial temperature (IIT)
at or above the limit of superheat.

Studies and analysis performed by Argonne National Laboratories indicated that the cold liquid should be finely divided. It may be valid to deduce that the "state of fineness" may relate to the severity of the reaction corresponding the amount of energy released. There is another aspect of the Argonne work which may be applicable to the reactions experienced in bleed-out simulations. Argonne determined that in addition to the requirement for the IIT to be at or above the limit of superheating for the cold fluid, the violence of the vapor explosion is related to the actual temperature of the fluids. Thus, as noted in bleed-out simulations, there are no explosions when the water temperature is above 140°F. The presence of the hot liquid and a sufficiently high IIT is assured because the temperature of molten aluminum is 1220°F. The presence of liquid water was postulated to be assured by surface cavities in the quench tank (pit) surfaces. It had been noted that explosions did not occur when these surfaces were smooth, e.g., glass, stainless steel, aluminum and coated surfaces (tarset, grease, paint, etc). In addition, the surface cavities "finely" divide the liquid water.

The remaining condition which needed to be satisfied was that the two liquids come into contact. The conceptual development of the impact shock cavity collapse initiation mechanism indicated the potential for aluminum flow induced impact shock other than at the initial approach to the quench tank surface. United Kingdom work at Ashton had shown that a shock, applied to the interface of liquid water over liquid tin, collapsed the separating vapor film. Thus it was postulated that an impact by the molten aluminum flowing over a surface of the quench tank would develop an impact shock when it reacted a second (or subsequent) surface. The above rationale completed the definition of the initiation mechanism which then had to be demonstrated.

Some of the aspects of the model defined above would be relatively easy to confirm. The demonstration that an impact shock developed to collapse the vapor film would not be easily accomplished. The shock formation and subsequent vapor film collapse is referred to as the trigger for the vapor explosion. Analysis had shown the potential for impact shock generation (Figs. 5.11 and C.16). The magnitude of the shock pressure depends upon the impact surface material and the aluminum flow speed. The conditions which may be encountered indicated that a shock pressure range of 2000 to 5000 psi could be realized. However, the energy associated with shock waves in this range was not defined nor were the requirements of the strength and energy necessary for collapsing a film known. Furthermore, in addition to these unknowns, the pressure/energy/film thickness interrelationships for the vapor film thickness which had to be collapsed was not defined.

There were two "obvious" possibilities for impact shock generation: the initial impact of aluminum on the first surface reached (which was subsequently shown not to take place) and surface flow to a second quench tank surface. The time frame of the explosions ruled out the initial impact and admitted the second possibility. Reactions took place in several gross experiments within 177 ± 13 msec after contacting the quench tank water (Section 9.4). This admits times at least as great as 216 msec (average plus 3 standard deviations). As shown in Fig. 5.1, explosions had been obtained in simulations most often between 140 to 215 msec after water contact and in one case after 700 msec. The most frequent time frame is closely correlated to side and corner impact times. These times may be obtained from Fig. 5.12 by adding the flow time through water of the 60 msec (Section 9.4). Figure 5.12 indicates that flow to a 6 inch radius (side of a 12 inch diameter or square tank) takes about 50 msec and over 8 inches (corner of a 12 inch square tank) about 65 msec. These times (110 msec and 119 msec) correspond to the lower time bound for the reactions most frequently observed. Flow resistance and non-ideal conditions could easily account for the upper time bound of the most frequently observed explosion. In Appendix C, additional quench tank surface

flow calculations are reported in Fig. C.19. The calculations indicate that the surface flow could take as long as 220 msec so that adding the time for flow through water of 60 msec provided an upper bound for the most frequent obtained reaction of 280 msec. This still does not take into account the longest time observed in a simulation, 700 msec.

Three rationales may be considered to explain the long time of 700 msec: the time was determined erroneously; shock conditions exist which have not been identified; or another trigger mechanism is involved in the interaction. Since this long time was the exception, the experimental evaluation of the postulated initiation mechanism was performed without resolving this aspect of the interaction.

13. INITIATION MECHANISM EXPERIMENTS

The initiation experiment program was designed to demonstrate the "most probable" mechanism postulated by the mechanism definition study, Section 12. The experimental program is reported in Appendix C and summarized in this section.

13.1 Overview

Seven experiments were performed using a No. 70 clay-graphite crucible provided with a 3-1/4 inch diameter internally (within the molten aluminum) sealed port and containing 50 pounds of molten aluminum. The total drop distance was 18 inches with the last 6 inches (in 6 cases and 1/64 inch in one case) being quench water contained in a 12 inch diameter 11 inch high glass cylindrical tank. The glass tanks were center mounted on 24 inch square surfaces of four types and sealed with silicon rubber. Data was obtained by means of: 16 mm, 1000 pps film; still photograph; thermocouples; an accelerometer attached to the tank bottom surface; a tank side aluminum sensor; and zero time and explosion time signals.

The aluminum drop temperatures were nominally 1525°F, ranging up to 1590°F. The quench water temperature ranged from 45°F to 60°F. Five types of quench surfaces were used: smooth and rough, concrete and steel; and taset coated rough concrete. Reactions were expected on the rough surfaces of which there were 3 concrete and 1 steel; and were not expected on the smooth surfaces, 1 each concrete and steel. One mild steam explosion resulted from the drop made on the rough steel surface. The drop made on a rough concrete surface, which was covered with only 1/64 inch of water, had an approximate 4 inch diameter area about 1/8 inch deep "crater" formed as a result of the interaction.

The mild steam explosion occurred at 156 msec after the aluminum contacted the quench water. The crater must have been formed in the concrete surface after 1 second, as there was no accelerometer record showing this event. There would have been an accelerometer output had the recorder been on, when the event took place. Data recording was terminated 1 second after the

start of the aluminum pour. The lack of reactions in the other two runs in which they were expected was attributed to the irregular leading edge geometry of the molten aluminum stream. This shape factor is thought to have the same effect as a small diameter stream, one 2-1/2 inches in diameter and less.

The thermocouple data showed that the aluminum remained liquid with the temperature dropping about 125°F making the nominal aluminum temperature above on the quench surface 1400°F. The in-surface thermocouples showed that the initial water temperature had not changed when aluminum reached the quench tank side wall except in the case of the explosion. In that case, the temperature was unchanged (for an average of the two sensors for 13 msec after the closest approach of aluminum to the bottom surface).

The aluminum stream did not impact the quench tank bottom surface as the flow direction changed from vertical to horizontal (radial). The thermocouples positioned 1/8 inch above this surface did not register until after the aluminum flow reached a quench tank side surface. Thus, the point of closest approach of the incoming aluminum stream was greater than 1/8 inch. This also indicates that the vapor layer or water/vapor layer was at least 1/8 inch thick.

The explosion which occurred took place just as the bottom surface of the quench tank was completely covered with molten aluminum. In all cases, the rate of temperature rise sensed by the thermocouples changed dramatically after a side surface of the quench tank was contacted by the aluminum flow.

13.2 Tangential Flow Impact Generated Shock

The analysis performed, prior to the conduct of the experiments, demonstrated that the initiation mechanism was directly related to radial flow produced shock. Photographic evidence presented in Appendix C (and the last paragraphs in Section C.5 and Section C.6.2) indicated that a tangential flow developed as a result of the radial flow. The tangential flow represents an important consideration from the standpoint of shock strength.

The relative impact speed of the aluminum could be twice as great under this condition as when it impacts a stationary surface. This concept was presented to the program review committee at the final meeting after the experimental program had been completed. It was not accepted then as having much significance. However, since this aspect of the flow appeared to have potential importance, some additional examination of this condition was made.

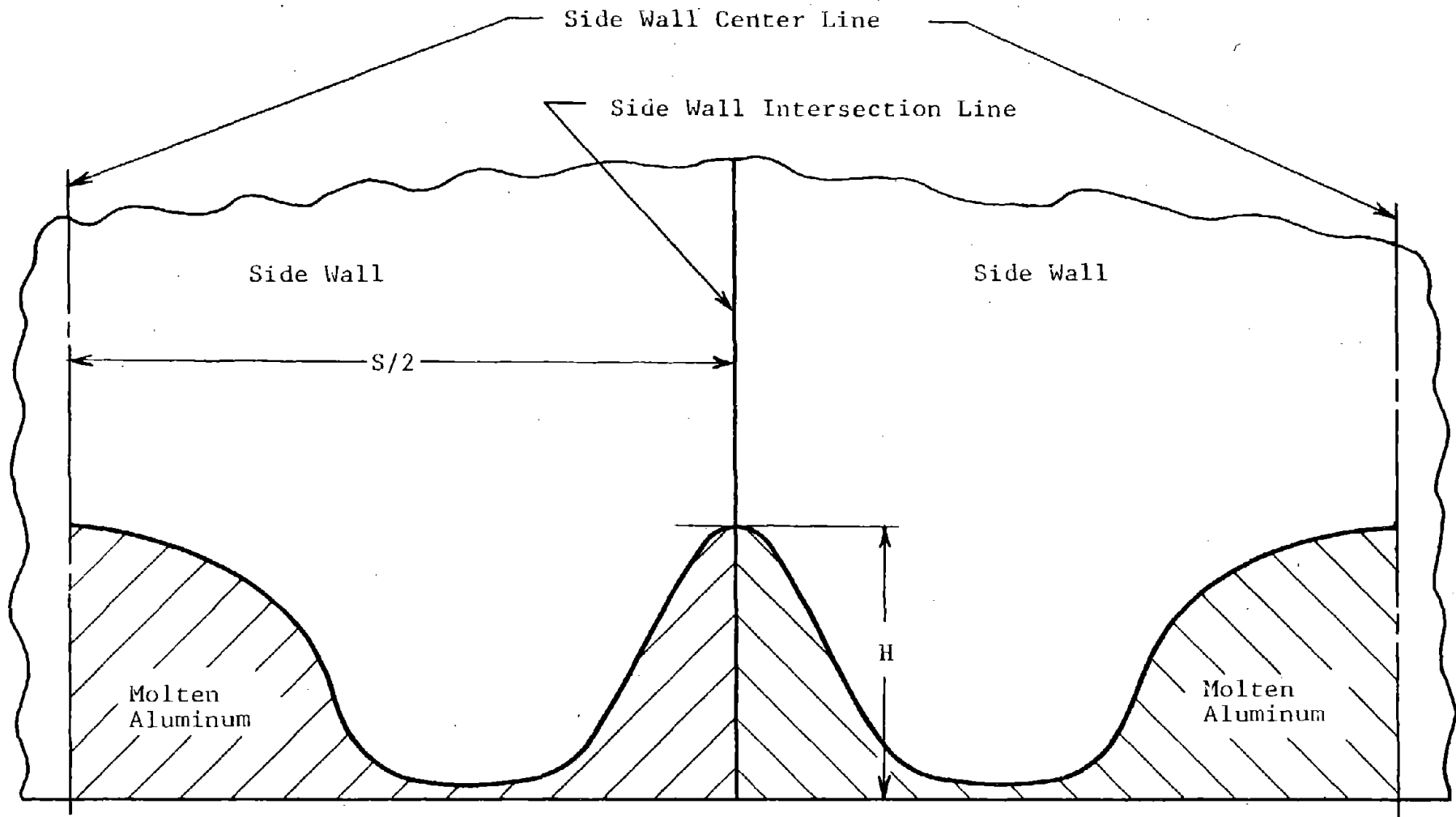
A seemingly unrelated observation made by the committee, as well as by the project staff, provided additional stimulus for closer examination of the tangential flow impact condition. The flow pattern developed by molten aluminum, upon impacting the sides of the circular quench tank, was continued flow up the wall rather than collecting, more or less uniformly, on the bottom of the quench tank as takes place in square tanks. The vertical flow reached a height of at least 12 inches. The potential energy of the aluminum at this height is equivalent to 96 ips or more (which is about the calculated radial speed). Thus there is a significant amount of kinetic energy in the flowing aluminum after it impacts the side wall. This means that in the square crosssection quench tanks, where the flow does not "climb the wall", part of the flow energy is still available. Furthermore, when two elements of flow meet, twice as much energy is available as was when the radial flow impacted the side wall.

Having previously accepted that "pure" radial flow could produce a significant impact shock and determining that considerable more energy could be involved in producing a shock by the counter tangential flows meeting, several crude experiments were made to verify the existence of the tangential flow and the way it varied as the flow reached the side wall when the flow vector was not perpendicular to the wall. A small rectangular clear plastic "quench tank" was filled with water and ink was forced into it from an eye dropper to simulate a bleed-out. The impact point of the ink was placed near a corner and the side walls so that the flow pattern could be observed as it developed. After some variation

IIT RESEARCH INSTITUTE

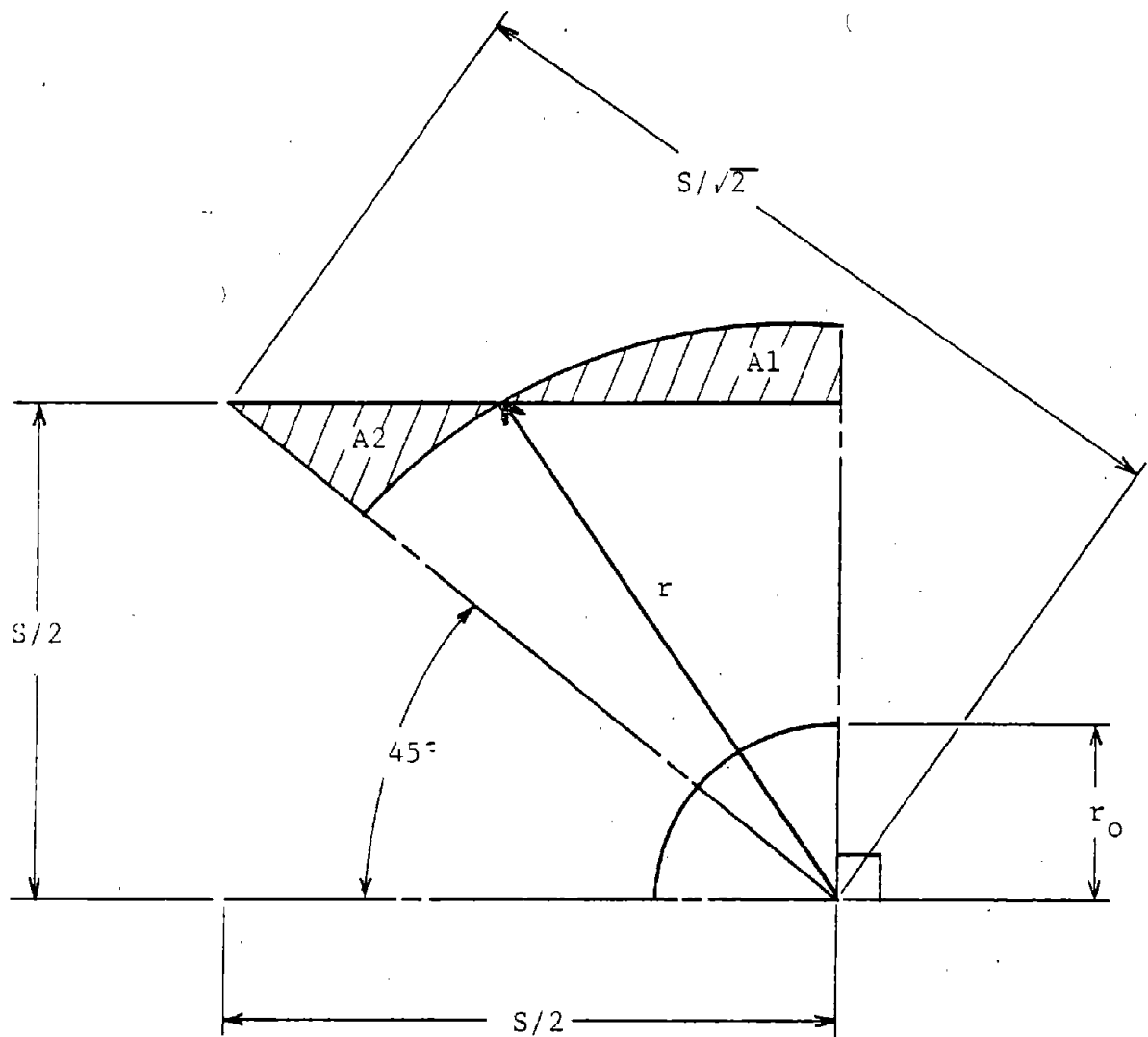
in the impact location and in the force used to eject the ink, the desired conditions were observed and they verified the expected results. Figure 13.1 shows a profile of the flow on the sides adjacent to a corner. The time at which this takes place is just after the flow has filled in the corner area on the tank surface. Fastex films of large scale experiments were viewed to ascertain if this pattern and the tangential flow existed. The film for Battelle run C-42 showed both patterns clearly. This run had a glass bottom, with a mirror showing the bottom flow patterns and a clear plastic side, also with a mirror. It took a considerable amount of study to be able to place objects and events in their proper relationship. But after doing this, the postulated flow pattern was clearly present. The review of the Battelle films also refocused attention on the number of natural initiations appearing to take place from/in the corner.

The tangential flow dynamics may be bounded by assuming there is no flow vertically on the quench tank side walls, as indicated in Fig. 13.1. This is a reasonable assumption for an upper bound and this condition is represented in Fig. 13.2. It shows that for a 12 inch square quench tank, flow to a radius of about 6-3/4 inches will completely cover the quench tank bottom surface. Whereas without considering this aspect of flow, the flow would have had to expand to almost 8-1/2 inches. If the molten aluminum which first reached the side of the tank is forced into the corner, the leading edge average speed would be almost 800 ips and since there would be a similar flow from the adjacent quadrant, the relative impact speed could approach 1600 ips. The radial impact speed is on the order of 100 ips, thus the tangential flow could give rise to 16 times the shock pressure, since it is linear with respect to speed. The tangential flow represents a significantly higher energy shock condition than the radial flow, 38,000 psi rather than 2400 psi. (Refer to Table D.1, in Appendix D, molten aluminum on molten aluminum.)



Exterior side view of corner development schematic for a square quench tank showing the vertical profile of aluminum on side walls just when the tank bottom surface is covered.

Figure 13.1 Flow Profile on Quench Tank Side Walls (Schematic)



S = side of square quench tank

r_o = radius of initial aluminum stream

r = radius of aluminum flow on quench tank surface when $A_1 = A_2$ (assuming no vertical flow on quench tank side walls)

$$\frac{1}{2}(S/2)^2 = \frac{45\pi}{360} r^2$$

$$r = S/\sqrt{\pi} \text{ for } S = 12 \text{ in.}, r = 6.770 \text{ in.}, S/\sqrt{2} = 8.485 \text{ in.}$$

$$\text{If } r = 100t; t = \frac{r-S/2}{100} = \frac{6.770-6.000}{100} = 7.7 \text{ msec}$$

$$\bar{u} = \frac{S/2}{t} = (12/2)/.0077 = 779 \text{ ips}$$

t = time, sec

Figure 13.2 Approximate Tangential Flow Impact Condition

13.3 "Free Standing" Vertical Flow

The impact resulting from tangential flow from two quadrants of the quench tank described in the previous section (13.2) may produce "free standing" vertical flow. (This may be easily demonstrated by pouring water from two containers on to a horizontal surface so that the flows meet.) The height such a vertical flow could attain has not been calculated nor has such a condition been visible in high speed motion pictures of interactions (most likely it would be difficult to detect unless the experiment was designed to show such a condition). This vertical flow would be very unstable and could be expected to "fall" or fold over from the top on one side or the other. The result of this would be a force applied on the aluminum covering the bottom of the quench tank. This could collapse the steam film (between the liquid water in the quench tank bottom surface cavities) and initiate very localized spontaneous nucleation. This local explosion would then be the shock source which propagates, collapsing the vapor film between the majority of the molten aluminum and liquid water, and triggers a vapor explosion of significant energy to produce the major explosion.

This "vertical" trigger would come later in the total interaction cycle than any of the other triggers identified. Assymetry in flow conditions, added to the time for the vertical flow to rise and then fall, could possibly add enough time to account for the longest interaction time reported for simulations (refer to Figure 5.1). However, it is indicated that other types of "triggers" may be identified by further analysis of the aluminum flow pattern.

13.4 Conclusions

It is concluded that the experiments demonstrated that the initiation mechanism for molten aluminum water explosions is spontaneous nucleation of quench water. The trigger for this event is most probably an impact generated shock produced by aluminum flow in the quench tank. This conclusion is substantiated by the thermocouple data which established that there is liquid water and

molten aluminum present throughout the primary time during which explosions have been obtained. Photomicrographs (Fig. C.8) of quench tank surfaces show that there are surface capillaries in rough surfaces which can contain liquid water and they also show (Fig. C.9) the lack of capillaries in smooth surfaces. The one explosion and the time at which thermocouples sensed temperature rise are very closely correlated to aluminum flow reaching quench tank vertical surfaces which in turn correlates to impact generated shock formation.

Further, it is concluded that the most frequent impact shock which triggers spontaneous nucleation is a result of tangential flow caused by flow deflection from the rectangular geometry of the quench tank. First contact by the flow at the side walls may provide the trigger, but the strength of this shock may be considerably less. Eccentricity of the incoming aluminum stream may give rise to a range of flow conditions other than the two relatively simple cases studied in the program. There apparently is a condition which has given rise to a "late" initiation, e.g., one taking place after twice the time the most frequent explosion occurs. Some phenomena such as "free vertical flow" may explain this long time. It is considered important to try to indicate that the late explosion fits into the vapor explosion initiation mechanism theory so that there is not unexplained data which would reduce confidence in the vapor explosion initiation mechanism. Since it seems reasonable triggers may be identified which would come late in the overall encounter, the late reaction need not be cause to reject the postulated initiation mechanism.

14. SIMULATION EQUIPMENT DESIGN

The simulation experiments conducted and the analysis made of the results have indicated the need for improved equipment design. Both the drop hardware and the sensors employed have room for improvement.

The importance of maintaining control over the geometry of the aluminum stream should be evident from the discussion presented in Appendix C, Section C.6.4. Control of the temperature at which the aluminum is dropped is poor and if/when the significance of the aluminum temperature is to be determined to any greater degree than it has, the drop crucible design should be changed to provide the necessary control.

It is recommended that the method used for opening the drop crucible be changed to eliminate or minimize any interaction with the aluminum stream geometry. External sealing, similar to that shown in Appendix C, Fig. C.12, could be made to work with some development. It is also recommended that an orifice larger than 3-1/4 inches be used. The drop crucible should be provided with a controlled heat source and well designed insulation so that the desired drop temperature can be achieved easily. Temperature sensors should be located: near the crucible wall; in the vicinity of the orifice; and near the central portion of the crucible cavity. A means should be provided to assure that the temperature at these locations are reasonably uniform before the drop is made.

Sensors which show the position of the aluminum stream during the simulation should be developed for use in place of thermocouples. Thermocouples are expensive to fabricate and install and are not necessary for obtaining this data. Thermocouples should be used, but not to obtain primary position data.

Photography should be employed to provide flow data during the interaction. This coverage should include: bottom, side and top views. The image should be as large as possible so that flow detail can be resolved to permit discernment of patterns which may collapse the steam film between the aluminum and quench tank surface.

MIT RESEARCH INSTITUTE

15. STUDY APPLICABILITY TO FURNACE CHARGING

The interaction between molten aluminum and water in furnace charging operations has important aspects which are considerably different from those in DC operations. The volume of aluminum is small and that of water large during the critical time period when bleed-outs occurred in DC operations. Conversely, in furnace charging operations, the volume of aluminum is by far the largest and the water, which is not supposed to be present, constitutes a very small volume. Reports on furnace charging explosions trace the presence of water to that which have been in soft drink bottles, or as snow or ice attached to the material being charged.

Some of the primary factors which effect explosions in DC operations and furnace charging are different. Water introduced during furnace charging is completely engulfed by molten aluminum; the surfaces of the furnace have no direct effect or influence on the interaction; gross aluminum flow conditions are not applicable; and in general, the reaction parameters presented in Section 4 have no real meaning in furnace charging operations. However, there is one very interesting similarity between these two commercial operations. Water may be introduced which is in hairline cracks or surface cavities of the metal charge into the furnace. In such a case, this liquid water and that in the surface cavities of quench pit surfaces is similar and the liquid water is in a finely divided state.

15.1 Experimental Data

Simulation experimental data is apparently almost totally lacking for furnace charging interactions. Some of the information available comes from post explosion investigations. Simulation of furnace charging interactions were conducted by the Reynolds Metal Company and are described in "Experimentally Produced Reactions of Molten Aluminum and Water" prepared by W. J. Roschke, dated June 8, 1961. Sixty-one experiments were conducted

relating to this type of encounter. The only explosions which were obtained were described as of the "mechanical steam pressure type". These occurred when 20 pounds of aluminum was poured over 25 to 70 ml (about 1 to 3 ounces) of water contained in 1 inch diameter capped steel pipe. Mechanical explosions also occurred when these pipes were dropped into 20 pounds of molten aluminum. The molten aluminum temperature range which produced these results varied from 1410°F to 2120°F. The mechanical explosions occurred only when steel tubes were used and not when the tubes were aluminum. In the case of aluminum, steam could be observed bubbling through and out of the molten aluminum overburden without reacting. In contrast, the mechanical explosion was described as "quite forceful at times but not in the magnitude of some of the explosions which occurred when molten metal dropped into water."

Reports on actual explosions and simulations do not quantify the time elapse from the introduction of water to the explosion. Times have been reported of 1 to 5 minutes for the explosion to take place after the furnace was charged. The Reynolds work did not report the time required for the water contained in tubes to explode, but did (qualitatively) for the bleed-out simulations. This leads to a conclusion that the time frame was much longer which would be consistent with the times reported for actual explosions.

15.2 Discussion

The scenario for furnace charging explosions may be divided into phases:

1. Induction

- Water introduced to a large mass of molten aluminum
- Water heated and confined by molten aluminum mass

2. Trigger

- Release of thermal energy stored in water
- Propagation of energy through molten aluminum

3. Reaction

IIT RESEARCH INSTITUTE

The phases of this scenario are analogous to that for DC bleed-outs. The induction period may be considerably longer as time may be required for transferring heat from the molten aluminum to the encapsulated water. A steam film is formed so that the main mass of liquid water must be heated through the film. The vapor and liquid may be considered as concentric spheres within an almost infinite molten aluminum heat sink. The sphere of water and vapor will have its temperature, and hence pressure increased as heat is transferred to it.

A trigger event may result from the interaction between the molten aluminum and the heated water and vapor. From the available data, the effect of such a trigger can be quite different in actual furnace explosions and in simulation reactions. Apparently considerable more energy is released by the trigger in furnace reactions. The postulation of an initiation mechanism, the trigger event in this case, should encompass the range of energies indicated to be released.

Propagation of the trigger must be consistent with the various levels of reaction which have been observed. In the case of simulations made with water contained in aluminum tubes, propagation consisted of steam venting with no accompanying disturbance. The observations made in similar simulations using steel pipe indicated that molten aluminum was splattered about. In contrast, furnaces are blown up and large quantities of molten aluminum dispersed over a considerable area.

The relationship between the various degrees of reaction may be related to the water confinement. In the case of the simulations the mass of molten aluminum was considerably less than that in commercial furnaces. Furthermore, the water may be introduced confined or unconfined. Confinement was provided by aluminum or steel tubes in simulations. Partial confinement in furnace operations would be provided if the water was introduced in cracks in the metal being remelted and in one case by a soft drink bottle (assumed uncapped). Unconfined water would come from ice or snow adhering to the metal being remelted.

IIT RESEARCH INSTITUTE

There would appear to be a significant difference between confined liquid and that unconfined or partially confined. In the case of container confined liquid, the vapor pressure will increase as heat is transferred to it and the container will weaken as it is heated. When the pressure exceeds the container strength, the container will usually fail locally at the weakest point, producing a "jet" like emptying action. The aluminum overburden in the simulations was only about 6 inches so that a relatively short vent path was available. The pressure developed at the rupture in the aluminum container would be considerably lower than that in steel container explaining the difference in the reaction degree. In both of these cases, the pressure within the container expands producing a jet with some significant speed which could reasonably be expected to penetrate 6 inches of molten aluminum.

The situation existing in the case of unconfined and partially confined liquid is considerably different. As the water and vapor are heated they can expand against the molten aluminum continually, rather than almost instantaneously after confinement fracture. Furthermore, the "flexible" confinement provided by the much greater mass of molten aluminum would be capable of maintaining a "sphere" of combined vapor and liquid, whereas it would not in the simulations performed. The significance in the differences between the simulations and furnace conditions, or rather between confined and unconfined liquid water, is that in the latter situation considerably more energy may be transferred from the molten aluminum to the water and the manner in which it is converted.

The concentration of energy in the "sphere" of vapor/liquid will be bounded and at some point the initiation action will occur. Candidate mechanism for the release of the energy are presented in Section 15.3. Regardless of the specific mechanism, a pressure pulse or shock will propagate through the mass of molten aluminum which is postulated to break it up into small particles of aluminum with unoxidized surfaces. The atmosphere

in the furnace may oxidize these surfaces providing additional energy. Under the proper condition of fresh surface area and furnace atmospheric chemistry, the temperature and hence the pressure of the atmosphere may be raised quickly to a high enough pressure to "explode" the furnace and displace considerable molten aluminum. The degree of the final reaction would seem to be directly relatable to the amount of water, the concentration of energy in this water and possibly to the energy release mechanism. Since the amount of water introduced into the furnace is considered relatively small, the production of hydrogen and its subsequent contribution to the explosion may not be significant.

15.3 Initiation Mechanism

The candidate initiation mechanisms described in Section 7 encompass three which appear to have primary application in furnace charging explosions. These are:

- Bubble collapse and rebound,
- Bubble collapse producing a jet, and
- Cavity collapse induced by a shock wave.

These mechanisms are closely related and elements of them all may be combined and considered as one mechanism. Shock produced cavity collapse was considered applied to hemispherical cavity, but is even more applicable to a bubble or spherical cavity. One consideration of this mechanism, in furnace charging, could dictate that the impact shock (which could cause cavity collapse) could arise from the impact of the furnace charged material on the molten aluminum in the furnace. The shock wave formed would have to be considered as reflected from internal furnaces surface and then engulfing the liquid/vapor bubble. The time for furnace reaction occurrence is quite late in relation to this shock formation so that it could be expected that the wave would have dissipated well before the initiation. Therefore, the contribution of initial impact shock waves is discounted.

The mechanism of the bubble collapse and rebound, and bubble collapse producing a jet may be the same mechanism as it may be impossible to maintain sufficient symmetry to achieve stabilized bubble collapse. Geometric assymetry during collapse would be expected to produce a jet. The jet could be fresh aluminum flowing into the bubble or vapor, or liquid flowing out of the bubble. In either case, the bubble dynamics are cyclic and are produced by heat exchange between molten aluminum and the vapor/liquid.

Two potential energy release mechanisms may operate during the bubble expansion and contraction process. Expansion of the bubble will increase the surface area providing unoxidized aluminum which may be oxidized. This will add heat to the vapor/liquid in the bubble. Bubble collapse may raise the vapor temperature to 2000°C or above which may permit aluminum oxidation in the presence of the oxide surface coating. If or when the bubble motion produces a jet, unoxidized aluminum will be exposed to vapor and liquid and be oxidized.

If the initial source of liquid water provides quite small volumes, spheres with diameters on the order of 0.1 mm (0.005 in.), a condition for a vapor explosion may be present. Such a condition could be envisioned as a result of snowflakes or ice crystals that were clinging to the furnace charge. Also liquid water in small cracks or in surface cavities could provide such a source. Under these conditions, liquid water in a finely divided state would exist. The bubble collapse may be construed to be vapor film collapse and result in a vapor explosion.

The combination of large and small water volumes may be a situation where the larger bubbles expand and contract providing a vapor film collapsing force. The small water volume, attached to, or in furnace charged metal surface cavities (similar to the quench tank surface), would be surrounded by a vapor film. If the time frame and the mass of metal was such that it did not conduct heat into the water to raise its temperature above 140°F;

the large bubble produced pressure wave could collapse the vapor film on the small volumes of water producing spontaneous nucleation of the liquid. The presence of large bubbles, to provide the force for film collapse on the small ones may not be required. The metal (being charged into the furnace) with surface capillaries containing liquid water may have a terminal speed of 36 to 72 ips when and if impacts a furnace surface. This impact would produce a shock, coupled efficiently to the metal bearing the liquid water, and collapse the vapor film initiating spontaneous nucleation. The transient time may be on the order of 1 to 6 seconds, which may be more or less depending on the depth of molten aluminum and the transient path. Except for the short time period, say less than 10 seconds, as compared to minutes reported for the occurrence of the explosion, this scenario could be viable.

The vapor explosions resulting in any of the preceding scenarios would act just as it would in DC bleed-outs. However, the amount of water present would be considerably less than that in DC explosions so that violence of the final reaction would be less. The net result of the explosion may be just as devastating if the furnace provides more confinement than the quench pits do. The expansion of the explosion product gases against the large volume of molten aluminum, instead of rigid concrete quench pit surfaces, could produce considerable displacement and increase the seriousness of the end result.

15.4 Conclusion

The sparseness of data for explosions resulting from furnace charging makes the selection of the most probable initial mechanism difficult and little confidence can be placed in any conclusion. However, in light of the present state of information, the mechanism involving heat transfer driving bubble expansion and collapse seems most likely to be present. The energy release mechanism is most likely either of, or some combination of the following:

- Aluminum oxidation of fresh cavity surface caused by bubble expansion and/or jet formation providing contact between water (and/or its vapor) and fresh aluminum.

- Spontaneous nucleation of liquid in small cavities resulting from: film collapse either by the collapse of the cavity contained in the water by its expansion contraction motion; or from pressure pulses stimulated by larger bubbles.

It appears that the simulations conducted were not performed in a manner which could simulate the actual condition present in a furnace. The liquid water was not introduced in a similar manner. There was an attempt to approach furnace conditions by trying to submerge or maintain ice cubes under/in molten aluminum. The ice could not be made to "penetrate" the molten aluminum. The simulations were made using 20 pounds of aluminum. This quantity appears to be quite small in relation to the actual furnace quantity, especially when the overburden of furnace molten aluminum is considered.

Adhering to the stated practice of ensuring that the metal to be charged into the furnace is dry should prevent explosions. A review of the procedures being used may be in order to make sure that the metal is thoroughly dry before charging. If preheating is used to accomplish this, some evaluation of heating time and temperature might be made - if it has not been done. The heating requirements for a large volume of metal containing small amounts of water might be considerably more than expected.

16. CONCLUSIONS

The Molten Aluminum - Water Explosion Initiation Mechanism Study has shown that the most probable initiation mechanism resulting from DC bleed-outs is spontaneous nucleation of liquid quench water contained in quench pit surface cavities. This liquid water is separated from the molten aluminum by a vapor film. The stability of this film, the number and size of the surface capillaries containing liquid water (below 140°F) and the strength of the stimulus available to collapse the separating film determine if and how violent a reaction will be. The amount of aluminum in the quench water and the distribution of aluminum in the water are important also in the violence of the explosion.

The three aspects of the vapor explosion which may be considered in eliminating the chance for an explosion are: liquid aluminum, liquid water and vapor film collapse. Liquid aluminum and liquid water are inherent components in the DC process. However, since the liquid water must be finely divided to produce a significant initiation, a large degree of safety is obtained by the current practice of coating the quench pit surfaces. This eliminates the surface cavities which would have provided the finely divided liquid water. (The only drawback to this safety measure is assuring that the coating is maintained continuously.) The use of smooth quench pit surfaces which would not become pitted as a result of operations might help in this aspect of explosion prevention. The stability of the vapor film and the energy source for collapsing it are directly related to the DC bleed-out conditions. (These can not be controlled as the occurrence is a random event with random combinations of bleed-out stream size and head.) The depth of the quench pit water is directly proportionate to the time that the incoming aluminum stream is in the water before terminating its vertical flow near a surface. In general, the longer times will permit the development of a thicker attached vapor film separating the aluminum from the pit surface and therefore require more of a stimulus to collapse the film and

initiate spontaneous nucleation of the surface liquid water. Flow dividers which reduced the bleed-out stream diameter also act to establish more and thicker vapor films attached to the aluminum. This effect is the same or quite similar to the effect of deep water in the quench pits.

The stimulus for collapsing the vapor film separating molten aluminum and liquid water is provided by the aluminum flow impacting a surface or upon itself, thereby producing a shock. The shock passes through the aluminum and water collapsing the film. If the shock is too weak for the film present, liquid-liquid contact will not occur and spontaneous nucleation will not take place. The size and geometry of the quench pits (and structures within the pit), in relationship to bleed-out impact location, might have an optimum relationship for reducing the effect of the shock stimulus. Shock waves expand spherically from their origin so that their strength reduces in proportion to the cube of the distance from the source. In addition, it appears that circular crosssection pits may reduce: the probability of shocks developing or the strength of a shock which may develop. When or where possible, this aspect of the interaction may be useful to exploit.

There appears to be a finite probability that an explosion may occur in the absence of a surface. This situation is similar to what occurs during furnace charging operations. The dumping of molten aluminum into water encompasses the possibility for mixing, resulting from flow, to encapsulate liquid water with liquid aluminum. Under this condition, expansion and collapse of the water cavities could take place and if small water cavities, about 0.005 inch in diameter, exist, the liquid could spontaneously nucleate. Cavity collapse in the case of the large sizes could initiate aluminum oxidation supplying energy to produce an explosion.

The study has established a firm basis for EXPLOSION INITIATION CHARACTERIZATION AND PREVENTIVE MEASURES FORMULATION. A program for accomplishing this is considerably different from establishing and quantifying the mechanism. Quantified characterization is required to assign meaningful safety margins and confidence levels in these margins. The objective of the program was to identify and define the initiation mechanism. This has been accomplished.

17. RECOMMENDATION

The initiation mechanism study has defined the most probable mechanism. The nuances of the molten metal-water interaction and equipment used, and that which should be used have been determined. Thus a firm basis has been established upon which to perform Phase II of the "Molten Aluminum - Water Explosion Initiation Mechanism and Prevention Study," "Explosion Initiation Characterization and Prevention Measures Formulation."

17.1 Initiation Characterization and Prevention Concept Formulation

The interaction of molten aluminum and water in a quench tank should be parametized. This will functionally define the inter-relationships of the significant independent variables.

Aluminum: stream diameter
weight
temperature
drop height

Water: depth
temperature
additives
type

Quench Tank: surface material
surface treatment
crosssection (geometry)

The significant dependent variables should include:

Aluminum: temperature
impact shock level
flow: at and through water;
over tank bottom;
at and around tank sides;
during bulk mixing after
bottom surface covered.

Water: temperature
 flow patterns
 film thickness

Events: film collapse
 initiation: time
 location
 strength

The dependent variables should be characterized, as applicable, as a function of: time and space. (Task 1)

This effort should be accomplished regardless of the acceptance or rejection of the vapor explosion being the initiation mechanism. The definition of the interaction parameters will provide a sound basis for: postulating, accepting and/or rejecting any candidate initiation mechanisms. If the mechanism is not a vapor explosion, it would be expected to be significantly more difficult to identify.

17.1.1 Equipment Development (Task 2)

The interaction of molten aluminum and water may be defined by determining parametric relationships through statistically designed factorial experiments. This will provide response equations relating the independent variables to the dependent variables. In order to do this, control of the independent variables must be much better than it has been. The instrumentation design used must be improved (over that which has been used) to assure obtaining the necessary data. Thus, an equipment/instrumentation-design/development task should be undertaken. Fractionalized factorial experiments should be conducted during the development of the equipment (and instrumentation) to assure the equipment is capable of providing the required data over the range of conditions which will be encountered. The data obtained in this process will be useful in itself.

17.1.2 Supporting Studies (Task 3)

If or when the vapor explosion is accepted as the initiation mechanism, correlating experiments should be performed which define vapor film stability in terms of shock strength. Experiments should be performed which relate aluminum flow parameters to impact shock strength levels to tie the film stability definition to the actual shock strengths which can be encountered. The stability of the film should be related to the temperature environment over the range of conditions which are expected in commercial direct chill operations. The flow patterns which can produce vapor film collapse that have not been defined should be.

17.1.3 Response Equation Validation (Task 4)

The conduct of Tasks 1 through 3 would be expected to establish predictive response equations. Operational conditions corresponding to a high probability (with a high confidence level) for obtaining explosions and for not obtaining explosions should be predicted and then verified. The selected conditions should be ones which were not evaluated in developing the response equations. This will establish the validity of the response equations and their usefulness for determining cause and effect relationships.

17.1.4 Explosive Parametric Study (Task 5)

The set of response equations should be exercised to illuminate the full range of interactions and develop a good understanding of the parameter interactions. The parameters which prevent or drastically reduce the probability of an explosion would be identified and reviewed with the Aluminum Association Task Group to determine the suitability of various prevention solutions for commercial operations. An experimental program should be developed and performed to validate the prevention solutions.

17.2 Implementation of Prevention Measures

The conduct of the "Initiation Characterizations and Prevention Concept Formulation Study" would be the final step required for implementation of the prevention measure study. This study should develop a fault tree for an explosion which could be used to predict the occurrence of an explosion. The influence of prevention measures in the reduction of explosion risk indicated by the fault tree would be used to select the most meaningful measures. The fault tree and prevention measures would be developed in concert with an Aluminum Association Task Group.

Specific prevention measure procedures and designs should be developed, detailed and documented. Statistical data should be generated to provide input for the fault tree so that meaningful risk prediction could be made. This aspect of work should also be accomplished in cooperation with the Aluminum Producers so that the results will be practical, meaningful and acceptable to the industry.

APPENDIX A
LITERATURE SURVEY REFERENCES

IIT RESEARCH INSTITUTE

LIST OF CATEGORIES

- (A) Aluminum Particle Ignition
- (B) Aluminum Oxidation
- (C) Aluminum Kinetics
- (D) Reaction Kinetics
- (E) Aluminum Physics & Thermodynamics
- (F) Liquid Metal-H₂O, Explosions
- (G) Liquid Aluminum-H₂O, Explosions
- (H) Liquid Explosions Phenomena
- (I) Instrumentation
- (J) Miscellaneous
- (K) Electrostatics & Electrical Effects

ALUMINUM PARTICLE IGNITION (A)

- D-1A "Effect of Aluminum on the Burning of Ammonium Perchlorate-Polyformaldehyde Mixtures", Zenin, A. A., et al, Combustion Explosion, & Shock Waves, 4(3), P. 165-168, 1968.
- D-2A "Combustibility and Ignitability of Mixtures of High-Calorific Metal Powders and Organic Substances with the Formula $C_xH_yO_z$ ", Gorbunov, V. V., et al, Combustion, Explosion, & Shock Waves, 4(2), P. 105-108, 1968.
- D-3A "Mass-Spectrometer Study of the Thermal Decomposition of Nitroglycerine Powder at High Temperature", Koroveinichev, O.P., et al, Combustion, Explosion, & Shock Waves, 6(3), P. 352-253, March 1973.
- D-4A "Excitation of Sodium of Certain Reactions Behind Shock Waves", Zaslanko, I. S., et al, Combustion, Explosion, & Shock Waves, 6(2), P. 175-182, Feb. 1973.
- D-5A "Ignition Limits of Aluminum Particles", Gurevich, M. S., et al, Combustion, Explosion, & Shock Waves, 6(12), P. 154-157, Apr.-June 1970.
- D-6A "Heterogeneous Ignition of an Aluminum Particle in Oxygen and Water Vapor", Gurevich, M. A., et al, Combustion, Explosion, & Shock Waves, 6(3), P. 291-297, March 1973.
- D-7A "Ignition and Combustion of Aluminum Particles in Hot Ambient Gases", Friedman, R. and Macek, A., Combustion, Explosion, & Shock Waves, 6(1), P. 9-19, March 1962.
- D-8A "Estimating Aluminum Particle Combustion Kinetics", Bartlett, R. W., et al, Combustion and Flame, 7(3), P. 227-234, Sept. 1963.
- D-9A "Effect of the Activity of Aluminum and Magnesium Powders on the Combustion of AP Compositions", Romodanova, L. D. and Pokhil, P. F., Combustion, Explosion, & Shock Waves, 6(1), P. 121-124, Jan.-March 1970.
- D-10A "Combustion and Ignition of Particles of Finely Dispersed Aluminum", Belyaev, A. F., et al, Combustion, Explosion & Shock Waves, 4(3), P. 182-185, 1968.
- D-11A "The Mechanism of Metal Particle Combustion", Pokhil, P. F., et al, Combustion, Explosion, & Shock Waves, 6(3), P. 356-358, March 1973.
- D-12A "Recent Experimental Results on the Combustion of Aluminum and Other Metals", Barrere, M., National Aeronautics & Space Administration, NASA-TT-F-13,043, July 1970.
(N70-32987)

IIT RESEARCH INSTITUTE

ALUMINUM PARTICLE IGNITION (A) (Contd)

- D-13A "Ignition and Combustion of Aluminum and Beryllium", Kuehl, D. K., AIAA Journal, 3(12), P. 2239-2247, Decm 1965.
- D-14A "Ignition Limits of a Metal Particle", Gurevich, M. A., and Stepanov, A. M. Combustion, Explosion, & Shock Waves, 4(2), P. 109-112, 1968.
- D-15A "Ignition of a Metal Particle", Gurevich, M. A., and Stepanov, A. M., Combustion, Explosion, & Shock Waves, 4(3), P. 188-192, 1968.
- D-16A "Ignition and Combustion of a Gas Suspension of Magnesium Particles", Gurevich, M. A., et al, Combustion, Explosion & Shock Waves, 6(3), P. 298-303, March 1973.
- D-17A "Combustion Temperature of Metal-Powder Aerosols", Zlobinskii, B. M., et al, Combustion, Explosion, & Shock Waves, 5(3), P. 298-305, Jul.-Sept. 1969.
- D-18A "Combustion of Pulse-Heated Single Particles of Aluminum and Beryllium", Prentice, J. L., Combustion Science & Technology, 1, P. 385-398, 1970.
- D-19A "Differences Between the Combustion of Aluminum Droplets in Air and in an Oxygen Argon Mixture", Prentice, J. L., and Nelson, L. S., J. Electrochemical Society, 115(8), P. 809-812, August 1968.
- D-20A "Apparatus for the Production and Ignition of Metal Droplets with a Pulsed Laser", Nelson, L. S., et al, Review of Scientific Instruments, 39(5), P. 744-747, May 1968.
- D-21A "Ignition and Combustion of Aluminum Particles in Hot Ambient Gases", Friedman, R. and Macek, A., Combustion and Flame, 6(1), P. 9-19, March 1962.
- D-22A "Ignition of Metals in Oxygen", White, E. L. and Ward, J. J., Defense Metals Information Center, Battelle Memorial Institute, U.S. Air Force Materials Laboratory, DMIC Report 224, Feb. 1966.
- D-23A "Combustion Characteristics of Powdered Aluminum", Belyaev, A. F., Ermolaev, B. S., Korotkov, A. I., and Frolov, Yu. V., Combustion, Explosion, and Shock Waves, 5(2), P. 142-149, April-June 1969.
- D-24A "Coalescence of Metal Particles During the Combustion of Metallized Ballistite Compositions and Fuel-Oxidizer Mixtures", Pokhil, P. F., Logachev, V. S., and Mal'tsev, V. M., Combustion, Explosion, and Shock Waves., 6(1), P. 76-85, January-March 1970.

ALUMINUM PARTICLE IGNITION (A) (Concl)

- D-25A "Spectroscopic Investigation of Metal Combustion", Brzustowski, T. A. and Glassman, I., Heterogeneous Combustion Progress in Astronautics and Aeronautics, Vol. 15, P. 41-73.
- D-26A "Letter to the Editors", Bartlett, R. W., Combustion and Flame, 8(4), P. 341-342, December 1964.
- D-27A "The active Combustion Mechanism of Single Al and Zr Strands in Oxygen as Determined by High Speed Polotgraphy", Maloney, K. M. and Pillay, T. C. M., Combustion and Flame, 18, P. 337-346, 1972.
- D-28A "Fundamentals of Combustion of Single Aluminum and Beryllium Particles", Macek, Andrej, Heterogeneous Combustion, P. 203-217.
- D-29A "Ignition and Combustion of Aluminum Particles in Hot Ambient Gases", Friedman, R. and Macek, A., Combustion and Flame, 6(1), P. 9-19, March 1962.
- D-30A "The Ignition of Inflammable Gases by Sparks from Aluminum Paint and Rusty Steel", Kingman, F.E.T., et al, J. Appl. Chemistry, 2, P. 449-463, 1952.
- D-31A "Oxygen Compativility of Materials", Lapin, Abraham, Air Projects and Chemicals, Inc., For Presentation of International Institute of Refrigeration Commission 3 Meeting on 14-15, November 1973.
- D-32A "Ignition of Metals in Reactive Atmospheres", Adams, M. J., Final Report, Air Products and Chemicals, Inc., August 1971.
- D-33A "Combustion of Powdered Metals in Active Media", Pokhil, P. F., et al, Foreign Technology Division, FTD-MT-24-551-73, n.d. (AD 769 576)

ALUMINUM OXIDATION (B)

- D-1B "Reduction of SiO by Molten Al", Prabriputaloong, K., et al, J. Amer. Ceramic Society, 56(4), P. 184-185, April 1973.
- D-2B "Kinetics of the Molten-Aluminum/Steam Reaction by the Levitation Method", Wilson, R. E., Reactor Safety II, P. 102.
- D-3B "Oxidation of Aluminum in the Temperature Range 400°-600°C", Smeltzer, W. W., J. Electrochemical Society, 103(4), P. 209-214, 1956.
- D-4B "On the Chemical Stability of Aluminum in the Composition of Industrial Explosives", Svetlov, B. Y. and Solntseva, N., Interdepartmental Commission on the Use of Explosives, P. 21-37.
- D-5B "Direct Observation of the Oxidation of Aluminum Single-Crystal Surfaces", Doherty, P. E. and Davis, R. S., J. Applied Physics, 34(3), P. 619-628, March 1963.
- D-6B "Electrical Properties and Defect Chemistry of Aluminum Oxide", Kroger, F. A., Dept. of Materials Science, Univ. of Southern California, Office of Naval Research, P. 1-5, Nov. 1971.
- D-7B "The Formation of Volatile Oxides by Furnace Construction Materials", Alcock, C. B., British Ceramic Society: Transaction, 60(2), P. 147-164, Feb. 1961.
- D-8B "Ionic Transport Numbers of Group IIa Oxides Under Low Oxygen Potentials", Alcock, C. B. and Stavropoulos, G. P., J. Amer. Ceramic Society, 54(9), P. 436-443, Sept. 1971.
- D-9B "Measurements of Electromotive Force Al₂O₃-Pitfalls and Results", Yee, J. and Kroger, F. A., J. Amer. Ceramic Society 56(4), P. 189-191, April 1973.
- D-10B "The Thermodynamic Properties of the Oxides and Their Vaporization Processes", Brewer, L., Chemical Reviews, 52, P. 1-11, 1953.
- D-11B "C. Boron-Aluminum Group Oxides", Brewer, L., Chemical Reviews, 52, P. 14-31, 1953.
- D-12B "I. Iron Group Oxides", Brewer, L., Chemical Reviews, 52, P. 32-35, 1953.
- D-13B "C. Boron-Aluminum Group Oxides, II.", Brewer, L., Chemical Reviews, 52, P. 51-53, 1953.

ALUMINUM OXIDATION (B) (Contd)

- D-14B "Effect of Applied Electric Field on the Mechanism of Oxidation of Metals and Alloys", Final Report, Berkowitz, J. B., et al Arthur D. Little, Inc., Report No. 74206, Naval Air Systems Command, 68 pages, Dec. 18, 71-Dec. 18, 1972.
- D-15B "Effect of Applied Electric Fields on the Mechanisms of Oxidation of Metals and Alloys", Third Quarterly Report, Berkowitz, J. B., Arthur D. Little, Inc., Report No. 74206, Naval Air Systems Command, Dec. 18, 71-Dec. 18, 72.
- D-16B "Kinetics of Iron and Aluminum Oxidation by Oxygen", Fontijn, A. and Kurzius, S. C., AeroChem. Research Lab., Inc., AeroChem TP-260, Advanced Research Projects Agency, 30 pages, July 1971.
- D-17B "Thin Oxide Films on Aluminum", Gulbransen, E. A. and Wysong, W. S., J. Physical Chemistry, 51, P. 1087-1103, 1947.
- D-18B "On the Ignition of Metal Particles", Khaikin, B. I., et al, Combustion, Explosion, & Shock Waves, 6(4), P. 412-422, Oct.-Dec. 1970.
- D-19B "Oxidation of High-Purity Aluminum and 5052 Aluminum-Magnesium Alloy at Elevated Temperatures", Cochran, C. N. and Sleppy, W. C., J. of Electrochemical, 108, P. 322-327, 1961.
- D-20B "High-Temperature Fast-Flow Reactor Studies of Metal Atom Oxidation Kinetics", Fontijn, A., Kurzius, S. C., and Houghton, J. J., AeroChem Research Laboratories, Inc., AeroChem TP-277, ARPA-DNA, (Prepared for Submission to the 14th International Combustion Symposium), March 1972.
- D-21B "Uber Die Brennbarkeit Von Metallen in Sauerstoff Bis 200 atm. Druck", Kirschfeld, L., Metall, 21, Jahrgang, Heft. 2, P. 98-102, February 1967.
- D-22B "Brennbarkeit Von Stahl und Gubeisen in Sauerstoff Bei Drucken Bis 150 atm", Kirschfeld, V. L., 39, Jahrgang, Heft. 7, P. 535-539, Juli 1968.
- D-23B "Die Verbrennungsgeschwindigkeit Von Eisendrahten in Sauerstoff Hohen Druckes", Kirschfeld, V. L., 32, Jahrgang Heft.1, P. 57-62, January 1961.

ALUMINUM OXIDATION (B) (Concl)

- D-24B "Einrichtung Fur Verbrennungsversuche an Metallen Unter Sauerstoffdrucken bis 200 atm und Brennbarkeit Von Eisendraht in Hockdruck-Sauerstoff", Kirschfeld, V. L., 36, Jahrgang, Heft.11, P. 823-826, November 1965.
- D-25B "Effect of Applied Electric Fields on the Mechanisms of Oxidation of Metals and Alloys", Berowitz, J. B. and Lee, W. D., Arthur D. Little, Inc., Naval Air Development Center, Third Quarter Report, n.d.
- D-26B "The Kinetics of Oxidation of Molten Aluminum in Oxidant Streams", Moskovits, M., Oxidation of Metals 5(1), P. 1-9, 1972.
- D-27B "Oxides and Hydroxides of Aluminum", Wefers, K. and Bell, G. M., Technical Paper No. 19, Alcoa Research Laboratories, 1972.

ALUMINUM KINETICS (C)

- D-1C "Metal-Water Reactions, VI" Analytical Formulations for the Reaction Rate", Technical Report, Epstein, L. F., Vallecitos Atomic Laboratory, General Electric Company, GEAP-3272, U.S. Atomic Energy Commission, Sept. 1959.
- D-2C "Metal Water Reactions. VII: Reactor Safety Aspects of Metal-Water Reactions", Technical Report, Epstein, L. F., Vallecitos Atomic Laboratory, General Electric Company Commission, Jan. 1960.
- D-3C "Metal-Water Reactions. IX: The Kinetics of Metal-Water Reactions-Feasibility Study of Some New Techniques", Furman, S. C., Vallecitos Atomic Laboratory, General Electric Company, GEAP-3338, U.S. Atomic Energy Commission, Jan. 1960.
- D-4C "Scientific Technological Mining Society Blasting", Selected Articles, Svetlov, B. Y., et al Foreign Technology Division, Wright-Patterson Air Base, FTD-HT-66-254, March 1967 (AD 660 249).
- D-5C "Action of V_2O_5 on the Burning Rate of Compositions Based on Ammonium Perchlorate and Metal Fuels", Romodanova, L. D., et al, Combustion, Explosion, & Shock Waves, 4(3), P. 186-187, Fall, 1968.
- D-6C "Metal-Water Reactions: .V. The Kinetics of Metal-Water Reactions-Low Pressure Studies", Furman, S. C., Vallecitos Atomic Laboratory, General Electric Company, U.S. Atomic Energy Commission, GEAP-3208, July 1959.
- D-7C "Frictional Sparking of Aluminum", Bailey, J. C., Trans., The Institute of Mining Engineers, 118 (4), P. 223-244, January 1959.
- D-8C "The Gaseous Species of the Al-Al₂O₃ System", Brewer, L. and Searcy, A. W., Amer. Chem. Soc. J., 73 (IV), P. 5308-5315, 1951.
- D-9C "Title in Russian), Beletskii, M. S. and Rapoport, M. B., Doklady Akad. Nauk S.S.S.R., 80, P. 751-754, 1951.
- D-10C "The Burning Rate of Aluminum and Magnesium Wire in Pure Oxygen and Oxygen-Water Vapor Atmospheres at Higher Pressures", Long, C. H. and Sebald, H., Western States Combustion Institute, WSCI-68-8, April 1968.

REACTION KINETICS (D)

- D-1D "Spectral and Photometric Study of the Flames of Model Fuel-Oxidizer-Metal Compositions", Pokhil, P. F., et al, Combustion, Explosion, & Shock Waves, 6(2), P. 129-136, April-June 1970.
- D-2D "Effect of Density on the Combustion of Aluminothermic Compositions", Dubrovin, A. S., et al, Combustion, Explosion, & Shock Waves, 6(1), P. 60-67, Jan.-March 1970.
- D-3D "Chemistry Under Pressure", Weale, K. E., Industrial Research, P. 50-52, June 1969.
- D-4D "Detonation: How This Process Occurs in Explosives", Shchilkin, K. I., Priroda (Nature), 53(8), P. 10-20, 1964.
- D-5D "Free Radicals in Charcoal and the Combustion of Compositions Containing Charcoal, Urbanski, T., et al, Explosivstoffe, P. 9-11, 1970.
- D-6D "A Reaction Mechanism for the Decomposition of Ammonium Nitrate", Koper, J. H., Explosivstoffe, P. 181-183, 1970.
- D-7D "Molecular Theory of Gases and Liquids", Bird, R. B., et al, John Wiley & Sons, Inc.
- D-8D "Spectroscopic Investigation of the Decomposition of Nitromethane in Shock Waves", Borisov, A. A., et al, Combustion, Explosion, & Shock Waves, 4(3), P. 222-227, 1968.
- D-9D "Activation Energy for Formation of Exicted Radicals in an Undisturbed Acetylene-Air Flame and in a Flame Reinforced by a High Frequency Discharge", Nesterko, N. A., et al, Combustion, Explosion, & Shock Waves, 4(3), P. 219-221, 1968.
- D-10D "Thermal Effects Which may Result in the Unexpected Ignition of Gaseous Mixtures", Dehn, J. T., U.S. Army Aberdeen Res. Development Center, Ballistic Research Lab., BRL-MR-2179, U.S. Army Material Command, April 1972. (AD 741 375)
- D-11D "A Computer Study of a Free-Radical Mechanism of Ethane Pyrolysis", Snow, R. H., et al, A.I. Ch. E. Journal, 5(3), P. 301-309, Sept. 1959.
- D-12D "Comment of Evidence for Nitrogen Trioxide in the Combustion of a Double-Base Propellant", Phillips, L., J. Physical Chemistry, 72 (6), II, P. 2279, 1968.

REACTION KINETICS (D) (Contd)

- D-13D "Excitation of Sodium in Certain Reactions Behind Shock Waves", Zaslonko, I. S., et al, Combustion, Explosion, & Shock Waves, 6(2), P. 175-182, April-June 1970.
- D-14D "Kinetics of the Combustion Reactions of Gas-Phase Systems", Kondrat'ev, V. N., and Vzryva, G. F., Combustion, Explosion & Shock Waves, 4(4), P. 253-257, 1968.
- D-15D "Reaction of Nitrogen with Burning Beryllium Droplets", Prentice, J. L., Combustion Science and Technology, 5, P. 273-285, 1972.
- D-16D "Chain-Thermal Auto-Ignition in H -Cl Mixtures", Borisov, A. A., Combustion, Explosion, & Shock Waves, 1(3), P. 6-10, July-Sept. 1965.
- D-17D "Determination of the Rate Constant of the Hydrogen-Hydroxyl Reaction", Azatyan, V. V., et al, Combustion, Explosion, & Shock Waves, 3(1), P. 46-50, Spring, 1967.
- D-18D "Use of a Pulse Mass Spectrometer to Investigate the High-Speed Processes Associated with the High-Temperature Decomposition of Ammonium Perchlorate", Korobeinichev, O. P., et al, Combustion, Explosion & Shock, 4(1), P. 19-22, Spring, 1968.
- D-19D "The Oxidation of Copper in the Temperature 1486 Range 200°-800°C", Tylecote, R. F., et al, J. Inst. of Metals, 81, P. 681-700; 1952-1953.
- D-20D "The Distillation of Lithium Metal", Epstein, L. F. and Howland, W. H., Science, 114, P. 443-444, 1951.
- D-21D "Metal-Water Reactions: II. Kinetics of the Reaction Between Lithium and Water Vapor", Deal, B. E. and Svec, H. J., J. Amer. Chem. Society, 75, P. 6173-6174, 1953.
- D-22D "The Rate of Reaction of Hydrogen with Throium", Peterson, D. T. and Westlake, D. G., J. Phys. Chemical, 63, P. 1514-1517, 1959.
- D-23D "Reaction Rate of Solid Sodium with Air", Howland, W. H., and Epstein, L. F., Ind. Engineering Chem. 49(11), P. 1931-1932, 1957.
- D-24D "Kinetics of the High Temperature Oxidation of Zirconium", Belle, J., and Mallett, M. W., J. Electrochem. Soc., 101, P. 339-342, 1954.

REACTION KINETICS (D) (Contd)

- D-25D "The Vapor Pressure of Inorganic Substances: V. Zirconium Between 1949-2054°K.", Skinner, G. B., et al, J. Amer. Chem. Soc., 73, P. 174-177, 1951.
- D-26D "Kinetics of the Uranium-Steam Reaction", Hopkinson, B. E., J. of Electrochemical Soc., 106, P. 102-106, 1959.
- D-27D "Combustion of Zirconium Droplets in Oxygen/Rare Gas Mixtures-Kinetics and Mechanism", Nelson, L. S., et al, Twelfth Symposium (International) on Combustion, P. 59-912.
- D-28D "Mechanism of Combustion Inhibition by Compounds Containing Halogen", Rosser, W. A., Wise, H., & Miller, J., The 12th Symposium (International) on Combustion, Vol. VII, P. 175-182.
- D-29D "The Quenching of Flame by Wire Gauzes", Palmer, K. N., The 12th Symposium (International) on Combustion, Vol. VII, P. 497-503.
- D-30D "On Some Reactions Occurring During the Explosion Induction Period", Voevodsky, V. V., The 12th Symposium (International) on Combustion, Vol. VII, P. 34-40.
- D-31D "Effects of Halogenated Extinguishing Agents on Flame Quenching and a Chemical Interpretation of Their Action", Belles, F. E., and O'Neal, C., Jr., The 12th Symposium (International) on Combustion, Vol. VII, P. 806-813.
- D-32D "Ignition Phenomena in Hydrogen-Air Mixtures", Rose, H. E. and Priede, T., The 12th Symposium (International) on Combustion, Vol. VII, P. 436-445.
- D-33D "The Combustion of Titanium and Zirconium", Harrison, P. L., The 12th Symposium (International) on Combustion, Vol. VII, P. 913-918.
- D-34D "Oxidation of Metal Alkyles and Related Compounds: The Ignition of Hydrocarbons", Badin, E. J., The 3rd Symposium (International) on Combustion, Vol. Flame and Explosion Phenomena, P. 386-389.
- D-35D "Kinetics Aspects of the Combustion of Solid Fuels", Arthur, J. R., Bangham, D. H., & Miss Bowring, J. R., The 3rd Symposium (International) on Combustion, Vol. Flame and Explosion Phenomena, P. 466-474.

REACTION KINETICS (D) (Contd)

- D-36D "The Mechanism of Chain Initiation in the Thermal Reaction Between Hydrogen and Oxygen", Lewis, B. and Elbe, G. V., The 3rd Symposium (International) on Combustion, Vol. Flame and Explosion Phenomena, P. 484-493.
- D-37D "Tulular Fast-Flow Reaction Studies at High Temperatures. 1. Kinetics of the Fe/O Reaction at 1600 K", Fontijn, A. and Kurizius, S. C., AeroChem Research Laboratories, Chemical Physics Letters, 13(5), P. 507-510, April 1, 1972.
- D-38D "Experimentelle und Thermodynamische Untersuchung Zur Reaktion Von Wolframdrahten Mit H O Bei Temperaturen Zwischen 1500 und 2800 K", Von, Almer, F.H.R. and Wiedijk, P., Z. Anorg. Allg. Chem., 385, P. 312-320, 1971.
- D-39D "Propagation of Gasless Reactions in Solids-II. Experimental Study of Exothermic Intermetallic Reaction Rates", Hardt, A. P. and Holsinger, T. W., Combustion and Flame, 21, P. 91-97, 1973.
- D-40D "Propagation of Lasless Reactions in Solid-I. Analytical Study of Exothermic Intermetallic Reaction Rates", Hardt, A. P. and Phung, P. V., Combustion and Flame, 21, P. 77-89, 1973.
- D-41D "A Theory of Water and Ionic Solution, with Particular Reference to Hydrogen and Hydroxyl Ions", Bernal, J. D. and Fowler, R. H., Journal of Chemical Physics, 1(8), P. 515-548, August 1933.
- D-42D "Intense and Transient Pressure, Temperature, and Irradiation Effects on the Ionization of Water", Lieberman, P. and Nagumo, G., IIT Research Institute, J6136-FR, Defense Atomic Support Agency, DASA-2341, September 1969.
- D-43D "Burning of a Particle of Low-Boiling Metal Moving Relative to a Gaseous Oxidizing Agent", Klyachko, L. A., Combustion, Explosion, and Shock Waves, 7(2), P. 199-202, September 1973.
- D-44D "Combustion of a Conglomerate of Magnesium Particles", Ozerov, E. S. and Skvortsov, I. I., Combustion, Explosion, & Shock Waves, 7(2), P. 191-194, September 1973.
- D-45D "Burning of Magnesium Particles in Water Vapor", Prachukho, V. P. et al, Combustion, Explosion, and Shock Waves, 7(2), P. 195-198, September 1973.

REACTION KINETICS (D) (Concl)

- D-46D "Mechanism of Action of Iron Catalysts on the Combustion of Composite Systems", Bobolev, V. K., Combustion, Explosion, and Shock Waves, 7(3), P. 317-324, November 1973.
- D-47D "The Effects of Chemical and Physical Parameters on the Burning Rate of a Liquid Droplet", Wise, H., et al, 5th Symposium (International) on Combustion, P. 132-141, 1955.
- D-48D "A Technical Mystery Under Vigorous Attack", Smith, R. B., Nucleonics, 14(II), P. 28-33, 1956.
- D-49D "Reaction of Flowing Steam with the Refractory Metals Niobium and Tantalum", Kilpatrick, M. and Lott, S. K., (Reprinted from), J. Less-Common Metals, 8, P. 299-305, 1965.
- D-50D "Reaction of Flowing Steam with Refractory Metals. I. Molybdenum (1100-1700°)", Kilpatrick, M. and Lott, S. K., J. Physical Chemistry, 69(5), P. 1-3, 1965.
- D-51D "Reaction of Flowing Steam with Refractory Metals. II. Rhenium (850°-1700°C)", Kilpatrick, M. and Lott, S. K., J. of Electrochemical Society, 113(1), P. 1-2, Jan. 1966.
- D-52D "Reaction of Flowing Steam with Refractory Metals, III, Tungsten (1000°-1700°C)", Kilpatrick, M. and Lott, S. K., J. of Electrochemical Society, 113(1), P. 1-2, Jan. 1966.
- D-53D "Catalysis in Deflagration of Explosives", Glaskova, A. P., Explosivstoffe, 4, P. 137-145, July-August 1973.

ALUMINUM PHYSICS & THERMODYNAMICS (E)

- D-1E "The Spreading of Liquid Metals on Solid Surfaces", Bondi, A., Chemical Reviews, 52, P. 417-423, 1953.
- D-2E "Destabilization of Vapor Film Boiling Around Spheres", Stevens, J. W. and Witte, L. C., Int. J. Heat Mass Transfer, 16, P. 669-678, 1973.
- D-3E "Identification of Boiling Regimes and a Reaction-Force Apparatur", Witte, L. C. and Henningson, P. J., J. Scientific Instruments (J. of Physics E), 2(2), P. 1101-1103, 1969.
- D-4E "Pressurization of a Solidifying Sphere", Hsiao, K. H., ASME Publication, 71-APM-AAA, J. of Applied Mechanics.
- D-5E "The Vapor Explosion-Heat Transfer and Fragmentation II. Transition Boiling from Spheres to Water", Stevens., et al, University of Houston, Dept. of Mechanical Engineering, Technical Report No. ORO-3936-3, April 1970.
- D-6E "The Vapor Explosion-Heat Transfer and Fragmentation IV. Rapid Quenching of Molten Metal", Witte, L. C., et al University of Houston, Dept. of Mechanical Engineering, Technical Report No. ORO-3936-6, August 1971.
- D-7E "The Vapor Explosion-Heat Transfer and Fragmentation V. Investigation of the Vapor Explosion Phenomenon using a Molten-Metal Jet Injected into Distilled Water", Bradley, R. H., et al University of Houston, Dept. of Mechanical Engineering, Technical Report No. ORO-3936-7, Oct. 1971.
- D-8E "Destabilization of Vapor Film Boiling Around Spheres", Stevens, J. W. and Witte, L. C., Inst. J. Heat Mass Transfer, 16, P. 669-678, 1973.
- D-9E "Maximum Stable Droplets in Dispersoids", Mugele, R. A., A.I.Ch.E. Journal, 6(1), P. 3-9, March 1960.
- D-10E "A Rate-Limited Model of Molten Fuel/Coolant Interactions: Model Development and Preliminary Calculations", Cho, D. H., et al, Argonne National Laboratory, ANL-7919, Atomic Energy Commission, March 1972.
- D-11E "The Viscosity of Molten Tin, Lead, Zinc, Aluminum, and Some of Their Alloys", Yao, T. P. and Kondic, V., J. Inst. of Metals, 81, P. 17-24, 1952/1953.

ALUMINUM PHYSICS & THERMODYNAMICS (E) (Contd)

- D-12E "A Precise Determination of the Viscosity of Liquid Tin, Lead, Bismuth, and Aluminum by an Absolute Method", Rothwell, E., J. Inst. of Metals, 90, P. 389-394, 1961/1962.
- D-13E "On the Instability of Small Gas Bubbles Moving Uniformly in Various Liquids", Hartunian, R. A. and Sears, W. R., J. of Fluid Mechanics, 3, P. 27-47, 1957.
- D-14E "On the Mechanism of Cavitation Damage by Nonhemispherical Cavities Collapsing in Contact with a Solid Boundary", Naude, C. F., and Ellis, A. T., J. Basic Engineering, 83(1), P. 648-656, March 1961.
- D-15E "Cavitation Bubble Collapse Observations in a Venturi", Ivany, R. D., Hammitt, F. G., and Mitchell, T. M., J. Basic Engineering, 88(3), P. 619-657, Sept. 1966.
- D-16E "The Initial Motion of a Gas Bubble Formed in an Inviscid Liquid", Walters, J. K. and Davidson, J. F., J. Fluid Mechanics, 17(3), P. 321-336, Nov. 1963.
- D-17E "Dynamics of Bubbles Moving in Liquids with Pressure Gradient", Yeh, Hsu-Chieh and Yang, Wen-Jei, J. of Applied Physics, 39(7), P. 3156-3165, June 1968.
- D-18E "Bubble Dynamics in a Non-Newtonian Fluid Subjected to Periodically Varying Pressures", Chan, K. S., and Yang, Wen-Jei, J. of Acoust. Soc. of America, 46(1), Part 2, P. 205-210, July 1969.
- D-19E "Dynamics of a Gas Bubble Moving in an Inviscid Liquid Subjected to Sudden Pressure Change", Yeh, Hsu-Chieh and Yang, Wen-Jei, J. Applied Physics, 40(4), P. 1763-1968, March 1969.
- D-20E "Dynamic Behavior of a Gas Bubble in Viscoelastic Liquids", Tanasawa, I. and Yang, Wen-Jei, J. Applied Physics, 41(11), P. 4526-4531, October 1970.
- D-21E "Bubbles and the Rocket Effect", Chincholle, L., J. Applied Physics, 41(11), P. 4532-4538, October 1970.
- D-22E "Heat Transfer from Spheres into Subcooled Liquid Sodium During Forced Convection", Witte, L. C., Baker, L., and Haworth, D. R., Transactions of the ASME., J. of Heat Transfer, P. 394-398, Nov. 1968.

ALUMINUM PHYSICS & THERMODYNAMICS (E) (Contd)

- D-23E "Oscillations of a Gas Bubble in Viscoelastic Liquids Subject to Acoustic and Impulsive Pressure Variations", Fogler, H. S., and Goddard, J. D., J. Applied Physics, 42(1), P. 259-263, January 1971.
- D-24E "The Interaction of Liquid Hydrocarbons with Water", Garland, G. and Atkinson, G., Dept. of Chemistry, Univ. of Maryland, Marine Safety Technology Div., Project No. 723261, October 1971.
- D-25E "Hazards of Spillage of LNG into Water", Burgess, D., Biordi, J. and Murphy, J., U.S. Dept. of the Interior, Bureau of Mines, PMSRC Report No. 4177, Office of Research and Development, Sept. 1972.
- D-26E "An Experimental Study of Transient Boiling", Rosenthal, M. W. and Miller, R. L., Oak Ridge National Laboratory, Carbide and Carbon Corporation, ORNL-2294, n.d.
- D-27E "Collapse of Spherical Cavities in Viscoelastic Fluids", Fogler, H. S. and Goddard, J. D., J. Physics of Fluids, 13(5), P. 1135-1141, May 1970.
- D-28E "The Initial Motion of a Gas Bubble Formed in an Inviscid Liquid" Walters, J. K. and Davidson, J. F., J. Fluid Mechanics, 12(1), P. 408-416, 1972.
- D-29E "On the Stability of the Spherical Shape of a Vapor Cavity in a Liquid", Plesset, M. S. and Mitchell, T. P., Quart. Appl. Mechanics, 13, P. 419-430, 1956.
- D-30E "XX. The Collapse of Cavitation Bubbles and the Pressures Thereby Produced Against Solid Boundaries", E. Cavitation, Benjamin, T. B. and Ellis, A. T., Phil. Trans., A-260, Plates 48 and 49, P. 221-240, 1966.
- D-31E "A Photographic Study of the Dynamics and Damage Capabilities of Bubbles Collapsing Near Solid Boundaries", Shulter, N. D. and Musler, R. B., J. of Engineering for Industry, (ASME), 87, P. 511-517, June 1965.
- D-32E "Machining High Purity Alumina", Linden Laboratories, Inc., U.S. Army Electronics Command, Eight Quarterly Report, July 30, 1966. (AD 640 695)
- D-33E "Pressure Generation by Molten Fuel-Coolant Interactions Under LMFBR Accident Conditions", Cho, D. H., et al, Proc. of Conference on New Developments in Reaction Mathematics and Applications, CONF-710302, Volume I of II, March 1971.

ALUMINUM PHYSICS & THERMODYNAMICS (E) (Concl)

- D-34E "Unsteady Stagnation Point Heat Transfer", Chao, B. T. and Jeng, D. R., ASME J. Heat Transfer, 87(2), P. 221-230, May 1965.
- D-35E "Heat Transfer and Fragmentation During Molten-Metal/Water Interactions", Witte, L. C., et al, ASME publication No. 73-WA/HT-28, ASME J. of Heat Transfer, P. 1-7, 1973.
- D-36E "Critical Speeds and Sizes of Liquid Globules", Hinze, J. O., Appl. Science Research, A1, P. 273-288, 1948.
- D-37E "Thermal Conductivity of Heterogeneous Materials", Gorrington, Robert L., Chemical Engineering Progress, 57(7), P. 53-59, July 1961.
- D-38E "Transmission of Sound in Molten Metals", Webber, G.M.B. and Stephens, R.W.B., Physical Acoustics: Principles and Methods, Volume IV-Part B, Applications to Quantum and Solid State Physics, Academic Press, P. 53-97, 1968.
- D-39E "Schallgeschwindigkeit und Kompressibilitat Von Quecksilber und Geschmolzenem Aluminium", Seemann, H. J. and Klein, F. K., Z. Angew. Phys., 19, P. 368-374, February 1965.
- D-40E "Ultrasonic Velocities of Sound in Some Metallic Liquids. Adiabatic and Isothermal Compressibilities of Liquid Metals at Their Melting Points", Kleppa, O. J., J. of Chemical Physics, 18(10), P. 1331-1336, October 1950.
- D-41E "Combustion of Powdered Metals in Active Media", Pokhil, P. F., et al, Foreign Technology Division, FTD-MT-24-551-73, n.d. (AD 769 576)

LIQUID METAL-H₂O, EXPLOSIONS (F)

- D-1F "Explosive Interaction of Molten Metals Injected into Water", Bradley, R. H., and Witte, L. C., Nuclear Science and Engineering, 48(4), P. 387-396, August 1972.
- D-2F "Molten Metal-Water Explosions", Flory, K., et al, Chemical Engineering Progress, 65(12), P. 50-54, Dec. 1969.
- D-3F "Melta/Water Explosions", Brauer, F. E., Nuclear Science and Engineering, 31(3), P. 551-554, March 1968. (G)
- D-4F "The Vapor Explosion", Witte, L. C., et al, J. of Metals, 22(2), P. 39-44, Feb. 1970.
- D-5F "Explosions from Molten Materials and Water", Lipsett, S. G., J. Fire Technology-Boston, 2 P. 118-126, 1966.
- D-6F "Experimental Study of Vapor Explosions", Enger, T. and Hartmen, D., Session VI, Paper 2, P. 2-12, n.d. 3rd International Conf. & Exhibition on Liquified Natural Gas, Sept. 24, 1972, Washington, D.C.
- D-7F "Metal-Water Reactions", Svec, H. J. and Staley, H. G., J. Electrochem. Soc., 105, P. 121-125, 1958.
- D-8F "A Technical Mystery Under Vigorous Attack", Smith, R. B., Nucleonics, 14(12), P. 29-33, 1956.
- D-9F "Ignition Characteristics of Metals and Alloys", Dean, L. E. and Thompson, W. R., J. Amer. Rocket Society, 31(7), P. 917-923, 1961.
- D-10F "Electrochemical Properties and Oxidation of Some Zirconium Alloys in Molten Salt at 300 C-500 C.", Atomic Energy of Canada Limited, Hubner, W. and Cox, B., Chalk River Nuclear Laboratories, AECL-4431, May 1973.
- D-11F "Fuel-Coolant Interactions in Submarine Vulcanism", Peckover, R. S., Buchanan, D. J., and Ashby, D.E.T.F., Culham Laboratory, CLM-P348, UKAEA Research Group, July 1973.
- D-12F "Interaction of Sodium with Molten UO₂ and Stainless Steel Using a Dropping Mode of Contact", Armstrong, D.R., et al, Argonne National Laboratory, ANL-7890, P. 1-23, Dec. 1971.
- D-13F "A Model for Fuel-Coolant Interactions", Buchanan, D. J., (Submitted for Publication in J. Phys. D., App. Phys.), CLM-P 361, P. 1-23, Plus Plates, August 1973.

LIQUID METAL-H₂O, EXPLOSIONS (F) (Concl)

- D-14F "Explosive Vapor Formation", Groenveld, P., J. Heat Transfer, ASME, 94(2), P. 236-238, May 1972.
- D-15F "Dynamic Mixing of Water and Lava", Colgate, S. A., and Sigurgeirsson, T., Nature, 244, P. 552-555, August 1973.
- D-16F "Spontaneous Nucleation in Supersaturated Water Vapor", Rodebush, W. H., Ind. Engineering Chem., 44, P. 1289-1291, 1952.
- D-17F "What Causes Kraft Dissolving Tank Explosions", I, Nelson, W. and Kennedy, E. H., Paper Trade Journal, 140, P. 50-56, 1956.
- D-18F "What Causes Kraft Dissolving Tank Explosions", II, Nelson, W. and Kennedy, E. H., Paper Trade Journal, 140, P. 30-32, 1956.
- D-19F "A Study into the Cause of Molten Explosions", Brauer, Fredrick, E., University of Kansas, Dept. of Chemical and Petroleum Engineering, 45 pages, April 1967.
- D-20F "An Experimental Study of the Water-Molten Metal Interaction", Paoli, Raphael, M., University of Kansas, Dept. of Mechanical and Petroleum Engineering, 79 pages, March 1968.
- D-21F "Molten Material-Coolant Interactions", Cho, D. H., et al, Trans. American Nuclear Society, 13(1), P. 385, 1970.
- D-22F "The Vapor Explosion-Heat Transfer and Fragmentation VII-Molten-Metal/Water Interactions Prior to a Vapor Explosion", Hsiao, K. H., et al, University of Houston, Department of Mechanical Engineering, Technical Report No. ORO-3936-11, Atomic Energy Commission, January 1974.

LIQUID ALUMINUM-H₂O, EXPLOSIONS (G)

- D-1G "Explosions Between Molten Aluminum and Water to the Aluminum Association", Rengstorff, G.W.P., et al, Battelle Memorial Institute, Columbus Laboratories, April 11, 1969.
- D-2G "Annual Summary Report on Explosions of Molten Aluminum and Water", Laber, D. and Lemmon, A. W., The Aluminum Association, Battelle Memorial Institute, P. A-58, Dec. 1970.
- D-3G "Chemical Engineering Division", Semiannual Report, Vogel, R. C., Levenson, M., & Masten, F. R., Argonne National Laboratory, ANL-6900, January-June 1964., SL 14,103.
- D-4G "Chemical Engineering Division", Summary Report, Lawroski, S., Vogel, R. C., Levenson, M., and Munnecke, V. H., Argonne National Laboratory, ANL-6648, May 1963.
- D-5G "Chemical Engineering Division", Summary Report, Lawroski, S., Vogel, R. C., and Munnecke, V. H., Argonne National Laboratory, ANL-6379, October 1961.
- D-6G "Chemical Engineering Division", Semiannual Report, Vogel, R. C., Levenson, M., and Munnecke, V. H., Argonne National Laboratory, ANL-6800, May 1964.
- D-7G "Experiments with a Series of Small, Pu-Plus-U-Fueled Fast-Reactor Criticals", (FARET Mockup-ZPR-3 Assembly 46), Hess, Al L., Keeney, W. P., and McVean, R. L., Argonne National Laboratory, ANL-7215, January 1970.
- D-8G "Chemical Engineering Division", Summary Report, Lawroski, S., Vogel, R. C., Levenson, M., and Munnecke, V. H., Argonne National Laboratory, ANL-6725, April, May, June, 1963.
- D-9G "In-Pile Molten Metal-Water Reaction Experiments", Elgert, O. J. and Brown, A. W., United States Atomic Energy Commission, Technical Information Service Extension, Oak Ridge, Tenn., IDO-16257, June 30, 1956.
- D-10G "Mechanism for Vapor Explosions", Buchanan, D. J. and Dullforce, T. A., Nature, 245, P. 32-34, Sept. 7, 1973.
- D-11G "The Reaction of Molten Uranium and Zirconium Alloys with Water", Higgins, H. M., U.S. Atomic Energy Commission, Aerojet General Corporation, AGC-AE-17, April 30, 1956.

LIQUID ALUMINUM-H₂O, EXPLOSIONS (G) (Concl)

- D-12G "Simulation of Nuclear Bursts at the Surface of Water by the Impaction of Molten Metal Droplets", Kriebel, A. R., URS Research Company, URS 7207-2, Office of Naval Research, April 1973. (AD 759 383)
- D-13G "Chemical Engineering Division", Summary Report, Lawroski, S. Vogel, R. C., and Munnecke, V. H., Argonne National Laboratory, ANL-6413, July, August, September, 1961.
- D-14G "Ursachen und Verhütung Von Al-H₂-Explosionen", Maischak, Von Klaus-Dieter and Feige, W., Neue Hutte, 15(11), P. 662-665, November 1970.

LIQUID EXPLOSIONS PHENOMENA (H)

- D-1H "Initiation of Detonation of Explosives", Kistiakowsky, G. B., Third Symposium on Combustion, Flame, & Explosion Phenomena, P. 560-571.
- D-2H "Measurement of the Chapman-Jouguet Pressure and Reaction Zone Length in a Detonating High Explosive", Duff, R. E., et al, J. of Chemical Physics, 23(7), P. 1268-1273, July 1955.
- D-3H "The Correlation of Explosive Power with Molecular Structure", Martin, A. R., et al, J. Applied Chem., 9, P. 310-316, June 1959.
- D-4H "Thermochemistry of Explosives", Thermochemistry of Explosives, Chapter V., P. 40-64.
- D-5H "Generalized Shock Adiabats for Organic Liquids", Voskoboinikov, I. M., et al, Combustion, Explosion, & Shock Waves, 3(4), P. 359-364, 1967.
- D-6H "Thermodynamic Investigation of the Shock Adiabats", Trofimov, V. S., Combustion, Explosion, & Shock Waves, 3(4), P. 352-358, 1967.
- D-7H "Excitation and Propagation of Detonation Processes in Weakly Initiated Liquid Explosives", Dubovik, A. V., et al, Combustion, Explosion, and Shock Waves, 3(4), P. 299-304, 1967.
- D-8H "Shock Initiation of Nitromethane", Walker, F. E. and Wasley, R. J., Lawrence Radiation Laboratory, University of California, URCL-71696, May 13, 1969.
- D-9H "Annealing Behavior of Recoil Cobalt-57 Atoms in Hexamine Nickel Chloride", Yoshihara, K., Nature, 204, P. 1296-1299, Dec. 26, 1964.
- D-10H "The Initiation of Liquid Explosives by Shock and the Importance of Liquid Break BU", Johansson, C. H., et al, Proc. Royal Society, 246, P. 160-167.
- D-11H "Critical Mass (Hypothesis and Verification) of Liquid Rocket Propellants", Report No. IX., Farber, E. A., Florida Engineering & Industrial Experiment Station, Univ. of Florida, NASA Project NAS10-1255, Sept. 14-16, 1971.
- D-12H "Characteristics of Liquid Rocket Propellant Explosion Phenomena", Farber, E. A., Florida Engineering & Industrial Experiment Station, Univ. of Florida, NASA Project NAS 10-1255, XXII(7), July 1968.

LIQUID EXPLOSIONS PHENOMENA (H) (Contd)

- D-13H "Characteristics of Liquid Rocket Propellant Explosion Phenomena", Farber, E. A., Florida Engineering & Industrial, Experiment Station, Univ. of Florida, NASA Project NAS 10-1255, XXI(8), August 1967.
- D-14H "Characteristics of Liquid Rocket Propellant Explosion Phenomena", Farber, E. A., Florida Engineering & Industrial, Experiment Station, Univ. of Florida, NASA Project NAS 10-1255, XXII(11), Nov. 1969.
- D-15H "No. 346: A Mathematical Model for Defining Explosive Yield and Mixing Probabilities of Liquid Propellants", "No. 347: A Systematic Approach for the Analytical Analysis and Prediction of the Yield from Liquid Propellant Explosions", Farber, E. A., Florida Engineering & Industrial, Experiment Station, Univ. of Florida, XX(3), March 1966.
- D-16H "No. 396: Characteristics of Liquid Rocket Propellant Explosion Phenomena, Part V: Thermocouple Grid Analysis of Two 25,000 lb Lox/RP Liquid Propellant Explosion Experiments", Farber, E. A., Florida Engineering & Industrial, Experiment Station, Univ. of Florida, XXI(11), Nov. 1967.
- D-17H "Final Report: Prediction of Explosive Yield and Other Characteristics of Liquid Propellant Rocket Explosions", Farber, E. A., et al, Florida Engineering & Industrial, Experiment Station, Univ. of Florida, NAS 10-1255, Oct. 31, 1968.
- D-18H "Rapid Phase Transformation During LNG Spillage on Water", Enger, T., and Hartman, D., Session VI, Paper 2., P. 1-26, n.d.
- D-19H "Explosives", Gurton, O. A., Wood, H. L., Kellock, S. C., and McAuslan, J.H.L., Reprinted from Reports on the Progress or Applied Chemistry, Vol. 55, P. 307-332, 1970.
- D-20H "Electrostatic Charge Generation and Auto-Ignition Results of Liquid Rocket Propellant Experiments", Farber, E. A., 14th Annual DOD Explosive Safety Seminar, New Orleans, La., P. 631-681, November 8-10, 1972.
- D-21H "LNG/Water Explosions: Cause & Effects", Katz, D. L. and Sliepcevich, C. M., Hydrocarbon Proc. Petrol. Refin., P. 240-244, November 1971.
- D-22H "Bubble Mechanism of Initiating an Explosion in a Liquid Layer After an Impact", Dubovik, A. V. and Bobolev, V. K., Combustion, Explosion, & Shock Waves, 7(2), P. 207-213, September 1973.

LIQUID EXPLOSIONS PHENOMENA (H) (Contd)

- D-23H "Some Regularities of the Initiation of an Explosion in Nitroglycerin During Collapse of Air Cavities After an Impact", Dubovik, A. V. and Bobolev, V. K., Combustion, Explosion, and Shock Waves, 7(2), P. 214-220, Sept. 1973.
- D-24H "Unusual Fire Hazard of LNG Tanker Spills", Fay, James, A., Combustion Science and Technology, 7, P. 47-49, 1973.
- D-25H "The Influence of the Surface Tension Difference on the Boiling of Mixtures", Hovestreyjdt, J., Chemical Engineering Science, 18, P. 631-639, 1963.
- D-26H "The Superheating of Liquids", Kenrick, F. B., et al, J. Physic. Chemical, 28, P. 1297-1307, 1924.
- D-27H "On the Limit Superheat", Wakeshima, H. and Takata, K., Journal of the Physical Society of Japan, 13(11), P. 1398-1403, November 1958.
- D-28H "The Pressure-Volume Relation of Superheated Liquids", Wismer, K. L., J. Phy. Chem., 26, P. 301-315, 1922.
- D-29H "Some Applications of Photography", Rayleigh, L., Nature, 1133(44), P. 249-254, July 16, 1891.
- D-30H "Superheat-Limit Explosions", Katz, D. L., Chemical Engineering Progress, 68(5), P. 68-69, May 1972.
- D-31H "LNG/Water Explosions: Cause and Effect", Katz, D. L. and Sliepcevich, C. M. Hydrocarbon Proc. Petrol. Refin., P. 240-244, Nov. 1971.
- D-32H "Droplet Size Distribution in Sprays", Mugele, R. A. and Evans, H. D., Industrial and Engineering Chemistry, 43(I), P. 1317-1325, 1951.
- D-33H "Interfacial Area in Liquid-Liquid and Gas-Liquid Agitation", Vermeulen, T., et al, Chem. Engrg. Progress, 51(I), P. 85F-94F, 1955.
- D-34H "The Laws of Expanding Circles and Spheres in Relation to the Lateral Growth of Surface Films and the Grain-Size of Metals", Evans, U. R., Faraday Society, Trans., 41, P. 365-374, 1945.
- D-35H "The Rate of Growth of Vapor Bubbles in Superheated Water", Dergarabedian, Paul, Journal Appl. Mech., 75, P. 537-545, n.d.

LIQUID EXPLOSIONS PHENOMENA (H) (Contd)

- D-36H "Supersaturation of Gases in Liquids", Kenrick, F. B., et al, Journal Phy. Chem., 28, P. 1308-1315, 1924.
- D-37H "Generalized Quantitative Criteria for Predicting the Rate-Controlling Mechanism for Vapor Bubble Growth in Super-Heated Liquids", Florschuetz, L. W. and Al-Jubouri, A. S., International Journal of Heat Mass Transfer, 14, P. 587-600, 1971.
- D-38H "Numerical Study of Two Fluid Rayleigh-Taylor Instability", Daly, Bart J., The Physics of Fluids, 10(2), P. 297-307, February 1967.
- D-39H "Dynamic Mixing of Water and Lava", Colgate, S. A. and Sigurgeirsson, T., Nature, 244, P. 552-555, August 1973.
- D-40H "Numerical Study of Large-Amplitude Free-Surface Motions", Harlow, F. H. and Welch, J. E., The Physics of Fluids, 9(5), P. 842-851, May 1966.
- D-41H "Maximum Superheating of Water as a Measure in Negative Pressure", Briggs, L. J., J. of Applied Physics, 26(8), P. 1001-1006, August 1955.
- D-42H "Bubble Growth and Pressure Relationships in the Flashing of Superheated Water", Hooper, F. C., et al, Volume 1 of 3, University of Toronto, Department of Mechanical Engineering, UTME-TP-6904, July 1969.
- D-43H "Bubble Growth and Pressure Relationships in the Flashing of Superheated Water", Hooper, F. C., et al, Volume 2 of 3, University of Toronto, Department of Mechanical Engineering, UTME-TP-6904, July 1969.
- D-44H "Bubble Growth and Pressure Relationships in the Flashing of Superheated Water", Hooper, F. C., et al, Volume 3 of 3, University of Toronto, Department of Mechanical Engineering, UTME-TP-6904, July 1969.
- D-45H "Observations on Bubble Growths in Various Superheated Liquids", Dergarabedian, Paul, Journal of Fluid Mechanics, 9(1), P. 39-48, September 1960.
- D-46H "Atomization of Liquids by Means of a Rotating Cup", Hinze, J. O. and Milborn, H., J. of Applied Mechanics, P. 145-153, July 1950.

LIQUID EXPLOSIONS PHENOMENA (H) (Contd)

- D-47H "The Rate of Growth of Vapor Bubbles in Superheated Water", Dergarbedian, Paul, J. Applied Mechanics, 20, P. 537-545, December 1953.
- D-48H "Air Bubbles in Water", Liebermann, Leonard, J. of Applied Physics, 28(2), P. 205-211, February 1957.
- D-49H "On the Conduction of Heat into a Growing Vapor Bubble", Forster, H. K., J. Applied Physics, 25(1), P. 1067-1068, August 1954.
- D-50H "An Experimental Study of Energy Transfer Processes Relevant to Thermal Explosions", Board, S. J., et al, International J. Heat Mass Transfer, 14, P. 1631-1641, 1971.
- D-51H "Transient Heat Transfer from a Hot Nickel Sphere Moving Through Water", Walford, F. J., International Journal Heat Mass Transfer, 12(12), P. 1621-1625, Dec. 1969.
- D-52H "Bubble Growth in Transient Pool Boiling", Yesin, A. O. and Jeffers, D. E., J. of the British Nuclear Energy Society, 8(4), P. 267-274, October 1969.
- D-53H "Heat Transfer and Critical Heat Flux in Transient Boiling, (I) An Experimental Study in Saturated Pool Boiling", Tachibana, F., et al, J. Nuclear Science and Technology, 5(3), P. 117-126, March 1968.
- D-54H "The Effect of Subcooling on the Onset of Transition Boiling", Witte, L. C., et al, Tran. American Nuclear Society, 12(2), P. 806, November 1966.
- D-55H "Selected Values of Critical Supersaturation of Nucleation of Liquids from the Vapor", Pound, G. M., J. of Physical and Chemical Reference Data, 1(1), P. 119-133, 1972.
- D-56H "The Top Millimeter of the Ocean", MacIntyre, Ferren, Scientific American, P. 62-77, 1974.
- D-57H "Growth of a Vapor-Filled Cavity Near a Heating Surface and Some Related Questions", Forster, K. E., The Physics of Fluids, 4(4), P. 448-455, April 1961.
- D-58H "Growth of a Vapor Bubble in a Superheated Liquid", Forster, H. K. and Zuber, N., J. Of Applied Physics, 25(4), P. 474-478, April 1954.

LIQUID EXPLOSIONS PHENOMENA (H) (Concl)

- D-59H "An Experimental Study of Surface Cooling by Bubbles During Nucleate Boiling Water", Rogers, T. F. & Mesler, R. B., A.I.Ch.E. Journal, 10(5), P. 656-660, Sept. 1964.
- D-60H "The Behavior of Water Under Hydrostatic Tension: I", Temperley, H.N.V. & Chambers, LL.G, Proceeding of the Physical Society of London, 58(328), Pt. 4, P. 420-436, July 1946.
- D-61H "The Effects of Bubble Translation of Vapor Bubble Growth in a Superheated Liquid", Ruckenstein, E. & Davis, E. J., International J. of Heat and Mass Transfer, 14(7), P. 939-952, July 1971.
- D-62H "Combustion of Powdered Metals in Active Media", Pokhil, P. F., et al, Foreign Technology Division, FTD-MT-24-551-73, n.d. (AD 769 576)
- D-63H "The Effect of Acceleration of the Nature of Combustion of Liquid Explosives", Margolin, L. D. & Ordzhonikidze, S. K., Foreign Technology Division, FTD-HT-23-1410-74, n.d.
- D-64H "Investigation Regarding the Effect of Thermophysical Parameters on the Ignition of Fuel Drops in a Gas Behind a Shock Wave Front", Gel'sand, B.Ye, et al, Foreign Technology Division, FTD-HT-23-1411-74, n.d.
- D-65H "The Effect of Pressure on the Burning Process of Aluminum Powders", Kalabukhov, G. V., et al, Foreign Technology Division, FTD-HT-1221-74, n.d.

INSTRUMENTATION (I)

- D-1I "Use of Infrared Imagery to Track In-Flight Ejecta Produced by a 100-Ton TNT Detonation of Granite", (Operation Mine Shaft), Lieberman, P., et al, IIT Research Institute, J6180-FR., May 1970.
- D-2I "Detection of Strong Shock Waves with Plastic Tapes", Champion, A. R., et al, Sandia Laboratories, SC-R-68-1676, Reprinted from: Review of Scientific Instruments., 39(3), P. 377-378, March 1968.
- D-3I "A Two-Camera System to Study Underwater Explosions", Pearson, J. and Gallup, R., Naval Weapons Center, NWC TP-5345, Naval Materiel Command, 24 pages, April 1972.
- D-4I "Metal-Oxide Metal (M-O-M) Detector", Kwok, S. P., et al, J. Applied Physics, 42(2), P. 554-563, Feb. 1971.
- D-5I "Directional Sensitivity of Hot Film Sensors in Liquid Metals", Hill, J. C. and Sleichner, C. A., Review of Scientific Instruments, 42(10), P. 1461-1468, Oct. 1971.
- D-6I "An Apparatus for the Study of Rapid Phase Transformation Kinetics in Metals", Ayers, J. D. and Barnes, W. C., Review of Scientific Instruments, 42(3), P. 302-304, March 1971.
- D-7I "Capsule for Studying the High Pressure Reactions of Hazardous Liquids", Cervený, W. J., et al, Review of Scientific Instruments, 42(3), P. 391-393, March 1971.
- D-8I "Optical Method of Determining Propellant Surface Temperature", Pokhil, P. F., et al, Combustion, Explosion, & Shock Waves, 3(3), P. 204-209, Fall 1967.
- D-9I "Measurement of the Thermal Pressure Coefficient (-) of Molten Salts", Cleaver, B., et al, Review of Scientific Instruments, 42(5), P. 578-579, May 1971.
- D-10I "Speed of Sound in Liquid Sodium from 1000 to 1500°C, Chasanov, M. G., et al, J. Applied Physics, 43(2), P. 748-749, Feb. 1972.
- D-11I "A Multiple-Pulse Ruby-Laser System for Dynamic Photo-mechanic: Applications to Transmitted and Scattered-Light Photoelasticity", Rowlands, R. E., et al, Experimental Mechanics, 9(9), P. 385-393, Sept. 1969.

INSTRUMENTATION (I) (Contd)

- D-12I "Furnace Periscope and Flow Visualization", Scorey, P. L., et al British Ceramic Society: Transaction, 60(5), P. 343-362, May 1961.
- D-13I "Operation of a Grid-Shuttered Image Converter Tube in the Piscosecond Region", Schelev, M. Y., et al, Review of Scientific Instruments, 43(12), P. 1819-1829, Dec. 1972.
- D-14I "An Intense Microsecond Flash Lamp", LeBlang, J. C., et al, Review of Scientific Instruments, 43(12), P. 1814-1818, Dec. 1972.
- D-15I "Optical Lever Observations of Impact Shock Waves", Gregson, V. G. and Zaker, T. A., IIT Research Institute, P. 1-9.
- D-16I "Eyes That Stop Time", Sinclair, M. P., Industrial Research P. 45-47, June 1969.
- D-17I "The Characteristics of the Acoustical Pulses Emitted by Boiling Bubbles in Water", Saxe, R. F. and Cothren, R. K., J. Acoustical Soc. of America, 48(5), Pt. II, P. 1257-1265, Nov. 1970.
- D-18I "Oscillations of a Gas Bubble in Viscoelastic Liquids Subject to Acoustic and Impulsive Pressure Variations", Fogler, H. S. and Goddard, J. D., J. Applied Physics, 42(1), P. 259-263, Jan. 1971.
- D-19I "Significant Audible Noise From Sodium-Water Reactions", Ying, S. P., and Scott, C. C., J. Acoustical Society of America, 49(5), Pt. II, P. 1393-1396, May 1971.
- D-20I "5: Emission of Light During Detonation", Dentonics, P. 177-189.
- D-21I "A Method for Performing High Precision Lattice Parameter Change Measurements of Quenched Aluminum", Eubig, C. and Tomizuka, T., Review of Scientific Instruments, 43(12), P. 1804-1810, Dec. 1972.
- D-22I "Microcalorimeter Measurements of Flame Emission", Zenin, A. A., et al, Combustion, Explosion, & Shock Waves, 4(2), P. 113-116, Summer 1968.
- D-23I "Hycam Instruction Manual", 16 mm High Speed Motion Picture Camera, Photo Instrument Division, Redlake.

INSTRUMENTATION (I) (Concl)

- D-24I "Sensitivity of Explosives to Initiation by Electrostatic Discharges", Brown, F. W., Kusler, D. J., Gibson, F. C., Bureau of Mines, U.S. Department of the Interior, Report of Investigations 5002, September 1953.
- D-25I "Surface Tension of Titanium, Zirconium, and Hafnium", Peterson, A. W., Kedesdy, H., et al, Journal of Applied Physics, 29(2), P. 213-216, February 1958.
- D-26I "The Application of the High-Speed Motion Picture Camera to Research on the Surface Tension of Liquids", Hauser, E. A., et al, J. Physical Chemistry, 20, P. 973-988, 1936.
- D-27I "A Miniature Pressure Transducer", Massey, B. S. and Kavrak, I., J. Science Instrumentation, 43, P. 569-571, 1966.
- D-28I "Available Dark", Photography, Norwood, James, Industrial Photography, 20(11), P. 24-26, November 1971.

MISCELLANEOUS (J)

- D-1J "Studies in the Molecular Forces Involved in Surface Formation. II: The Surface Free Energies of Simple Liquid Mixtures", Belton, J. W. and Evans, M. G., Faraday Society, Transactions, 41, P. 1-21, 1945.

ELECTROSTATICS & ELECTRICAL EFFECTS (K)

- D-1K "Frictional Electricity in Missile Systems", Molmud, P., J. American Rocket Society, 29(1), P. 73-75, Jan. 1959.
- D-2K "Account of a Hydro-Electric Machine Constructed for The Polytechnic Institution and of Some Experiments Performed by its Means", Faraday, M., Philosophical Magazine, 23, P. 194-202, 1843.
- D-3K "Explosibility of Metal Powders", Bureau of Mines, Report of Investigation 6516, Department of the Interior, Jacobson, M., et al, 1964.
- D-4K "The Theory of Sound", Strutt, J. W. and Rayleigh, B., New York Dover Publications, Volume I., 1945.
- D-5K "What Metals will Throw a Spark", Anon, Metal Progress, 83, P. 33, September 1953.
- D-6K "Frictional Sparking Hazards with Aluminum", Anon, Light Metals, 21, P. 167-168, June 1958.
- D-7K "Triboluminescence and Triboelectrification by the Motion of Mercury over Glass Coated with Scintillator Dyes", Kerzthelyi, C. P. and Bard, A. J., J. Electrochem. Soc.: Solid-State Science and Technology, P. 1726-1729, Dec. 1973.
- D-8K "Gaseous Reactions and Luminescence Initiated by Triboelectricity", DePaoli, S. and Strausz, O. P., Canadian J. of Chemistry, 48, P. 3756-3757, 1970.
- D-9K "Generation of Light by the Relative Motion of Contiguous Surfaces of Mercury and Glass", Dybwad, G. L. and Mandeville, C. E., The Physical Review, 161(3), P. 527-532, Sept. 1967.
- D-10K "On the Equilibrium of Liquid Conducting Masses Charged with Electricity", Rayleigh, Lord, London Philosophical Magazine 5(14), P. 184-186, 1882.
- D-11K "Electrochemical Cells and Electrical Conduction of Pure and Doped Al_2O_3 ", Brook, R. J., Yee, J., and Kroger, F. A., Amer. Ceramic Society, 54, P. 444-451, 1971.
- D-12K "Some Electromechanical Effects on Dielectrics", Kao, K. C., British J. of Applied Physics, 12, P. 629-632, Nov. 1961.

APPENDIX B
MATRIX ISOLATION STUDY

IIT RESEARCH INSTITUTE

APPENDIX B

MATRIX ISOLATION STUDY

B.1 INTRODUCTION

The purpose of the matrix study was to determine the existence and thermodynamic constants of chemical species produced in the water molten aluminum reaction which are not currently predicted by available thermodynamic data ⁽¹⁾. In particular the gaseous species AlOH, or possibly some other hydroxy species of aluminum, was sought which could possibly be formed in the reaction $\text{Al(l)} + \text{H}_2\text{O(g)} = \text{AlOH(g)} + \text{H(g)}$. This reaction with the possible formation of gaseous aluminum products could be of prime importance in understanding the reaction initiation of molten aluminum and water. Although these experiments are made at low pressure, the basic thermodynamic constants can be used to determine mechanisms under the explosion conditions existing in the field tests and in the manufacturing process.

B.2 EXPERIMENTAL

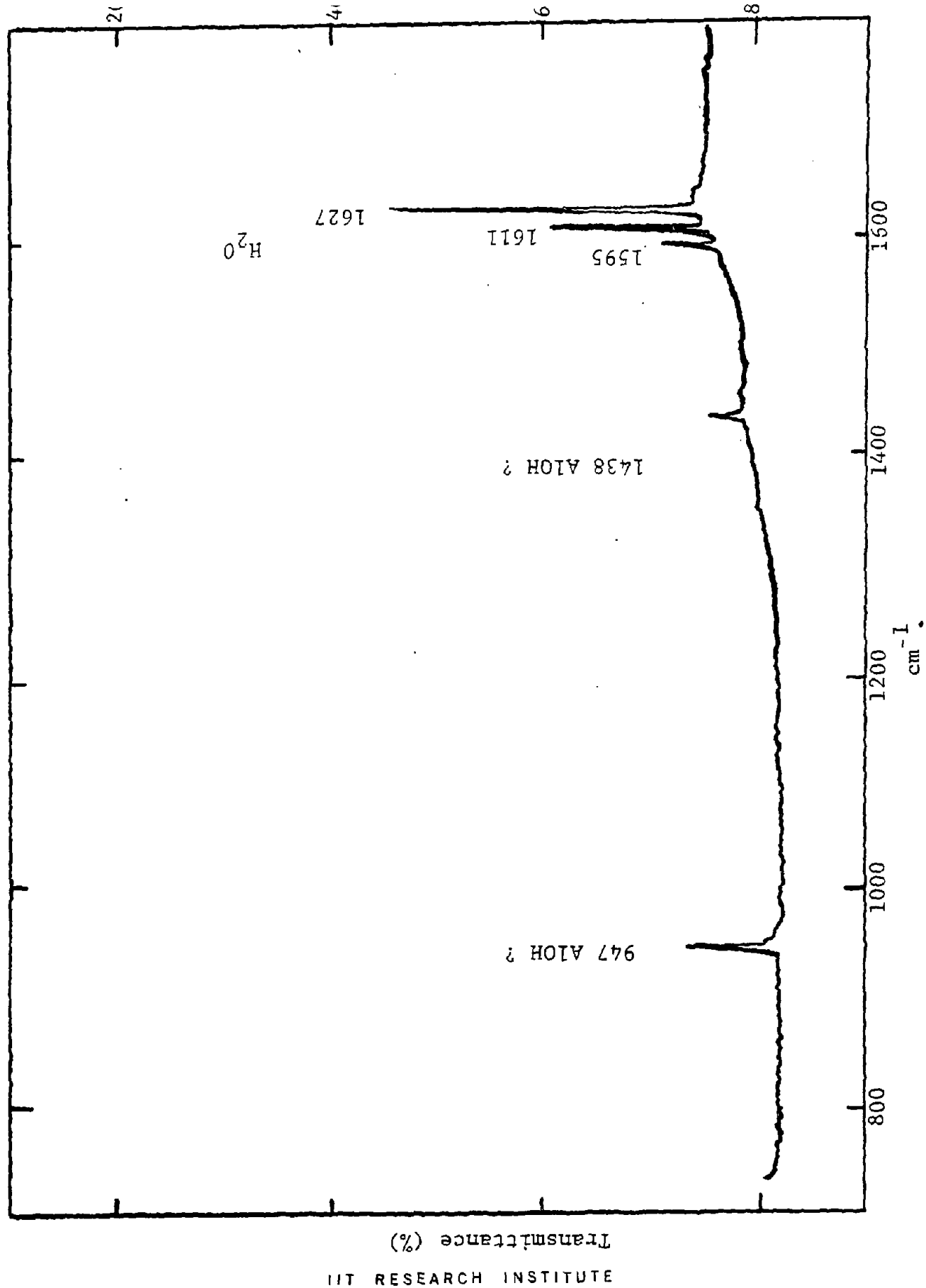
In order to pursue the above study, the technique of matrix isolation, in conjunction with infrared spectroscopy, was used to study the reaction. The aluminum, (99.999 percent pure) was contained in aluminum oxide effusion tube with an orifice 0.025 inch diameter. The latter was surrounded by a tantalum susceptor which was heated by electric induction. Provision was made to pass water vapor over the heated aluminum. The pressure of the water vapor over the heated aluminum was controlled at about 10^{-4} - 10^{-5} atm. The vapor species effusing from the reaction cell were isolated in argon matrices at high dilution and the IR spectrum recorded on a Perkin-Elmer 621 spectrometer in the range 4000-200 cm^{-1} .

B.3 RESULTS

A series of two experiments were made in which water vapor was passed over molten aluminum in the temperature range 1350 to 2460°F. In Figure B-1 part of an IR spectrum of the vapor species effusing from the reaction cell at a temperature of 1535°F is shown. By far the most intense absorption bands are those of unreacted water vapor at about 1600 cm^{-1} . In addition two weaker absorption bands were observed at 1438 and 947 cm^{-1} . These latter two bands were observed in several experiments in the temperature range 1380 to 1880°F. Relative absorption band intensity measurements made on these two features (947 and 1438 cm^{-1}) indicated that the same molecular species was responsible for both of them. The only other absorption bands occurring in the spectrum not shown in Figure B-1 were those of the high frequency vibration of H_2O at about 3600 cm^{-1} . In experiments performed with the reaction cell temperature in the range 2280 to 2460°F the 947 and 1438 cm^{-1} absorption bands were absent, and the water vapor bands at about 1600 cm^{-1} were markedly reduced in intensity.

It was demonstrated in later experiments that all the water vapor passing over the molten aluminum at these temperatures had reacted and that the weak H_2O absorption bands represented a residual background level. A new series of absorption bands appeared at about 1000 cm^{-1} and these are shown in Figure B-2. From previous studies by this writer ^(2,3) these absorption bands may be readily assigned to the species Al_2O which is known to be formed by the reaction of molten aluminum with aluminum oxide at these temperatures.

From the data obtained in these experiments it appeared possible that the 947 and 1438 cm^{-1} absorption bands could possibly be assigned to a gaseous species AlOH . For such a molecule, three infrared active frequencies would be expected, an Al-O stretching mode at about $900\text{-}1000\text{ cm}^{-1}$, an Al-O-H bending mode at about $1400\text{-}1600\text{ cm}^{-1}$ and an O-H stretching mode at about $3300\text{-}3600\text{ cm}^{-1}$.



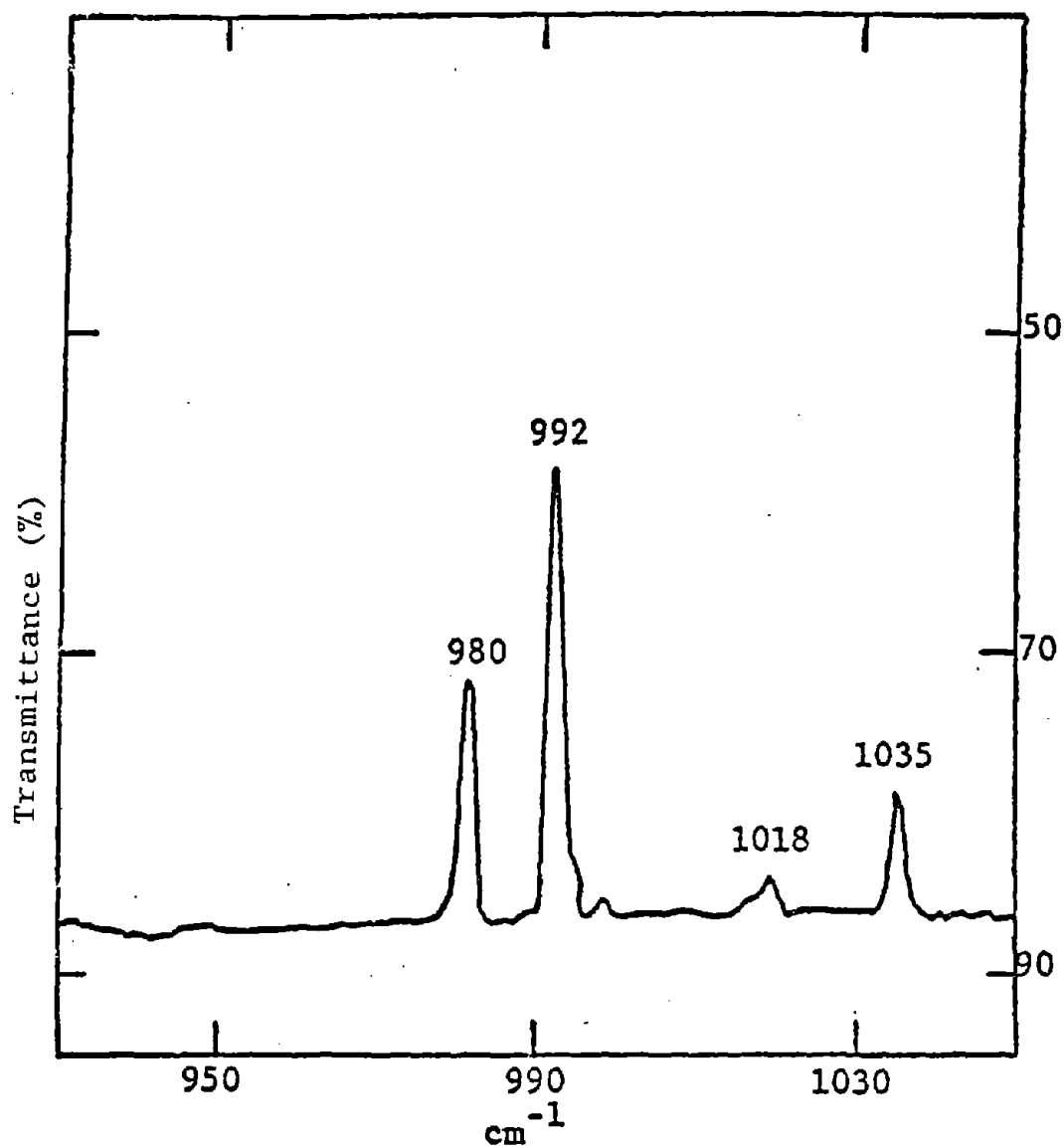


Figure B-2 IR Spectrum of Al_2O_3 Formed in the Reaction of Molten Aluminum and Water Vapor at 2450°F .

Although in the present study no absorption band corresponding to an O-H stretching vibration was observed, possibly due to its low extinction coefficient, the magnitudes of the two observed frequencies of 947 and 1348 cm^{-1} are indeed compatible with the existence of AlOH.

In an attempt to gain further evidence as to the possible existence of AlOH, a series of 10 experiments were performed in which water vapor containing about equimolar amounts of H_2^{16}O and H_2^{18}O were passed over the molten aluminum in the aluminum oxide effusion tube. A temperature range from 1425 to 2460°F was examined, starting initially at the lower temperature and increasing in approximately 180°F increments. Up to a temperature of 2140°F the only absorption bands observed were those of the water vapor. These are shown in Figure B-3 and the presence of the two isotopic species is clearly evident. No absorption bands at 947 or 1348 cm^{-1} were recorded. At the temperature of the next experiment, 2320°F, a very weak absorption band due to the H_2^{16}O species was present and some weak bands due to Al_2O . At 2460°F the spectrum was basically the same except that the Al_2O bands were now much more intense. However, there were no absorption bands corresponding to the two isotopic species Al_2^{16}O and Al_2^{18}O by the reaction between molten aluminum and the water vapor. It must therefore be concluded that the formation of Al_2O is the result of the reaction $4\text{Al} + \text{Al}_2\text{O}_3 = 3\text{Al}_2\text{O}$, with the bulk of the Al_2O_3 for the reaction being provided by the effusion cell itself. It is not clear why the 947 and 1348 cm^{-1} absorption bands did not appear in this series of experiments as opposed to the earlier set of experiments in which only pure H_2^{16}O was used. It was observed that in the latter series of experiments there appeared to be a reduced mass-flow of water vapor through the effusion cell. If indeed AlOH is formed in the molten aluminum water reaction, it could be that the reduced flow rate through the effusion tube in the isotopic series of experiments might have resulted in the AlOH being destroyed before egress from the effusion tube could have occurred.

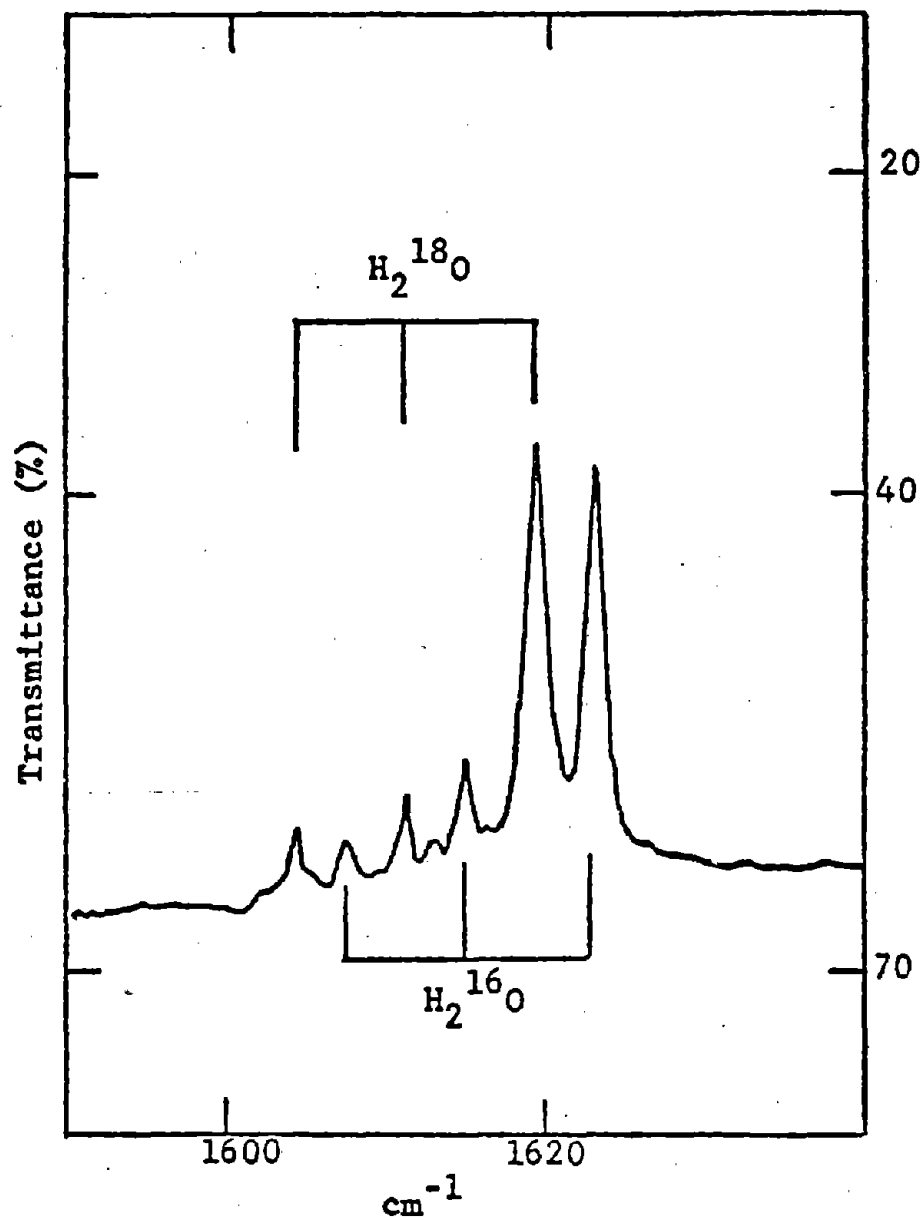


Figure B-3 IR Spectrum of the Water Vapor Species H_2^{16}O and H_2^{18}O at about 1620 cm^{-1} .

Finally, two experiments were made in which a small amount of ferric oxide, Fe_2O_3 , was added to the aluminum metal in the effusion cell. In the first experiment with the effusion cell at 1600°F the infrared spectrum only showed the presence of water vapor, while in the second experiment, run at 2330°F, the water vapor absorption bands had almost completely disappeared and the Al_2O spectrum was present. The latter is shown in Figure B-4, which is essentially the same as that shown in Figure B-2 with the deception of the presence of an absorption band at 948 cm^{-1} which does not occur in the nondoped spectrum. At this time it is not possible to state the origin of this absorption band.

B.4 CONCLUSIONS

1. The extent of the reaction between water vapor at pressures of 10^{-4} to 10^{-5} atm, and molten aluminum below temperatures of about 2250°F is at best only slight.
2. The extent of the reaction between water vapor, at pressures of 10^{-4} to 10^{-5} atm, and molten aluminum above temperatures of about 2300°F appears to be essentially complete.
3. There is a possibility that the species AlOH may exist as a gaseous molecule at much lower temperatures (i.e., below about 1900°F) than might be anticipated from currently available thermodynamic data. If this possibility is correct, the reaction $\text{Al(l)} + \text{H}_2\text{O(g)} = \text{AlOH(g)} + \text{H}$ could be the primary reaction leading to an energy release in the water-molten aluminum system.
4. The possible influence of iron oxide on the molten aluminum water vapor reaction is unclear based on the present data.

B.5 REFERENCES

1. JANAF Thermochemical Tables, Dow Chemical Co., Mich.
2. A. Snelson, J. Phys. Chem., 74, 2574 (1970).
3. A. Snelson, Final Report, Thermodynamic Properties of Rocket Combustion Products, AFRPL Contract F04611-69-C-0093, (1970).

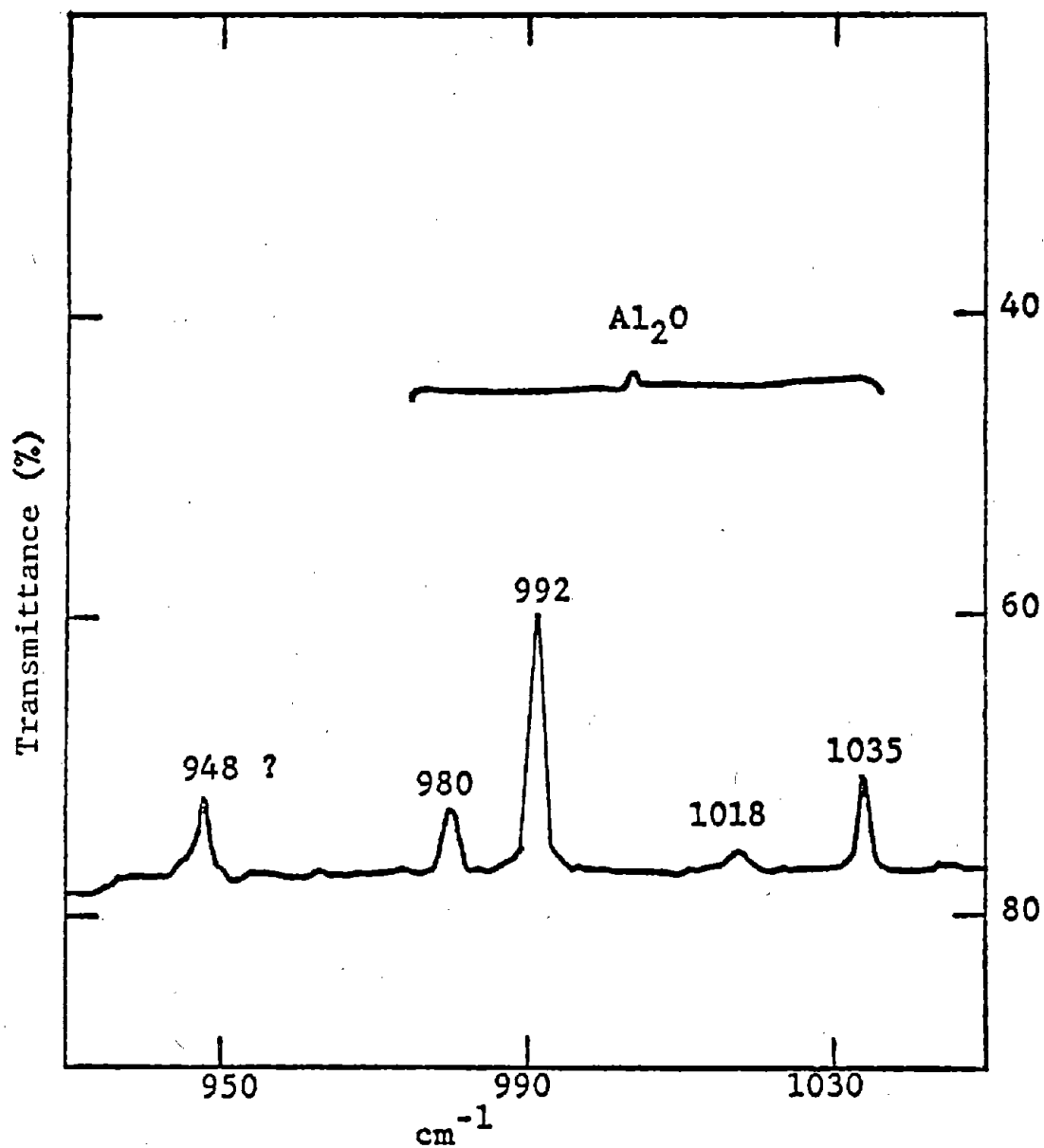


Figure B-4 IR Spectrum of Al₂O₃ Formed in the Reaction of Molten Aluminum and Water Vapor in the Presence of Ferric Oxide at 2330°F.

APPENDIX C

MOLTEN ALUMINUM-WATER EXPLOSION
INITIATION MECHANISM EXPERIMENTS

TABLE OF CONTENTS

	<u>Page</u>
C.1 OBJECTIVE, SCOPE AND DISCUSSION	C-1
C.2 EQUIPMENT	C-3
C.2.1 Quench Tank	C-5
C.2.2 Drop Crucible	C-8
C.3 INSTRUMENTATION	C-11
C.4 RANGE SETUP AND OPERATION	C-15
C.5 EXPERIMENTAL RESULTS	C-18
C.6 DISCUSSION	C-26
C.6.1 Evidence that Aluminum and Water are Liquid	C-28
C.6.2 Evidence of Intimate Liquid/Liquid Contact	C-29
C.6.3 Smooth Quench Tank Surface Experiments	C-37
C.6.4 Leading Edge	C-38
C.6.5 Miscellaneous Characteristics	C-42
C.6.6 Heat Transfer Considerations	C-47
C.7 CONCLUSIONS	C-49

LIST OF ILLUSTRATIONS¹

<u>Figure</u>		<u>Page</u>
C-1	Schematic of Equipment Setup	C-50
C-2	Schematic of Quench Tank, Accelerometer and Support Stand	C-51
C-3	Actual Sensor Locations	C-52
C-4	Concrete Quench Tank Bottom Surface	C-53
C-5	Quench Tank Stand	C-54
C-6	Quench Tank Bottom Surfaces Smooth and Rough Steel	C-55
C-7	Quench Tank Bottom Surfaces Smooth and Rough Concrete	C-56
C-8	Quench Tank Bottom Surfaces Rough Steel and Rough Concrete	C-57
C-9	Quench Tank Bottom Surfaces Smooth Steel and Smooth Concrete	C-58
C-10	Schematic of Simulation Setup with New Drop Crucible	C-59
C-11	Drop Fixture Assembly	C-60
C-12	Drop Bucket Assembly	C-61
C-13	Top and Bottom Plate	C-62
C-14	Slide	C-63
C-15	Aluminum Weight and Speed at Water Surfaces	C-64
C-16	Aluminum Flow Characteristics After Initial Impact on Quench Tank Bottom	C-65
C-17	Efflux Speed and Weight Flow at Drop Crucible Versus Time (Calculated)	C-66
C-18	Weight and Speed Versus Time at Quench Tank Water Surface (Calculated)	C-67
C-19	Calculated Flow Speed and Time Versus Radial Distance for Two Stream Radii (Frictionless Axisymmetrical Navier-Stokes Flow)	C-68

¹ Note: All the illustrations are at the end of the Appendix.

LIST OF ILLUSTRATIONS¹(Cont'd)

<u>Figure</u>		<u>Page</u>
C 20	Melt Furnace and New Drop Crucible	C-69
C-21	Views of Simulation Site and Aluminum Transfer	C-70
C-22	Quench Tanks: Before and After	C-71
C-23	Partial Record for Experiment 2, Temperature, Quench Tank Bottom Acceleration and Time	C-72
C-24	Partial Record for Experiment 3, Temperature, Quench Tank Bottom Acceleration and Time	C-73
C-25	Partial Record for Experiment 4, Temperature, Quench Tank Bottom Acceleration and Time	C-74
C-26	Partial Record for Experiment 5, Temperature, Quench Tank Bottom Acceleration and Time	C-75
C-27	Partial Record for Experiment 6, Temperature, Quench Tank Bottom Acceleration and Time	C-76
C-28	Partial Record for Experiment 7, Temperature, Quench Tank Bottom Acceleration and Time	C-77
C-29	Partial Record for Experiment 8, Temperature, Quench Tank Bottom Acceleration and Time	C-78
C-30	Faxtex Film Frame Enlargements Showing Initial Portions of Aluminum Streams	C-79
C-31	Faxtex Film Frame Sequence from Experiment No. 6, Mild Steam Explosion (Rough Steel Quench Tank Bottom Surface)	C-80
C-32	Temperature Profiles, 1/8 inch above surface	C-81
C-33	Circumferential Flow Producing an Impact Shock in a Round Quench Tank	C-82
C-34	Shock Pressure Versus Molten Aluminum Impact Speed (Calculated)	C-83
C-35	Average Rate of Temperature Rise Versus Average Aluminum Radial Flow Speed	C-84
C-36	Boiling Force Envelopes Versus Time	C-85
C-37	Temperature Rise Representing Film Thickness Versus Initial Aluminum Volume Entering Quench Water	C-86
C-38	Quenching Curve (Norm Cochran's Data, Alcoa Replotted	C-87
C-39	Aluminum Temperature Versus Quench Time	C-88

¹ Note: All the illustrations are at the end of the Appendix

APPENDIX C
MOLTEN ALUMINUM-WATER EXPLOSION
INITIATION MECHANISM EXPERIMENTS

C.1 OBJECTIVE, SCOPE AND DISCUSSION

The objective of the experiments was to establish circumstantial evidence that the initiation mechanism is or is not a vapor explosion. This evidence was to consist of time related data on: aluminum temperature and position; quench tank bottom temperature; and quench tank acceleration. The data was to be obtained for quench tank bottom surfaces which are: smooth and which contain surface cavities; made of concrete and steel; and for a surface coated with tarset.

It was predicted that the smooth and coated surfaces would not produce initiation reactions, whereas the other surfaces would. The surfaces which do not produce reactions are expected to be hotter than the ones that do. The position time data for the initial aluminum flow over the quench tank should indicate that the aluminum impacts the tank side wall at a speed on the order of 100 ips. The temperature of the aluminum very near the bottom surface should be above 1220°F, corresponding to its liquid state, up to and including the time of an initiation.

The conditions in the experiments are designed to show the importance of the quench tank bottom surface in obtaining an initiation. It is expected that the instrumentation will establish that the aluminum was liquid during the time frame in which it is most probable for an initiation to take place. It is also expected to establish that the aluminum impact speed on the quench tank side wall is of sufficient magnitude to produce a shock capable of collapsing a steam film. Furthermore, the time of this impact and an initiation are expected to be correlated quite strongly, giving credence to a cause and effect relationship. The significance of a surface containing cavities and no cavities was expected to be demonstrated in two ways. First, the direct correlation of initiation and no initiation and second by differences in surface temperature. The higher surface temperature,

IIT RESEARCH INSTITUTE

in the absence of surface cavities, was predicted due to the lack of a steam film, or a reduced steam film thickness. The initial impact of the aluminum on the quench tank bottom was predicted to force all or almost all of the water and steam away from the bottom surface and the radial flow to the tank sides was expected to do the same. If there was liquid water initially in the surface texture, then a steam film can be reformed; whereas if there were no surface cavities to contain liquid water, then the steam film can not reform. In the latter case the hot aluminum may be in direct or almost direct contact with the bottom and it should be hotter as a result.

It was postulated that, under simulation conditions which produce two out of three explosions, a trigger reaction always takes place. The reason that an explosion does not always occur is believed to be related to either the strength of the trigger and/or the concentration of the aluminum and water, in the vicinity of the trigger. Improper levels in either of these two factors or relationships between them could preclude normal detection of the reaction taking place. It was expected that detection of quench tank body motion through acceleration would be a more "sensitive" means for determining that there was or was not a trigger, than those which have been used previously. In this manner it is believed that each experimental condition which should provide an initiation will, as evidenced by body motion, rather than two out of three as evidenced by a violent reaction.

The simulation conditions which probably produce an explosion are:

Aluminum Temperature	$\geq 1382^{\circ}\text{F}$
Drop crucible opening	$\geq 3\text{-}1/4$ inches
Drop height	= 18 inches
Water depth	= 6 inches
Water temperature	= 32°F to 130°F
Quench tank bottom surface	= nonsmooth (Rough, with surface capillaries)
Aluminum weight	≥ 50 pounds

These are considered to be the base line conditions for the experiments with two exceptions: the drop crucible opening and aluminum weight. A new drop crucible has been designed and fabricated which has a 3-1/2 inch diameter opening. This crucible will hold about 34 pounds of aluminum but 26 pounds will match or exceed the flow conditions from No. 60 and No. 70 crucibles with 50 pounds flowing through a 3-1/4 inch diameter orifice during the critical reaction period. The most important design feature of the drop crucible is the orifice seal. It has been made external to the crucible in an attempt to obtain consistent and regular initial portions of the aluminum stream. The opening device used in previous experiments is located within the drop crucible, surrounded by molten aluminum. If the new design does not function properly, the conventional crucible will be used.

The primary variable in the experiment is the quench tank bottom surface. If sufficient funds are available, the water depth and aluminum temperature will be made variables. Table C.1 shows the matrix of experimental conditions planned. It is expected that six runs can be made. Two provisional experiments are shown to permit flexibility in the event that field operations progress well, so that the time budgeted may include these two conditions.

C.2 EQUIPMENT

A schematic of the overall experimental set-up is shown in Fig. C.1.¹ A fastax camera, nine thermocouples and one accelerometer were used to obtain data. Data from these sensors was recorded on magnetic tape by a tape recorder with 14 channels. One channel was used for time and for each thermocouple and two channels for the accelerometer. The accelerometer output was recorded at two levels of amplification, low and high gain to facilitate obtaining marginal and strong signals. The thermocouple and accelerometer leads were bundled below the quench tank and brought out to preamplifiers and thereafter to the tape recorder. The aluminum temperature in the drop crucible was monitored with a separate chart recorder. The zero time break wire and

¹ All of the figures are at the end of this appendix.

TABLE C-1

MATRIX OF PLANNED EXPERIMENTAL CONDITIONS*

Condition Number	Quench Tank Bottom			Aluminum Temperature	Water Depth	Initiation Predicted
	Material	Surface	Coating			
1	Concrete	Cavities	None	1380° F	0 in. (wet)	Yes
2	Concrete	Cavities	None	1380° F	6 inches	Yes
3	Concrete	No Cavities	None	1380° F	6 inches	No
4	Concrete	Cavities	Tarset	1380° F	6 inches	No
5	Steel	No Cavities	None	1380° F	6 inches	No
6	Steel	Cavities	None	1380° F	6 inches	Yes
7**	Concrete	Cavities	None	1240° F	12 inches	No
8**	Concrete	Cavities	None	1380° F	12 inches	Yes

* 3-1/2 inch diameter drop crucible opening; 12 inch diameter glass quench tank; aluminum weight for all runs will be 26 pounds or greater.

** Provisional experiments to be made if cost permits.

explosion breakwire modulate the time signal to show the time that aluminum flow starts and when the explosion occurs. The fastax camera will provide overall documentation.

C.2.1 Quench Tank

A schematic of the quench tank is shown in Figure C.2. Glass jars obtained for the original gross experiments were modified for use. The bottoms of these jars were cut off and the remaining cylinder placed on the drop surface. Silicon rubber were used to seal the glass cylinder on the concrete and steel drop surfaces. The accelerometer was attached to the bottom of the drop surface (required one point attachment). The support frame holds the portion of the drop surface which extends past the glass cylinder. Sufficient clearance was provided under the support frame to preclude the accelerometer impacting the rigid support surface, and for bringing out the leads from the thermocouples and accelerometer.

Figure C.3 is a schematic showing the location of the various sensors and the elevation of the thermocouples with respect to the impact surface. The first seven thermocouples are positioned so that they monitor the temperature about 1/8 inch above the impact surface. These locations provided a means of determining the radial position (including symmetry) of the flow. Since this data is obtained as a function of time for known positions of the thermocouples, average flow speeds may be calculated. Gage 7 is placed at the glass cylinder wall so that the time the aluminum reaches this impact surface will be defined. Holes for the leads were drilled through the impact surface and sealed with silicon rubber. The contact sensor, at locations M and M1, was added after the third experiment.

Two steel quench tank bottom surfaces were prepared, one each by treatments 1 and 2 shown in Table C.2. Six concrete quench tank bottom surfaces were prepared according to Table C.3 and Figure C.4. Details of the quench tank stand are shown in Figure C.5. Photomicrographs were made of each type of quench

TABLE C-2

SPECIFICATION FOR STEEL QUENCH TANK BOTTOM SURFACE

December 19, 1974

- Low carbon steel plate (1010 - 1020) cold rolled.
- Twenty-four ($-1/16$) inches by 24 ($-1/16$) inches by $3/16$ inch thick.
- Treatment 1: Chemically degrease.
- Treatment 2: a) chemically degrease as in treatment 1; b) grit blast; c) oven heat for 60 minutes at 1200°F ; d) air cool to room temperature; and e) rinse with clean water.
- Drill through holes in quench tank bottom surface per Figure 3, Schematic of Thermocouple and Accelerometer Locations.
 1. At location A - drill $5/32$ inch and tap with 10-32 thread.
 2. At locations 1 through 9 drill $1/8$ inch diameter holes.
- Drill two - $1/8$ inch diameter holes through one corner as shown for concrete surface, Figure 4. (For tying up thermocouple leads.)

TABLE C-3

SPECIFICATION FOR CONCRETE QUENCH TANK BOTTOM SURFACE

- Mortar (ASTM C109)
Compressive strength > 3000 psi (@ 8 days, 3 tests, \bar{F}_c
6233 psi)
Mix: water/cement/sand: 0.5/1.0/2.75
Sand: 61% ASTM C190
39% ASTM C109
- Cure for ten days at high humidity (100% RH at 70°F)
- Prepare six test cubes, two (2) inches/side
- Surface finish
 - A. Smooth with hand trowel
 - B. Cover "A" finish with "neat" cement and trowel
- Slabs to be 24 inch x 24 inch x 3/4 inch per Figure C-4
- Drill 9 through holes 1/16 inch diameter at thermocouple location 1 through 9 shown in Figure 3, "Schematic of Thermocouple and Accelerometer Locations", use drill template which is located by means of hole "A", 10-32 thread, for accelerometer.
- Drill two 1/8 inch diameter holes through one corner as shown in Figure 4 (for tieing up thermocouple leads).

tank surface and are shown in Figs. C.6, C.7, C.8 and C.9. Smooth and rough steel surfaces are shown in Fig. C-5; smooth and rough concrete surfaces are shown in Fig. C.6; rough steel and rough concrete are shown in Fig. C.7; and smooth steel and smooth concrete are shown in Fig. C.8. The contrast between rough and smooth surfaces is striking and substantiates the concept of retained liquid water in the surface capillaries. The comparison of rough surfaces of both materials (Fig. C.7) indicates a difference. The steel surface appears more uniform and to have smaller capillaries than the concrete surface. No significance has been attributed to this difference.

C.2.2 Drop Crucible

The spatial relationship between the new drop crucible and the quench tank stand are shown in Fig. C.10. Clearance has been provided between the top of the quench tank and the bottom of the crucible for the safety cover. Figures C.11 through C.14 describe the new drop crucible.

The aluminum weight flow and speed characteristics have been calculated for 26 pounds flowing from the new crucible (18 inch drop, 12 inch air and 6 inch through water). These calculations are based upon the crucible geometry: the bottom section, 5-1/2 inch long, has a 3.548 inch diameter which is the port opening and has a volume of 54.4 cubic inch (4.6 lb); the transition section is five inches long and has a 72.5 cubic inch volume (6.1 lb) and the top section is 20 inches long with a 5.047 inch diameter and has a total volume of 400.1 cubic inches (33.9 lb). Twenty-six (26) pounds of aluminum fill the crucible to a level which is 11-5/32 inch below the top. The efflux speed from the crucible, V_o is:

$$V_o = \sqrt{2gh}$$

where: h = head in crucible

g = gravitational acceleration

The time to flow between two head levels, t_o , is:

$$t_o = \sqrt{2/g} (D/d)^2 \left[\sqrt{h_1} - \sqrt{h_2} \right]$$

D = applicable crucible diameter

d = orifice diameter

h_1 = initial head

h_2 = final head

The speed at the water surface, V_a , is:

$$V_a = \sqrt{2gh + V_o^2}$$

h = air drop height

The time for the flow through air, t_a , is:

$$t_a = (V_a - V_o)/g$$

The total time to reach the water surface, t , is:

$$t = t_o + t_a$$

Table C.4 presents calculations made to show the flow characteristics. The weight and speed at the water are plotted in Fig. C.15.

The initial flow characteristics along the bottom of the quench tank have been calculated to assist in evaluating the event history. These calculations are based upon the condition that the flow of aluminum in the stream (Q_o) must equal the radial flow (Q_R):

$$Q_o = \pi r_o^2 V$$

$$Q_R = 2\pi r h u$$

where: r_o = vertical stream radius

V = vertical speed

r = horizontal flow radius

h = height of horizontal leading edge

u = speed of horizontal leading edge

TABLE C-4

CALCULATED PARAMETERS FOR FLOW FROM DROP CRUCIBLE*

Weight Out (lbs)	At Crucible		At Water	
	Time (sec)	Speed (ips)	Time (sec)	Speed (ips)
0	0	122	.086	156
5	.051	112	.143	148
10	.107	102	.206	140
15	.169	90	.277	131
21.4	.299	65	.435	118
26	.640	0	.894	98

*3-1/2 inch diameter orifice.

TABLE C-5

QUENCH TANK INITIAL BOTTOM FLOW PARAMETERS

Time (sec)	Speed (u) (ips)	Position (r) (inch)	Leading Edge Thickness (h), inch
0	0.0	0.0	6.0
0	23.0	1.774	6.0
.009	25.9	2.0	4.7
.040	38.9	3.0	2.1
.062	51.8	4.0	1.2
.079	64.8	5.0	0.8
.093	77.7	6.0	0.5

Defining u as shown below¹, equating the two flows and solving for h yields:

$$u = dr/dt = \dot{r} = V(r/2h_o)$$

$$h = h_o(r_o/r)^2$$

The flow parameters shown in Table C.5 were calculated using these last two equations with:

$$h_o = 6 \text{ inches}$$

$$V = 155.5 \text{ ips}$$

$$r_o = 1.774 \text{ inches}$$

The parameters in Table C.5 are plotted in Fig. C.16 as a function of radial position.

Characterization calculations have also have been made for the conventional No. 70 drop crucible with an initial aluminum weight of 50 pounds flowing through a 3-1/4 inch diameter orifice. Figures C.17, C.18 and C.19 show the results of these calculations. Flow speed and time are shown in Fig. C.19 for two aluminum stream radii and the influence of aluminum flow in water instead of air. The quench tank water has a significant retardation effect on the flow parameters.

C.3 INSTRUMENTATION

Analysis of various aspects of the pour dynamics and experimental data available have lead to the information and requirements presented. Table C.6 presents the expected temperature profiles as a function of location and time. Table C.7 presents the acceleration characteristics expected for both concrete and steel quench tank bottom surfaces. It was required that the response of the surface be determined experimentally prior to running a test. Two calibrations are required for the accelerometer. Table C.8 shows the expected event time relationships.

¹For frictionless axisymmetrical Navier-Stokes flow.

TABLE C-6

EXPECTED TEMPERATURE PROFILE

$T_o = 1400^\circ\text{F}$, 12 inch air drop, 6 inch water, 3.5 inch pour diameter

Thermocouple ①		Time Reading Expected, msec	Temperature Range Expected, °F
Number	Location (inch)		
1	1	125	1150-1250 ②
2	2	134	1150-1250
3	3	165	1150-1250
4	5	187	1150-1250
5	3	165	1150-1250
6	3	165	1150-1250
7	5.8125	218	1150-1250
8 ③	1 ③	218 ④	IWT ⑤-1250
9 ③	1 ③	218 ④	IWT ⑤-1250

- ① Chromel-alumel thermocouple wire 0.010 inch diameter.
 ② All calibrated to read 32 to 1600°F.
 ③ These couples flush with surface, the others 1/8 inch above surface.
 ④ Reading expected to be IWT at least to this time.
 ⑤ IWT = initial water temperature.

TABLE C-7

ACCELERATION CHARACTERIZATION AND INSTRUMENTATION REQUIREMENTS
(QUENCH TANK BOTTOM)

Concrete (24 inch square supported 3 inch/side = 18 inches,
3/4 inch thick)

- Period: 6 msec
- Maximum G's after initial impact:
 - 1.5 msec
 - 4.5 msec
 - 7.5 msec or
 - every 3 msec after first 1.5 msec
- Maximum G's expected from initial impact of molten aluminum on bottom $3.9 \leq G's \leq 7.8$

Steel (24 inch square supported 3 inches/side = 18 inches,
3/16 inch diameter)

- Period: 15 msec
- Maximum G's after initial impact:
 - 3.75 msec
 - 11.25 msec
 - 18.75 msec or
 - every 7.5 msec after first 3.75 msec
- Maximum G's expected from initial impact of molten aluminum on bottom $2.8 \leq G's \leq 5.6$

Instrumentation

- Channel 13 full scale deflection - 15 G's
- Channel 12 cover the lowest possible signal (limited by "noise") to meet channel 13 minimum readable signal.
- Preliminary accelerometer check before each test (with or without water as called for by test) strike quench tank bottom plate at center on top side (use wood and hammer) and record frequency.

TABLE C-8

EVENT TIME ESTIMATE

(3.5 inch diameter tap, 26 pounds, 12 inch air, 6 inch water)

Event	Time, use
Start fastax camera	-500
Start pour (pull plate seal)	0
Leading edge at water	86
Leading edge at tank bottom	125
Five pounds through water surface	143
Leading edge at tank side	218
Earliest time initiation expected	218
Ten pounds through water surface	206
Start of most likely time range for an initiation	232
Fifteen pounds through water surface	277
End of most likely time range for an initiation	332
21.4 pounds through water surface	435
Expected latest time for initiation	812
Twenty-six pounds through water surface (If aluminum and water are mixed 50-50 the mixture will be 6 inches up from tank bottom, e.g., at initial water line)	894
Twenty-six pounds in tank, all aluminum (no mixing), 2.89 inches above tank bottom	921
"Last flow to tank side"	990
Expected end of pour dynamics	1,000
Fastax camera film run out	2,000

Table C.9 shows the recorder channel assignments. It should be noted that the output from thermocouples 1 and 9 were placed on channels 1, 9, 10 and 11. Channels 10 and 11 are provided for obtaining the highest possible reading. (A side contract sensor was substituted for the maximum temperature reading from thermocouple 9 on channel 11 after the third experiment.)

A 16mm 100 foot capacity fastex camera loaded with color film was to be used for overall documentation of the event. Millisecond timing marks were provided. The running time was about two seconds with 1/2 second before the start of the pour.

Still photographs showing the overall set-up were made. Still pictures of the quench tank before and after each experiment were taken.

C.4 RANGE SETUP AND OPERATION

The instrumentation and ancillary equipment were shipped to the experimental site, at Kingsbury, Indiana, and range setup started on Friday, January 17, 1975. The major problem encountered was opening the new drop crucible. The opening problem involved two factors: adjusting the four bolts which seal the slide and aligning the pull cable, to prevent binding during opening. On Wednesday, January 22, a checkout of the crucible opening and instrumentation was made successfully using water in place of aluminum. Black and white fastex movies were taken of the pour which showed that the flow front was as desired, but the stream expanded into the space between the bottom of the crucible and the seal retaining plate. Although this would be undesirable if it took place with aluminum, it was judged that the higher surface tension of aluminum might prevent this from happening.

The first experiment was attempted on January 23, but the crucible would not open. Two factors were noted which could account for this. First, although the hot clearance at the

TABLE C-9
TAPE RECORDER CHANNEL ASSIGNMENTS

Channel Number	Sensor	
1	Couple 1	30°F to 1600°F
2	Couple 2	30°F to 1600°F
3	Couple 3	30°F to 1600°F
4	Couple 4	30°F to 1600°F
5	Couple 5	30°F to 1600°F
6	Couple 6	30°F to 1600°F
7	Couple 7	30°F to 1600°F
8	Couple 8	30°F to 1600°F
9	Couple 9	30°F to 1600°F
10	Couple 1	Maximum reading possible
11	Couple 9	Maximum reading possible Experiments 1, 2 and 3
11		Contact sensor Experiments 4 through 8
12	Accelerometer, minimum G's possible	
13	Accelerometer, full scale 15 G's	
14	Timing Marks (tenths of millisecond) Modulate once each with signals from: Zero time break wire and Explosion break circuit	

slide plate had been checked after heating with a torch and found not to change, the hot aluminum apparently did cause a reduction in clearance which would increase the required opening force to overcome the additional friction. Second, the crucible section at the slide valve is much smaller than at the main portion of the crucible and was believed to cool much more rapidly and the aluminum there could have solidified quickly. Three unsuccessful attempts were made to drop the aluminum, with adjustments being made in the seal retaining bolts each try. The major portion of the aluminum was still molten when the experiment was aborted. The axial heat loss through the reduced section at the orifice was apparently enough to solidify the aluminum there. The new drop crucible was removed and replaced with the No. 70 drop crucible which had a 3-1/4 inch diameter orifice and a conventional internal seal device. This resetup was completed on January 24th and the first successful experiment conducted.

Figure C.20 shows the melt furnace (View a), melt crucible removal from the furnace (View b), the installation of the new drop crucible (View c) and a close-up of the new crucible (View d). The steel frame structure in the left side of View c was used to support a cable and weight used to open the new drop crucible. A cable was attached to the slide valve, which may be seen in View d, which passed through three pulleys, terminating at the weight. The weight was restrained by a cable. The pour was started by cutting the restraint cable with a linear shaped charge.

Zero time was established by a breakwire attached to the rigid structure and weight. The breakwire consisted of two bare wire ends lightly twisted together which were pulled apart as the weight dropped. The separation of the wire modulated the time base record showing the start of the experiment.

Figure C.21 shows views of the simulation site and aluminum transfer. View a shows the No. 70 drop crucible installed at the drop location with the fastex camera in the foreground, 35.5 feet from the quench tank. View b shows the crucible opening

arrangement. The drop weights are on the right and cable support arm is on top of one vertical steel posts. A weight of 105 pounds was used to open the crucible and the weight "free falls" about 4-1/2 inches and then drops 4-1/2 inches more to the ground. View c shows a closeup of the crucible, quench tank, tank safety cover, and "bull" torch used to preheat the drop crucible. The cable system for opening the crucible is in view at the upper right. The taut cable on the right is the weight restraining cable. Zero time was obtained as described previously. View d shows the cart used to move the molten aluminum from the melt furnace to the drop site and the transfer of molten aluminum to the drop crucible. Figure C.22 shows photographs of quench tanks "before and after". View a shows the conductive paint circuit, around the bottom of the glass quench tank, and leads from it (on the left). Fracture of the tank opens this circuit which modulates the time base record, as the zero time signal does. The contact sensor leads may be seen in the right background. Insulation was stripped from the ends of two wires and they were placed about 1/4 inch apart and 1/16 inch above the quench tank bottom surface. The wires extend up straight for about 1-1/2 inch and then were spread apart, with an included angle of about 90 degrees. The quench water acted as a series resistor of about 1500 ohm which, under the applied voltage, produced a signal. When the aluminum shorts the bare wire ends, the signal drops showing the presence of aluminum.

C.5 EXPERIMENTAL RESULTS

Seven actual experiments were conducted which produced data, but only one initiation was obtained. A mild steam explosion resulted from experiment No. 6, which had a quench tank bottom surface made of rough steel. The experiments correspond to the matrix shown in Table C.1, except that: the actual experiment number is one greater than the condition number in the table; all of the aluminum temperatures were 1525°F to 1590°F; six inches

of water were used in experiment No. 8, condition No. 7 and the last condition listed in the table was not evaluated. Experiment 8 was a repeat of experiment No. 3, both evaluations of condition 2 in Table C.1. Since it was anticipated that a rough concrete surface would produce an explosion and one was not obtained on the initial attempt, this condition was repeated. The aluminum temperatures were higher than planned for two reasons: first it was desired to avoid having the aluminum solidify and cause a time delay and second, the seal in the drop crucible leaked intermittently which was undesirable. Thus the aluminum was transferred from the melt crucible hot, about 1800°F, and allowed to cool at the drop site to about 1700 to 1750°F before transfer to the drop crucible. Transfer to the drop crucible provided a temperature drop to about 1550° to 1600°F.

Table C.10 summarizes the bulk of the data obtained from the experiments. Figures C.23, 24, 25, 26, 27, 28 and 29 show photographs made of actual records, except that the records used for data reduction had a greatly expanded time base. The top three traces are the three thermocouples at the three inch radial position (thermocouples 3, 5, and 6 in Fig. C.3). The next lower trace in Fig. 23 and 24 is the thermocouple at the quench tank edge (Thermocouple 7, Fig. C.3) whereas in the other figures this trace is the quench tank side contact sensor (M and M1 in Fig. C.3) before the aluminum shorts the circuit. The fifth trace in Figures C.23 and C.24 has no data as the side contact sensor was not used and this is the "zero" position, whereas in the others the fifth trace is the thermocouple at the quench tank side. The next two traces are the high gain output from the accelerometer, and the timing base.

Figure C.23 for experiment No. 2 shows a lot of signal distortion caused by stray 60 cycle signals. This condition was reduced by the addition of multiple ground wires in experiment No. 3 and further improved in experiment No. 4 by using an electrically insulated accelerometer mounting stud.

TABLE C-10
SUMMARY OF FINAL SIMULATION EXPERIMENTS
(50 POUNDS ALUMINUM, No. 70 DROP CRUCIBLE, 3-1/4 INCH DIAMETER ORIFICE,
16-1/2 INCHES TOTAL DROP DISTANCE, 11-5/8 INCH INSIDE DIAMETER GLASS
SIDE QUENCH TANK, UNTREATED TAP WATER)

SIMULATION NOS.	2	3	4	5	6	7	8
ITEMS							
DATES 1975	1/24	1/27	1/28	1/29	1/29	1/30	1/31
Initial Temperatures:							
Aluminum (°F)	1525	1590	1525	1525	1525	1575	1525
Water (°F)	45	56	58	55	46	60	60
Air (°F)	44	32	38	32	30	31	36
Water Depth (inch)	1/64	6	6	6	6	6	6
Quench Tank Bottom Surface	Concrete	Concrete	Concrete	Concrete	Steel	Steel	Concrete
Quench Tank Surface Treatment	None	None	Neat Cement	Target	Blast/Oven	Acetone	None
Quench Tank Surface Condition	Rough	Rough	Smooth	Smooth	Rough	Smooth	Rough
Initiation Reaction:							
Predicted	Yes	Yes	No	No	Yes	No	Yes
Achieved	No	No	No	No	Yes*	No	No
At Time of Tank Side Impact:							
Radial Speed (ips)	80	59	44	73	55	101	65
Shock Pressure (psi)	1850	1330	1000	1650	1250	2220	1450
Temperatures at Radial Locations from Center, (°F):							
1/8 inch above surface:							
1 inch	115	1455	865	220	1415	360	1350
2 inches	55	1355	1350	280	1380	350	1340
3 inches (average of 3)	45	290	1000	775	1330	70	610
5 inches	45	56	NR	600	1460	60	225
5.8 inches	45	56	58	55	1210	60	NR
At surface:							
1 inch (average of 2)	45	56	95	540	1100	110	80
Maximum Temperatures at Radial Locations from Center:							
1/8 inch above surface, (°F)							
1 inch	950	1455	1345	1285	1415	1380	1350
2 inches	1230	1455	1350	1495	1380	1515	1340
3 inches (average of 3)	1235	1485	1500	1340	1330	1300	1340
5 inches	905	1355	G.O.	1500	1460	1095	1475
5.8 inches	1360	1280	1395	1435	1210	1500	G.O.
At surface:							
1 inch (average of 2), (°F)	45	160	290	1140	1100	705	240
Pour Start to Water Contact, (msec)	331	336	347	244	311	345	282
Aluminum at:							
Water (msec)	0	0	0	0	0	0	0
Quench Tank Surface (msec)	0	76	76	93	100	102	109
Start of Temperature Rise at Radial Locations from Center:							
1/8 inch above surface: (msec)							
1 inch	57	92	92	112	108	89	92
2 inches	64	100	92	99	113	89	101
3 inches (average of 3)	90	117	123	115	125	110	115
5 inches	119	167	G.O.	172	159	137	141
5.8 inches	116	222	216	199	159	174	N.R.
Aluminum at Tank Side, (msec)	67**	118**	198	186	162	100	148
End of Temperature Rise at Radial Locations From Center:							
1/8 inch above surface: (msec)							
1 inch	188	109	262	662	157	137	118
2 inches	393	120	190	662	157	145	164
3 inches	249	161	251	299	152	235	195
5 inches	393	198	G.O.	209	177	519	201
5.8 inches	373	408	277	555	163	416	N.R.
Boiling Signal Reduced Markedly, (msec)	N.R.	270	266	215	N.R.	240	246
Quench Tank Broke, (msec)	393	721	630	662	157	519	620

* Mild Steam. ** Average from fastex film other times from contact sensor. G.O. = Gate Open; N.R. = No Record or Data.

The zero time and quench tank break signals show fairly clearly, in Fig. C.24 through C.29, as a change in the vertical deflection of the lowest trace. The initial accelerometer signal was produced by the overpressure from the drop weight line cutting charge. In most cases this charge cut the zero time breakwire, as may be noted by the close time sequence of these two events. Figures C.26 and C.29 show a considerable separation in these two events, indicating that the cutting charge did not break the zero time wire.

In Figs. C.25 and C.27, the leak from the drop crucible produced drops which caused the early accelerometer signal. However, the main rise of the accelerometer output signifies that the aluminum has just contacted the water surface in the quench tank. Variations in the initial rise of this signal may be attributed to the geometry of the leading portion of the aluminum stream. Figure C.30 is a composite of frames from the fastex films showing this portion of the streams. Table C.11 summarizes the geometric characteristics determined from the films. Table C.12 summarizes the force time relations obtained from the accelerometer data.

The fastex film was used to establish aluminum flow along the quench tank surface and data is presented in Table C.13. The aluminum stream is shrouded or sheathed in a steam film and it is not certain if the measurements are made to the aluminum or the steam film. However, they are closely coupled and whichever it was may not have a significant effect on the overall interpretation of the data. The distances reported in Table C.13 for the right and left side may be used to calculate the nominal stream diameters, shown in Table C.14. The differences in the diameters listed in Table C.11 and C.14 could arise from several factors:

- the associated steam film thickness
- the leading edge slowed down in relation to the main stream due to the flow through the quench water which enlarged the diameter

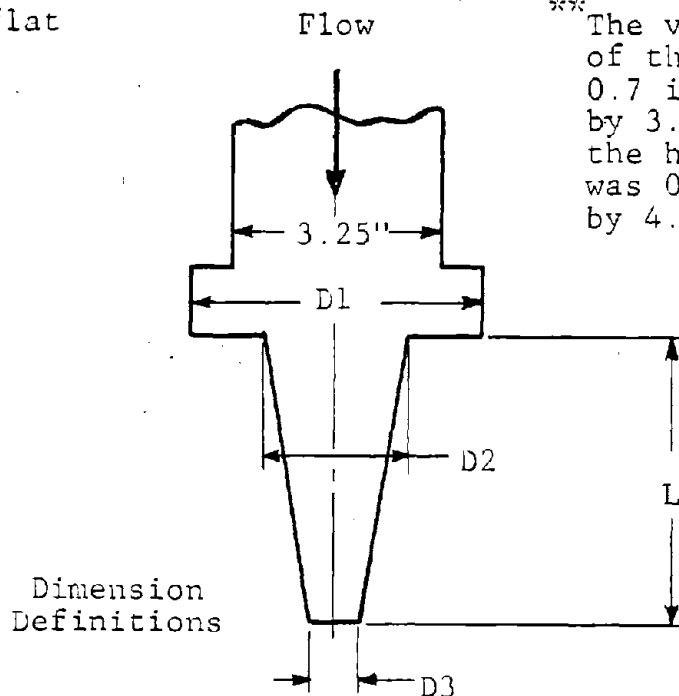
TABLE C-11

ALUMINUM STREAM LEADING END GEOMETRY DATA
TAKEN FROM FASTEX MOVIES (FIGURE C-30)

Item Experiment Number	Diameter, inches			Length, L inches	Comments
	D1	D2	D3		
2	5.9	0.6	0.6	11.8	D3 Split
3	5.9	2.1	2.1	8.3	Bend at D3*
4	5.6	2.4	0.6	5.9	Small Bend at D3
5	5.2	2.4	2.2	7.1	Straight: D2 to D3
6	4.9	1.9	1.6	5.2	Big Bend at D3; Mild Steam Explo- sion
7	5.4	2.2	1.1	7.1	Bend at D3
8	5.7	2.2	$\frac{1.1}{0.7}$	$\frac{4.3}{3.3}$	D3 Split,** 1 Split* Contacts Side

* Appears more flat
than round.

** The vertical part
of the slit was
0.7 inch diameter
by 3.3 inch long,
the horizontal part
was 0.9 inch diameter
by 4.3 inch long.



IIT RESEARCH INSTITUTE

TABLE C-12

FORCE/TIME CHARACTERISTICS FOR QUENCH TANK
BOTTOM SURFACE BASED ON ACCELEROMETER DATA

Experiment Number Item	2	3	4	5	6	7	8
Time at (msec):							
Aluminum at Water*	0	0	0	0	0	0	0
End First Force Change	0	96	17	10	36	15	11
Start Second Force Change	60	157	59	179	154	61	51
End Second Force Change	87	270	84	215	-	83	81
Start Third Force Change	119	-	185	-	-	206	176
End Third Force Change	**	-	266	-	-	240	246
Second to Third Force Change	-	546	-	469	-	-	-
Third to Fourth Force Change	-	-	524	-	-	402	466
Fourth to Fifth Force Change	-	-	-	-	-	512	-
Force Levels (lbs):							
First	15	327	80	342	261	84	144
Second	49	34	288	49	***	270	323
Third	**	19	42	19	-	120	49
Fourth	-	-	19	-	-	87	23
Fifth	-	-	-	-	-	21	-

*Start of first signal. **Record not readable. ***Explosion.

TABLE C-13

ALUMINUM FLOW POSITION DATA FROM FASTEX MOTION PICTURES

Experiment Number Item	2	3	4	5	6	7	8
Aluminum at (msec):							
Water	0	0	0	0	0	0	0
Tank Bottom	0	76	76	93	100	102	109
Tank Right Side	67	123	171	138	137	146	159
Tank Left Side	67	114	132	120	152	118	156
Flow Distance (inch):							
Right Side	5.0	3.4	5.0	3.2	2.2	4.4	4.4
Left Side	5.7	1.8	2.0	2.0	2.6	1.7	1.9
Radial Flow Time (msec):							
Right Side	67	47	95	45	37	44	50
Left Side	67	38	56	22	52	16	47
Radial Flow Speed (ips):							
Right Side	75	72	53	71	60	100	88
Left Side	85	47	36	74	50	106	40
Average	80	60	44	73	55	103	64

TABLE C-14
INDICATED ALUMINUM STREAM DIMENSIONS
AT START OF RADIAL FLOW

Experiment Number	Indicated Initial* Stream Diameter, inch	Radius, inch
2	0.9	0.4
3	6.4	3.2
4	4.6	2.3
5	6.4	3.2
6	6.8	3.4
7	5.5	2.2
8	5.3	2.6

*Quench tank inside diameter less sum of radial flow distance listed in Table C-13.

- the ability to detect early flow is hindered because the leading edge of the flow is quite "thick" until the flow has reached a radial position of 3 inches (effective diameter of about 6 inches) as indicated in Fig. C.16

A sequence of fastex film frames from experiment No. 6, showing the events preceding the mild steam explosion, is presented in Fig. C.31. This sequence is typical of the aluminum and water interaction obtained except for the explosion. The motion of the leading edge of the aluminum through the water, until it is in close proximity with the quench tank bottom surface, appears to depend upon the geometry of the stream. The resistance of the water retards the motion of the front, in relationship to the main Section (that with the 3-1/4 inch diameter). The apparent amount of steam around the leading edge also appears to be proportionate to its diameter. There is apparently more vapor when the diameter is smaller. The geometry of the leading edge also seems to be important. Leading edges which have "lips" slow down more than those that don't and the more the bend, the greater the retardation.

A particularly interesting effect was thought to be noted from Views 8, 9, and 10 in Fig. C.31. Light, apparently reflected from molten aluminum rising up the back side of the tank, makes it look like there is circumferential flow in addition to radial flow. This reflection has disappeared in View 10 and the initiation is evidenced in View 11. Thus there may well be an important impact shock resulting from the circumferential flow from front and back impacting.

C.6 DISCUSSION

It is postulated that spontaneous nucleation of water is the initiation mechanism in molten aluminum-water explosions. The intensity of the explosion depends upon the amount of energy released and the mass of aluminum and water which are influenced.

The necessary and sufficient conditions for this initiation mechanism are:

1. Liquid Aluminum
2. Liquid Water
3. Intimate contact of the two liquids

The experiments were conducted to establish data revelant to these conditions. The thermocouples provide direct data on the physical state of the two materials and thereby establish the first two conditions. The third condition depends upon the dynamics of the aluminum and water interaction which was not instrumented directly. Thus, circumstantial evidence has to be used to establish that intimate contact between the liquids was achieved.

The seven experiments conducted had been expected to produce four initiation reactions whereas only one took place. The lack of initiations is attributed to the small diameters of the initial portions of the incoming aluminum streams, as shown in Fig. C.30 and described in Table C.11. It is believed that if the new drop crucible had functioned as desired, this would not have been the situation and the predicted initiations would have taken place. The lack of initiations may weaken the case that can be put forth, that the trigger of the initiation reaction is an impact generated shock. However, it seems clear that the initiation mechanism is spontaneous nucleation of surface contained liquid water. The data does provide a firm basis for the characterization of the molten aluminum-water interaction. This data, coupled with the work of others, is believed to establish that a water vapor explosion triggered by an impact shock is the most probable initiation mechanism.

The most surprising aspect of the data is that the initial portion of the aluminum stream did not contact the bottom surface of the quench tank as was expected. The surface impact was apparently prevented by a composite layer of water and vapor. The stability of this layer was great enough to change the flow direction from vertical to horizontal radial flow. The basis for this

IIT RESEARCH INSTITUTE

observation is that the thermocouples 1/8 inch above the bottom surface of the quench tank did not sense any temperature until, on the average, 40 msec after the aluminum flow reached its initial closest point to the bottom surface. Experiments 7 and 8 were exceptions to this at the 1 and 2 inch locations. However, liquid water was still present at the 1 inch location at the time the aluminum reached the quench tank walls. Even more significantly, aluminum temperatures were not sensed for quite some time (on the average, 47 msec) thereafter, except in the case of the explosion. That this was true for the second experiment, when the concrete surface was just wet, was totally unexpected. In this case, the initial portion of the aluminum stream was about 0.6 inch in diameter and split in two.

C.6.1 Evidence that Aluminum and Water are Liquid

The primary instrumentation was designed to establish the physical state of the aluminum and water by measuring the temperature environment at/near the quench tank bottom. It was expected: that the quench tank bottom would contain liquid water at, or close to the initial temperature until an initiation; and that the aluminum would be molten throughout the time period in which an initiation could take place. It is believed that these two conditions have been established. Temperature profile data is presented in Fig. C.32 and is considered quite significant.

The initial aluminum temperature was 1525°F in five of 7 cases and is shown at that value. The average of all the maximum temperature measured was just under 1400°F, indicating that the overall average temperature drop during a bleed out simulation is about 125°F. This is in good agreement with data reported from other investigations. The average of the maximum temperature at each of the thermocouple locations is also shown and substantiates that the overall average is representative of the aluminum temperature existing during the pouring period for all of the simulations.

This then establishes the first requirement for conditions under which a vapor explosion can take place: the heat source must be liquid and at a temperature greater than the limit of superheat for water. The liquid temperature of aluminum (1220°F) is always above this value (512°F to 572°F) and the instantaneous interfacial temperature between 1220°F aluminum and 130°F water is 1115°F, well above the superheat limit.

The second condition which is necessary for a vapor explosion is that liquid water is present. Table C.10 lists the average of the measured temperatures at the quench tank surface, thermocouples (TC) 8 and 9 located one inch from the tank center, at the time the aluminum reached the tank side walls. Except for experiments 5 and 6, these temperatures were well below the boiling temperature for water. In experiment No. 5 the initial water temperature was 55°F and this did not change for 33 msec after the start of radial flow at TC No. 8 and after 8 msec at TC No. 9. Similarly, in experiment No. 6, which resulted in the mild steam explosion, these times were 10 and 16 msec. Thus, it is clear that liquid water was present and that the second requirement for an initiation is satisfied.

C.6.2 Evidence of Intimate Liquid/Liquid Contact

Intimate contact between the molten aluminum and liquid water in the surface cavities of the quench tank bottom surface is postulated to be achieved by collapsing the separating vapor film with a shock. The shock is produced by a molten aluminum impact. Before conducting this experimental program, this impact was predicted to take place at the quench tank side walls. As a result of the simulations performed, especially experiment 6, another impact condition has been identified. Any lack of symmetry in the quench tank (such as square tank cross section) or the position of the aluminum stream in relation to the tank axis of symmetry, will produce an aluminum flow component along the tank walls. In a quench tank with a circular cross section, as shown in Fig. C.33, this flow will have two components which meet. The speed of each component should be about equal so that

MIT RESEARCH INSTITUTE

the relative speed, when the two flow components meet, will be twice that of each and a significant liquid-liquid aluminum impact will occur and produce a shock.

C.6.2.1 Primary Evidence

The experiments were selected to provide four initiations, including experiment 2 which had only a wet surface. The occurrence of the initiation was to be directly correlated to the time at which the aluminum contacted the quench tank wall producing a shock and in this manner demonstrate the cause and effect relationship. In addition, the aluminum radial flow speed was to be determined and used to calculate the strength of the resulting impact shock. The strength was expected to be of a magnitude which could be judged capable of collapsing a stream film. This latter criteria is subjective as: the relationship between shock strength and the thickness of vapor film, which it can collapse, is not know; the thickness of the film is not known; and the rate of shock energy dissipation has not been established. Photographic and sensor data showed that the initiation/explosion took place just after the instant aluminum completely covered the quench tank bottom surface. Views h, i and j in Fig. C.31 are photographs of the sequence of events preceding the explosion. Fig. C.27 shows actual sensor response for the explosion. The thermocouples at the 3 inch location were sensing aluminum temperature and the couple at the 5.8 inch location was sensing the initial water temperature prior to the explosion. The two surface thermocouples at the 1 inch position, not shown in Fig. C.27, were still indicating the initial water temperature. It may be seen, in the figure, that the explosion and the sharp temperature rise, at the 5.8 inch location, occur "simultaneously" and the other sensor records show that the surface thermocouples do likewise. The revelant data is summarized in Table C.15. Thus, it seems reasonable to conclude that the impact of the two circumferential flow components or the final radial flow impact on the side wall, collapsed the steam film and established intimate contact between the liquid aluminum and liquid water.

TABLE C-15
EXPLOSION END EVENT SEQUENCE

Data Source	Event	Time (msec)	Adjusted Time (msec)
Photographic	Aluminum at Quench Tank Right Side	137	140
	Aluminum at Quench Tank Left Side	152	155
	Explosion	153	156
	Quench Tank Breaks	163	157
Sensor	Quench Tank Breaks	157	157
	Thermocouple 1/8 inch above Quench Tank Surface, 5 inches from Center Starts Sensing	159	159
	Thermocouples on Quench Tank Surface, 1 inch from Center Start Sensing	159	159
	Thermocouple 1/8 inch above Quench Tank Surface at Side Wall Starts Sensing	162	162
	Side Contact Sensor Registered	163	163

The data used to establish the above cause and effect relationship is based upon sensor and photographic data. The separate records and the short time span of the trigger make it difficult to identify the event sequence with the precision necessary for microsecond events. The short time span makes the sensor response time important in establishing the precise event time sequence. In addition there is no way of knowing where the initiation took place. As a result of these factors, all of the raw sensor data does not correspond exactly with the events. The data in Table C.15 based upon the photographs shows that the explosion took place 153 msec after the aluminum contacted the quench tank water surface and that the tank broke 10 msec later. The sensor data shows that the tank broke before the thermocouples of interest started sensing and the aluminum reached the tank side. Since there is not a precise common time base between the two data sources, a time shift between like events of several milliseconds is reasonable. The event used to establish time correspondence between both data sources was when the aluminum just contacted the water. This time is clearly established by the accelerometer signal, but not quite as easy to determine from the film. However, the time of uncertainty in determining this point on the film is less than five frames, about 5 msec and most likely is determined within 3 msec. The time at which the tank broke is much more difficult to determine from the film and could easily be in error by ± 5 msec. The precision of determining the explosion from the film is within 1 frame or 1 msec which is also the case for the aluminum being at the left side of the tank. The error in determining the time at which the aluminum contacted the right side of the tank is estimated to be greater because there was no clear event demonstrated as there was for the left side contact and the explosion. (Light reflection made the left side contact easy to determine.)

Based upon the above, it seems reasonable to adjust the film data by adding 3 msec to the time for left contact and explosion and to deduct 6 msec from time the tank broke. This basis was used to obtain the "adjusted time" column shown in Table C.15.

This established the final event sequence as starting with the aluminum contacting the left tank wall and; the explosion taking place 1 msec later; the tank breaking 2 msec later; the 5 inch elevated and 1 inch surface thermocouples starting to read 3 msec later and the thermocouple at the tank edge starting to sense 7 msec later. This range of times for the critical events seem reasonable and is judged to substantiate the cause and effect relationship between the final aluminum contact with the quench tank side wall and the explosion.

This is the only "hard" data available to establish that an impact shock took place and triggered the vapor explosion. The secondary data available to substantiate the potential existence of a shock is the radial speed of the aluminum flow at the time of the quench tank side wall contact. This data was calculated from the fastex film and shown in Table C.10. The speed represent an average of two values and the shock strength is based upon this average value. Table C.13 shows the data upon which these values are based. Figure C.34 shows the relationship between aluminum speed and impact shock strength. The secondary data substantiates the hypothesis.

C.6.2.2 Secondary Evidence

A comparison of the shock strengths listed in Table C.10 shows that the strength calculated for experiment 4 was the lowest, 1000 psi; that for the explosion it was 1250 psi; and that all of the others were greater. Thus, in comparison to the explosion, experiment 6, the shock strength for all of the others (except for No. 4) should have been sufficient to collapse a steam film similar to that which was present in experiment 6. Since experiments 2, 3 and 8, in addition to 6 were the only ones for which a reaction was expected, it may help to demonstrate that the film collapse mechanism could have been present by establishing conditions which could have prevented a reaction. Since shock levels greater than that calculated for experiment 6 are ascribed to be present in experiments 2, 3 and 8, establishing that the vapor film was thicker than it was in the case of the explosion so

that it would not be collapsed sufficiently to obtain the necessary contact between liquids would accomplish this. In addition, the case for the existence of a shock may be enhanced if a relationship between the start of temperature rise on the quench tank bottom surface and the aluminum flow arriving at the side walls of the quench tank can be shown.

Figure C.32 shows temperature profiles 1/8 inch above the bottom surface of the quench tank and the average temperature for two locations on the bottom surface. Since, for all practical purposes, the aluminum temperature in the water is the same for all the experiments and the aluminum is the heat source, the thickness of the layer of water and vapor should be directly proportionate to the temperature measured. Specifically, if at corresponding times the 1/8 inch high thermocouples: sense aluminum temperature, the layer is equal to or less than 1/8 inch thick; if they sense temperatures less than aluminum temperature, the layer is greater than 1/8 inch thick; and in the last case, the lower the temperature sensed, the thicker the layer. Now, referring again to Fig. C.32, the unique temperature distribution which occurred in experiment 6 is shown clearly. Based upon the logic just presented, all of the other films existing at the time the aluminum impact the side wall were considerably thicker than the one in which the explosion took place.

Table C.10 lists the temperature at the time aluminum reached the quench tank wall. A comparison of these temperatures for experiments 2, 3, 6 and 8 shows clearly that the thermocouples 1/8 inch above the quench tank bottom surface, 3 inches and further from the center and the surface thermocouples, 1 inch from the center, sensed much lower temperature for experiments 2, 3 and 8 than in experiment 6. This emphasizes the results summarized in Fig. C.32.

An assessment of the thermocouple response data at the time which aluminum contacted the side wall of the quench tank was made in an attempt to establish a correlation. The records are not good enough to do this analytically, but a strong impression results

IIT RESEARCH INSTITUTE

that there is a physical relationship. A review of sensors data presented in Figs. C.23 through C.29 provides examples of the apparent relationship between aluminum contacting the side wall and the start of the temperature rise at the side wall. Figures C.25, 26, 27 and 28 illustrate this effect. The contact sensor is located 120 degrees away from the tank side thermocouple in Fig. 25 and 165 degrees away in the other figures. Thus, it is possible that the aluminum was above the thermocouple when the side contact occurred and the impact could have reduced the film thickness.

Comparing the side wall contact times listed in Table C.13 and that in Table C.10 with the times that the thermocouples started sensing, also shown in Table C.10, provides other possible correlations. Table C.16 summarizes these comparisons. In experiment 2, the individual times temperature was sensed at the 3 inch location were 106, 78 and 85 msec (average shown is 90) and side contact was at 67 msec. In experiment 3, the side wall contact times were 114 and 123 msec (Table C.13) whereas the average of the start of temperature rise at the 3 inch thermocouple location was 117 msec (Table C.10) and the individual times were 108, 116 and 126 msec.

In experiment 4, the left side tank contact was at 132 msec with one of the 3 inch thermocouples sensing at 136 msec and the contact sensor registered at 198 msec with the 5.8 inch thermocouple sensing at 216 msec. In experiment 5, the tank left side contact took place at 120 msec with one of the surface thermocouples sensing at 126 msec and the contact sensor registered at 186 msec with the 5.8 inch thermocouple sensing at 199 msec.

Experiment 6 has been presented previously. The aluminum reached the tank left side at 118 msec in experiment 7 with one of the 3 inch thermocouples sensing at 124 msec; also the side contact sensor registered at 163 msec with the 5.8 inch thermocouple sensing at 174 msec. In the eighth experiment the above type of correlation was not present, but in Fig. C.29, the thermocouple at 120 degrees and 3 inches appears to exhibit an increase in slope at the time the contact sensor registered.

IIT RESEARCH INSTITUTE

TABLE C-16
SIDE WALL CONTACT AND START OF TEMPERATURE RISE

Experiment Number	Side Contact Times (msec)	Time Thermocouple Started to Sense (msec)	Thermocouple Location	
			Radial (inch)	Height (inch)
2	67	78	3	1/8
2	67	85	3	1/8
2	67	106	3	1/8
3	114	116	3	1/8
3	123	126	3	1/8
4	132	136	3	1/8
4	198	216	5.8	1/8
5	120	126	1	0
5	186	199	5.8	1/8
7	118	124	3	1/8
7	163	174	3	1/8
8	Figure C-29 shows slope changes at the 3 inch 120° gage at time of side contact.			

Unfortunately, the above observations do not provide a rigorous cause and effect relationship. However, there appears to be a relationship rather than a random happenstance. It is believed that the lack of correlation arises because of the assortment of geometries of the initial portion of the aluminum stream (shown in Fig. C.30) and from the instrumentation arrangement. The irregular aluminum geometry is thought to produce much more nonuniform flow over the quench tank bottom surface than regular geometry would. Thus the film between the aluminum and tank bottom would be considerably more irregular and it could collapse from the flow irregularity. The large "collar" shown in Figure C.30 and described in Table C.11, produced a significant perturbation when it reached the quench tank water surface and also could have when it reached the flow already established. It could certainly have produced steam film collapse. The high speed movies were not clear enough to determine the times at which these events occurred. The steam film around the aluminum and the conductive paint break circuit on the quench tank obscured the view.

It is concluded that there is an impact generated shock which is capable of collapsing the steam film. A better demonstration of this would have been obtained if the leading edges of the aluminum streams had been larger and uniform.

C.6.3 Smooth Quench Tank Surface Experiments

Experiments 4, 5 and 7 were conducted with smooth surfaces for which no reaction was expected and none was obtained. However, just as in the other experiments, the leading edges of the aluminum stream were not of regular diameter or length as shown in Fig. C.30 and Table C.11. The descending order of stream size corresponds to experiments No. 5, 7 and 4. The stream in experiment 5 had a more favorable geometry than was present in the explosion, experiment 6, and the stream in experiment 7 was not much different from the one in the explosion. The leading edge of the stream in experiment 4

was considerably smaller or less favorable for initiation than those in 5, 6, or 7. With this qualification, experiments 5 and 7 may be considered substantiation that simulations made on smooth surfaces do not produce explosions.

Before conducting the experiments it had been predicted that the aluminum impact on the tank bottom would collapse or drive off the water/vapor film. Under this condition the thermocouples would start sensing temperature as soon as the flow reached them. In the case of rough surfaces, it was postulated that the steam film would reform and provide insulation so that the bottom surfaces would be cooler than a smooth surface which contained no water (to vaporize and reform a film). Since the aluminum did not contact the bottom immediately, these predictions are not meaningful. Data relating to the time at which temperature was sensed by the surface thermocouples did not provide a basis for deducing comparisons between rough and smooth surfaces. It is believed that the variation in the aluminum stream caused greater variations in the experimental results than the natural phenomenon which was being attempted to be detected.

C.6.4 Leading Edge

The geometry of the leading portions of the aluminum streams in the seven experiments varied considerably. This condition has been referred to repeatedly in the discussion presented so far. Figure C.30 shows the geometry for each experiment. The fastex film showed that the edge in experiment 2 was split resembling an inverted "V" with the opening down. In experiment 8, there also was a split, with one edge being at about right angles to the main stream. This portion of the stream contacted the tank wall before the stream reached the bottom. Table C.11 describes some of the gross features which could be scaled from the film. The scaling was made on the basis that the main portion of the stream had 3-1/4 inch diameter.

Long of Alcoa showed that the diameter of the crucible opening was a critical parameter in the interaction of molten aluminum and water, however the number of simulations was limited. The data indicated that 2-3/4 inches was the minimum orifice at which an explosion would occur, based upon obtaining no reaction in one simulation at each of the following orifice diameters: 3/4 inch, 1-1/2 inches and 2-1/2 inches. In addition, one simulation each with 2-3/4 inches and 4 inches and 22 simulations (performed with quench tanks having rough steel surfaces and under the same baseline conditions used in the current experiments) produced reactions. Hess and Brondyke of Alcoa made 51 simulations under the baseline conditions, using rough steel surfaces, and obtained 33 reactions. This poses an interesting question, did Long get 100 percent reactions (rather than 65 percent) because he ran 22 rather than 51 experiments; or was there another difference in the two sets of experiments?

It is believed that there is an uncontrolled variable which is not described by the drop crucible orifice diameter. The seven different initial geometries of the aluminum stream were all obtained from the same equipment (diameter orifice and orifice plug) being opened in the same manner (dropped weight). There was one variable which was not accurately controlled in the opening process: the free fall distance of the opening weight before it started to move the orifice plug. The cable used to support the weight, until cut by the linear shaped charge, was assembled individually for each experiment and precise control over its length was not provided. The free fall was about 4-1/2 inches, but it was not measured or controlled. The motion of the orifice plug through the aluminum could effect the initial flow and hence the geometry of the initial portion of the aluminum stream. This same effect could have been operating in Hess and Brondyke's and Long's experiments and could have been the difference between the two sets of Alcoa experiments. If there was better control in these two Alcoa series (than in IITRI's), the opening conditions (drop weight) could have been different with each providing a

"mean" geometry for all of the experiments which was different. Under this assumption, Long's mean geometry could have been more favorable for obtaining reactions than in Hess and Bron-dyke's experiments. In the absence of specific data, except for that just obtained, this represents a reasonable assumption. If the assumption is correct, the conditions obtained in these last IITRI experimental series provided a less favorable mean geometry than the other experiments did.

The leading portion of the aluminum stream is considered quite important because it is believed to play a significant role in the initiation mechanism. The major role is the effect on the film separating the molten aluminum and liquid water and the secondary role is the effect upon the flow produced shock which collapses the film. Although this concept is speculative, in that it has not been demonstrated, it is logical. It is concerned with the relative stability of the stream film formed between the molten aluminum and water and/or the quench tank surface. The stability of the vapor film is considered to have two characteristics:

- resistance to collapse,
- thickness.

These characteristics are important in relation to the strength of the shock available and required to collapse the film and provide liquid aluminum-liquid water contact. If the film requires too strong of a shock to collapse the thickness, intimate contact between the liquids will not be obtained. This rationale applies to irregular films in that the amount of contact required to release sufficient energy to obtain a identifiable reaction must be achieved. The strength of the shock is bounded by the initial aluminum head (initial aluminum weight and drop height) and the aluminum flow characteristics on or near the quench tank surface (which in part depends upon the head). These flow characteristics also depend upon the geometry of the aluminum stream.

The uncontrolled geometry of the leading edge of the aluminum stream was a superimposed condition in the experiments. This condition is believed to account for the lack of initiations in experiments 3 and 8 which should have produced explosions. It is also believed to have had a significant effect in experiment 2, but this may well be an entirely different case because of the vast differences in quench tank water depth. The small, irregular initial portion of the aluminum stream in experiments 3 and 8 are considered to be equivalent to streams which would have come from smaller diameter orifice openings in the drop crucible. The postulation is that they were effectively less than 2-1/2 inches in diameter and for this reason explosions were not obtained.

Experiment 2 was based upon observations provided by the Aluminum Association Task Group for Molten Aluminum-Water explosions. They noted, from past experience, and interpreted that the accidental pouring of molten aluminum on damp surfaces produced "pops" which could be considered explosions. It is believed, based upon the experiments just conducted, that this is not the case. Concrete contains hydrated water and upon rapid boiling this water can be vaporized and "blow out" concrete with an associated "pop". This is a mechanical explosion and does not have the energy release rate of a vapor explosion. In experiment 2, an area of concrete about 4 to 5 inches in diameter and on the order of 1/16 inch to 1/8 inch deep was found missing from the quench tank concrete surface after the experiment. The accelerometer trace should have shown this action even though the trace was distorted badly from a strong 60 cycle signal. It is believed that the mechanical explosion took place after the data recording period of about 1 second. The amount of mass removed by the mechanical explosion should have produced strong signal which should have been evident, regardless of the 60 cycle noise. On this basis, experiment 2 is not considered to have been a potential simulation of an explosion.

C.6.5 Miscellaneous Characteristics

The primary data has been used to develop some additional characteristics of the simulation. The temperature time response data have been used to provide an indication of the rate of temperature rise. The accelerometer data has been used to provide envelope boiling force rate data. The estimated dimensions of the leading portion of the aluminum stream have been used to estimate the initial volume of metal contacting the quench water and the calculated flow speed used to estimate the additional volume of aluminum in the quench tank at the time that the flow reached the tank side walls.

These types of data should relate to the interaction process and it was thought they would aid in understanding or verifying the results expected. This goal was not realized to any significant extent, but the results are presented because they may have a value in the future when a greater level of understanding is reached or when further study is performed.

C.6.5.1 Temperature Response Data

The average temperature rise at each thermocouple location is shown in Table C.17. The data was obtained by dividing the total change in temperature by the total time it took for the rise. In most cases this is a reasonable representation. The data has been grouped in three sections: experiment 2 by itself; experiments 3, 6 and 8, which were expected to react, form the next group, and the remaining experiments, which were made on smooth surfaces, comprise the last group. With the exception of experiment 2, averages for each group are shown for each similar gage location, both for the group and the experiment. The overall average temperature rise rate is shown for each experiment and for each group.

The overall average for each group indicates apparent significant differences. The average rise rate in experiment 2 was less than half of that for the smooth tank bottoms. The rough

TABLE C-17

AVERAGE RATE OF TEMPERATURE RISE

Experiment Number Item	Rough Surface 2 ***	Rough Surface				Smooth Surface			
		3	6	8	Average (3,6,8)	4	5	7	Average (4,5,7)
$\Delta T/\Delta t$ °F/msec									
1**	6.9	82.3	29.7	49.6	53.9	7.6	2.2	27.5	12.4
8	0	1.3	18.8	0.1	6.7	0.6	4.6	0	1.7
9	0	0	29.9	0.6	10.2	0.3	9.5	6.7	5.5
Average (8&9)	0	.6	24.4	0.3	8.5	0.4	7.1	3.3	3.6
2	3.6	70.0	30.3	20.3	40.2	13.2	2.6	26.0	13.9
3	4.7	65.4	44.1	15.2	41.6	9.2	25.3	6.5	13.7
5	9.1	25.8	13.2	20.9	20.0	8.2	5.2	27.1	16.8
6	13.9	25.7	65.7	12.4	34.6	27.6	4.3	7.5	13.1
Average (3,5,6)	9.2	39.0	41.0	16.2	32.1	15.0	11.6	17.0	14.5
4	3.1	41.3	78.7	23.6	47.9	N.R.*	39.1	2.7	20.9
7	4.9	6.6	291.0	N.R.*	148.8	21.9	3.9	5.0	10.3
Overall Average	5.1	57.7	66.8	17.8	44.9	11.1	10.7	13.2	12.0
Average Radius Flow Speed at Quench Tank Side, ips	80	60	55	64	60	44	73	103	73

* N.R. means no record.

** Numbers refer to thermocouple locations in Figure C-3.

*** 1/64 inch of water.

surfaces exhibited almost four times the average rate of temperature rise as did the smooth ones. There does not seem to be a logical basis to account for this correlation other than the surface roughness. The average rates of temperature rise are plotted in Fig. C.35 as a function of the average aluminum radial flow speed at the quench tank side. This plot clearly shows the correlation of temperature rise rate with flow speed by surface roughness. Since the normal heat transfer per se is not believed to be a parameter of importance, the significance may be that the film between the aluminum and a rough surface is less stable than the film between aluminum and a smooth surface. Flow over a rough surface could be envisioned as being relatively more turbulent and thereby increases heat transfer and producing conditions closer to nucleate or transition boiling. This aspect of the data would appear to bear further investigation.

C.6.5.2 Boiling Characterized by Accelerometer Data

Data has been presented on the boiling force which produced significant accelerations of the quench tank bottom surface. The frequency of the boiling force was on the order of 7800 cycles per second. The envelope values of the boiling forces were reported in Table C.12 and show forces as great as 340 pounds. It does seem that the shape of the acceleration records, and hence the associated driving force, has a correspondence to the initial geometry of the leading edge of the aluminum stream.

The data reported in Table C.12 have been plotted in Fig. C.36. If it is assumed that the force time curve obtained for the explosion in experiment number 6 represents the typical signature, some observation about the other results may be made. From the force time profiles it could be expected that experiment number 5 would have produced an explosion. The initial rate of boiling force rise was greater than that in the explosion. The quench tank bottom surface was tarset, which precludes surface cavities containing liquid water. Thus, it may be concluded that the

This high frequency might explain the trouble Battelle was reported to have had in trying to interpret their pressure records.

leading edge geometry and flow conditions would have produced an explosion if the tarset coating had not been present. In contrast, the initial force rise rate obtained in experiment number 3 was considerable less than occurred in the explosion. The quench tank surface was rough concrete and an explosion was expected. Therefore, it is concluded that the aluminum stream leading edge was improper for an explosion to occur.

The initial force rise rate in experiment number 8 (rough concrete surface) would appear to be great enough to produce an explosion except that it did not persist long enough. It is postulated that the stream geometry produced this effect and a steam film was formed which could not be collapsed. It may be seen that the initial rise is interrupted and then continue at about the same rate as it was initially. The initial force rise rates in experiment numbers 4 and 7 were low in comparison to the explosion. The initial force rise was interrupted and then continued at a rate greater than took place when the explosion occurred. Again, the characteristics of the steam leading edge are presumed to produce the force-time profiles shown.

Experiment 2 is clearly in a class by itself. It was made in a rough concrete surface but had very little quench water. It would be reasonable to assume that the quench water was vaporized rapidly which limited the boiling force obtainable.

C.6.5.3 Initial Aluminum Volume

In an effort to provide evidence on the effect of the aluminum stream volume and explosion initiation potential, data was prepared relating to the volume of aluminum in the initial portion of the aluminum streams. Table C.18 presented estimates of aluminum and water volumes. The volume of aluminum is estimated as that present when it reached the closest point to the quench tank bottom surface, and when the aluminum flow reached the tank side wall. The initial volume ratio, water to aluminum, may be considered an indication of the steam film thickness formed or rate of

TABLE C-18

ALUMINUM AND WATER VOLUMES AND AVERAGE TEMPERATURES

Experiment Number Item	2	3	4	5	6	7	8
Quench Tank Surface	Rough Concrete	Rough Concrete	Smooth Concrete	Tarset on Concrete	Rough Steel	Smooth Steel	Rough Concrete
Water Volume, cubic inch	2	637	637	637	637	637	637
Aluminum Volume, cubic inch:							
Initial	0*	29	10	30	13	15	13
Total at Time of Side Contact	2	98	167	165	129	126	116
Volume Ratios, Water to Aluminum:							
Initial	0*	22	64	21	49	42	49
At Side Contact	1	6.5	3.8	3.9	4.9	5.1	5.5
Average Temperature Rise 1/8 inch above Tank Surface at Time Aluminum at Tank Walls	11	486	821	442	1305	89	731

*The water "depth" was only about 1/64 inch so there was hardly any aluminum in the "water" and then the volume-ratio was "infinite" initially.

aluminum cooling. The lower the ratios, the thinner the film and the lower the cooling rate. In comparing the value of the ratios shown in Table C.18, that for number 6 (the explosion) should be used as a reference point. All ratios lower should have thinner steam films and cool more slowly. The initial ratios show that only experiments 2 and 4 are greater and the ratios at side contact for numbers 3, 7 and 8 are greater. The stream leading portion geometry accounts for the variations shown. Experiment 2 is clearly a case separate from the others.

The average temperature rise is plotted as a function of the volume of aluminum in the quench tank as the time of side wall contact (shown in Table C.18) in Fig. C.37. There seems to be two lines of correlation corresponding to average temperature rises above 800°F and below. This again indicates a strong correlation between stream layer thickness at the quench tank surface and the aluminum stream volume.

C.6.6 Heat Transfer Considerations

It is postulated that the interaction of molten aluminum and water depends upon the steam film thickness and stability. This in turn is related to the aluminum/water quenching curve which has not been defined for the temperature range of interest, 1200°F to 2000°F. An estimate of this quenching curve for some selected conditions is shown in Fig. C.38. There are three regions of specific interest in the quenching curves:

- Stable film boiling
- Transition boiling (unstable film and nucleate, boiling)
- Stable nucleate boiling

In addition to the relationship between temperature and boiling regions, the time required to go from one boiling region to another may be significant. This postulation rests on the aluminum flow dynamics in the quench tank because the assumed shock which can collapse the steam film may take place within a fixed time range. Then the combination of boiling region and time become important. Figure C.39 shows an estimate of the

temperature time relationship for the data shown in Fig. C.38. The upper 3 curves in Fig. C.38 represent conditions which are not conducive for explosions. Similarly, in Fig. C.39, the left hand 3 curves represent conditions under which explosions take place and the right hand 3 curves, conditions under which they do not.

The data of Fig. C.38 and C.39 were obtained with 40 gram samples of aluminum and the time in Fig. C.39 could be expected to be different for the simulations. However, the trends illustrated could be expected to be valid.

In order to reconcile the occurrence of explosions and the data, the following interpretations are made. First, the films existing during the film boiling temperature range are more stable than those present during transition boiling temperature range. Secondly, this stability is defined in terms of the shock strength necessary to collapse the film and that the flow produced shock levels are not strong enough to collapse films in the film boiling temperature range, while they may be strong enough to do so in the transition temperature range. Thirdly, when the aluminum temperature is in the nucleate boiling range, below the critical heat flux, there may be liquid-liquid contact and a vapor explosion could result.

It is emphasized that this third condition is most likely, not applicable to actual commercial operations because it is highly unlikely that serious bleed outs, streams on the order of 5 inches in diameter, can be cooled to the temperature range for nucleate boiling in the time frame of a potential initiation. Thus, under the state of understanding at this time, any attempt to drop the aluminum temperature into the nucleate boiling range may be expected to result in reaching the transitioned temperature range sooner and enhancing the possibility of an explosion. In addition, at this time, the advisability of maintaining a 10 foot depth of water in the pits below the casting operations should be reevaluated. Based upon the material being presented, the quenching effect of the water depends upon the diameter of the aluminum flowing through the water. The reasoning being advocated

suggests that there is a dangerous water depth range bounded on either side by a safe depth. The bounds on these depths are related to the aluminum stream diameters and the continuous length of the stream at this diameter. The ratio of water to aluminum may be the important characteristic.

Table C.18 was prepared to show what might be called interaction characteristics. The various stream geometries encountered in the experiments covered a wide range, with initial volumes of aluminum varying by a factor of 10. The corresponding aluminum to water volume ratios varied by a factor over 60. The interaction of the aluminum and quench water is thought to occur in two stages, as evidenced by the experimental results. The first stage is related to the initial portion of the aluminum stream. If the volume of this part of the stream is large compared to the volume of water, a thick stream film may be formed which could represent a safer condition than when a thin film is present. The thin film may occur when the aluminum volume is small in comparison to the water volume, but not small enough to cool rapidly.

C.7 CONCLUSIONS

It is concluded that the most probable molten aluminum-water explosion initiation mechanism is spontaneous nucleation of liquid water. This liquid water is contained in surface capillaries and must be present for an initiation to take place. The vapor film separating the molten aluminum and liquid water must be collapsed in order to obtain the liquid-liquid contact necessary for spontaneous nucleation. An impact produced shock is the most likely stimulus for collapsing the vapor film between the two liquids and triggering the vapor explosions.

The energy released by the initiation will depend upon the surface area over which liquid-liquid contact is obtained and on the number and size of capillaries containing liquid water in this area. The interaction of the initiation energy and bulk aluminum water mixture will depend upon the mixture ratio of these liquids in the vicinity of the initiation site.

IIT RESEARCH INSTITUTE

The prevention of molten aluminum-water explosions may be accomplished by preventing the liquid water from being spontaneously nucleated and this may be accomplished by elevating the liquid water temperature to a level above 140°F or by eliminating it through the use of smooth surfaces (surfaces without capillaries). It appears that liquid water at 140°F or higher temperatures will not spontaneously nucleate. Since liquid-liquid contact (aluminum and water) must be obtained to initiate an explosion, preventing this will eliminate an explosion. Control over the vapor film stability and/or minimizing or controlling the film collapsing stimulation may also preclude an initiation. The way to achieve this control is not well defined. Evidence is on hand which indicates that the vapor film stabilizing additives may accomplish this. Control over the strength of the impact shock may be harder to achieve, but could be possible. The size of the bleed-out appears to be important in this aspect of the interaction. Further study is needed to clarify these aspects of the interaction.

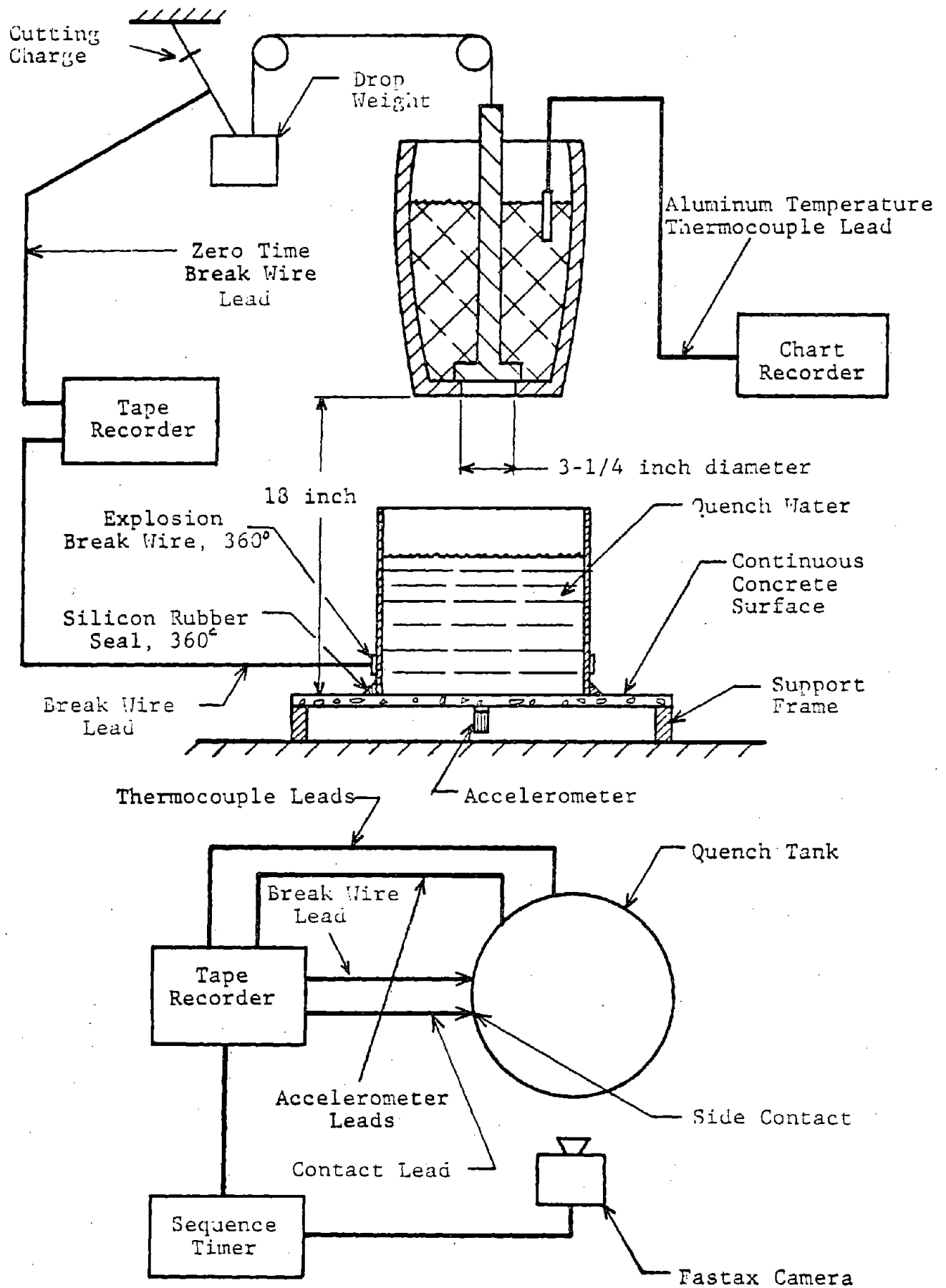


Figure C-1 Schematic of Equipment Setup

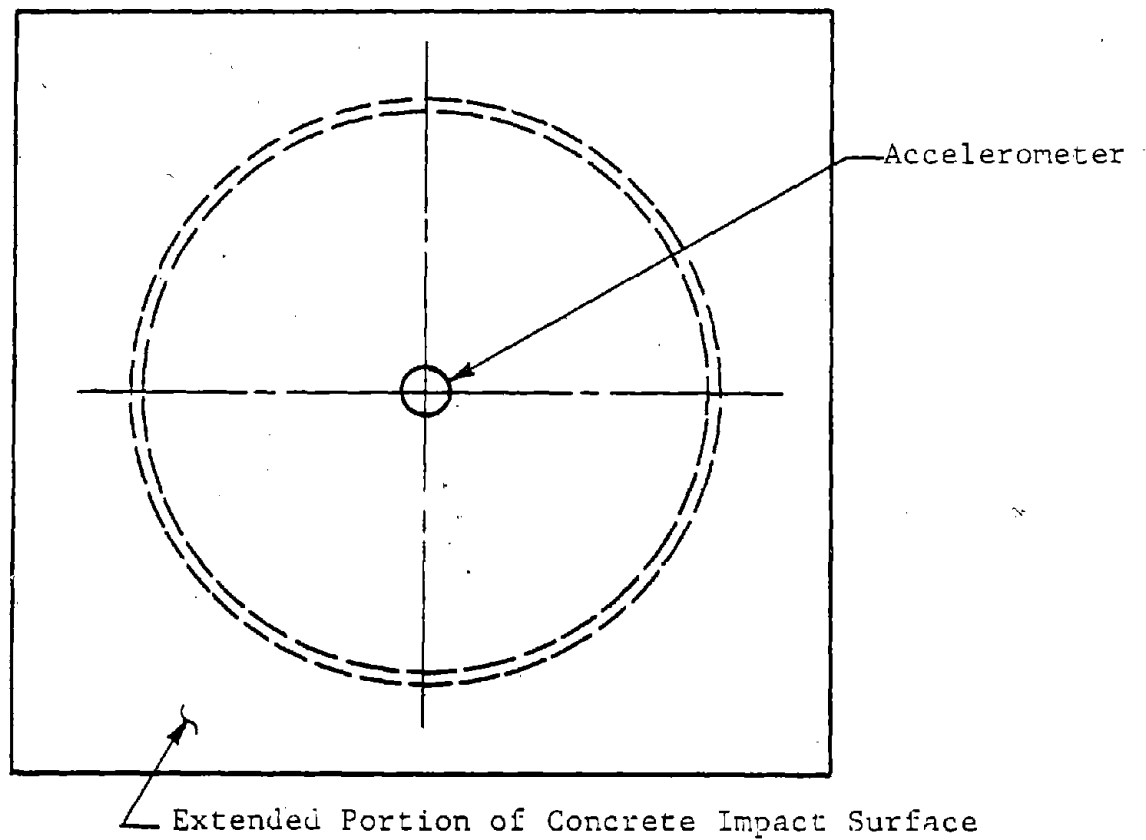
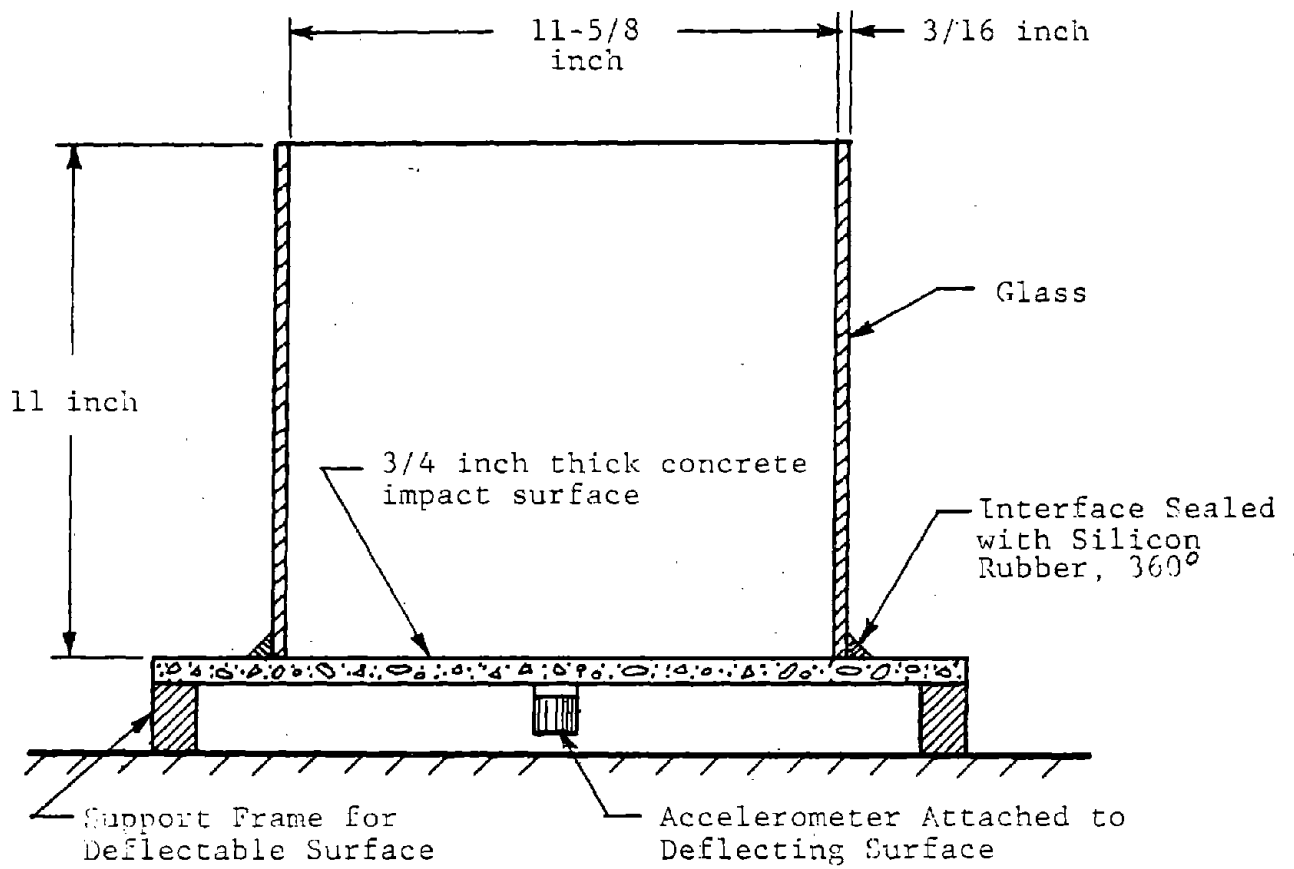
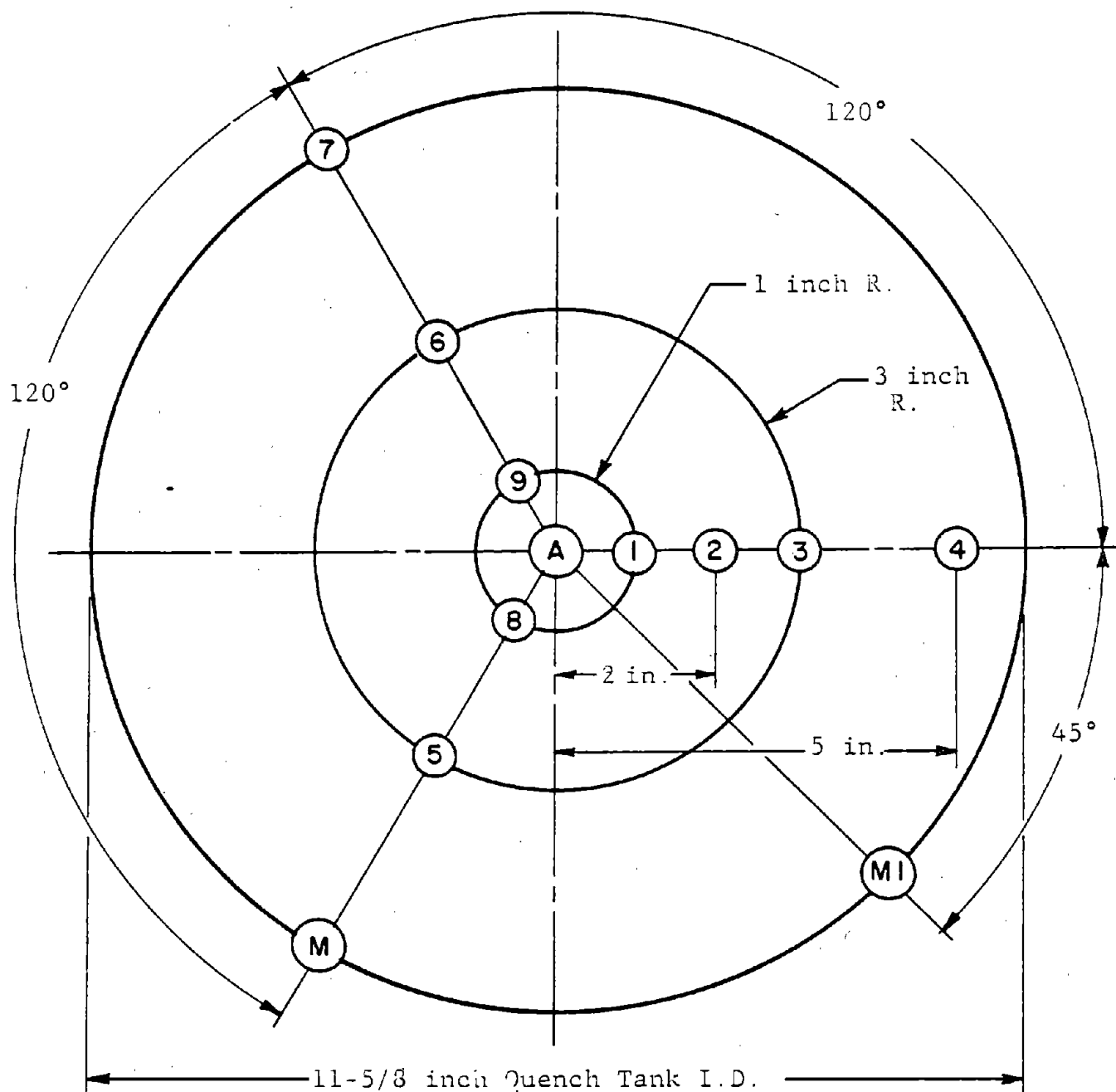


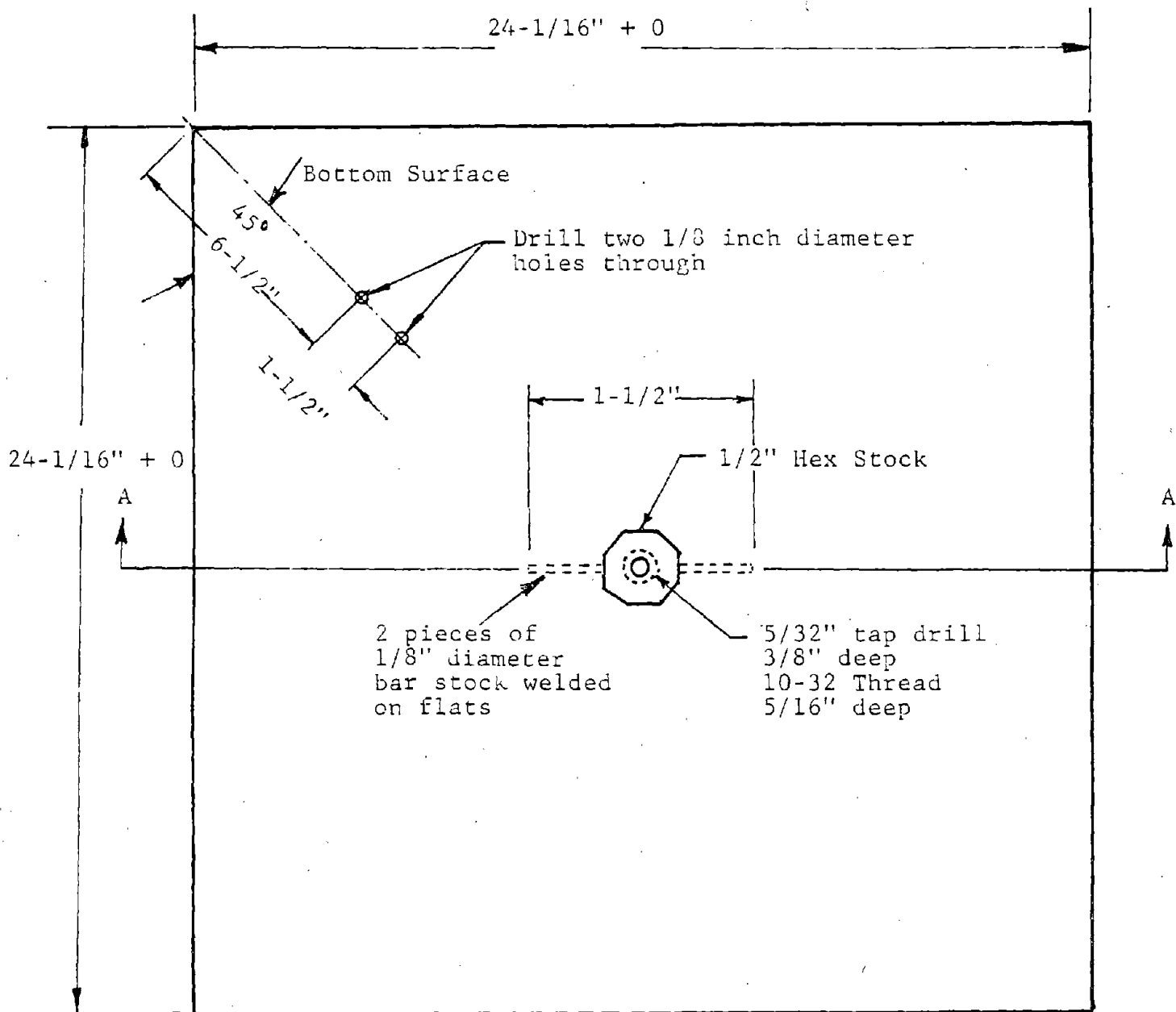
Figure C-2 Schematic of Quench Tank, Accelerometer and Support Stand



Thermocouple Numbers	Elevation
1 Through 7	1/8 inch Above Bottom
8 and 9	0 inch Above Bottom

A - Designated accelerometer location
M - Designates contact sensor location experiment 4
M1 - Designates contact sensor location experiments 5-8

Figure C-3 Actual Sensor Locations



Slab weight approximately 37.5 pounds

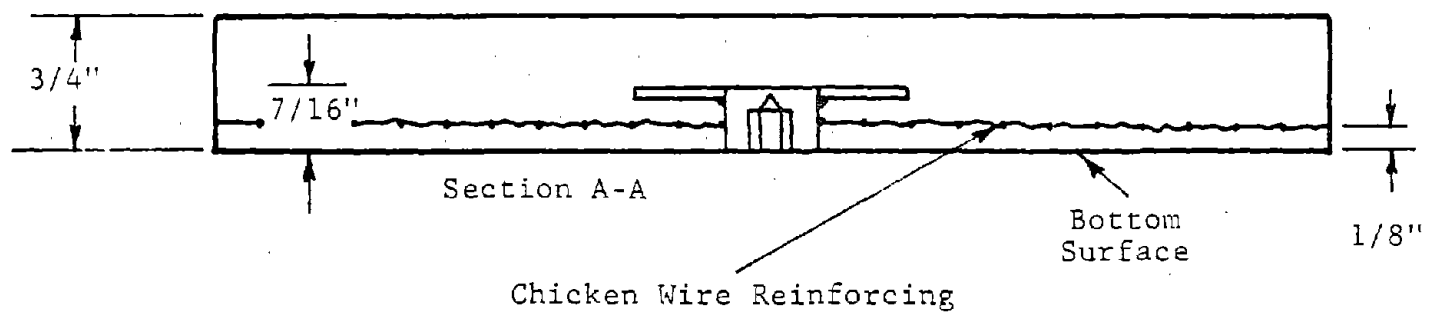


Figure C-4 Concrete Quench Tank Bottom Surface

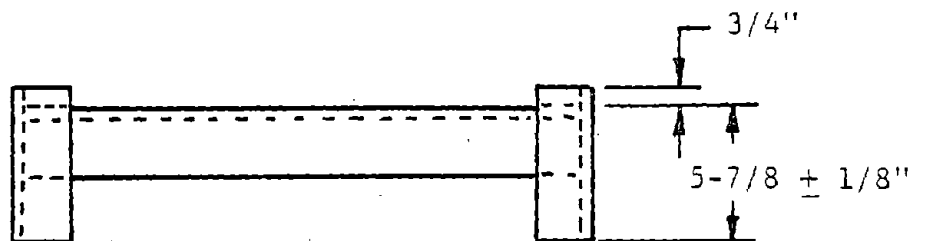
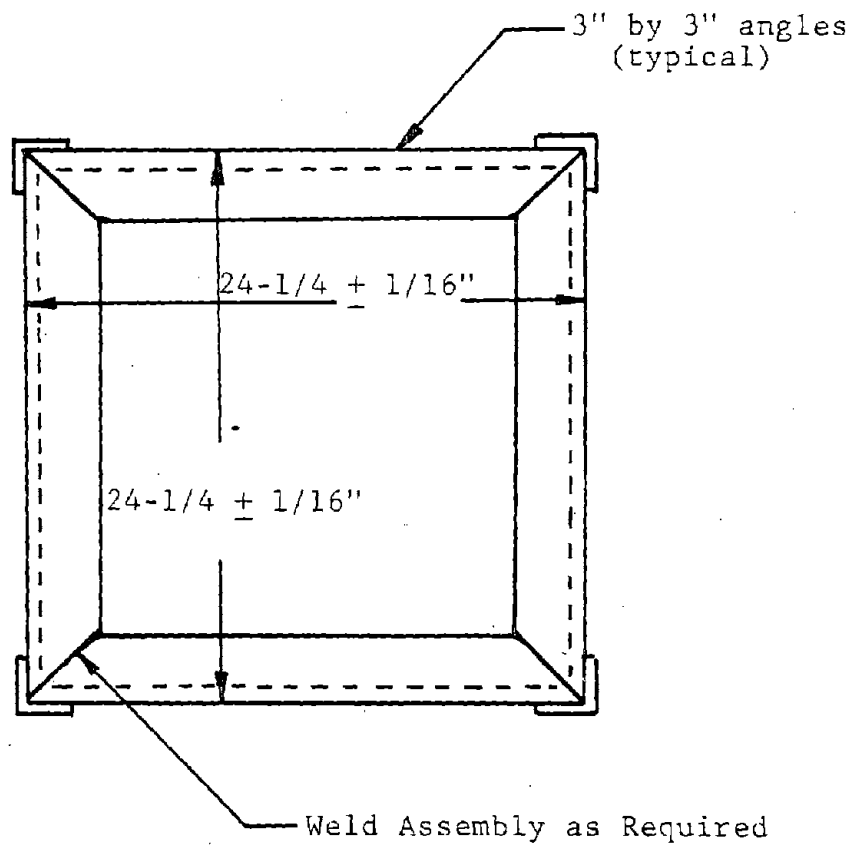
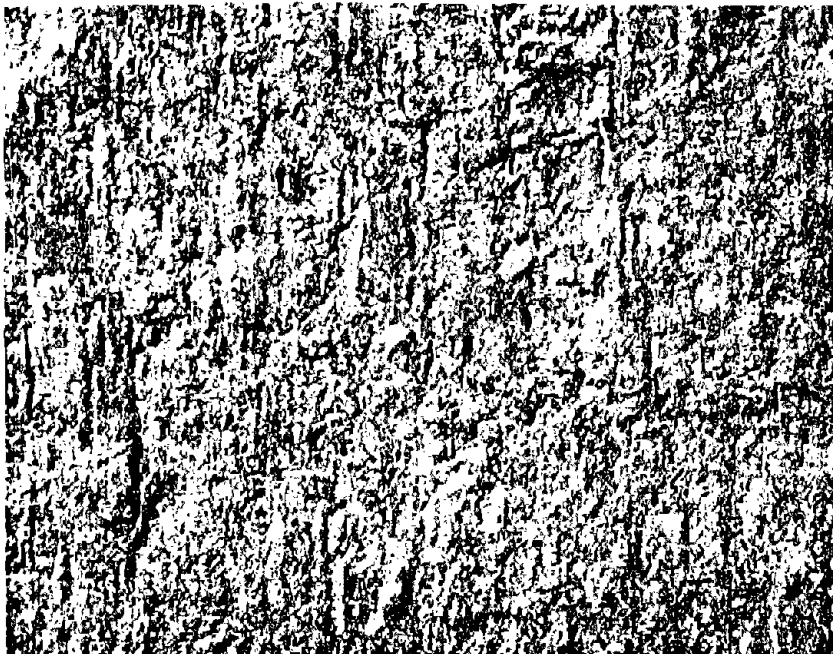


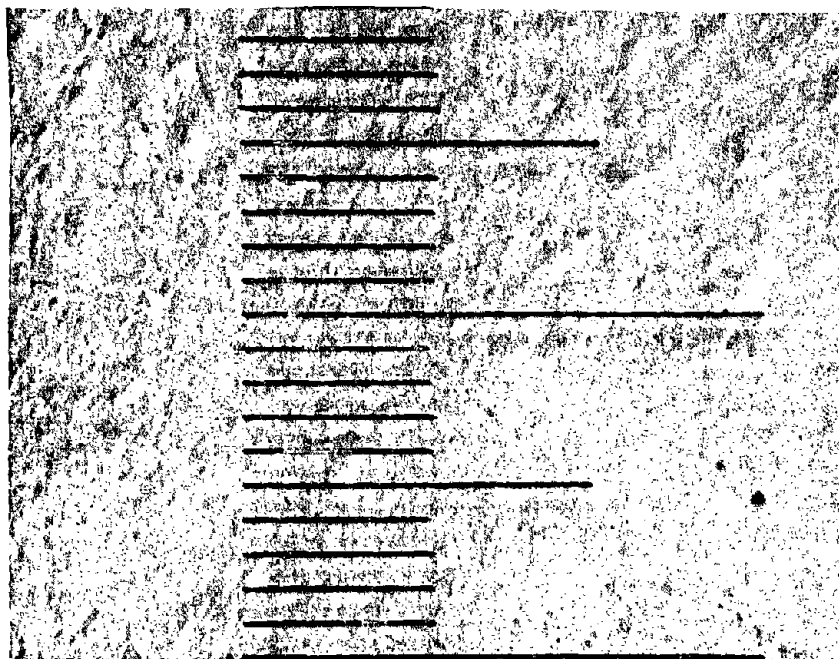
Figure C-5 Quench Tank Stand



a

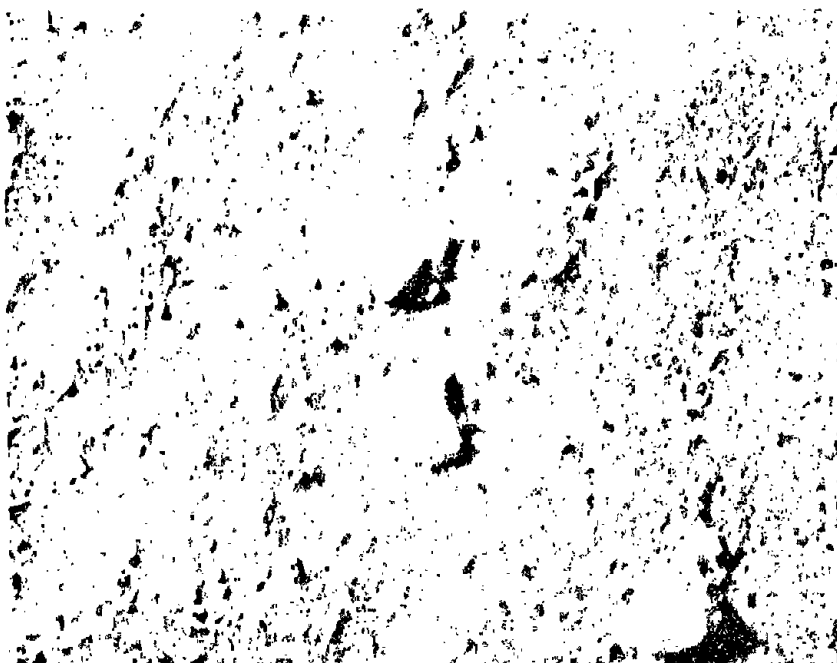


b

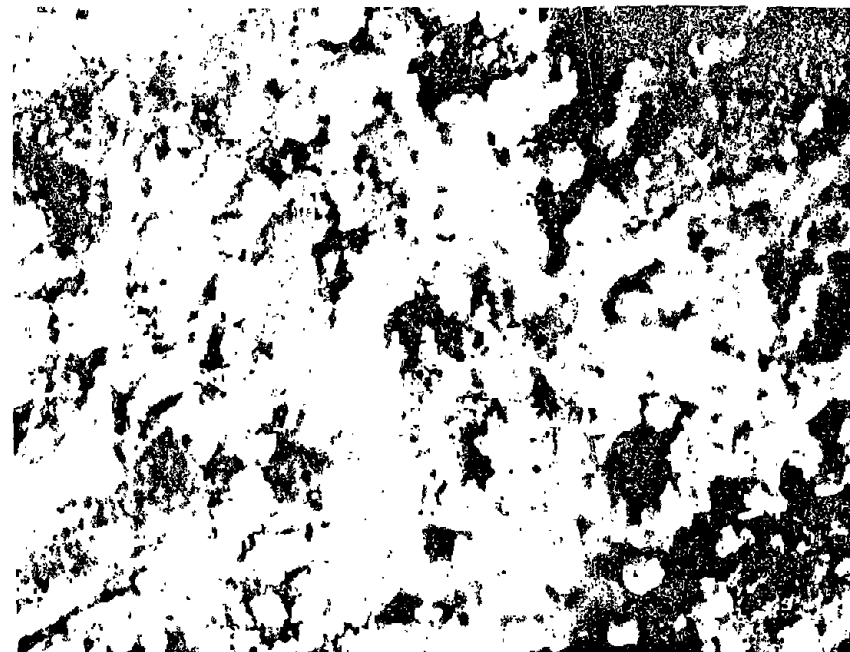
ViewTitle

- a Smooth Steel: low carbon (1010-1020) steel degreased with acetone
- b Rough Steel: low carbon (1010-1020) steel degreased with acetone, grit blasted, oven heated at 1200 °F for 60 minutes, air cooled to room temperature and rinsed with clean water.
- c All views magnified 48.3 times.
Smallest grid division is 0.1 mm.

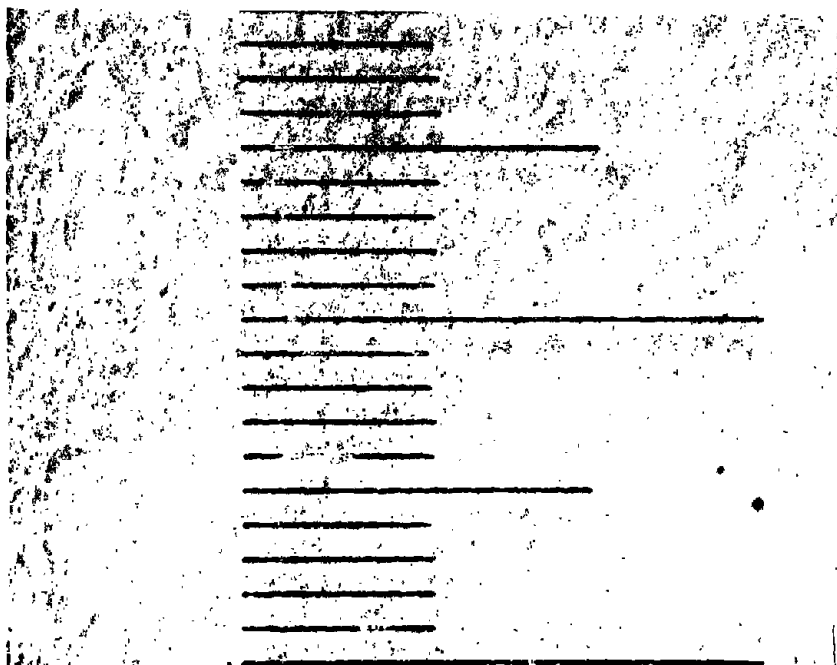
Figure C-6 Quench Tank Bottom Surfaces
Smooth and Rough Steel



a



b

ViewTitle

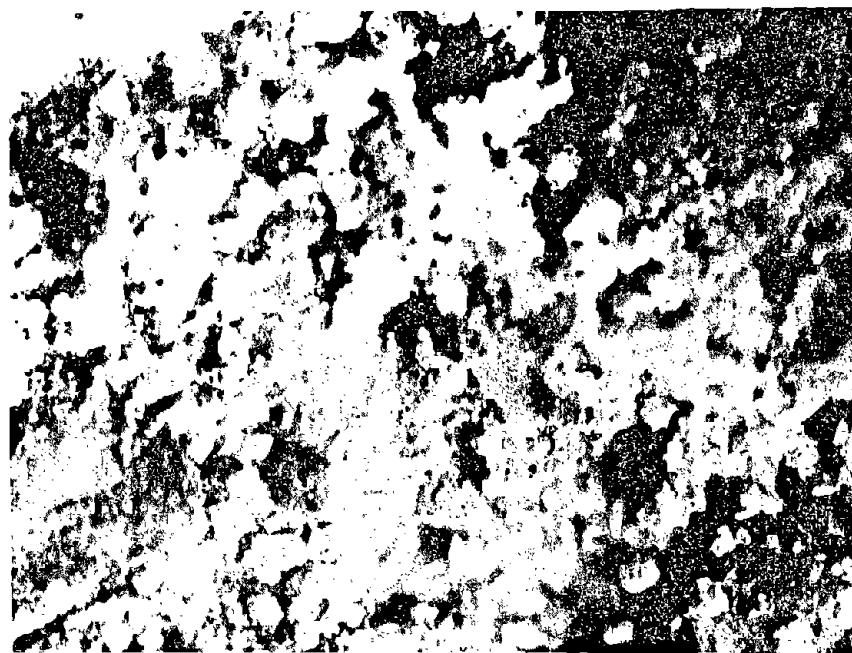
- | | |
|---|---|
| a | Smooth Concrete: neat cement
over mortar (ASTM C109) |
| b | Rough Concrete: mortar (ASTM C109) |
| c | All views magnified 48.3 times.
Smallest grid division is 0.1 mm |

Figure C-7 Quench Tank Bottom Surfaces
Smooth and Rough Concrete

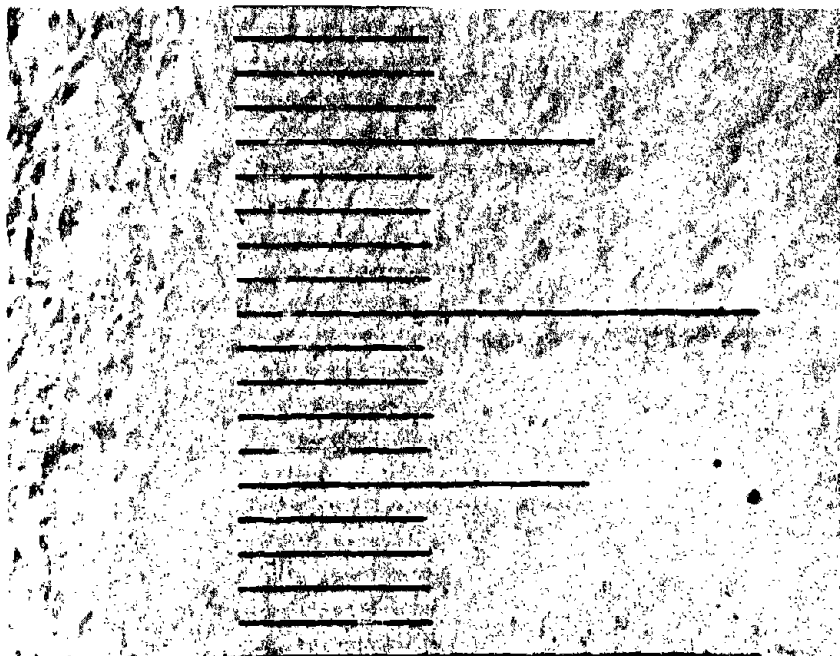




a



b



c

ViewTitle

- | | |
|---|---|
| a | Rough Steel: low carbon (1010-1020) steel degreased with acetone, grit blasted, oven heated at 1200°F for 60 minutes, air cooled to room temperature and rinsed with clean water. |
| b | Rough Concrete: mortar (ASTM C109) |
| c | All views magnified 48.3 times.
Smallest grid division is 0.1 mm. |

Figure C-8 Quench Tank Bottom Surfaces
Rough Steel and Rough Concrete

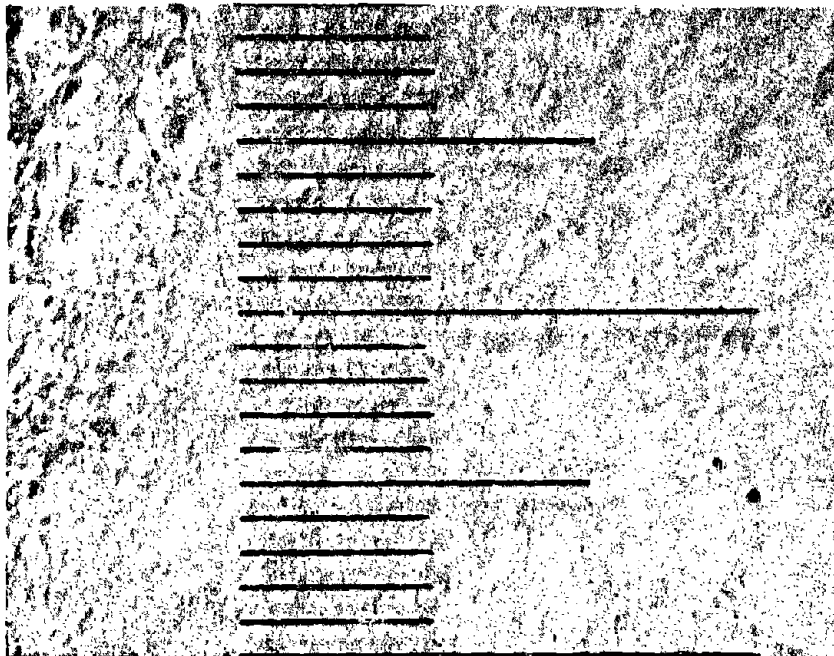




a



b



c

View

Title

- | | |
|---|--|
| a | Smooth Steel: low carbon (1010-1020) steel degreased with acetone |
| b | Smooth Concrete: neat cement over mortar (ASTM C109) |
| c | All views magnified 48.3 times.
Smallest grid division is 0.1 mm. |

Figure C-9 Quench Tank Bottom Surfaces
Smooth Steel and Smooth Concrete



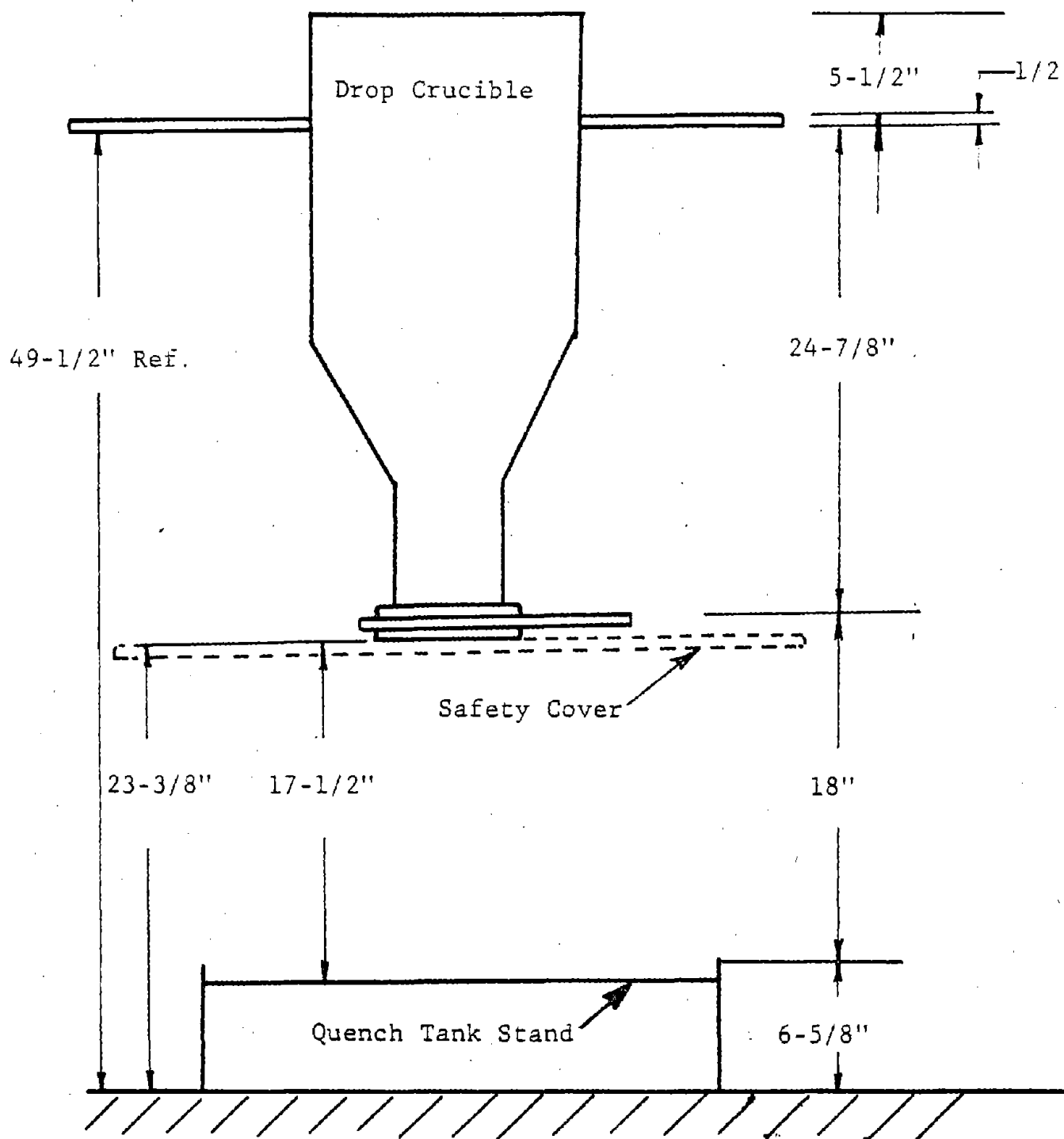
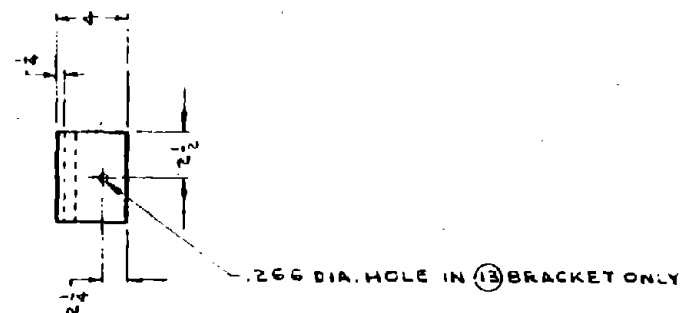
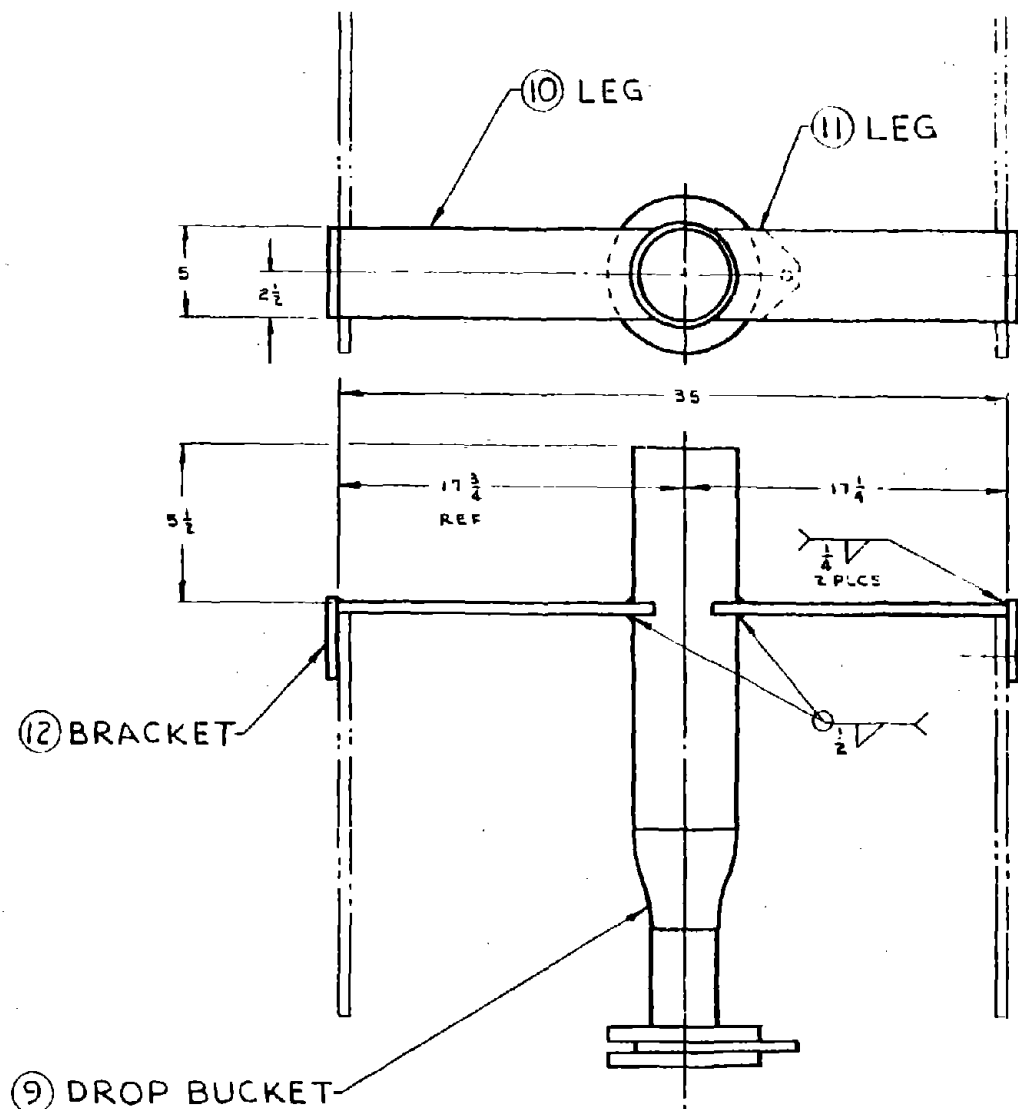


Figure C-10 Schematic of Simulation Setup
With New Drop Crucible



- DRILL HOLE IN FIELD TEST FIXTURE AND
INSERT $\frac{1}{4}$ IN. DIA. ALUMINUM ROD OR
ALUMINUM BOLT

(13) BRACKET

NOTE • BE SURE THAT (10) AND (11) LEGS ARE
PROPERLY ORIENTED WITH (9) DROP
BUCKET BEFORE WELDING

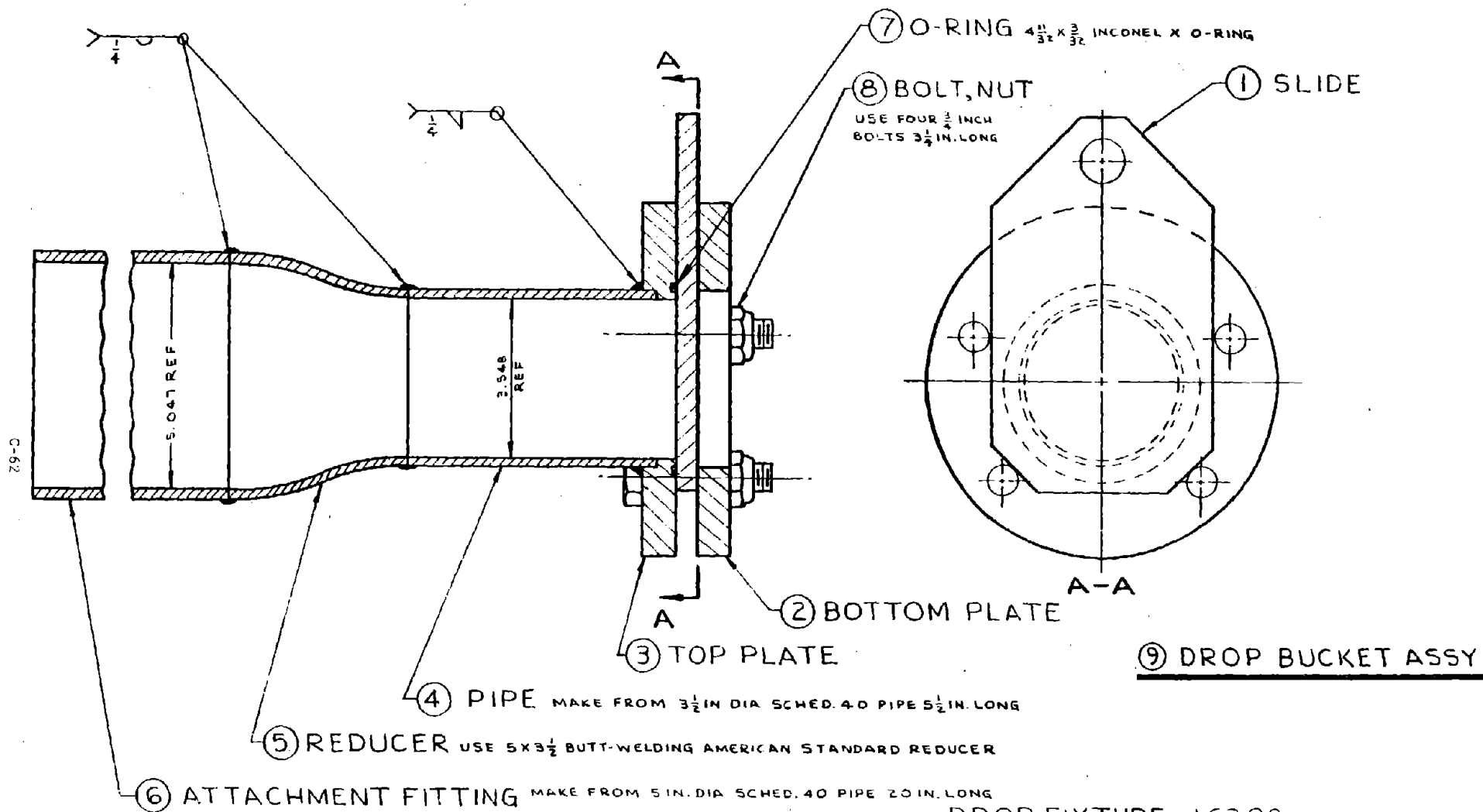
• LEGS AND BRACKETS TO BE MADE FROM $\frac{1}{2}$ IN.
1010-1020 STEEL PLATE

DROP FIXTURE J6309

12/12/74 E.P. BERGMANN

FIGURE C-11

SHT 1 OF 4



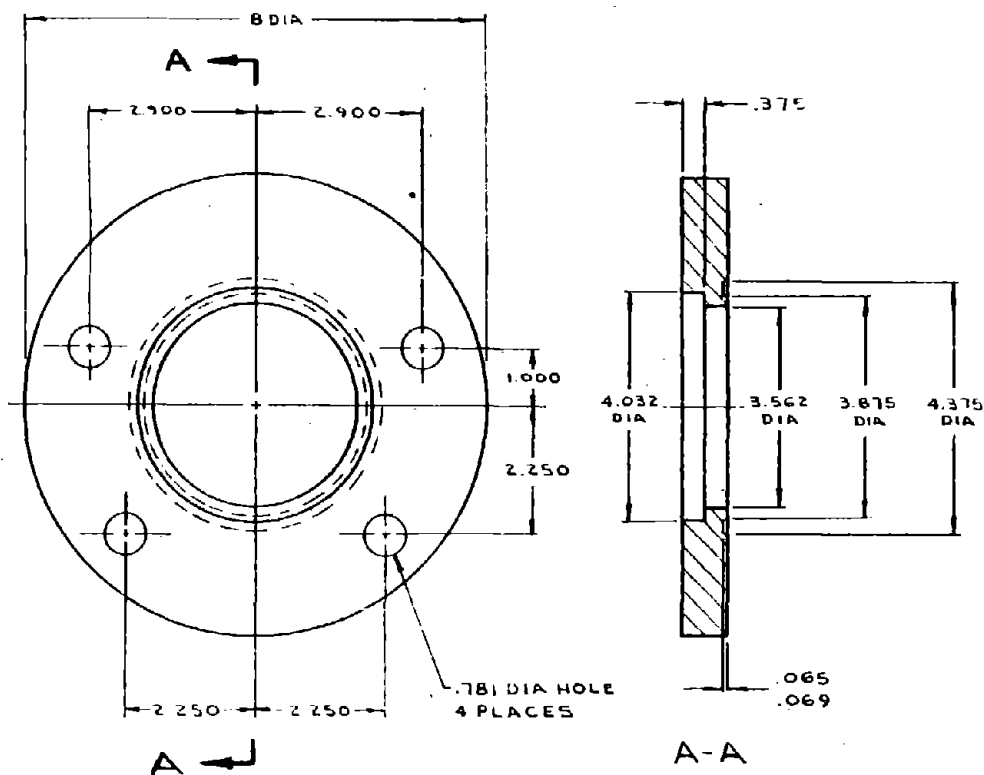
DROP FIXTURE J6309

12/10/74 E.P. BERGMANN

FIGURE C-12

SHT 2 OF 4

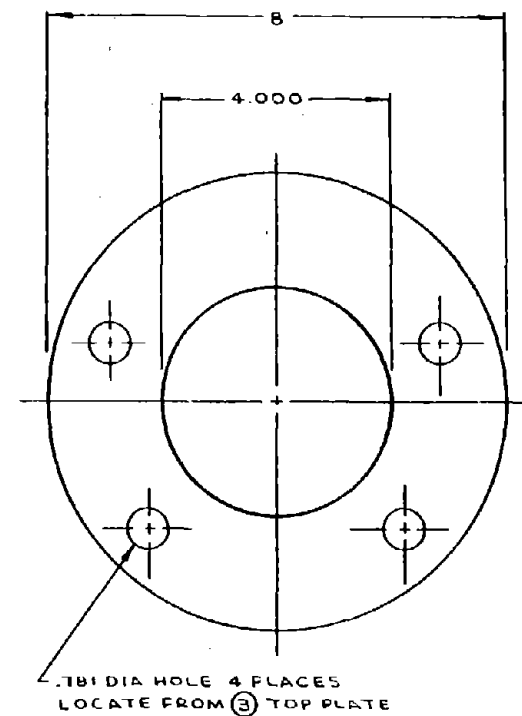
SCALE = $\frac{1}{2}$



③ TOP PLATE

- MAKE FROM $\frac{3}{4}$ IN. THICK 1010-1020 STEEL PLATE
- UNLESS OTHERWISE NOTED TOLERANCES ON DECIMAL DIMENSIONS $\pm .005$ IN., ON FRACTIONAL DIMENSIONS $\pm \frac{1}{32}$

SCALE = $\frac{1}{2}$



② BOTTOM PLATE

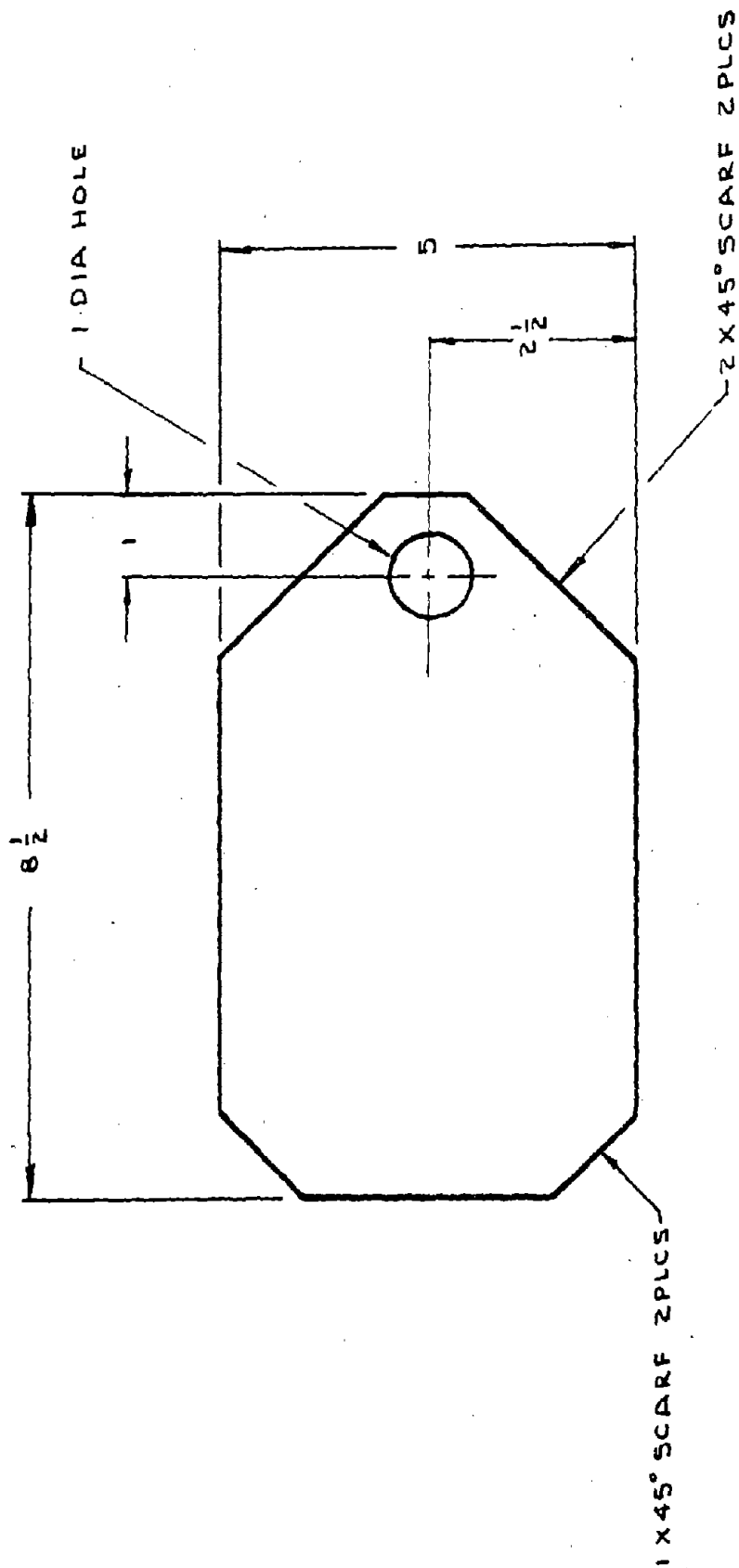
- MAKE FROM $\frac{3}{4}$ IN. THICK 1010-1020 STL PLATE
- UNLESS OTHERWISE NOTED TOLERANCES ON DECIMAL DIMENSIONS $\pm .005$ IN., ON FRACTIONAL DIMENSIONS $\pm \frac{1}{32}$

DROP FIXTURE J6309

12/11/74 E.P. BERGMANN

FIGURE C-13

SHT 3 OF 4



C-64

① SLIDE

- MAKE FROM $\frac{1}{2}$ IN. 1010-1020 PLATE (STL)
- GRIND FINISH BOTH FACES OF SLIDE
- TOLERANCES ON DIMENSIONS $\pm \frac{1}{32}$

DROP FIXTURE J6309

12/11/74 E.P. BERGMANN

FIGURE C-14

SHT 4 OF 4

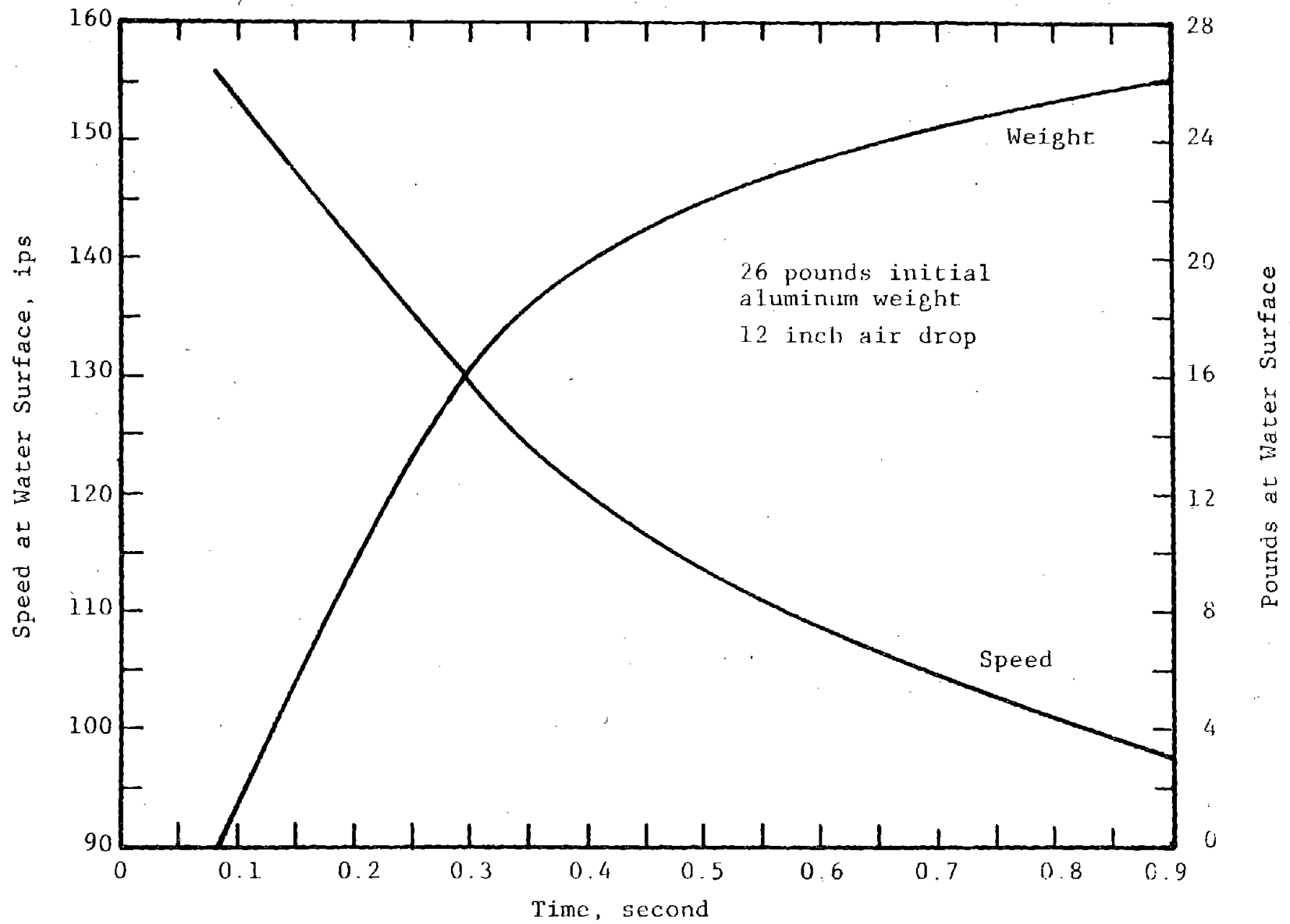


Figure C-15 Aluminum Weight and Speed at Water Surface

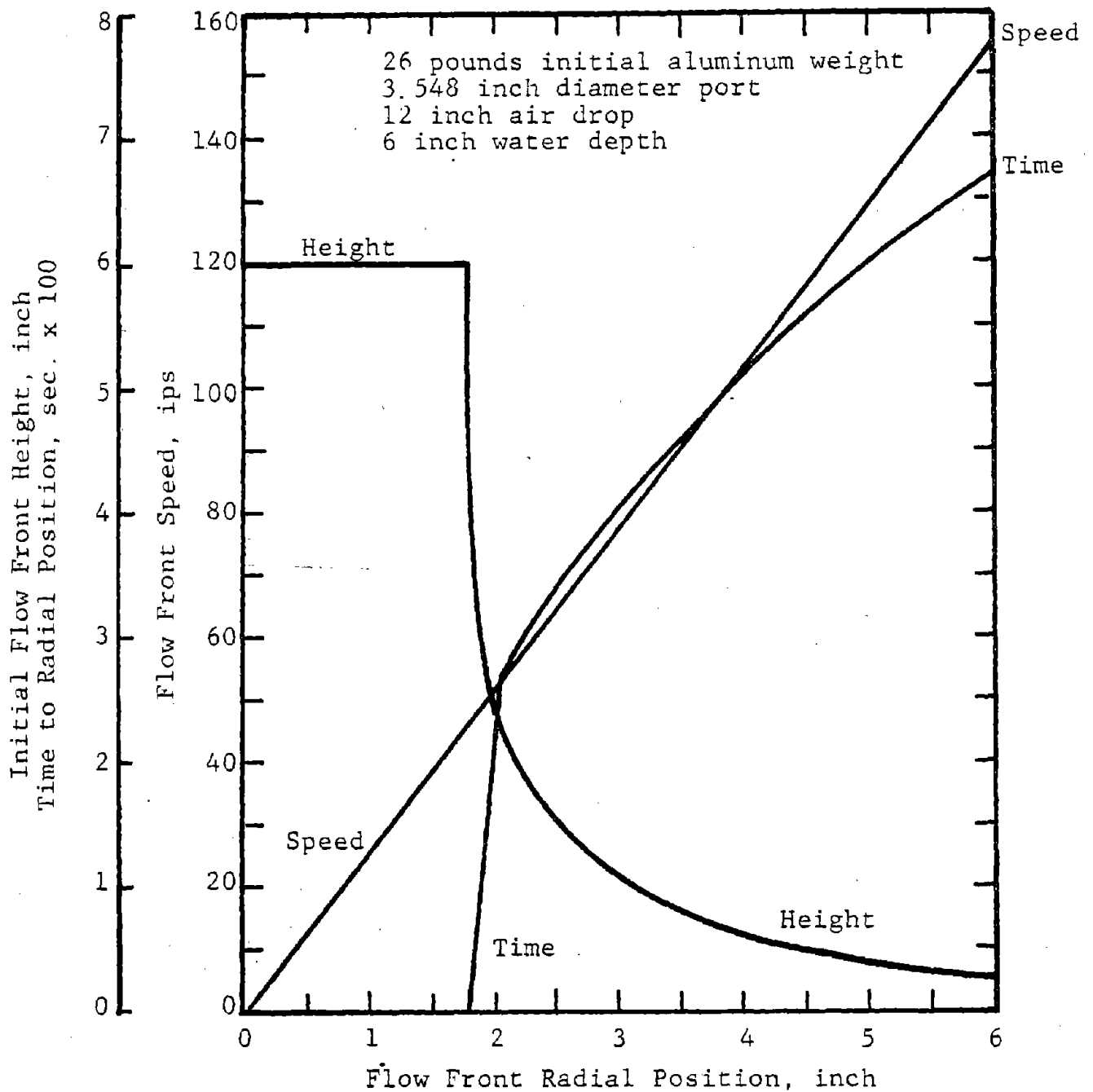


Figure C-16 Aluminum Flow Characteristics After Initial Impact on Quench Tank Bottom

C-67

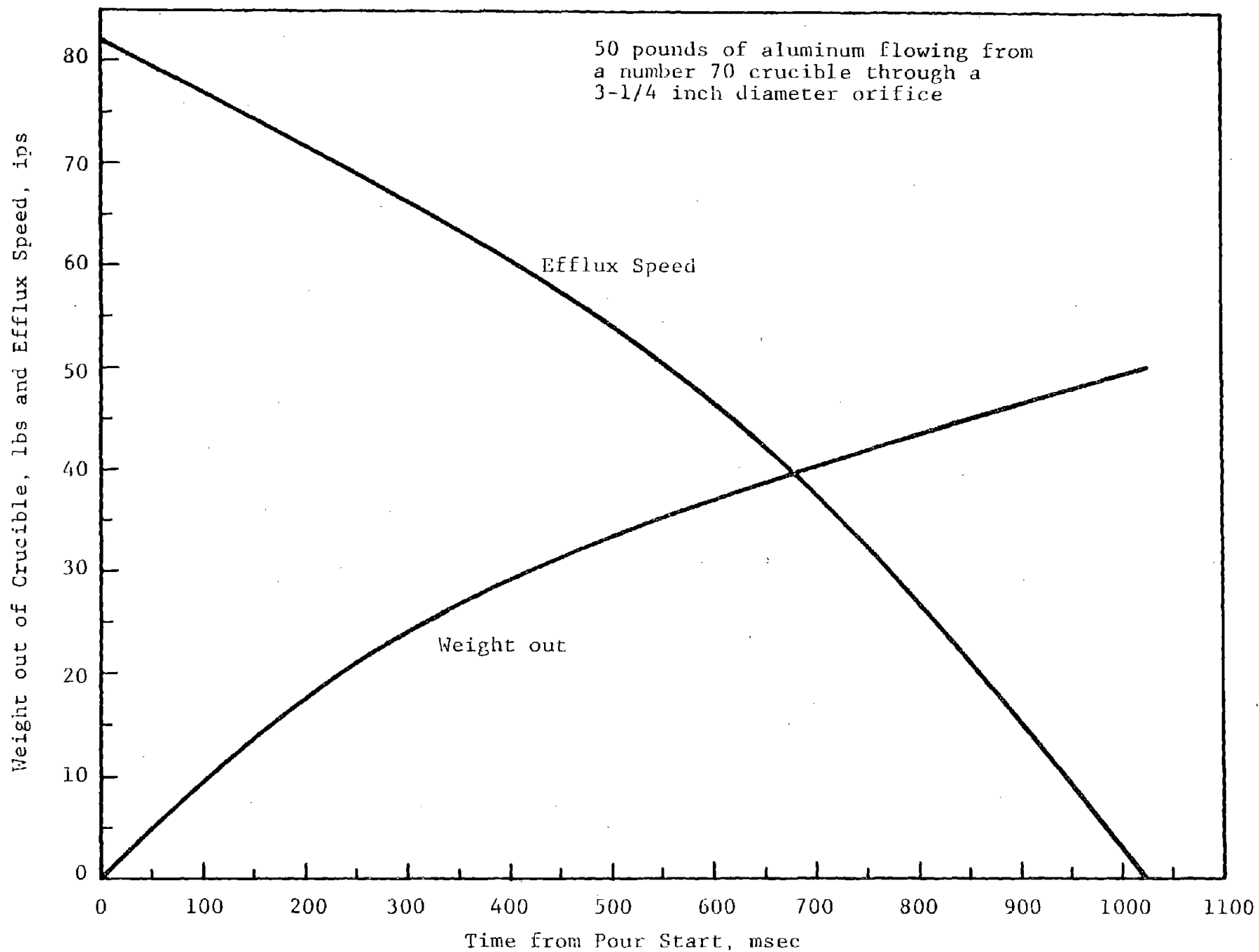


Figure C-17 Efflux Speed and Weight Flow at Drop Crucible Versus Time (Calculated)

50 lbs of aluminum flowing from a Number 70 crucible
through a 3-1/4 inch diameter orifice at quench tank
water surface after falling 12-1/2 inches

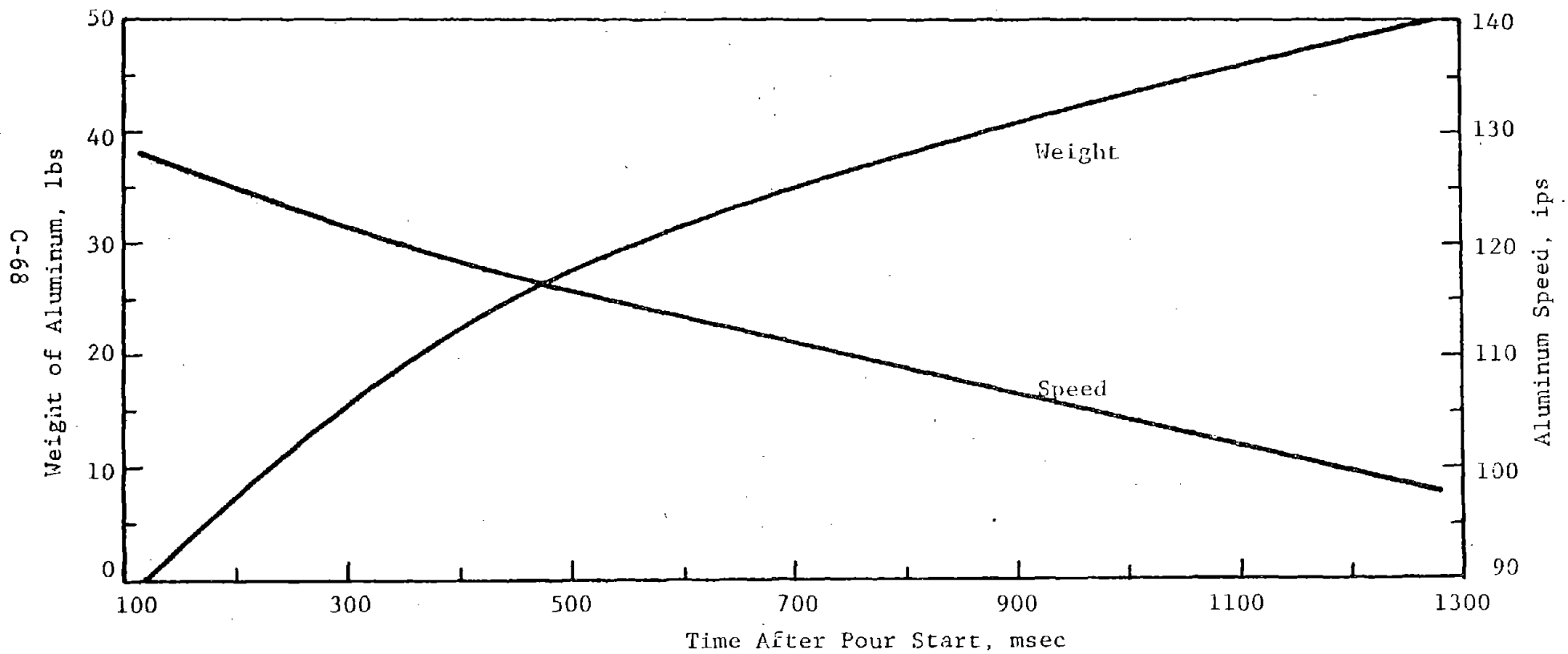


Figure C-18 Weight and Speed Versus Time at Quench Tank Water Surface (Calculated)

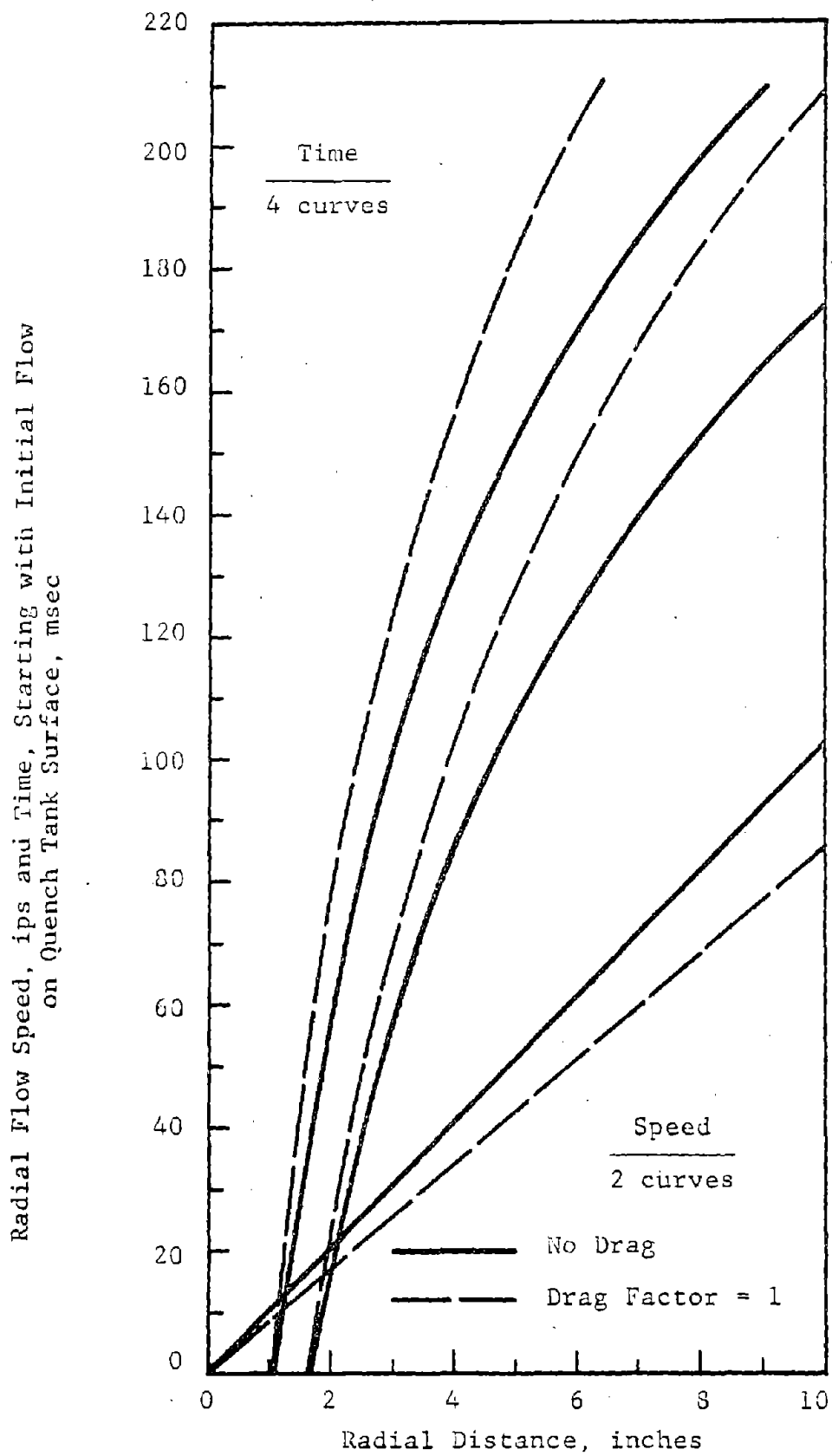
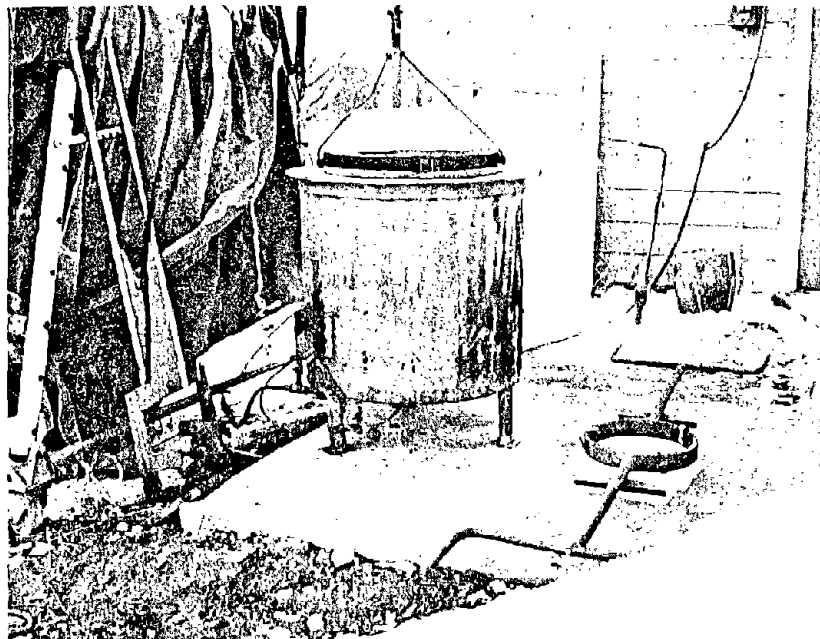
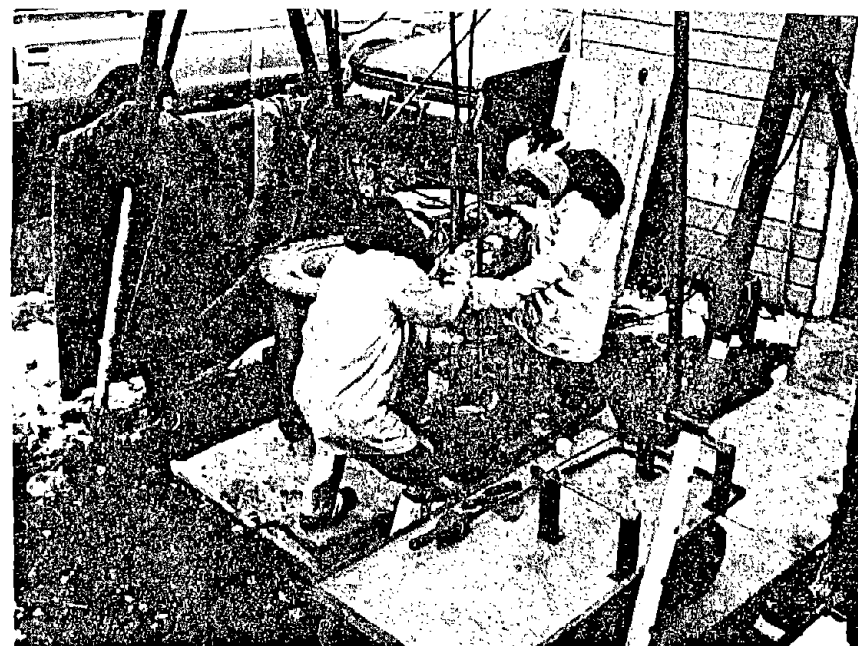


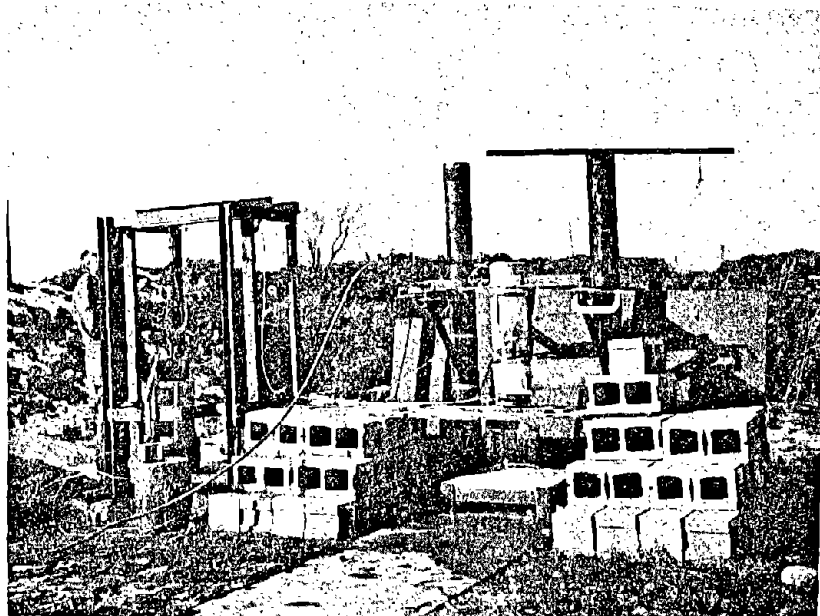
Figure C-19 Calculated Flow Speed and Time Versus Radial Distance for Two Stream Radii (Frictionless Axisymmetrical Navier-Stokes Flow)



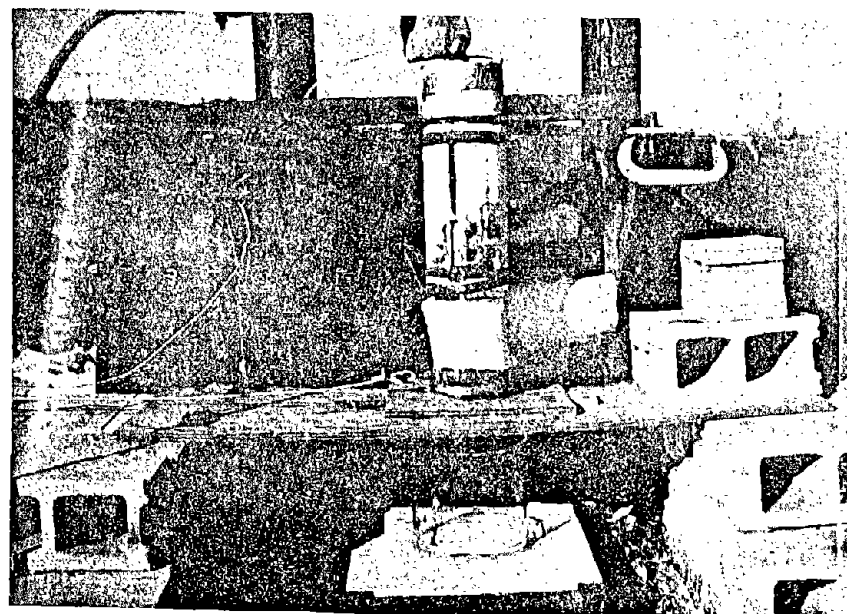
a - Melt Furnace



b - Melt Crucible Removal From Furnace

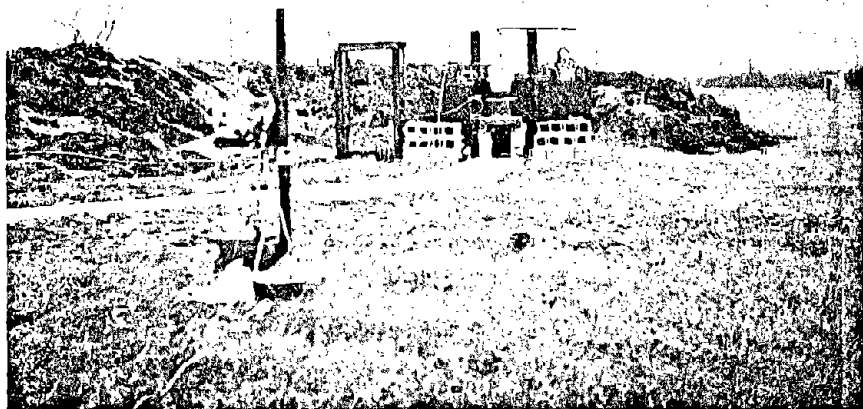


c - New Drop Crucible Installation

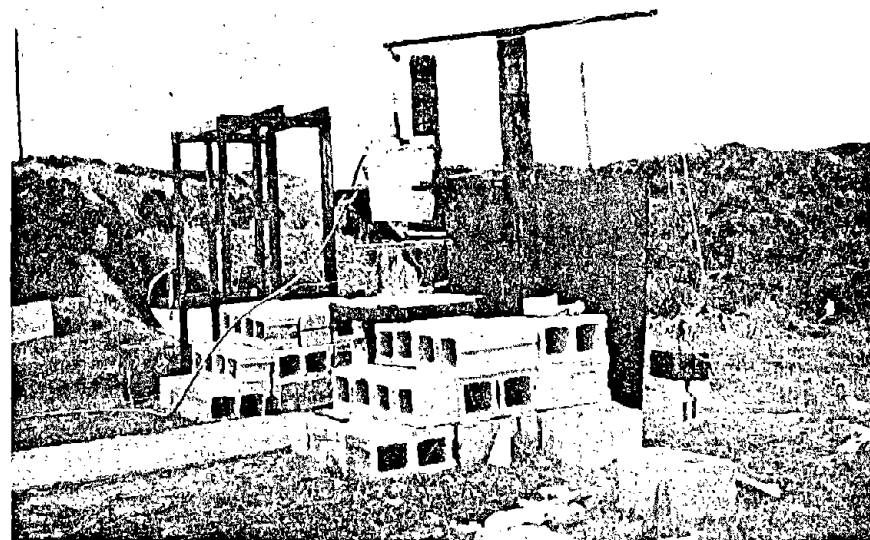


d - New Drop Crucible

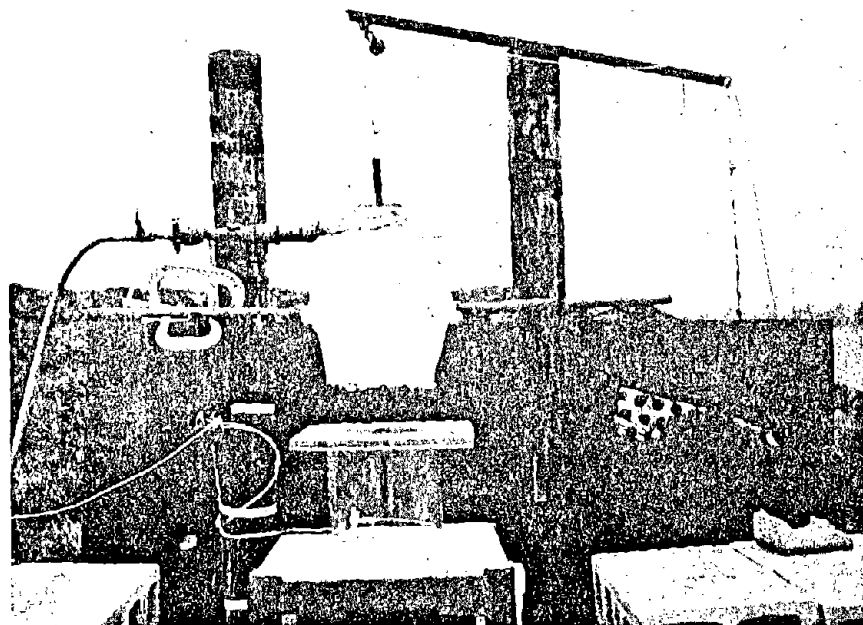
Figure C-20 Melt Furnace and New Drop Crucible



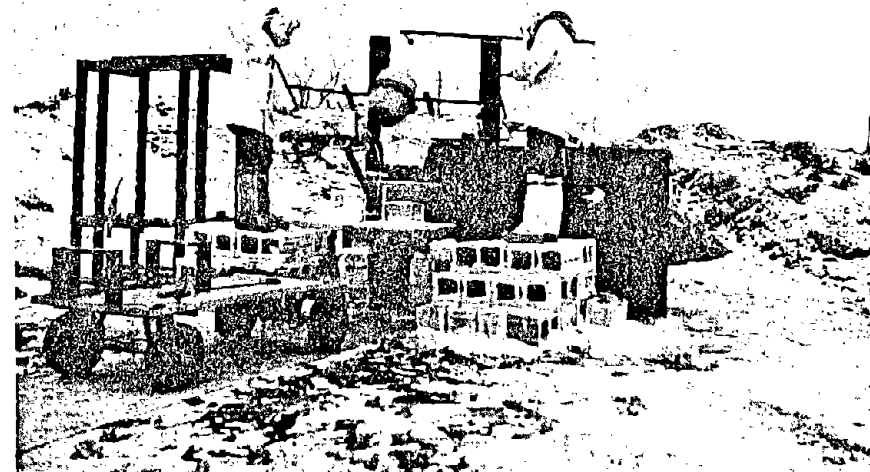
a - Overall View of Simulation Setup



b - Arrangement for Opening Drop Crucible



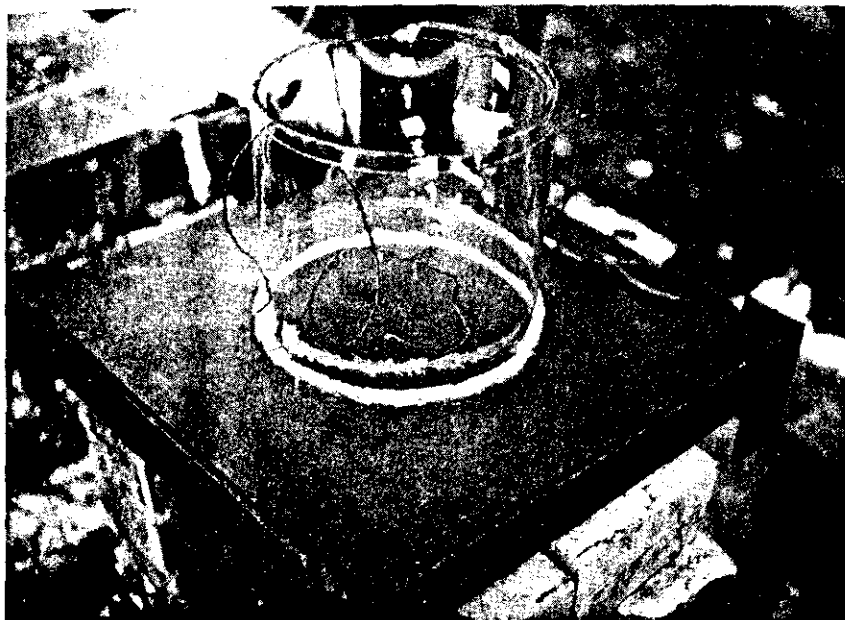
c - Second Simulation: Crucible Insulation and Preheating with Bull Torch



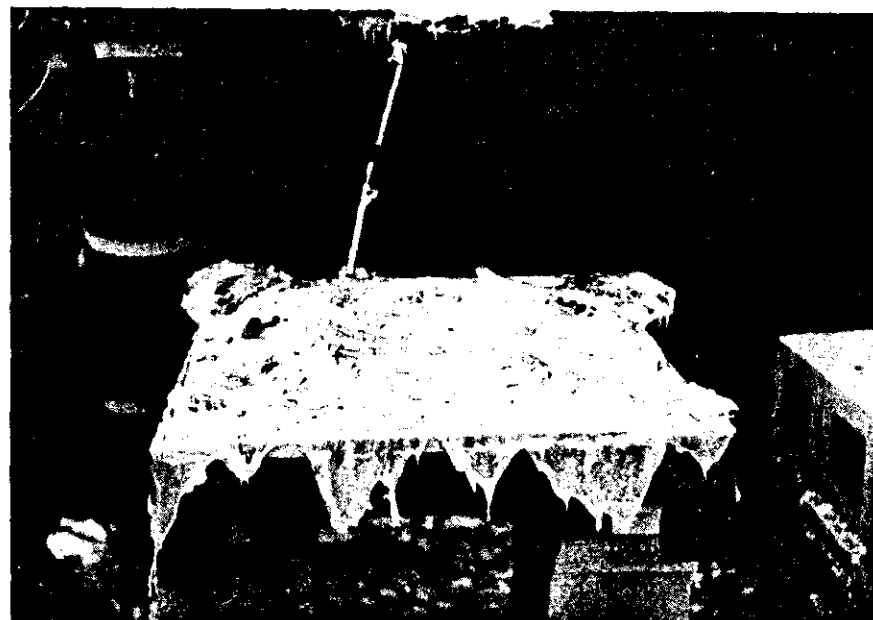
d - Second Simulation: Transfer of Molten Aluminum to Drop Crucible

Figure C-21 Views of Simulation Site and Aluminum Transfer

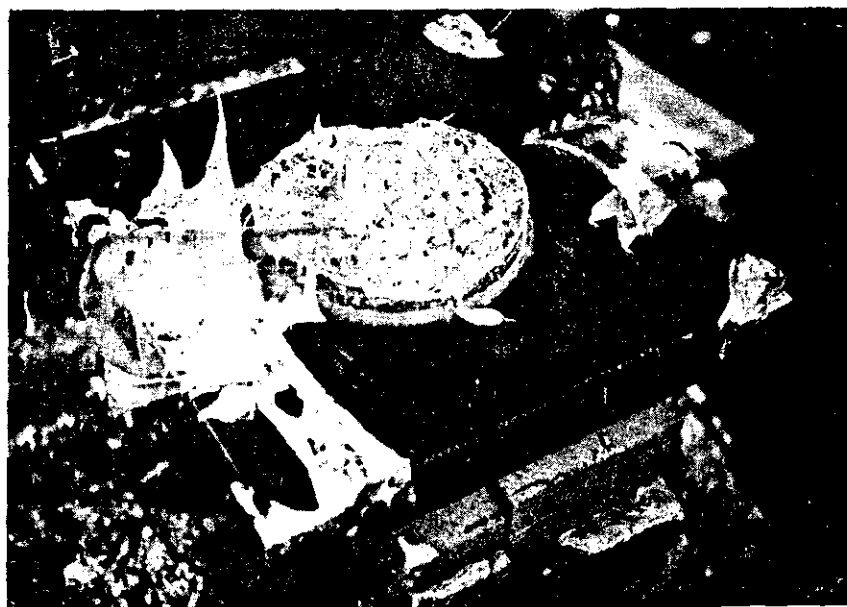




a - Rough Steel Bottom Quench Tank
Before Simulation No. 6



b - Rough Concrete Quench Tank Bottom After
Simulation No. 2 (1/64 inch Deep Water)



c - Taret Coated Concrete Quench Tank Bottom
After Simulation No. 5 (6 inch Deep Water)



d - Rough Concrete Quench Tank Bottom After
Simulation No. 8 (6 inch Deep Water)

C-73

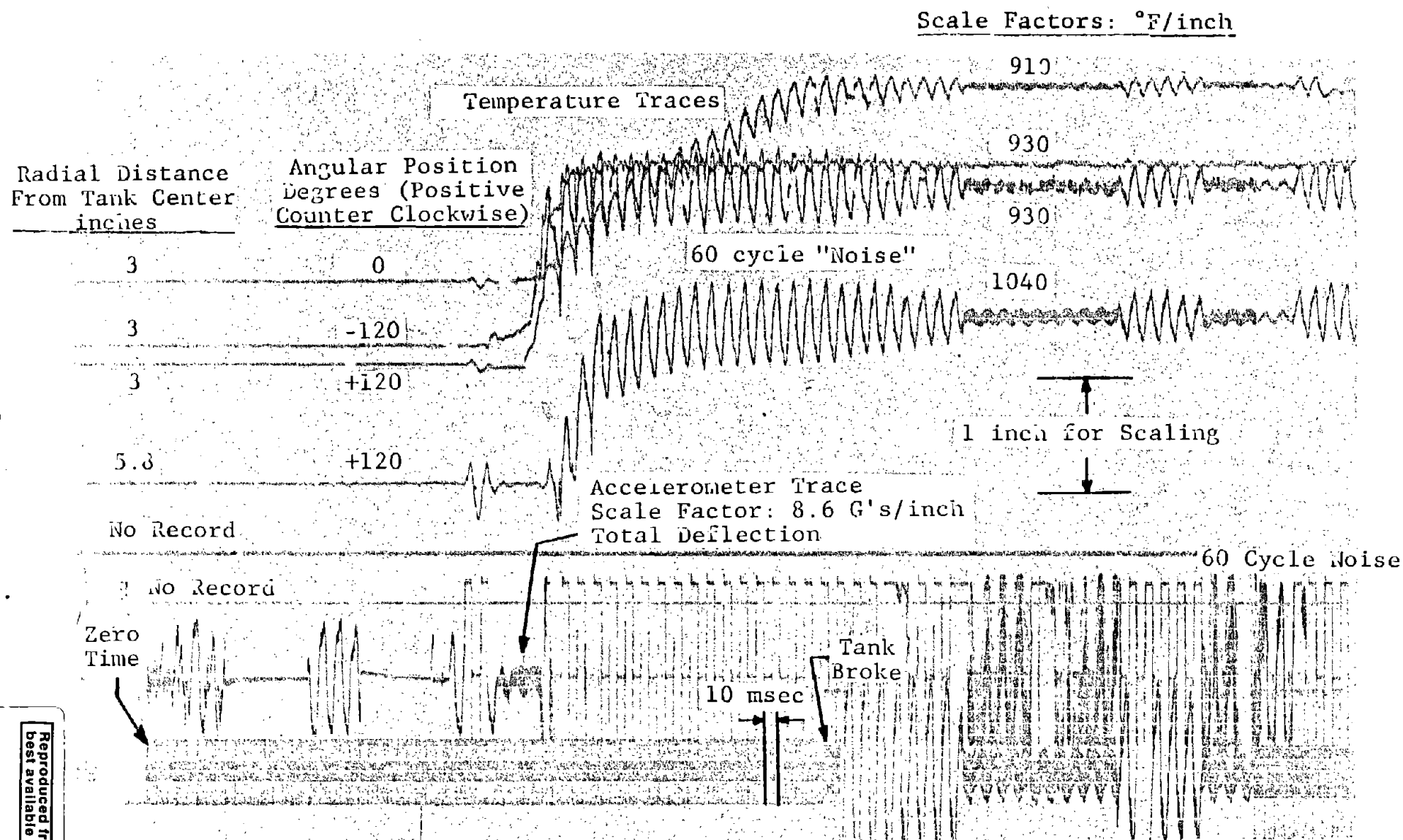


Figure C-23 Partial Record for Experiment 2, Temperature, Quench Tank Bottom Acceleration and Time

Scale Factors: °F/inch

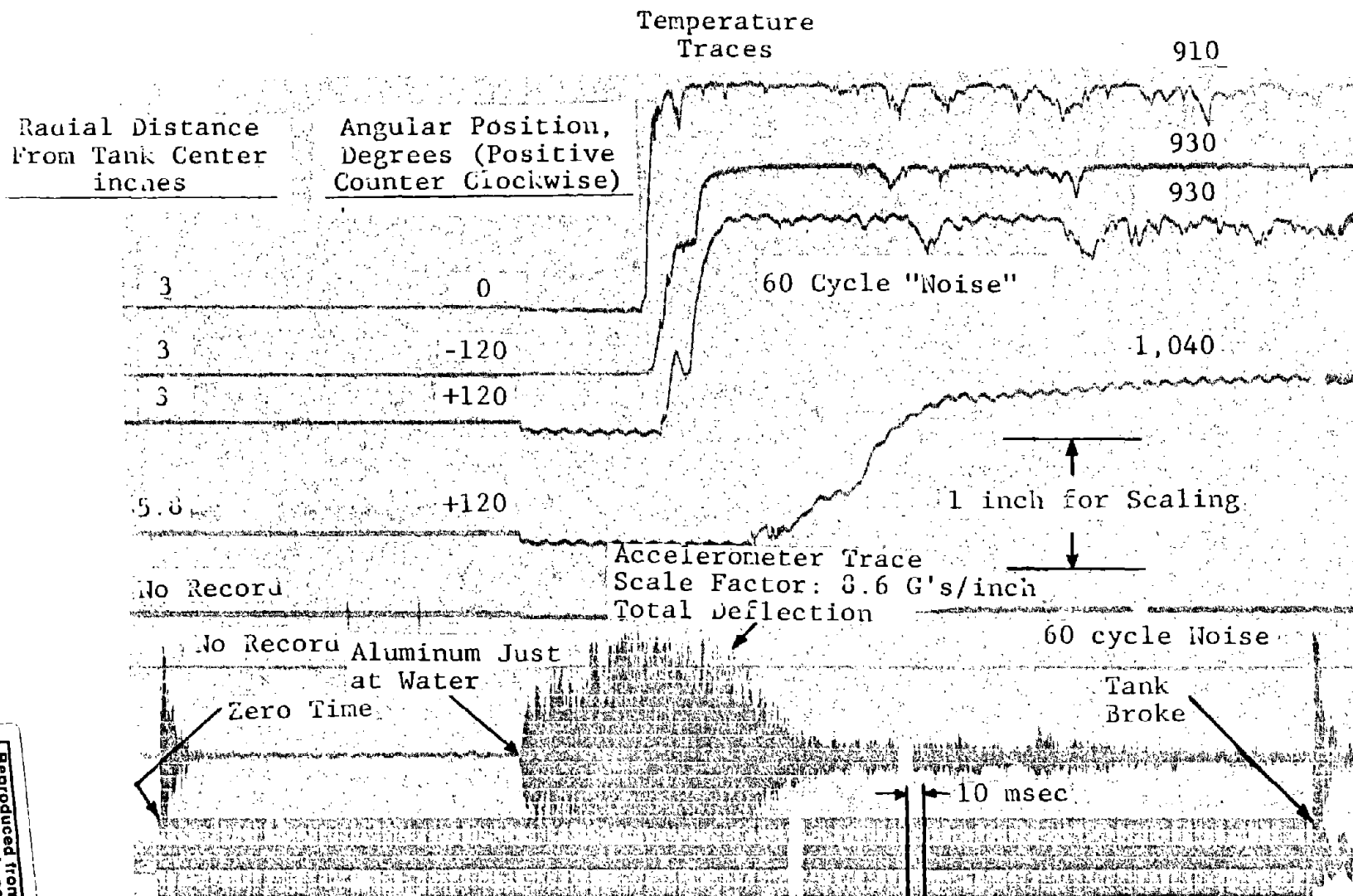


Figure C-24 Partial Record for Experiment 3, Temperature, Quench Tank Bottom Acceleration and Time

C-74

Reproduced from
best available copy.

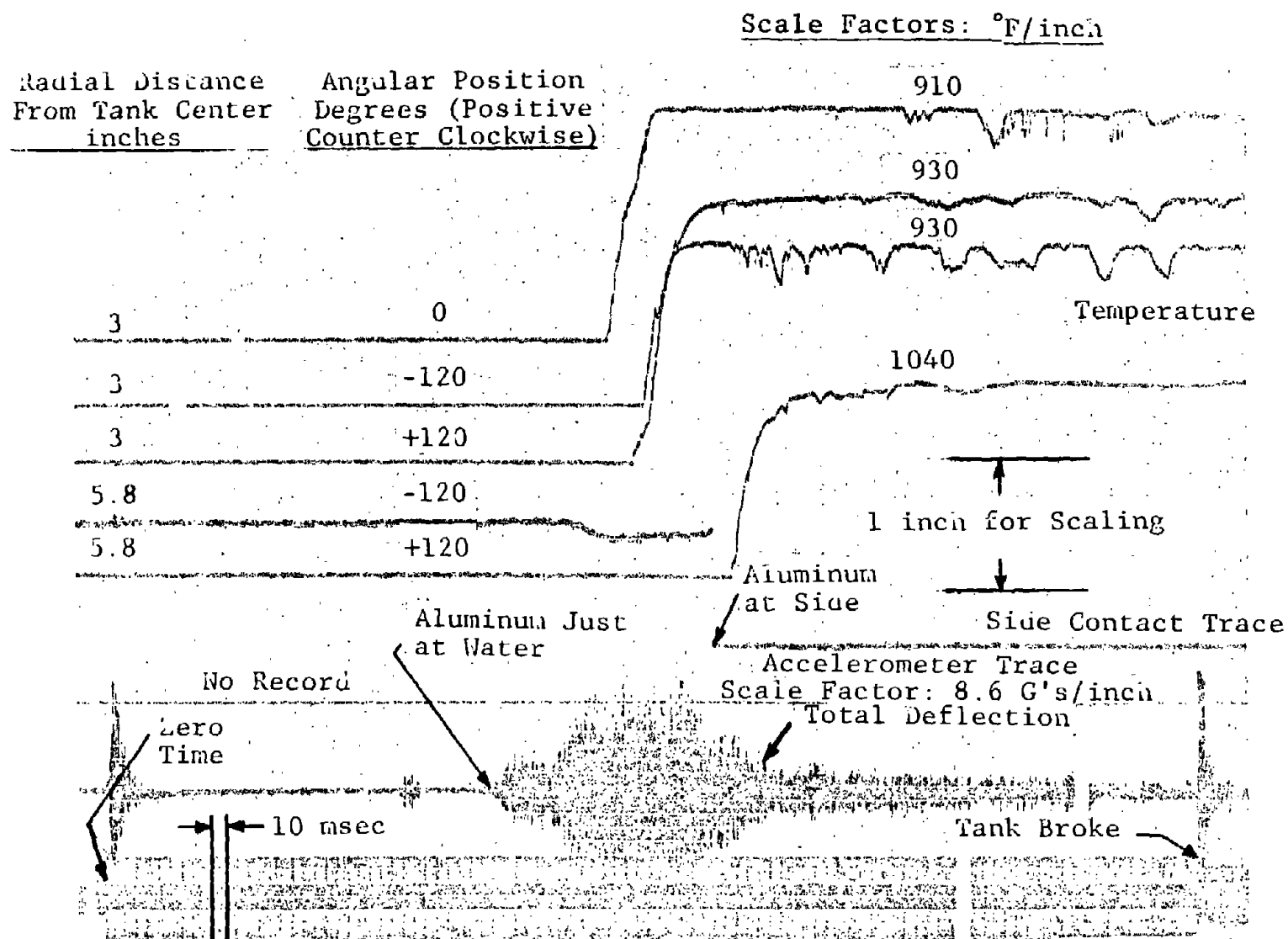


Figure C-25 Partial Record for Experiment 4, Temperature, Side Contact, Quench Tank Bottom Acceleration and Time

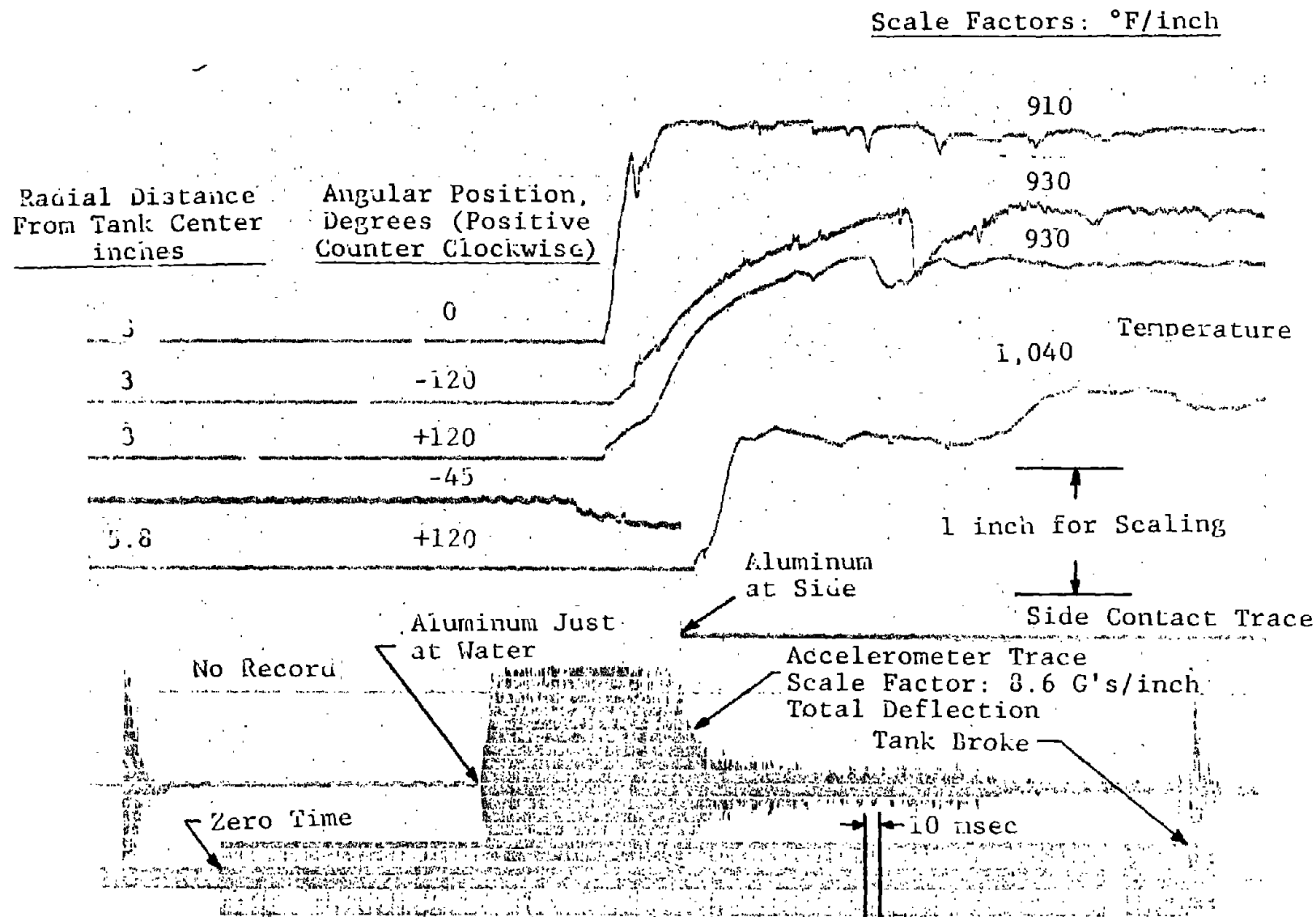


Figure C-26 Partial Record for Experiment 5, Temperature, Side Contact, Quench Tank Bottom Acceleration and Time

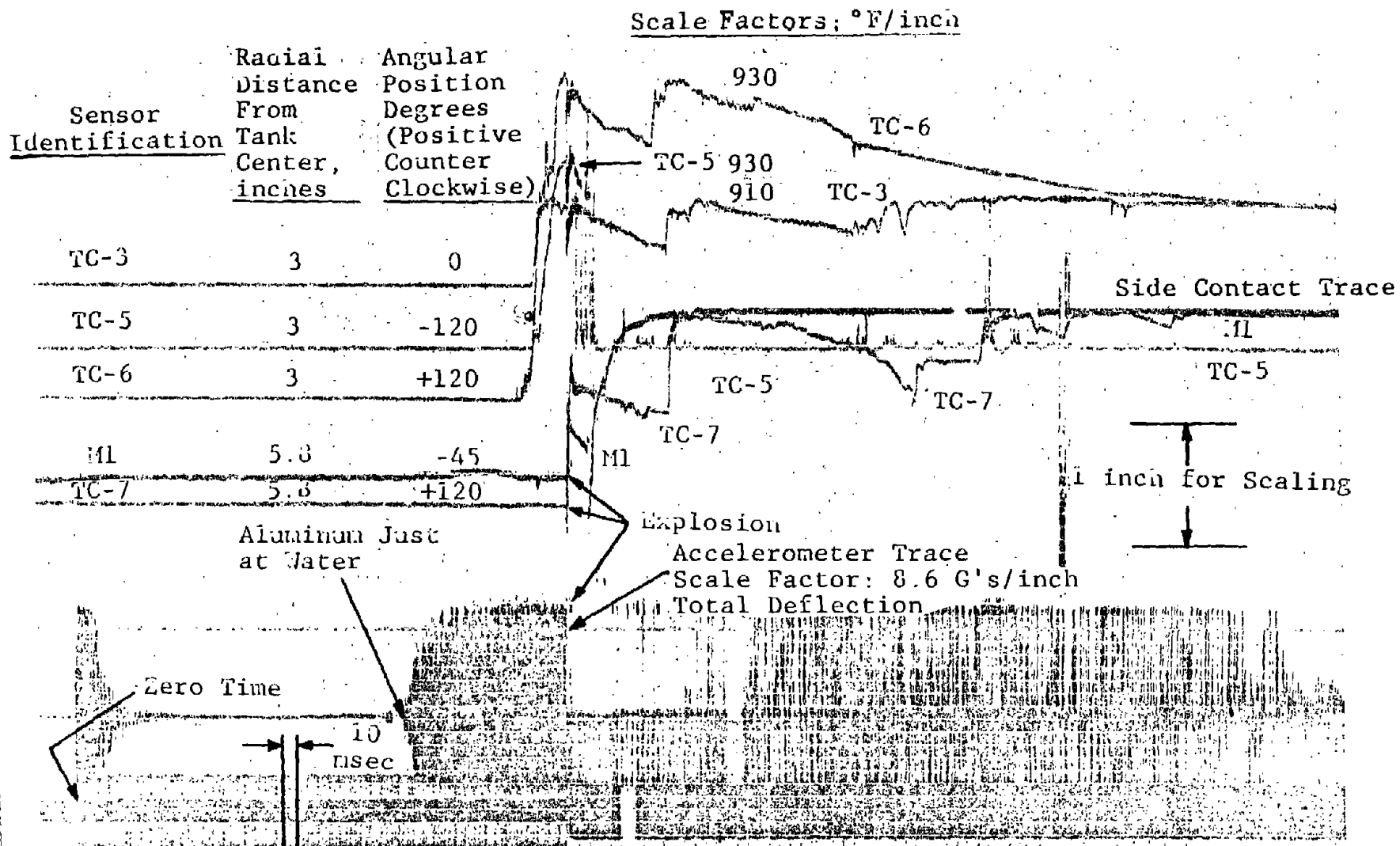


Figure C-27 Partial Record for Experiment 6, Temperature, Side Contact, Quench Tank Bottom Acceleration and Time

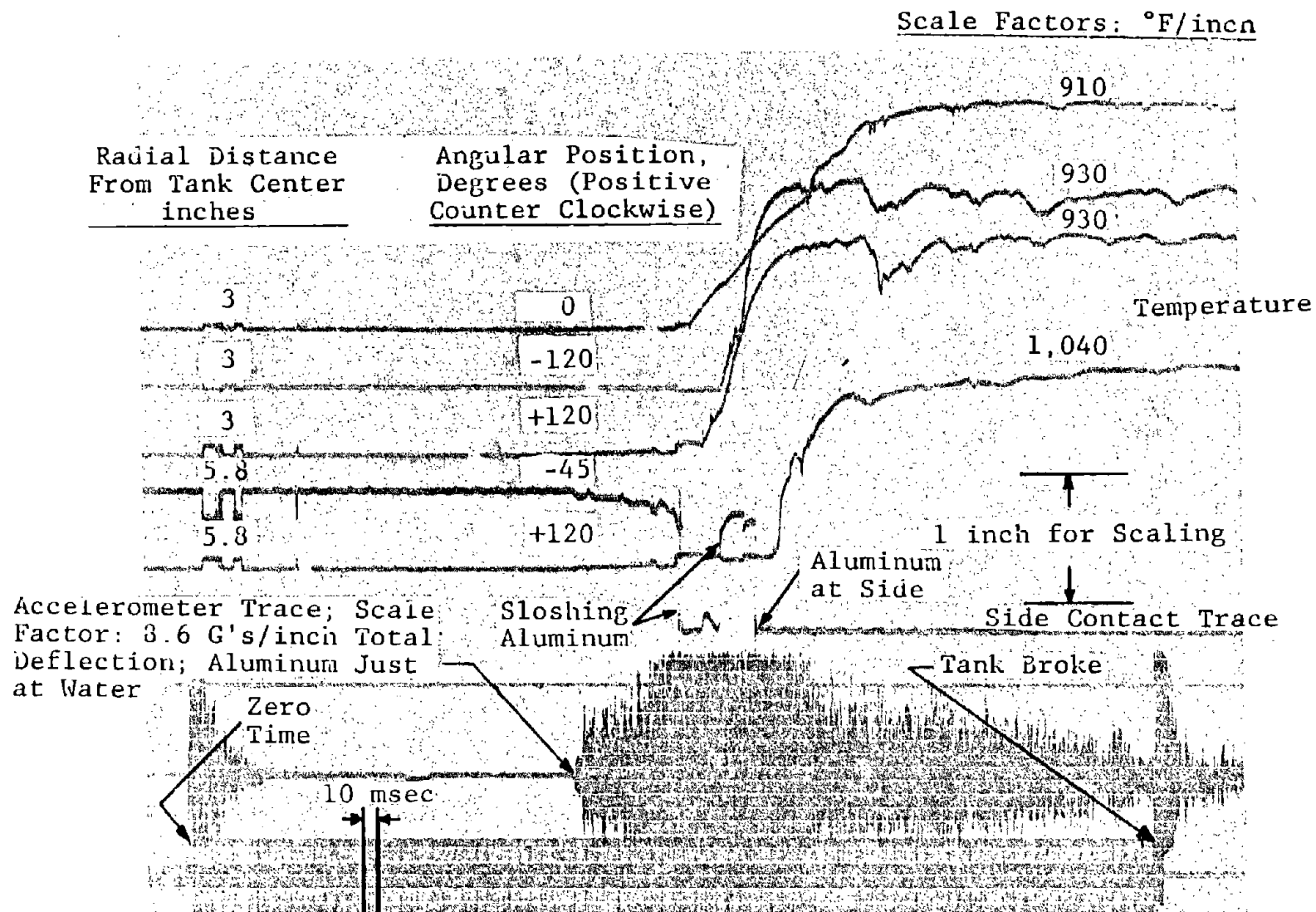
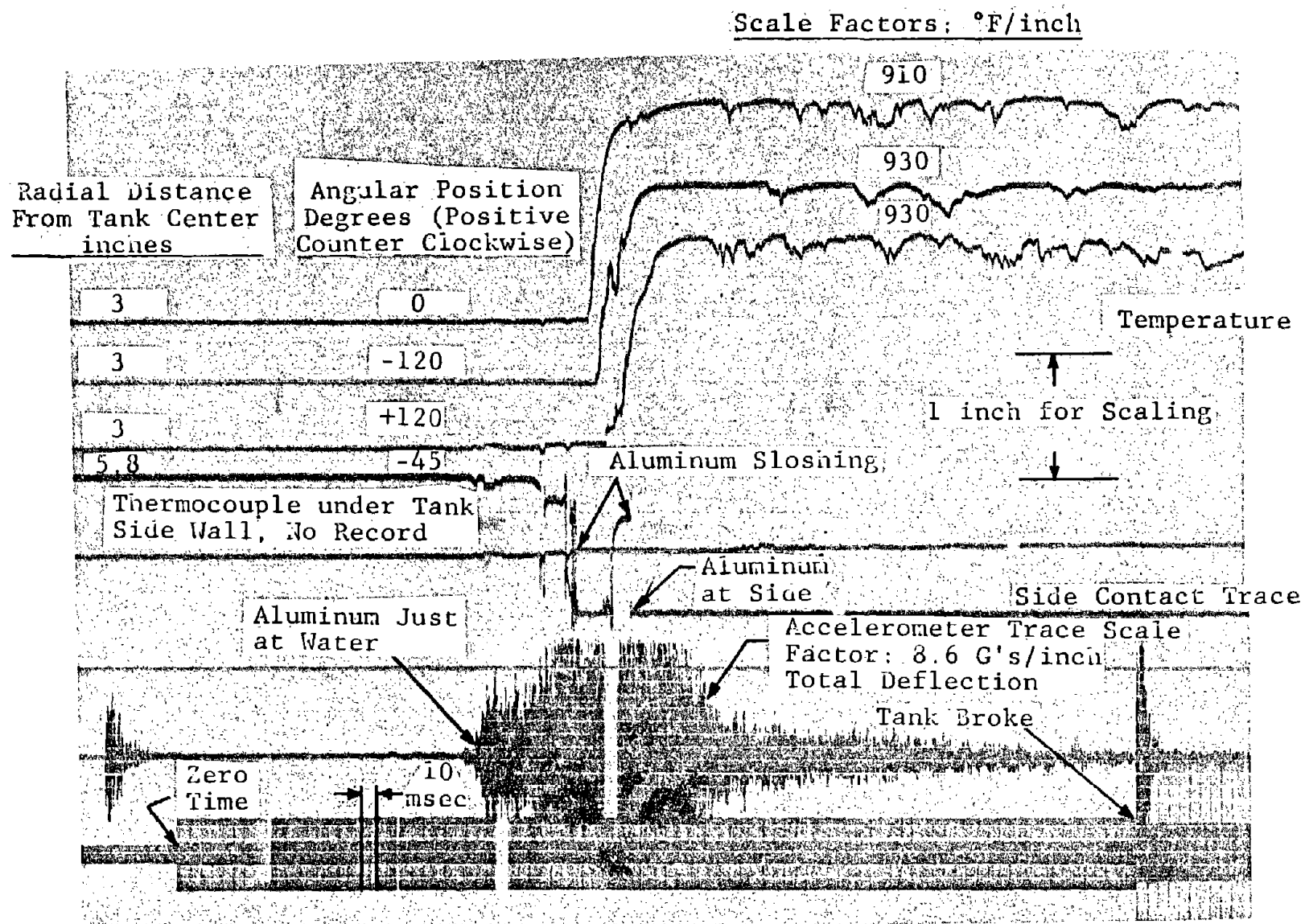


Figure C-28 Partial Record for Experiment 7, Temperature, Side Contact, Quench Tank Bottom Acceleration and Time



Reproduced from
best available copy.

Figure C-29 Partial Record for Experiment 8, Temperature, Side Contact, Quench Tank Bottom Acceleration and Time

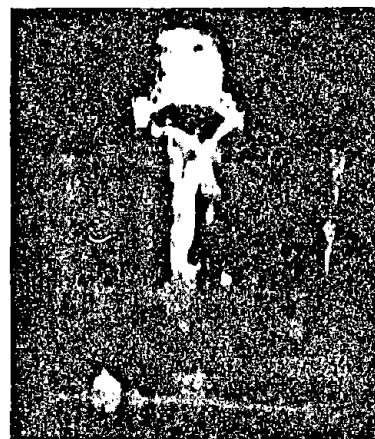
Reproduced from
best available copy.



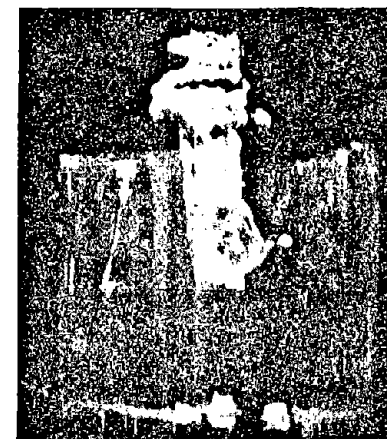
a - Experiment 2



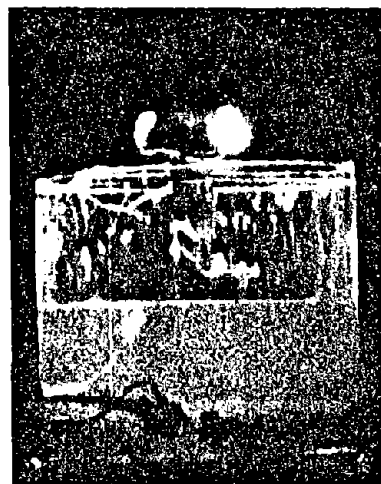
b - Experiment 3



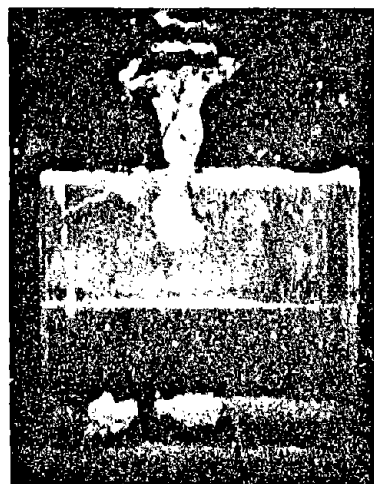
c - Experiment 4



d - Experiment 5



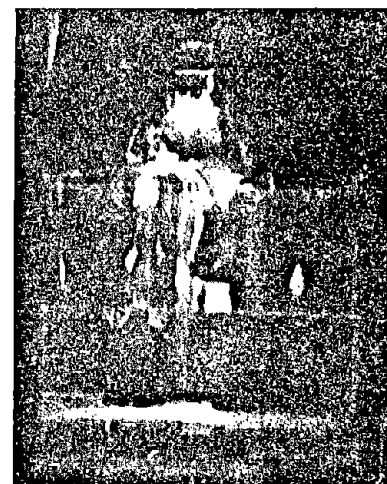
e - Experiment 6



f - Experiment 7

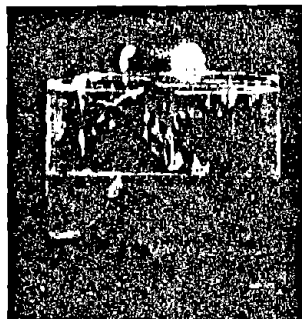


g - Experiment 8

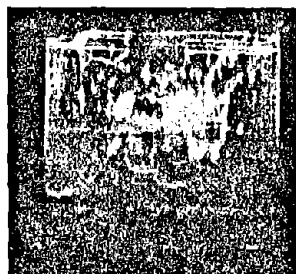


h - Experiment 9

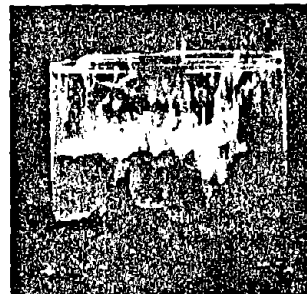
Figure C-30 Fastex Film Frame Enlargements Showing Initial Portions of Aluminum Streams



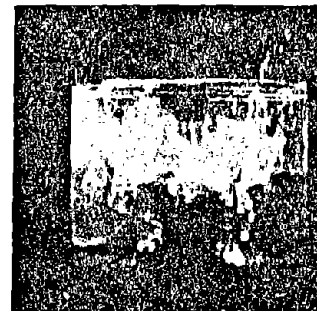
a - Just at Water



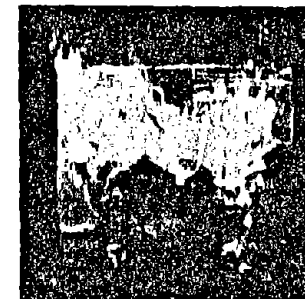
b - About 25 Percent to Bottom, Large Steam Film



c - About 30 Percent to Bottom, Larger Steam Film



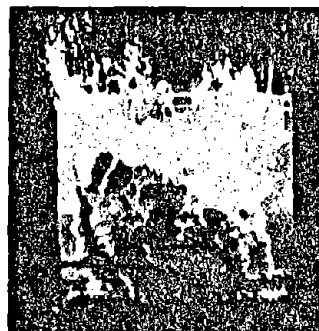
d - About 70 Percent to Bottom, Smaller Steam Film



e - At Bottom (about 1/8 inch above)



f - At Right Side



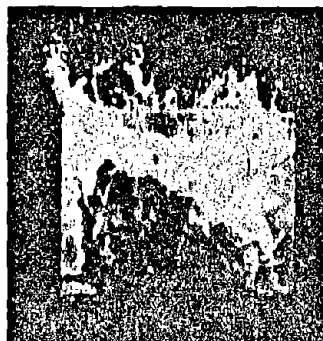
g - Flow Starting Up Wall and near Left Side



h - Flow Higher up Wall, Nearer Left Side and Flow up Back Wall Reflection Visible at Left



i - Flow Higher up Wall, Front and Back Radial Flow Almost Meet on Left



j - Front and Back Flow Just Meet on Left



k - Initiation Has Taken Place, Tank Venting Starting on Left and Extending on Right



l - Propagation of Initiation to Tank Top and Further Venting on Left and Right

Figure C-31 Fastex Film Frame Sequence from Experiment No. 6, Mild Steam Explosion (Rough Steel Quench Tank Bottom Surface)



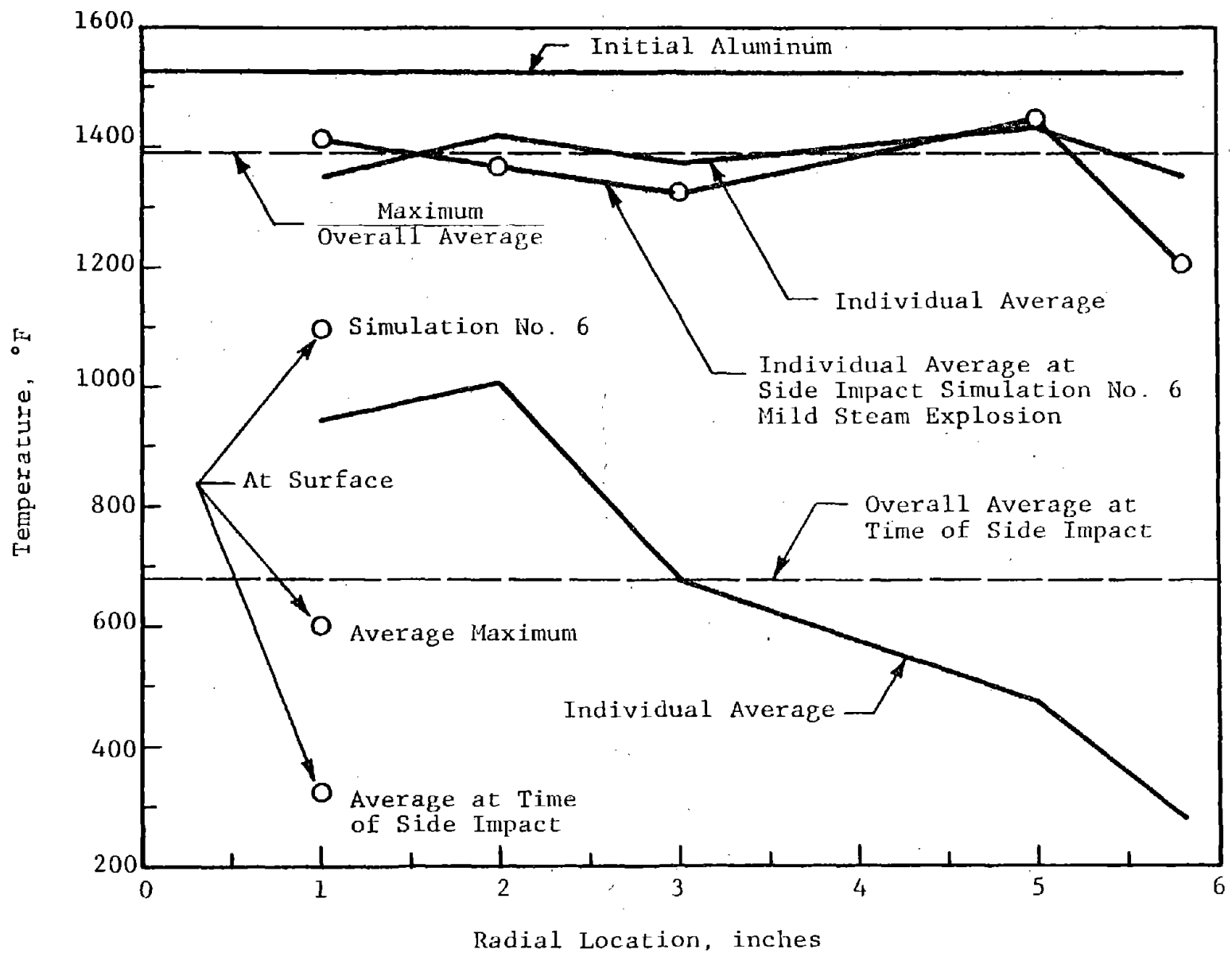
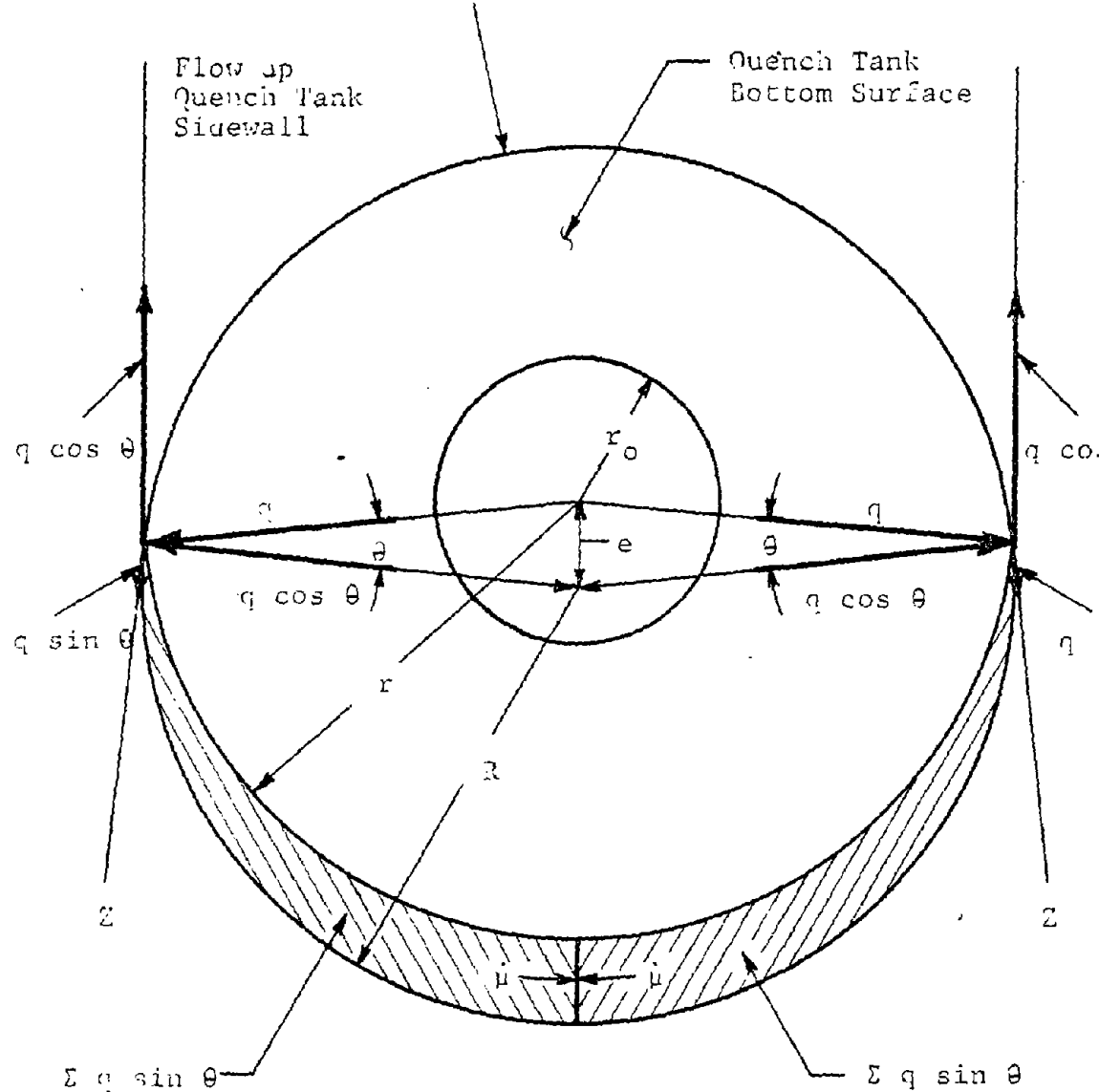


Figure C-32 Temperature Profiles, 1/8 inch Above Surface



- R = Quench tank radius
- r = Aluminum flow radius on tank bottom
- e = Eccentricity between aluminum stream impact center and tank center
- r_o = Aluminum stream initial radius
- q = Portion of radial flow, cubic inches per second
- $\sum q \sin \theta$ = Portion of radial flow which accumulates in circumferential flow
- \dot{u} = Aluminum circumferential flow speed at the time $r \leq R+e$ producing an impact speed of $2 \dot{u}$ which gives rise to an impact shock

Figure C-33 Circumferential Flow Producing an Impact Shock in a Round Quench Tank

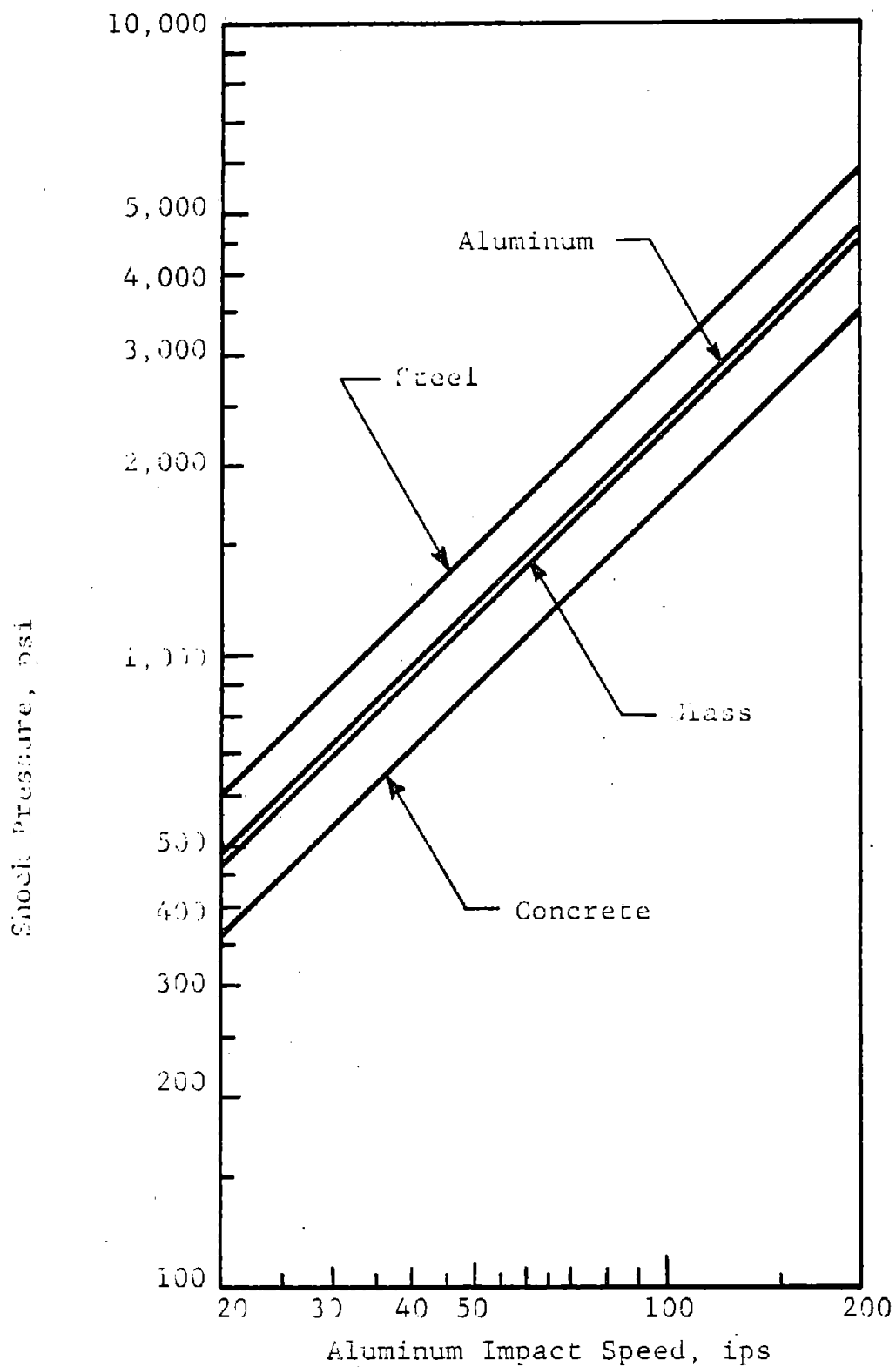


Figure C-34 Shock Pressure Versus Molten Aluminum Impact Speed (Calculated)

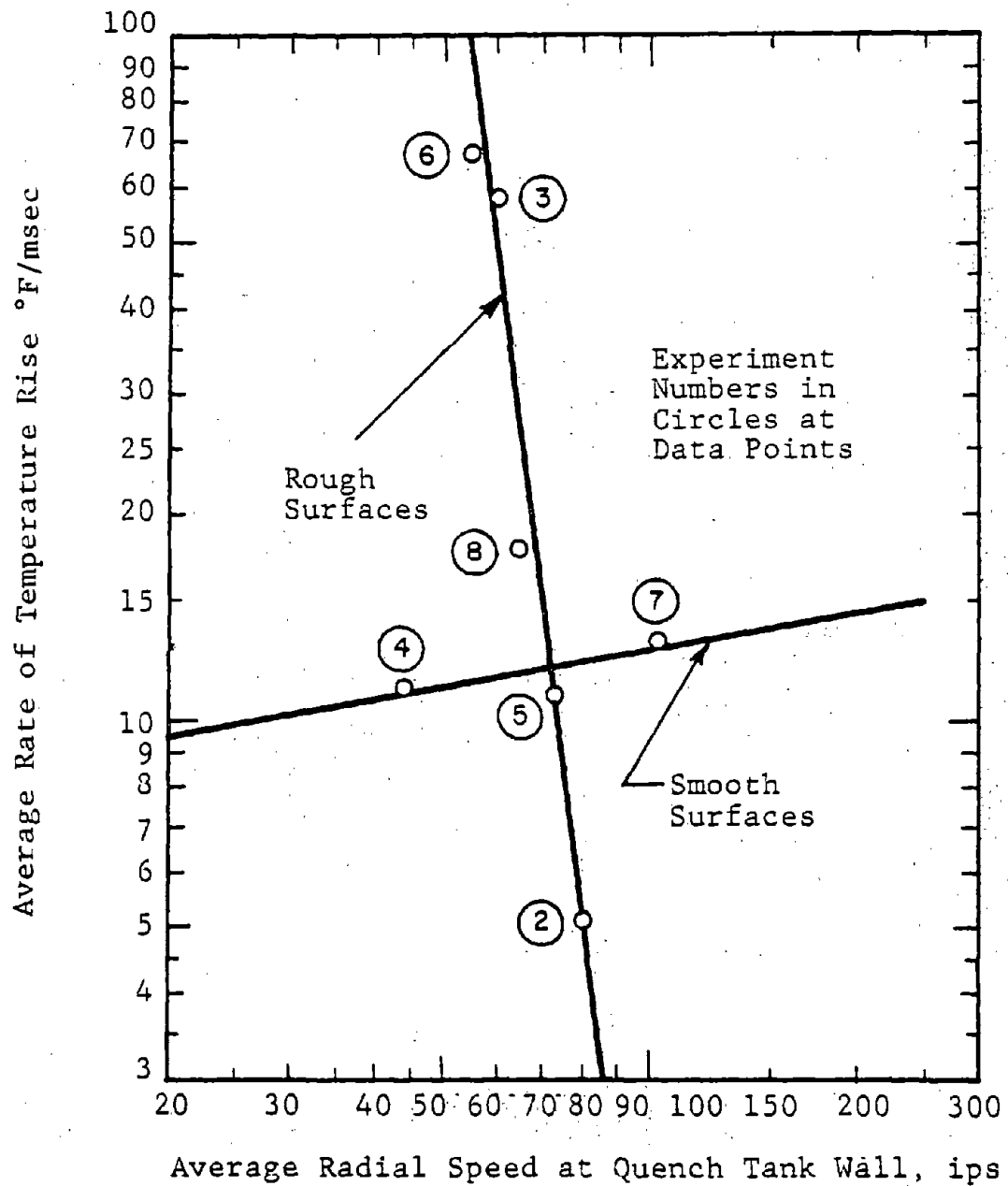


Figure C-35 Average Rate of Temperature Rise
Versus Average Aluminum Radial Flow Speed

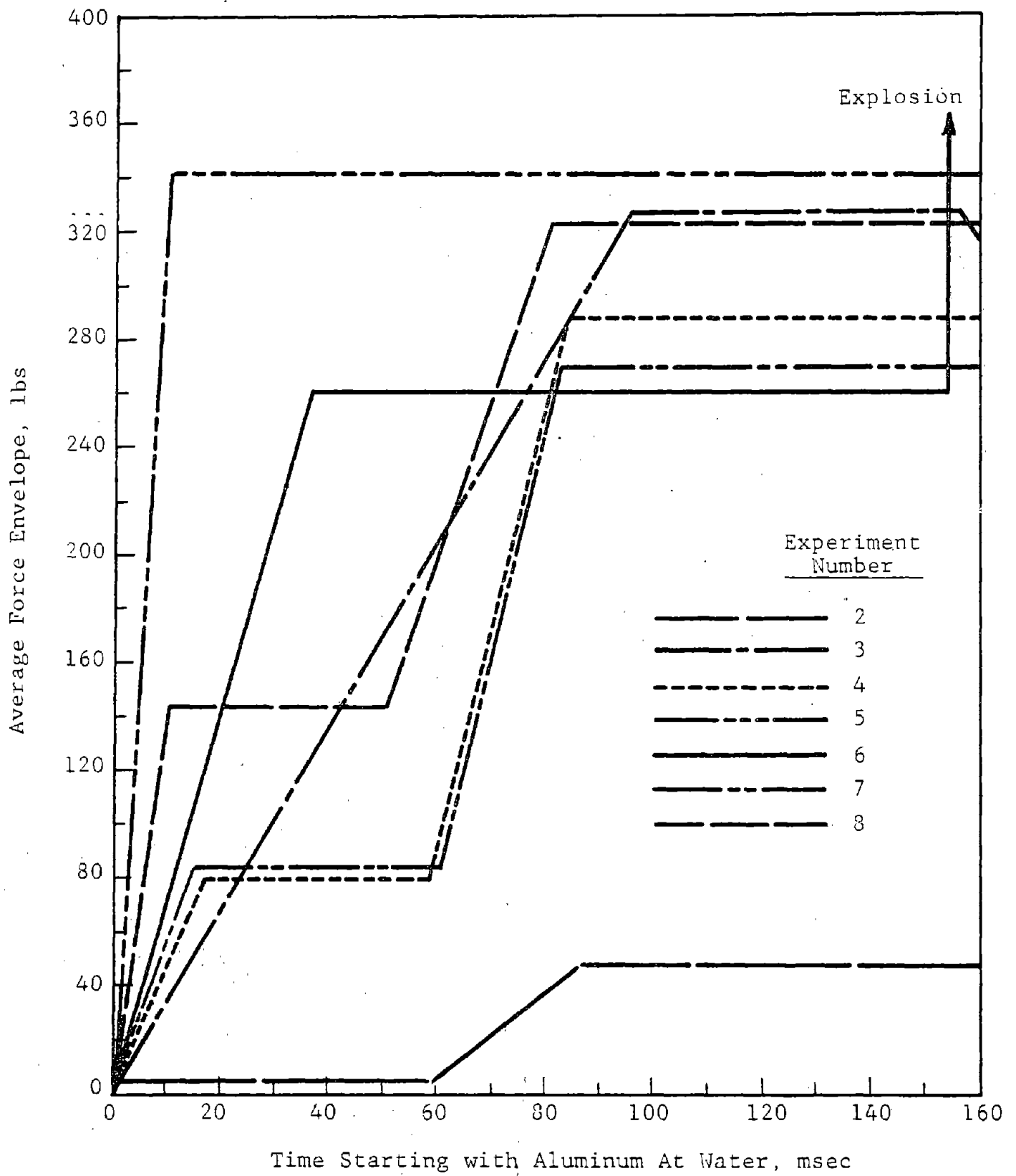


Figure C-36 Boiling Force Envelopes Versus Time

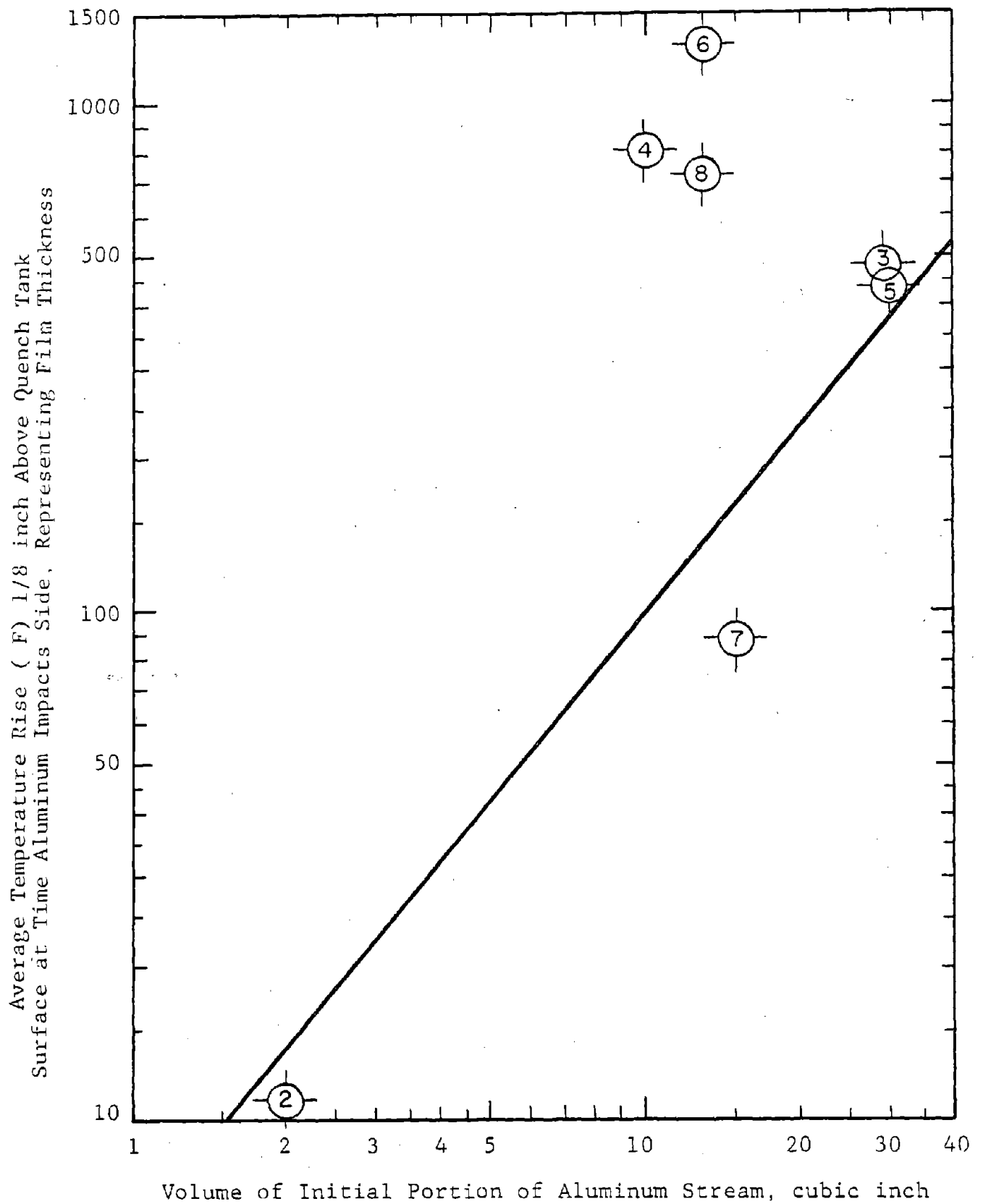


Figure C-37 Temperature Rise Representing Film Thickness Versus Initial Aluminum Volume Entering Quench Water

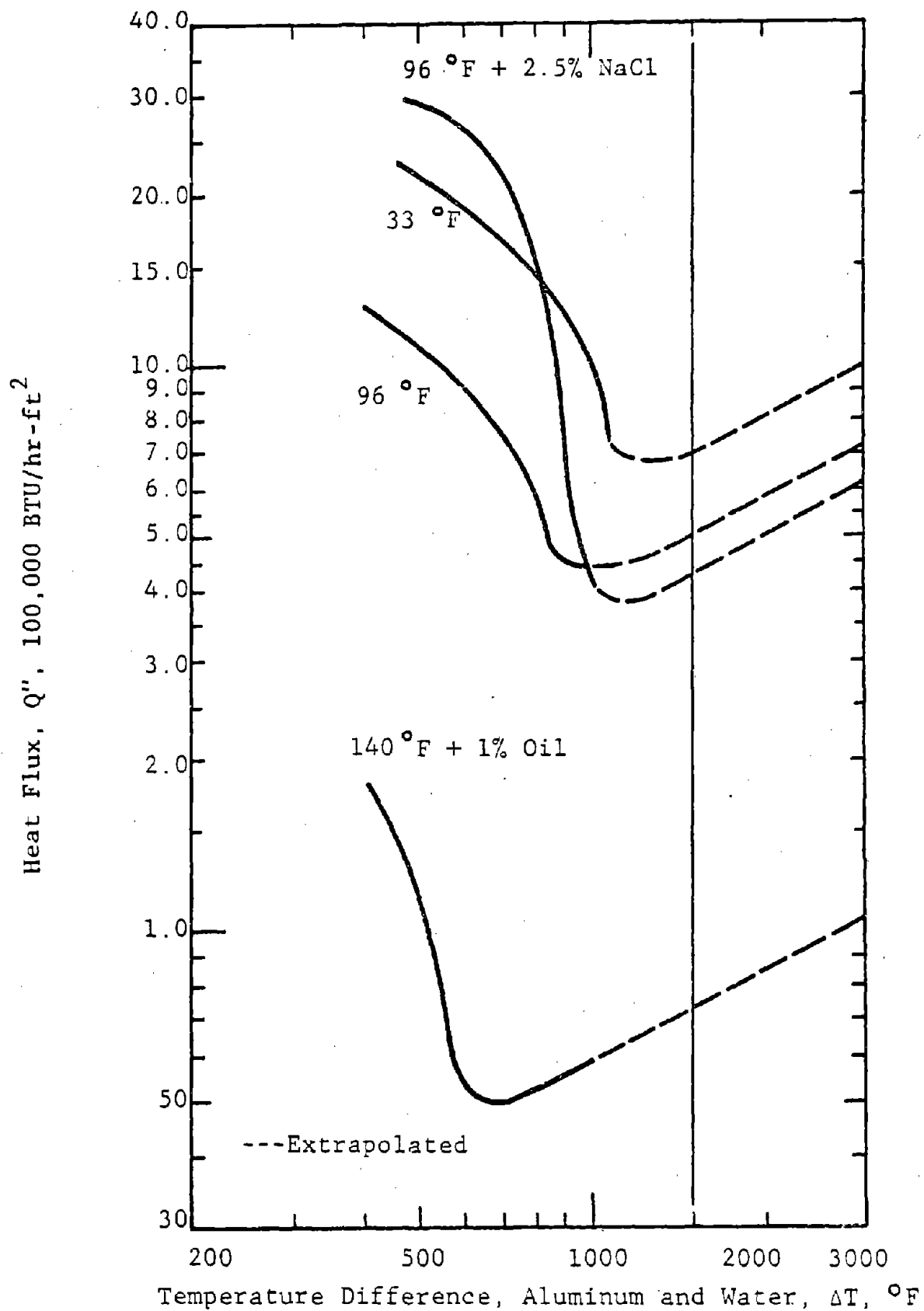


Figure C-38 Quenching Curve (Norm Cochran's Data, Aloca) Replotted

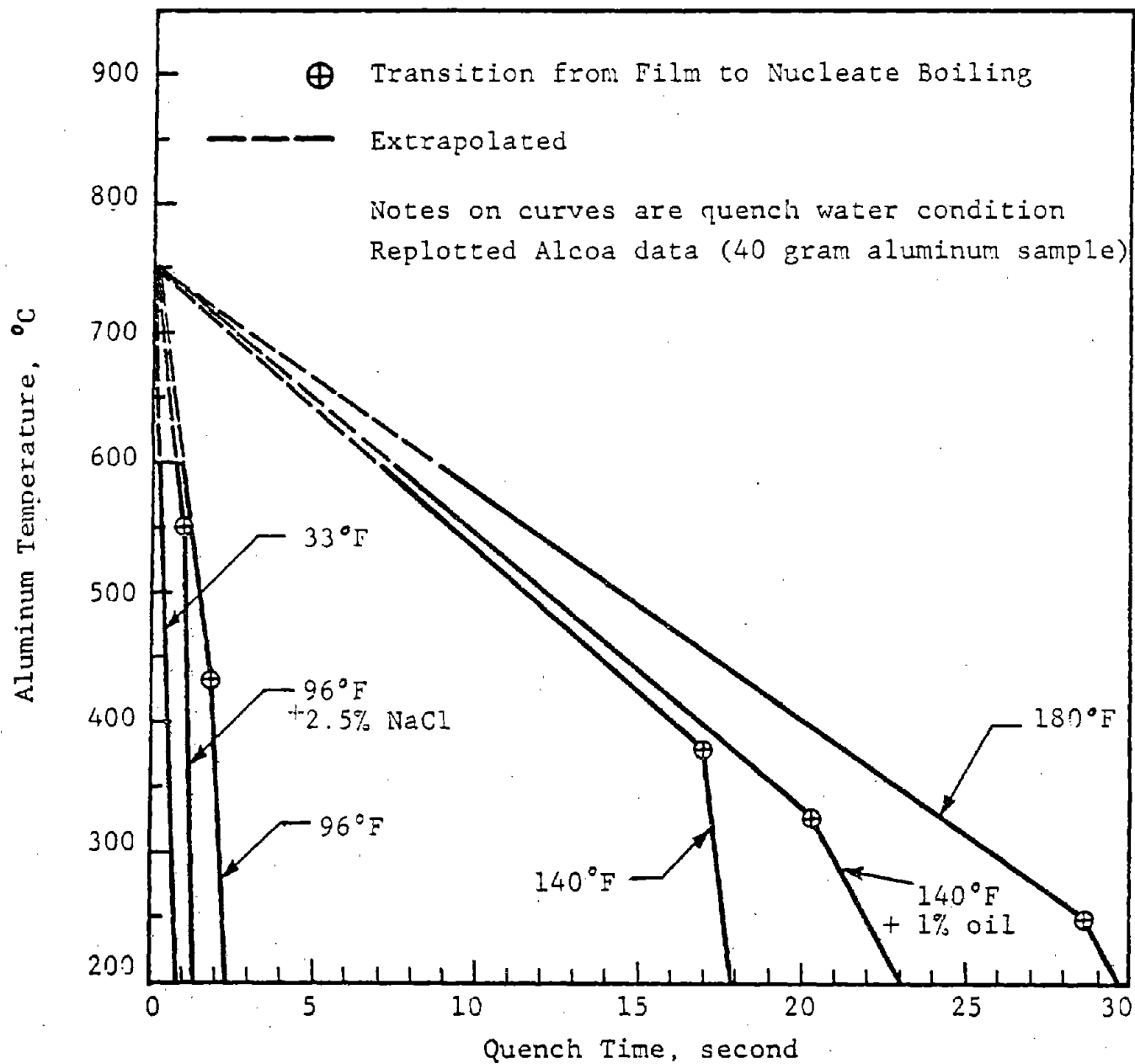


Figure C-39 Aluminum Temperature Versus Quench Time

APPENDIX D
IMPACT SHOCK-CAVITY COLLAPSE
INITIATION MECHANISM

IIT RESEARCH INSTITUTE

IMPACT SHOCK-CAVITY COLLAPSE INITIATION MECHANISM

D.1 Model Description

This Appendix presents a rationale for incorporating an impact generated shock as the first step in the initiation mechanism. The rationale is based upon relating the conditions which are important for the generation and duration of the impact shock (which will produce high temperature) to those conducive to molten aluminum-water reactions. The impact considered is that which could occur as the leading surface of the incoming aluminum initially approaches the quench pit (or tank) surface. It is postulated that if an impact does take place, a shock will be formed.

The important characteristics of the mechanism of cavity collapse under an imposed shock wave are:

- Aluminum particle speed in the shock wave, μ_0
- Initial density of the vapor in the collapsing cavity, ρ_0
- Sound speed in aluminum, c
- Radius of the impacting aluminum stream, R_0
- Initial radius of the collapsing cavity, r_0

Other important "derived" parameters are: the duration of the shock which is proportionate to R_0/c ; the cavity collapse time which is proportionate to r_0/μ_0 and ρ_0 ; temperature of the vapor in cavity after significant collapse, which is proportionate to ρ_0 ; and the acoustic impedance of aluminum, Z_A , which depends upon its temperature.

The value of μ_0 depends upon the aluminum stream velocity at initial impact and the physical characteristics of the surface impacted. The particular characteristic of the surface, in this respect, is its acoustic impedance, Z , which is equal to the produce of its speed of sound and density. In this connection, the impedance of the aluminum is significant. The value of ρ_0 depends upon the amount of heat transferred into the vapor film surrounding the aluminum at impact. This in turn depends upon: the water and aluminum

initial temperatures, the velocity of the aluminum in the water; the chemistry of the water; the local pressure; and the water depth. A higher temperature steam will have a lower density than lower temperature steam and a low ρ_0 promotes developing high temperatures during cavity collapse. The sound speed in aluminum depends to some degree upon its temperatures as does its density. The greater the ratio of the impedance of the impact surface to that of the aluminum, the smaller the value of μ_0 and the less hazardous will be the effect of the impact. The radius of the impacting stream of aluminum is a happenstance arising from a bleed-out which may occur during direct chill casting operations. As shown above, the value of R_0 is very important in determining how long the shock wave will persist, which in turn relates to the amount of cavity collapse and hence, the vapor temperature rise. The time which is available for a specific cavity to be collapsed by the shock wave depends upon its radial position on the impact surface. Cavities close to the stream center line will be engulfed longer by the shock than those farther out. The time required for cavity collapse depends on two factors, r_0 and μ_0 ; small values of r_0 and large values of μ_0 correspond to short collapse times. For equal temperature rises in collapsing cavities, going from positions near R_0 to the stream axis, the corresponding r_0 could be larger. Or, if the cavities are all about the same size, the temperature in the outer cavities (near R_0) will be lower than those near the axis. This latter example is more likely to be the case, e.g., the r_0 's will all be of the same order of magnitude. Thus, large diameter streams will provide more vapor raised to higher temperatures than will smaller streams with equal μ_0 's.

The factors which determine the value(s) of r_0 which may be encountered have been presented in Section 5.4.3 of the report body and the significance of r_0 is presented here. However, it seems reasonable that the characteristics of the impacted surface, the impact (aluminum) speed, vapor film thickness and interfacial surface tension (aluminum/water/impact surface) would be important. In this regard, experiments conducted under simulated bleed-out conditions indicated reductions in explosion frequency when various

surface coatings were present. This could relate to the entrapment of vapor and the cavity size. However it could also effect the impact condition, as the coating would change the impedance of the impact surface. Examination of some solidified aluminum obtained from the small scale physics experiments revealed cavities with diameters on the order of 0.020 inches which is in agreement with predictions.

Bleed-out simulation experiments have shown that the same factors which are significant in obtaining explosions are important in the potential for a shock produced cavity collapse mechanism. These simulation experiments have shown the following important factors, in addition to impact surface conditions, which bound the occurrence of explosions:

- Drop height
- Drop height with water depth
- Aluminum stream diameter
- Aluminum temperature
- Initial water temperature

From the point of view of the postulated initiation mechanism, these factors seem to point clearly to its applicability. A minimum drop height corresponds to a minimum particle speed in the shock (μ_0). The fact that initial aluminum temperature must be above a specific value relates to the potential for heat transfer and that the aluminum be molten upon impact. Corresponding to this is the bound placed upon drop height and water depth. The height corresponds to a speed and this speed through the water depth corresponds to a time for heat transfer. Since the density of the trapped vapor, at the impact surface, is important in developing high temperature, the heat transfer conditions proceeding impact are important. If the time is too short, e.g., the drop height, too great for the water depth, the vapor density will not be low enough. If the water depth is too great for the drop height, nucleate boiling may be approached more closely and again the film density will not be as low as if the vapor were in a superheated state. In addition, the aluminum near the vapor layer may have lost enough temperature to adversely effect the cavity collapse and associated events. The

existence of a minimum aluminum stream diameter is consistent with the shock theory. If the diameter is too small, the shock wave dissipates too fast and cavity collapse is not enough to start a chemical reaction.

Certain other aspects of experiments and actual plant explosions seem to fit the shock theory. For example: the surface coating effect, already discussed, and the minimum stream diameter, as produced by passing the aluminum through a grid; and the plant incident reported to have resulted in an explosion when a bleed-out impacted a vertical wall, below the pit water level. In this latter case, it would seem that a transient phenomena, such as the shock wave, could be established in the molten aluminum with vapor entrapped and in microseconds could go into the propagation phase, as the impacted materials continued "falling" under the acceleration of gravity. This portion of the bleed-out would have been in reasonable proximity to later portions of the bleed-out so that the trigger energy could propagate into it and an explosion result. A difficulty in applying the shock initiation mechanism to the molten aluminum-water reaction arises when the effect of aluminum kelp on the impact surface is taken into consideration. This is the likely condition in direct chill plant operations. Simulation experiments have been conducted with kelp and steel balls on the impact surface in which explosions were obtained. The presence of these materials would appear to interfere with the development of the impact generated shock wave as they could act as flow dividers, reducing the stream diameter. It is noted that the simulations were made from a greater drop height (30 inches rather than 18 inches) which would increase the aluminum impact speed and the resulting shock pressure would be higher. This may be significant in explaining why kelp and steel balls did not preclude an explosion. The effect on aluminum kelp and steel balls on the impact surface may be explained on the basis that they aid in entraining vapor. If this is the case, it would seem that the negative effect which they could have on the impact is less important than steam entrapment enhancement. This could

indicate the critical nature of entrapment. In particular, it would seem that the aluminum kelp would, in part, act as a flow divider, e.g., breakup the aluminum stream into flows with diameters smaller than critical. On the other hand, the impact of the molten flow on the kelp, before the bottom surface, could establish a different shock wave pattern than would be present without the kelp. Each surface of kelp would initiate a separate shock wave, differing in time of origin and associated with different vapor entrapment patterns. The analysis of this condition would be quite difficult. The impact on steel balls would similarly be difficult to analyze, but would be quite similar in effect. The effect of both kelp and balls is to extend the time for vapor entrapment and shock wave development. This may enhance the conditions for developing the shock.

D.2 MODEL ANALYSIS

Analysis was performed on the impact generated shock wave produced in the molten aluminum stream to provide quantification. It was desired to relate the aluminum stream diameter, collapsing cavity radius, collapse time and temperature to the experimental conditions known to be conducive to explosions. The parameters selected for this analysis were an 18 inch drop height, 3-1/4, 2-3/4 and 2-1/2 inch diameter aluminum streams and an aluminum temperature of 750°C (1382°F). It was assumed that the initial water temperature and the water depth would provide a film of 300°C (572°F) superheated steam trapped between the aluminum stream and impact surface. The impact speed of the aluminum was taken as 300 cm/sec (118 ips, which for practical purposes is the free fall speed of the stream).

D.2.1 Impact Parameters

The relevant parameters which are used to calculate the shock wave produced by the impact are:

- Aluminum stream radius, R_0 (cm)
- Initial aluminum speed, V (cm/sec)
- Particle speed at impact, U_0 (cm/ μ sec)
- Aluminum density, ρ_a (gm/cc)

- Aluminum sound speed, C_a (cm/ μ sec)
- Aluminum impedance, $Z_a = \rho_a C_a$ (mb- μ sec/cm)
- Impact surface material density, ρ_I (gm/cc)
- Impact surface material sound speed, C_I (mb- μ sec/cm)
- Impact surface material impedance, $Z_i = \rho_I C_I$ (mb- μ sec/cm)

The conditions at impact, for two materials to maintain contact (not separate), are that the shock pressure (P) in each material and the particle speeds (U) are equal. The equations representing the shock pressure in the aluminum (P_a) and in the surface (P_I) are:

$$P_a = Z_a [V - U_o]$$

U_o

$$P_i = Z_i U_o$$

Equating the two pressure and solving for U_o gives:

$$U_o = (V) Z_a / (Z_a + Z_i) = V / (1 + Z_i / Z_a)$$

The foregoing relationships are based upon the assumption that the thickness of the impacted surface is great enough so that a shock will not reflect during the time of interest.

There are two important time intervals associated with the shock wave collapsing the cavities at the impact interface:

- The time required for a cavity to collapse, t_c
- The time the shock wave engulfs the cavity, t_s

The cavity collapse time is proportionate to the cavity radius divided by the particle speed and the shock time is proportionate to the radial position of the cavity in the aluminum stream divided by the sound speed in aluminum. The time the shock engulfs a cavity on the axis of aluminum stream is:

$$t_s = R_o / C_a$$

and the time at any radial position, R, is:

$$t_s = (R_o - R) / C_a$$

The cavity radius, R_c , which can be collapsed in the time t_s is:

$$R_c \approx U_o t_s \quad \text{or}$$

$$U_o \approx (R_o - R) / C_a$$

The time required to collapse a cavity with a radius R_c is:

$$t_c \approx R_c / U_o$$

The change in the cavity radius is also proportionate to these parameters:

$$\Delta R_c \approx U_o (R_o - R) / C_a$$

so that the amount of collapse in a cavity of a given radius will be determined by shock particle speed and cavity radial position. The amount of collapse is critical in raising the trapped vapor temperature (and pressure) by adiabatic compression and the degree of instability which results in the formation of a jet of "fresh" aluminum.

The shock pressure accelerates the particles during cavity collapse so that the time for cavity collapse is less than the relationship shown, which is why it was stated as proportionate to the initial particle speed.

Table D.1 provides a summary of material and shock related parameters. Asphalt and epoxy are included as their characteristics are indicative of surface treatments such as taret. The other materials are typical impact surfaces. The impact shock pressures and particle speeds, shown for steel, solids aluminum, glass and concrete, were used in an existing IITRI computer code to calculate the collapse of spherical cavities in spheres of molten aluminum. In each case the initial cavity radius was taken as 0.05 cm (about 0.02 inch) and was assumed to contain steam at 300°C initially. Table D.2 summaries the times to approximate equal cavity compression ratios with the associated cavity pressures and temperatures.

Table D.1

SHOCK CHARACTERISTICS FOR VARIOUS MATERIALS AND MOLTEN ALUMINUM DROPPED FROM 18 INCHES
(IMPACT SPEED 300 cm/sec)

Material	Density ρ (gm/cm ³)	Sound Speed C (cm/ μ S)	Impedance ρC (mb- μ s/cm)	Speed Factor (SF)* $1 + \frac{\frac{1}{(\rho C)} x}{(\rho C)_a}$	Pressure Factor $(\rho C)_x SF$	Particle Speed (cm/sec)	Pressure	
							(kb)	(lb/in. ²)
Concrete	2.40	.347	0.833	0.569	0.474	171	0.142	2,060
Mild Steel	7.84	.360	2.822	0.280	0.790	84	0.237	3,440
Glass	2.50	.545	1.363	0.447	0.609	134	0.183	2,650
Solid Aluminum	2.70	.544	1.469	0.428	0.629	128	0.189	2,740
Asphalt	1.00	.090	0.090	0.924	0.083	277	0.025	360
Epoxy	1.20	.267	0.320	0.775	0.248	233	0.074	1,080
Molten Aluminum	2.34	.470	1.100	0.500	0.550	150	0.165	2,390
Liquid Water	1.00	.150	0.150	0.880	0.136	264	0.041	590

* $(\rho C)_x$ refers to the impact surface properties, $(\rho C)_a$ refers to molten aluminum properties.

Table D.2

TYPICAL COLLAPSE TIMES, PRESSURES AND TEMPERATURES FOR CAVITIES 0.05 CM RADII INITIALLY
IN 750°C ALUMINUM DROPPED 18 INCHES ON THE MATERIALS SHOWN (CAVITY CONTAINED 300 C STEAM)

Material	Time (μsec)	Volume Ratio (-)	Pressure (psi)	Temperature (°C)	Time (μsec)	Volume Ratio (-)	Pressure (psi)	Temperature (°C)
Concrete	3.019	.0119	4,960	2,040	3.075	.0038	23,670	3,040
Glass	3.167	.0120	4,960	2,040	3.224	.0038	22,010	3,030
Solid Aluminum	3.195	.0116	5,130	2,060	3.253	.0037	24,610	3,070
Steel	3.459	.0113	5,320	2,080	3.515	.0036	24,190	3,100

As shown in Table D.2, there is no appreciable difference in the collapse conditions. Impact on steel takes about 14 percent longer to reach the same conditions as on concrete. Impacts on solid aluminum and glass require about 5 percent more time to reach the same collapse condition as drops on concrete.

As indicated in Table D.2, a volume ratio, V_R (final to initial) of 0.0038 will increase the initial vapor temperature and pressure by factors of about 10 and 1,600, respectively. The constant of proportionality, K , needed to estimate the average particle speed may be obtained from the data in the table. The change in cavity volume required to obtain the temperature and pressure increase is:

$$V_R = [R/R_c]^3$$

$$R = R_c \sqrt[3]{V_R}$$

$$\Delta R = R_c - R = R_c [1 - \sqrt[3]{V_R}]$$

The change in radius is also,

$$\Delta R = KU_o t_s$$

so that:

$$K = R_c [1 - \sqrt[3]{V_R}] / [U_o t_s]$$

and for concrete; values from Tables D.1 and D.2 are:

$$C_a = .470 \text{ ca}/\mu\text{sec}$$

$$U_o = .00171 \text{ cm}/\mu\text{sec} (171 \text{ cm}/\mu\text{sec})$$

$$t_s = 3.075 \mu\text{sec}$$

$$R_c = 0.05 \text{ cm}$$

and K is:

$$K = 80.3$$

A cavity on the axis of a 3-1/4 inch diameter stream of aluminum will be in the shock wave for:

$$t_s = \frac{R_o}{C_a} = \left(\frac{3.25 \times 2.54}{2} \right) / .470 = 8.785 \mu\text{sec}$$

The maximum cavity radius which could be collapsed there would be about 0.143 cm which corresponds to a 0.1 inch diameter cavity. A .040 inch (.05 cm radius) diameter cavity would have to be 0.57 inch in from the outside diameter of the stream to be engulfed long enough to be collapsed.

It has been reported that the molten aluminum stream diameter should be 2-3/4 inches or greater to produce an explosion and that a 2-1/2 inch diameter will not. A 2-1/2 inch diameter corresponds to a shock compression time, for a cavity on the stream axis, of 6.76 sec which can collapse a cavity diameter of about 0.086 inch. Since a 0.04 inch diameter cavity must be 0.57 inch in from the aluminum stream diameter, all the cavities within a central "core" of the stream, having a diameter of 1.36 inch¹, could be collapsed if their diameters were between 0.040 inch and 0.085 inch. If a mean cavity has a 0.05 inch diameter and half of the core surface area contained cavities, approximately 370 cavities would be collapsed. The weight of water vapor (v) contained in the cavities is:

$$w = 4(10^{-4}) 370 \left(\frac{1}{2}\right) \left(\frac{4\pi}{3}\right) \left(\frac{.05 \times 2.54}{2}\right)^3 = 0.79 (10^{-4}) \text{ grams}$$

The chemical energy which could be released by aluminum oxidation² with this weight of steam is about 0.44 calories³. On the same basis as calculated for the 2-1/2 inch diameter stream, the 2-3/4 inch stream could release 0.62 calories, about 40 percent more chemical energy. If the chemical energy is considered distributed over the respective aluminum stream diameters at a thickness of the collapsed radius⁴ the specific energy added is about 0.45 cal/gm

¹ $\left[\frac{2.5}{2} - .51\right] 2 = 1.36$

² About 1.7 times as much aluminum reacts as steam and about 3330 gram-calories/gram of aluminum are released.

³ Gram-calories.

⁴ Collapsed radius = 0.006 inch.

$[1.88 (10^{-5}) \text{ mb-cc/gm}]^1$ for the 2-3/4 inch diameter stream and 0.39 cal/gm $[1.63 (10^{-5}) \text{ mb-cc/gm}]$ for the 2-1/2 inch diameter. This corresponds to approximately 15 percent more specific energy added in the case of the larger diameter. The energy change (Δe) is proportionate to the particle speed (u) in a shock wave which is proportionate to the shock pressure (P). These relations are:

$$\Delta e = 0.5 \mu^2$$

$$U = \sqrt{2\Delta e}$$

$$P = \rho C U \quad (\rho C = 1.1 \text{ mb-}\mu\text{s/cm})^2$$

In terms of particle speed, the larger stream would have a particle speed of $0.0084 \text{ cm}/\mu\text{sec}$ and the smaller stream $0.0072 \text{ cm}/\mu\text{sec}$. These speeds correspond to shock pressures of 134,000 and 115,000 psi respectively, for the larger and smaller streams.³

These shock pressure values seem quite significant, about 60 times the impact shock pressure and 6 times the cavity collapse pressure after the volume has been reduced to about 0.4 percent of its initial value. It would seem that the criteria for explosion stated on the basis of stream diameter may be made equivalent to the magnitude of the chemical energy released. This is quite reasonable because the energy in the shock wave dissipates during propagation unless energy is added. Thus, it may be indicated that about 0.6 calorie is required to be released through aluminum oxidation and that 0.4 calorie is insufficient for an initiation.

$$^1 \left(\frac{\text{cal}}{\text{gm}} \times 4.186 \right) (10^{-5}) = \frac{\text{mb-cc}}{\text{gm}} = \frac{\text{cm}^2}{\mu\text{sec}^2}$$

² The chemical energy, particle speed and shock pressure for a 3-1/4 inch diameter aluminum stream would be proportionately greater.

³ $\text{mb} = 14.5 (106) \text{ psi}$

D.2.2 Surface Treatment

The shock induced initiation model can be used to take the effect of impact surface treatment into account through impedance and shock waves reflected by the surface coating. The impact surface coating is considered thin, e.g., there is time for the shock wave, in the coating, to reflect from the substrate many times during the cavity collapse period. The sequential reflections of the shock wave from both interfaces (molten aluminum and substrate) cause the shock wave conditions to build up (in the molten aluminum) to approach that of a direct impact on the substrate. Thus, instead of an instantaneous "jump" at impact to the conditions which would prevail under direct contact, the full effect is spread out in time.

In order to provide a specific illustration, the impact of molten aluminum at 300 cm/sec (representing an 18 inch drop) on a .015 inch (.038 cm) coating of asphalt over concrete was considered. First, as indicated in Table D.1, this impact directly on concrete would provide shock conditions with a pressure of 2060 psi and a particle speed of 171 cm/sec. The same impact on the asphalt produces an initial shock with 360 psi and 277 cm/sec. These latter conditions are both the reflected (into the molten aluminum) and transmitted (into the asphalt) waves. The wave travels with an acoustic speed of .090 cm/ μ sec and has to travel a path twice the thickness of the coating (.076 cm) which will take 0.844 μ sec. Halfway through this time period, the initial wave reaches the concrete surface. This wave is reflected and transmitted, however, the concrete is assumed sufficiently thick so that no waves are reflected from its far surface and so we are only concerned with the reflected wave in the asphalt. The shock condition presented in Section D.2.1 applies as shown below.

$$P_{as} = Z_{as} [2U_1 - U_2]$$

$$P_c = Z_c U_2$$

Where the "as" subscript stands for asphalt and "c" for concrete. U_1 is the particle speed from the initial impact, 277 cm/sec and U_2 is the particle speed which results from the reflected wave and P is the reflected shock pressure.

Since

$$P_{as} = P_c$$

$$U_1 = 2U_1Z_{as}/(Z_{as}+Z_c) = 54 \text{ cm/sec}$$

$$P_2 = Z_c U_2 = 650 \text{ psi}$$

When this wave reaches the molten aluminum-asphalt interface, the shock conditions are:

$$P_a = Z_a(V-U_3) \quad (V = 300 \text{ cm/sec, the impact speed})$$

$$P_{as} = Z_{as}U_3 + (Z_c - Z_{as})U_2$$

Where the subscript "a" refers to the aluminum, "3" to the shock condition at the current aluminum-asphalt interface and the other subscript have the same meaning as previously defined.

Since, $P_{as} = P_a$,

$$U_3 = VZ_a/(Z_a+Z_{as}) - U_2(Z_c - Z_{as})/(Z_a+Z_{as}) = 243 \text{ cm/sec}$$

$$P_3 = Z_a(V-U_3) = 910 \text{ psi}$$

This process is repeated and the final shock state approaches the conditions for an impact of molten aluminum on cement without asphalt. Figure D.1 depicts the pressure and particle speed in the shock as a function of time at the axis of the aluminum stream. As shown, the shock pressure and particle speed reach the instantaneous values, when no asphalt layer is present, in 8.44 sec. The impact shock is a compression wave and it is reflected (rarefraction wave) from the stream outside diameter as a tension wave which nullifies the compression wave. The rarefraction wave travels at the same speed (acoustic) as the compression wave, thus, the compression shock is weakened near the outside diameter of the aluminum stream.

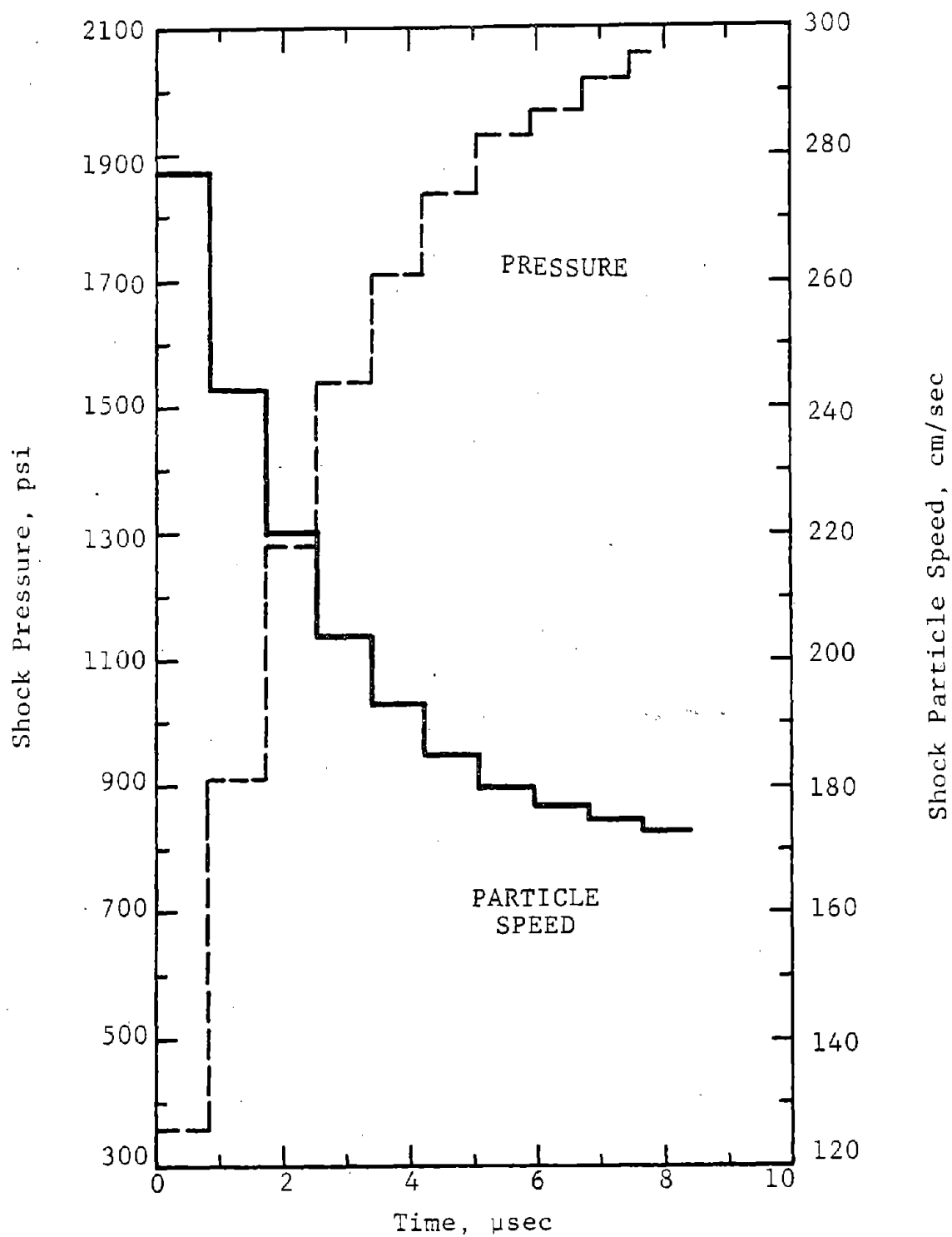


Figure D.1 Shock Pressure and Particle Speed Versus Time for Molten Aluminum Impacting Concrete at 300 cm/sec with a 0.015 inch Thick Asphalt Layer (Axial Conditions)

The effect of the tension wave and asphalt coating on concrete is shown in Fig. D.2. The shock pressure time curve is the same as in Fig. D.1, but the coating was taken as twice as thick (.030 inch) thereby doubling the time at each pressure level (as replotted). The shock pressure-position-time curve for the same impact without an asphalt coating is also shown in Fig. D.2 to provide a direct comparison. The shock wave engulfs an axial cavity in a 3-1/4 diameter (about a 4 cm radius) molten aluminum stream for 8.8 μ sec. As shown in Fig. D.2, the shock pressure, at the axial position (4 cm) will have just reached about 1800 psi and will have had an average pressure acting of about 1200 psi. This is less than 60 percent of the pressure level that would have acted had there been no 0.030 inch thick asphalt coating on the concrete surface. Calculations were not made to determine the amount of cavity collapse or the diameter cavity which could be collapsed sufficiently to sustain chemical reaction. However, it seems clear that the effect of impact trigger would be significantly mitigated. Therefore, it is reasonable to assume that the effect of this type of protective coating (one with a low impedance) is to "eliminate" the trigger.

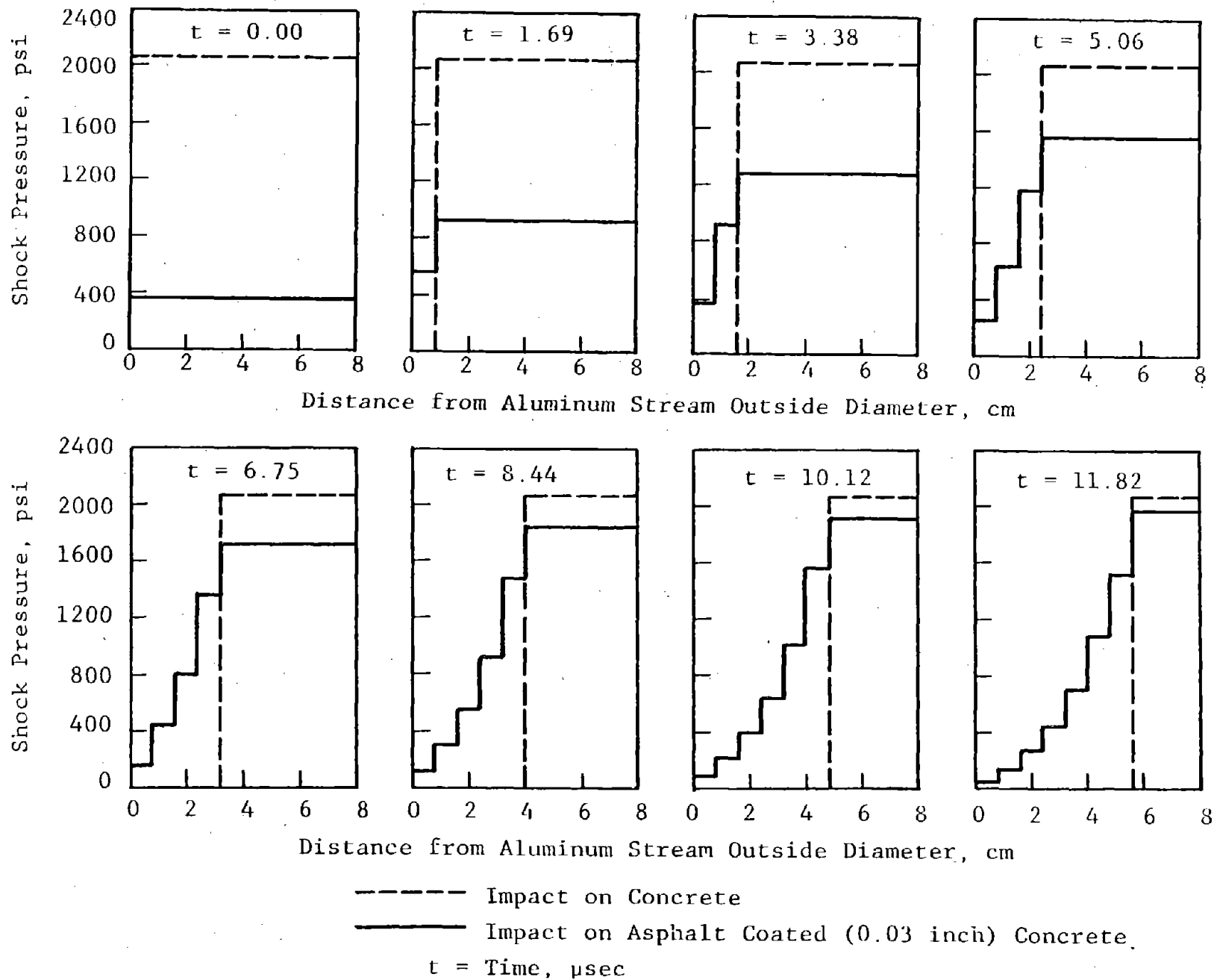


Figure D.2 Shock Pressure Versus Radial Position at Eight Times for Molten Aluminum Impacting Two Different Surfaces at 300 cm/sec